University Libraries
University of Nevada, Las Vegas

5-15-2018

Static and Dynamic Quantitative Microbial Risk Assessment of Potable Reuse Paradigms

Erfaneh Amoueyan
amooeyan.a@gmail.com

www.manaraa.com

STATIC AND DYNAMIC QUANTITATIVE MICROBIAL RISK ASSESSMENT OF

POTABLE REUSE PARADIGMS

By

Erfaneh Amoueyan

Bachelor of Science in Engineering – Civil Engineering
Babol University of Technology
2008

Master of Science in Engineering – Civil and Environmental Engineering
University of Mazandaran
2011

A dissertation submitted in partial fulfillment
of the requirements for the

Doctor of Philosophy – Civil and Environmental Engineering

Department of Civil and Environmental Engineering and Construction
Howard R. Hughes College of Engineering
The Graduate College

University of Nevada, Las Vegas
May 2018

Dissertation Approval

The Graduate College
The University of Nevada, Las Vegas

April 5, 2018

This dissertation prepared by

Erfaneh Amoueyan

entitled

Static And Dynamic Quantitative Microbial Risk Assessment Of Potable Reuse Paradigms

is approved in partial fulfillment of the requirements for the degree of

Doctor of Philosophy – Civil and Environmental Engineering
Department of Civil and Environmental Engineering and Construction

Daniel Gerrity, Ph.D.
Examination Committee Chair

Sajjad Ahmad, Ph.D.
Examination Committee Member

Haroon Stephen, Ph.D.
Examination Committee Member

Krystyna Stave, Ph.D.
Examination Committee Member

Kaushik Ghosh, Ph.D.
Graduate College Faculty Representative

Kathryn Hausbeck Korgan, Ph.D.
Graduate College Interim Dean

ii

Abstract

In recent years, potable reuse applications have become more common due to population growth and increased water demand, especially in communities with limited or variable water resources. However, there are concerns about potential exposure to pathogens and chemical compounds in treated wastewater. Therefore, advanced wastewater treatment processes are of paramount importance in any potable reuse system. The overall aim of this study was to develop and implement static and dynamic QMRAs to compare public health risk in various potable reuse scenarios. *Cryptosporidium*, norovirus, adenovirus, and *Salmonella* were chosen as the target pathogens. The research evaluated the performance of full advanced treatment (FAT) trains consisting of reverse osmosis (RO) and advanced oxidation processes (AOPs), which are required in California for planned IPR systems that directly inject recycled water into local aquifers or discharge to surface water. The study also explored ozone-biological filtration as an alternative for FAT trains by comparing its public health risk to that of the RO-based treatment train. Treatment process performance and resultant public health risks were modeled using the STELLA 10.1 system dynamics software package. The system dynamics model accounted for the possibility of unit process failure and subsequent effects on downstream treatment process performance (i.e., 'domino effects'). The model also compared typical vs. outbreak scenarios and identified the components and operational conditions that were most critical to minimizing public health risks in each of the potable reuse paradigms.

The dynamic disease transmission model incorporated secondary transmission and immunity through implementing different epidemiological states. In this study, dynamic disease transmission model was focused on norovirus which is the most common cause of acute gastroenteritis diseases in the US.

This study indicated that combined annual risk of infection was lower in DPR systems with direct distribution (median risk= 5.4×10^{-8} and 1.2×10^{-6} for ozone-based DPR and RO-based DPR, respectively) compared to the IPR systems and DPR with blending. Generally, potable reuse treatment trains with surface water utilization resulted in similar risk of infection which exceeded the benchmark risk of 10^{-4}. The model also identified 120 days and 150 days of storage time at 10°C and 20°C of temperature as the most critical parameters in *de facto* reuse systems when targeting *Cryptosporidium* and adenovirus, respectively. Included secondary transmission and immunity resulted in up to 8 orders of magnitude higher risk of norovirus than the static framework (depending on the treatment train). However, results of this study indicated that potable reuse systems were sufficiently robust to handle the high concentration of norovirus during outbreak conditions and that disease incidence of norovirus was mainly attributed to secondary transmission pathway. However, these results may change if other pathogens are considered in dynamic disease transmission model.

iv

Acknowledgment

I would like to express the deepest appreciation to my advisory committee chair, Dr. Daniel Gerrity for all his support, guidance, encouragement, and advice throughout this research. I would like to thank my committee members for their valuable time and suggestions. I would also like to extend my thanks to Dr. Joseph Eisenberg and the epidemiology group at the University of Michigan, School of Public Health for providing helpful feedback and comments.

Finally, I am extremely grateful to my family and friends for their love and support through all these years. I would particularly like to single out my sister for her mental support not only throughout this research, but throughout my entire life.

Table of Contents

List of Tables

x

List of Figures

List of Acronyms

AdV	Adenovirus
AOP	Advanced Oxidation Process
BAC	Biological Activated Carbon
CAS	Conventional Activated Sludge
CCL	Contaminant Candidate List
CDF	Cumulative Distribution Functions
CDPH	California Department of Public Health
CI	Cumulative incidence
DALYs	Disability Adjusted Life Years
DDW	California Division of Drinking Water
DPR	Direct Potable Reuse
DT	Delta time
DWTP	(Conventional) Drinking Water Treatment Plant
EPA	Environmental Protection Agency
ESB	Engineered storage buffer
FAT	Full Advanced Treatment
FCV	Feline calicivirus
FS	Factor Sensitivity
FUT2	Fucosyltransferase 2
HBGAs	Histo-blood group antigens
ILIS	International Life Sciences Institute
IOD	Instantaneous Ozone Demand

IPR	Indirect Potable Reuse
LRV	Log removal value
LT2	Long Term 2 Enhanced Surface Water Treatment Rule
MF	Microfiltration
MNV	Murine norovirus
MPN	Most probable number
NDMA	N-nitrosodimethylamine
NF	Nanofiltration
NMED	New Mexico Environment Department
NoV	Norovirus
NWRI	National Water Research Institute
O_3	Ozone
PDF	Probability Distribution Functions
QMRA	Quantitative Microbial Risk Assessment
qPCR	Quantitative polymerase chain reaction
RO	Reverse Osmosis
RWCs	Recycled Water Contributions
SDWA	Safe Drinking Water Act
SWTRs	Surface Water Treatment Rules
TCEQ	Texas Commission on Environmental Quality
TCID50	Tissue Culture Infective Dose
TDS	Total Dissolved Solids
TOC	Total Organic Carbon

TOrCs	Trace Organic Compounds
UF	Ultrafiltration
UV/H$_2$O$_2$	Ultraviolet/Hydrogen Peroxide
WHO	World Health Organization
WWTP	(Conventional) Wastewater Treatment Plant

1   Introduction

Climate change, population growth, urbanization, and increased water demands create intense pressure on finite natural water resources. Consequently, the need for more efficient use of water resources (i.e., conservation, reuse, and alternative water sources) is particularly critical for communities with limited or variable water resources (Asano et al., 2007). Recently, water reuse has become more common, especially in arid and semi-arid regions. It can also be beneficial in coastal regions with saltwater intrusion and communities with compromised water quality (Gerrity et al., 2013). Water reuse can be implemented to provide non-potable water for industry and irrigation purposes or potable water for augmenting drinking water supplies (NRC, 2012). However, there are always concerns about potential exposure to pathogens and chemical compounds in treated wastewater.

It is estimated that at least 9.1% of the global disease burden and 6.3% of all deaths are due to waterborne diseases that could be prevented by improved sanitation and hygiene (Pruss et al., 2008). It is widely recognized that water plays an important role in transporting microbial contamination that contributes in disease transmission and outbreaks (LeChevallier & Au, 2004). As a result, quantifying the microbial risk associated with exposure to contaminated water serves as a fundamental component of public health protection.

Many indirect potable reuse (IPR) and direct potable reuse (DPR) projects throughout the world employ reverse osmosis (RO) and an advanced oxidation process (AOP) to ensure adequate protection of public health (CDPH, 2014). In California, this 'full advanced treatment' (FAT) train is required for direct injection in groundwater replenishment applications and for surface water augmentation to address both known [e.g., pathogens and carcinogenic chemicals such as *N*-nitrosodimethylamine (NDMA)] and unknown potential health risks. RO-based

1

treatment trains can achieve very low concentrations of total dissolved solids (TDS), which is important for systems with high TDS inputs from local source waters and/or water softeners (Venkatesan et al., 2011). In addition, RO is also effective in reducing the total organic carbon (TOC) concentration in the finished product water, which aids in meeting stringent TOC requirements (e.g., 0.5 mg/L of wastewater-derived TOC; CDPH, 2014). However, implementation of RO is hindered by its high capital and operations and maintenance costs, high energy consumption, and concerns related to brine disposal in inland applications. As a result, some communities are already employing or exploring feasibility of ozone-biological filtration systems as an alternative to FAT systems. Therefore, it is critical to address microbial risk associated with alternative ozone-biological filtration systems to ensure public health protection.

Direct exposure to waterborne pathogenic microorganisms (i.e., primary transmission) is one of the most important factors in risk estimation. Risk associated with primary transmission can be calculated using published dose response functions coupled with pathogen doses based on ingestion of contaminated water. However, there are other factors that play important roles in the transmission of infectious diseases. Some studies have focused on secondary disease transmission, while also acknowledging the importance of immunity in estimating the spread of disease within a community (Brookhart et al., 2002; Eisenberg et al., 1996; Eisenberg et al., 2004; Soller & Eisenberg, 2008). Secondary transmission includes person-person or person-environment-person transmission (Soller & Eisenberg, 2008). These secondary transmission pathways can lead to significantly increased infection rates for certain pathogens (Eisenberg et al., 2004).

The current study aimed to incorporate each of these components into a potable reuse QMRA. The QMRA was developed using a system dynamics platform (STELLA 10.1, ISEE

Systems, Lebanon, NH) and allowed for assessments of the equivalency of potable reuse systems and treatment trains, the relative significance of treatment failures on water quality and public health, and the relative significance of primary versus secondary disease transmission pathways in the context of potable reuse. The system dynamics model was validated based on suggestions in Sterman (2000). These tests included structure assessment, dimensional consistency, parameter assessment, integration error (time step and numerical integration method), behavior reproduction, extreme condition tests, and sensitivity analyses.

This dissertation includes a literature review followed by three interdependent chapters that build upon information learned during earlier phases of the research:

- Chapter 3 focused on *Cryptosporidium* risk associated with *de facto* reuse, planned IPR, and DPR systems employing ozone-biofiltration treatment trains. The contents of this chapter were published in Water Research: "Amoueyan, E., Ahmad, S., Eisenberg, J. N., Pecson, B., & Gerrity, D. (2017). Quantifying pathogen risks associated with potable reuse: A risk assessment case study for *Cryptosporidium*. Water Research, 119, 252-266." References to Amoueyan et al. (2017) throughout the dissertation refer to this publication and to Chapter 3 of this dissertation.

- Chapter 4 expanded the static QMRA model to include a direct comparison of the potable reuse systems in Chapter 3 with RO-based treatment trains. Chapter 4 focused on four pathogens: *Cryptosporidium*, norovirus, adenovirus, and *Salmonella* because of their importance to gastroenteritis worldwide. This chapter will soon be submitted for publication. References to Amoueyan et al. (2018) later in the dissertation refer to Chapter 4 of this dissertation.

3

- Chapter 5 expanded the static QMRA framework to the dynamic level to incorporate multiple disease transmission pathways and time-dependent distributed delays for critical epidemiological states, such as post-infection immunity. This chapter focused on norovirus as the target pathogen because it is highly contagious so secondary transmission is known to be a critical factor for propagation of norovirus through a community.

The following sections describe the research questions and corresponding hypotheses that were addressed in this study:

1.1 Quantifying and comparing public health risks associated with different potable reuse treatment trains

RQ1: How do public health risks vary by potable reuse paradigm (i.e., IPR vs. DPR), by treatment train (e.g., ozone-biofiltration vs. RO-based treatment trains), and by different target pathogens?

H1: Potable reuse systems are safe and sustainable alternatives to conventional drinking water and can reliably meet a benchmark annual risk of 10^{-4}. Also, ozone-biofiltration is equivalent to RO-based treatment trains with respect to public health protection. Different waterborne pathogens pose different risk of infection depending on the treatment unit processes employed in each of the potable reuse systems. As previous studies (Forss & Ander, 2011) reported that risk of infection in potable reuse system was driven by *Cryptosporidium*, the hypothesis is that *Cryptosporidium* results in higher risk than other pathogens in potable reuse systems.

1.2 Evaluating the effects of unit process failures on public health risk

RQ2: How do unit process failures affect treatment train performance and public health?

H2: Failure in one or more treatment barriers will adversely affect the overall performance of the treatment train and lead to unacceptably high risk of infection.

Assuming the various treatment processes are operating as intended, one can estimate the log removal/inactivation credits expected for each pathogen in each potable reuse system using experimental/published data. However, failures during advanced treatment may have a significant detrimental impact on the total log removal/inactivation of pathogens. To address this issue, the potential impacts of process failures were incorporated into the model to evaluate whether the treatment trains are sufficiently robust to adequately protect public health during sub-optimal operation. The hypothesis is that IPR treatment trains are less sensitive to failure in treatment processes and the additional storage time provided in environmental buffer could compensate for the effect of failure.

1.3 Determining critical conditions affecting public health risk

RQ3: What are the most significant design/operational parameters affecting public health risk?

H3: Sensitivity analysis can be performed to find the most significant parameters/operational conditions and best inform the decision-making process in development of design or operational criteria for different potable reuse treatment trains. The hypothesis is that environmental buffers in IPR systems play an important role in public health protection.

1.4 Impacts of secondary disease transmission and pathogen-shedding from infected individuals on overall public health risk

RQ4: How do secondary disease transmission and post-infection immunity affect public health?

5

H4: Inclusion of secondary disease transmission leads to an increased risk of infection due to a greater number of pathogen-shedding individuals in the community. Higher number of infectious individuals would lead to higher concentration of pathogen shedding into the wastewater and ultimately higher concentration of pathogen in final drinking water. Incorporating post-infection immunity decreases disease incidence among the community compared to the condition with no immunity to the disease.

The answers to these research questions will aid in identifying the most critical parameters/operational conditions in implementation of potable reuse systems; therefore, contribute to the improvement of the decision-making processes in development, operational designs, and the overall reliability of potable reuse systems.

2   Background and literature review

2.1   Potable reuse

Generally, there are two types of potable reuse systems: indirect potable reuse (IPR) and direct potable reuse (DPR). Both systems use advanced treated wastewater for drinking purposes. The key difference is the use of an environmental buffer as a discharge or blending point in IPR systems which also acts as a psychological barrier (Khan, 2013; USEPA, 2012), while the DPR system utilizes additional engineered treatment processes, expanded monitoring efforts, or an engineered storage buffer to compensate for reduced response retention time (Tchobanoglous et al., 2015). In addition to providing new source of drinking water, employing advanced wastewater treatment processes in potable reuse applications can also decrease the adverse effects of discharging conventionally treated wastewater into 'pristine' water resources (Gerrity et al., 2014). A common form of IPR is known as unplanned IPR or *de facto* reuse (Rice et al., 2013; Rice et al., 2015), in which intake water to drinking water treatment plants is withdrawn from a water body that receives effluent from an upstream wastewater treatment plant. Although these systems are employing potable reuse, they are not officially recognized as reuse projects. Therefore, they may not have plans or permits specifically addressing the augmentation of the downstream community's source water with wastewater effluent (Cotruvo & Bell, 2014). Fig. 2.1 illustrates a schematic diagram of potable reuse paradigms.

First DPR system was implemented in Windhoek, Namibia, in which the reclaimed water is blended with the treated water downstream of the drinking water treatment facility and within the drinking water distribution system (NRC, 2012; Tchobanoglous et al., 2015). Since, no relationship could be found between diarrheal diseases or mortalities in the community and

7

exposure to drinking water, this system could serve as a successful development of potable reuse

project with no environmental buffer (NRC, 2012).
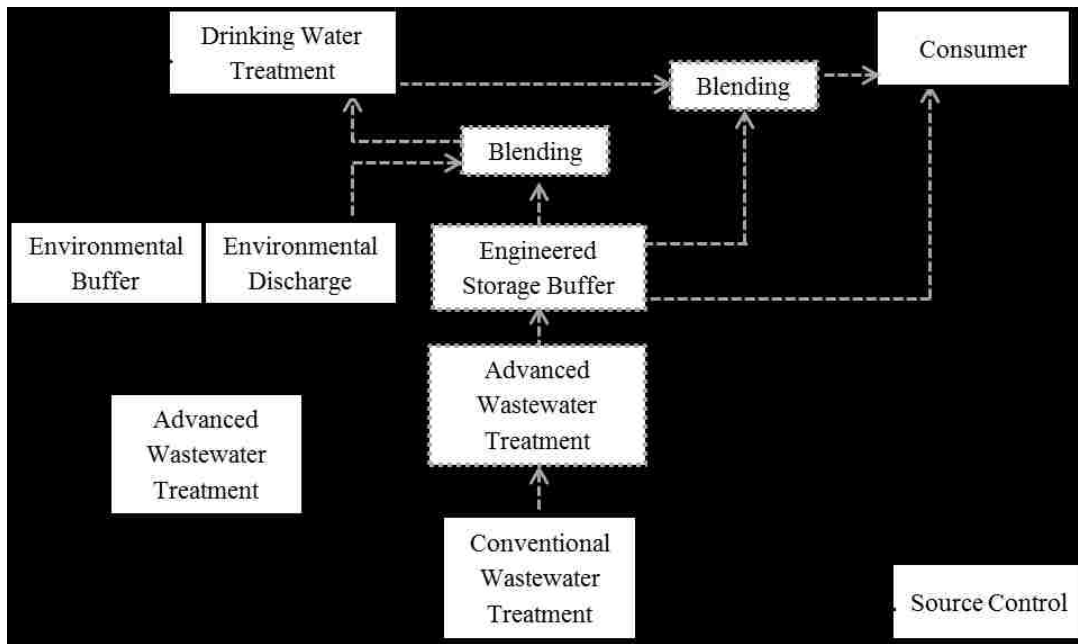
Figure 2-1. Schematic diagram of potable reuse paradigms.
Solid lines represent travel of water through an IPR system, and dashed lines represent travel of water through a DPR system (Gerrity et al., 2013).

At this time, Texas is the only state in the US with existing DPR system (Big Spring)

(Tchobanoglous et al., 2015; WHO, 2017), while IPR systems are more widespread throughout

the US states in California, Nevada, Arizona, Texas, Virginia, Georgia, and Florida which are

implemented based on state regulations and guidelines or regulated on a case-by-case basis

(Tchobanoglous et al., 2015)

Different potable reuse systems throughout the world that are successfully implemented

are listed in Table 2.1.

8

Table 2-1. Potable reuse projects throughout the world

Potable Reuse Project	Potable Reuse Application	Treatment process (after secondary treatment)	Reference
Montebello Forebay, California, USA	IPR with groundwater replenishment	Media filtration, SAT, Cl2	Sloss et al. (1996)
Goreangab plant, Windhoek, Namibia	DPR	O3, DAF, rapid sand filtration, O3, BAC, GAC, UF, Cl2	Tchobanoglous *et al*. (2015)
Orange County, California, USA	IPR with groundwater replenishment	Cl2, MF, RO, AOP (UV/H2O2)	Tchobanoglous *et al*. (2015)
Hueco Bolson recharge project, El Paso Water Utilities, Texas, USA	IPR with groundwater replenishment	PAC, lime clarification, media filtration, O3, GAC, O3, Cl2	Gerrity et al. (2013)
NEWater, Singapore	IPR with surface water augmentation	UF, RO, UV	WHO (2017)
UOSA, Fairfax county, Virginia, USA	IPR with surface water augmentation	Lime clarification, media filtration, GAC, Cl2, chloramination	Gerrity et al. (2013)
Big Spring, Texas, USA	DPR	MF, RO, AOP (UV/H2O2), blending, media filtration, Cl2	Tchobanoglous *et al*. (2015)
Beenyup groundwater replenishment scheme, Perth, Australia	IPR with groundwater replenishment	UF, RO, UV	WHO (2017)
Gwinnett County, Georgia, USA	IPR with surface water augmentation	Chemical phosphorus removal, UF, O3, GAC	Gerrity et al. (2013)

2.2   Microbial criteria

One of the primary concerns in potable reuse applications is potential exposure to

pathogenic microorganisms in the final product water. At this time, no federal regulations have

been established specifically for DPR. The California Division of Drinking Water (DDW) and

the National Water Research Institute (NWRI) recently established stringent

requirements/guidelines for pathogen removal in potable reuse applications to achieve the

benchmark risk of 10^{-4} per person per year (CDPH, 2014). Both frameworks specify 12-log and

10-log reductions for viruses and *Cryptosporidium*, respectively, while DDW also requires 10-

9

log reduction of *Giardia* and NWRI recommends 9-log reduction of bacteria. The recommended

guideline may vary statewide and on a case by case basis. Although, there is no specific

guideline in Texas for DPR projects, Texas Commission on Environmental Quality (TCEQ)

requires at least 8- 5.5- 6 log reductions of viruses, *Cryptosporidium*, and *Giardia*, respectively,

after secondary treatment of wastewater (TWDB, 2015). Higher log removals may be required

based on site-specific data. For example, TCEQ requires 9- 5.5- 8 log reductions of virus,

Cryptosporidium, and *Giardia*, respectively, for the Wichita Falls DPR project (Tchobanoglous

et al., 2015). However, since the recommended guidelines by TCEQ utilizes secondary treated

wastewater as the starting point and does not give any credit to conventional wastewater

treatment as California and NWRI criteria do, it is likely to achieve the same quality of water as

California and NWRI at the end point. Expert panel recommended any of these approaches (i.e.,

NWRI expert panel approach, California IPR approach, or TCEQ DPR approach) could be

adopted by New Mexico Environment Department (NMED) for DPR projects on a case by case

basis (NWRI, 2016b). Australian guidelines for water recycling utilizes a health target of 10^{-6}

DALYs pppy (Disability adjusted life years per person per year) which requires 8.1- 9.5- 8 log

reductions of *Campylobacter*, viruses, and *Cryptosporidium,* respectively, for untreated

wastewater. Because of these extensive levels of treatment, potable reuse systems must rely on

robust and redundant barriers achieving high disinfectant doses, reliable physical removal (e.g.,

media or membrane filtration), and/or prolonged aquifer storage (Gerrity et al., 2014). In theory,

many of these barriers are capable of achieving these treatment benchmarks under optimal

conditions, but periodic operational upsets or even complete failures might have significant

adverse impacts on public health. Moreover, there is significant uncertainty in determining

10

appropriate operational targets for certain parameters, specifically dilution ratio and storage time in environmental buffers.

Depending on the process included in each treatment train, different log removals of pathogens may be achieved. Pathogen log reduction credits for different treatment processes are shown in Table 2.2.

Table 2-2. Pathogen log removal credits for different treatment processes

Treatment unit Process	Expected Log reduction Credits			
	Virus	*Giardia*	*Cryptosporidium*	Total coliform bacteria[b]
Conventional activated sludge (CAS)	1[b]	0[b]	0[b]	2
Microfiltration (MF)	0[a]	4[a]	4[a]	4
Ultrafiltration (UF)	1[a]	4[a]	4[a]	4
Reverse Osmosis (RO)	1.5[a]	1.5[a]	1.5[a]	2
Biological Activated Carbon (BAC)	0[a]	0[a]	0[a]	0
UV/AOP	6[a]	6[a]	6[a]	6
Ozone (min CT=1 mg*min/l)	5[a]	3[a]	0[a]	4
Free chlorine	6[a]	3[a]	0[a]	4

[a]Tchobanoglous et al. (2015)
[b] Trussell et al. (2016)

2.3 Reliability framework

Many potable reuse treatment trains are capable of satisfying public health requirements during periods of optimal performance. However, there is always the possibility of a failure in one or more treatment barriers that could affect the performance of downstream processes (i.e., a 'domino effect') and the overall log removals in a treatment train. With the widespread implementation of potable reuse, it is important to fully understand the "4Rs" framework in relation to public health (Fig. 2.2): reliability (providing a safe and reliable source of drinking water) through redundancy (multi-barrier approach based on additional treatment or monitoring), robustness (significant attenuation of a broad range of contaminants), and resiliency (automated response to failures during treatment) (Pecson et al., 2015). The fundamental goal of the 4Rs

11

approach is to reduce the frequency and severity of system failures and to properly respond to failures if they occur.
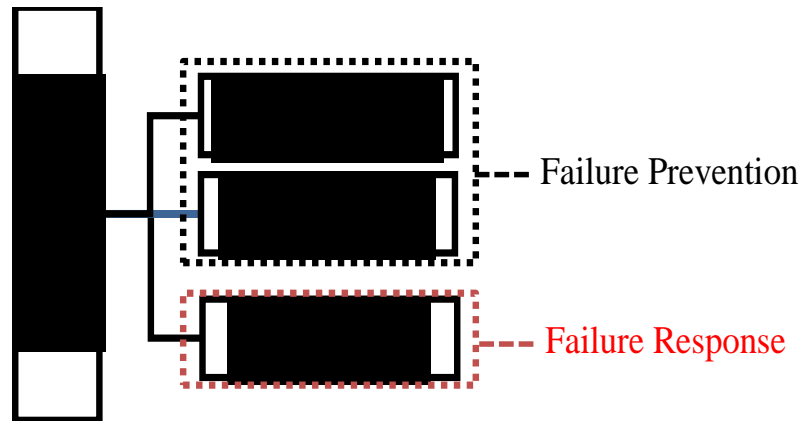
Figure 2-2. Representation of a reliability framework for potable reuse systems

Evaluating failure modes in a wastewater treatment plant and their associated consequences was first described in Mallory & Waller (1973). More recently, Forss & Ander (2011) conducted a comprehensive QMRA that studied the effects of treatment process failures in a DPR application. Beyond that study, there are few frameworks for incorporating treatment process failures into potable reuse QMRAs so the associated implications for water quality and public health are unclear.

Characterizing the significance of treatment process failure is critical for comparisons of IPR and DPR. According to NRC (2012), environmental buffers may not always be necessary to provide adequate public health protection. Instead, advanced treatment processes may allow for purified water to be delivered directly into a drinking water distribution system. On the other hand, a recent study indicated that blending advanced treated water with raw surface water upstream of a conventional drinking water treatment plant may still offer significant reductions

12

in public health risks (Soller et al., 2016). As a result, further investigations are required to fully understand the impact of environmental buffers in water quality.

2.4   Alternative ozone-biofiltration treatment trains

Due to sustainability concerns with RO (Gerrity et al., 2014), some communities are already employing or exploring the feasibility of ozone-biofiltration (Gerrity et al., 2013), as this treatment combination is equally capable of satisfying most public health criteria (Trussell et al., 2016). Ozone-biofiltration is unable to remove TDS without the use of RO or significant blending ratios, but some systems with low-TDS source waters may not require TDS reduction—even in DPR applications. Also, in the presence of precursors, there is a potential formation of disinfection by-products (DBPs) during ozonation (Gerrity et al., 2014). However, the public health risks associated with ozone-biofiltration need to be better characterized and communicated to overcome the perception (or reality) of RO as a superior treatment process. Using O3-BAC as an alternative for RO-based treatment trains (i.e., MF-RO-UV/H2O2) could save up to $51 million in capital cost and up to $4.3 million in O&M costs (Gerrity et al., 2014)

Several existing (or recently decommissioned) ozone-biofiltration trains are shown in Fig. 2.3 (Gerrity et al, 2013). The treatment train in Figure2.3A is employed in Gwinnett County, GA, USA (also includes lime softening). The treatment train in Figure 2.3B was employed in Gerringong, New South Wales, Australia, but has recently been decommissioned. The treatment train in Figure 2.3C is employed in El Paso, Texas, USA (also includes PAC in secondary treatment process and lime softening). Specifically, Figure 2.3A represents the advanced treatment train for planned IPR, and Figure 2.3B is similar to the advanced treatment train for DPR.

13
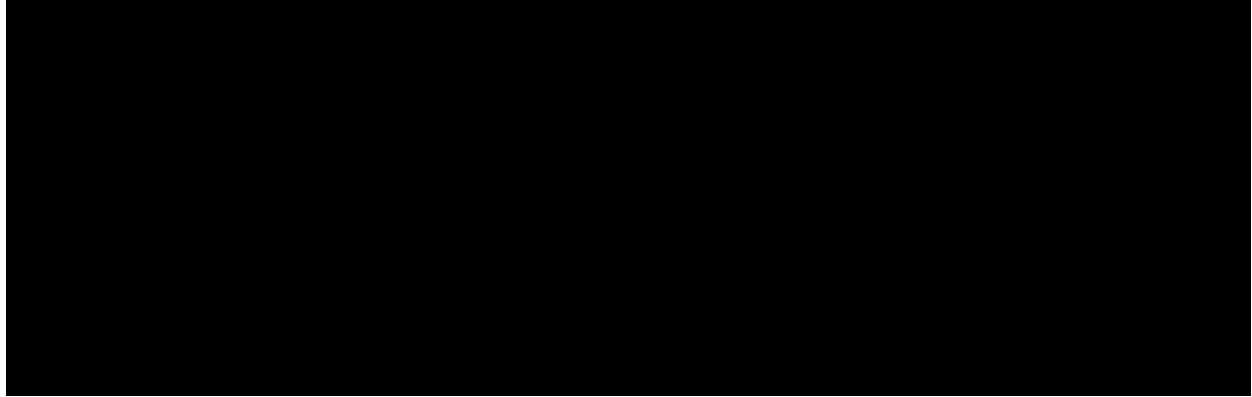
Figure 2-3. Examples ozone-based treatment trains for the production of high quality product water for potable reuse applications

There is insufficient evidence to determine whether potable reuse potentially poses greater risks than more conventional drinking water systems, or whether potable reuse is actually a safer and more reliable option. Additional studies are needed to address these questions, with the ultimate goal of informing future regulatory and operational decision-making processes. One tool that is often used to aid in these decision-making processes, particularly in the context of public health, is a quantitative microbial risk assessment (QMRA), which is an iterative modeling approach that relies on statistical probabilities to assess the risks posed by exposure to one or more pathogenic microorganisms.

2.5   Quantitative Microbial Risk Assessment (QMRA)

Health risk and probability of infection associated with exposure to a pathogen in drinking water can be determined by a quantitative microbial risk assessment (QMRA) (Haas et al., 2015). QMRA is a powerful tool, particularly in potable reuse applications, because it employs mathematical models to evaluate the performance and reliability of water reuse systems. The results of the QMRA can be used to characterize the overall public health risks, identify adverse outcomes, and ultimately aid in risk management, risk communication, and decision-making (Beaudequin et al., 2015). A general framework for QMRA consists of four fundamental steps

14

including: 1) *problem formulation and hazard identification* which collects general information about the microbial agent (pathogens) and the adverse health effects, 2) *exposure assessment* which estimate the probability of infection given a known dose of pathogens using mathematical dose-response relationships, 3) *dose-response assessment* which estimates the pathogen dose corresponding to the expected pathogen exposure, and 4) *risk characterization* which integrates information from the previous steps to estimate the risk of infection and characterize the significance of the risk within a specific context (Petterson et al., 2006).

Generally, there are two types of QMRAs: static and dynamic. The key difference between these two models is time dependency, which means the number of individuals susceptible to infection is time-invariant in a static model and time-variant in a dynamic model. Comparison between static and dynamic QMRA is shown in Table 2.3. Both static and dynamic QMRAs have been used to facilitate decision making in municipal, recreational, and agricultural applications (Soller et al., 2006; Olivieri et al., 2014a; Olivieri et al., 2014b). QMRAs have also been used to evaluate risks associated with *de facto* reuse along the Trinity River (Wu, 2015), hypothetical IPR scenarios (NRC, 2012), and even DPR (Forss & Ander, 2011; Soller et al., 2016).

Ames et al. (2014) conducted a static QMRA to evaluate the effect of wet weather overflows on the effluent from the wastewater treatment plant in Oakland, California and the quality of San Francisco Bay receiving water. The annual risk due to exposure to adenovirus and *Giardia* spp. was estimated which resulted in more than one order-of-magnitude below the EPA benchmark level for recreation events expect for the worse case outfall location.

15

Table 2-3. Comparison of static and dynamic QMRA

Static QMRA	Dynamic QMRA
The number of individuals susceptible to infection is time invariant	The number of individuals susceptible to infection is time variant
Direct exposure (environment-to-person)	Direct (environment-to-person) and indirect exposure (person-to-person/ person-to-environment-to-person)
Individual-based risk	Population-based risk
Potential for secondary transmission of infection or disease is typically not considered or assumed as a constant factor if it is.	Potential for secondary transmission of infection or disease is considered and the magnitude of transmission is a function of susceptible, infected and immune population.
Immunity to infection from microbial agents is typically not considered.	Exposed individuals may not be susceptible to infection or disease because they may already be infected or may be immune from infection due to prior exposure.
Dose-response function is the critical health component.	The dose-response function is important; however, factors specific to the transmission of infectious diseases may also be important.

Table adapted from Olivieri et al. (2014b)

The California Department of Public Health (CDPH) has performed a static QMRA to assess the public health risk associated with increasing the use of recycled water for irrigation purposes (Olivieri et al., 2014). The QMRA resulted in median annual risk in the range of 10^{-8}-10^{-4} for enteric viruses, *Cryptosporidium*, *Giardia,* and *E. coli* which was compliant with the benchmark risk.

Forss & Ander, 2011 conducted a comprehensive static QMRA in the New Goreangab water reclamation plant in Windhoek, Namibia. The study evaluated microbiological quality of water under different operational conditions including optimal, sub-optima, and outbreak condition. Ozonation and ultrafiltration (UF) processes were found to have significant impact on reduction of *Giardia* and *Cryptosporidium*, respectively. The study also proposed the use of UV light as an effective process for further removal of *Cryptosporidium* especially during outbreak

16

conditions. It has been suggested that incorporating more realistic failure times in QMRA framework would result in more accurate results.

More recently, Soller et al. (2017) and Soller et al. (2018) have performed QMRA to evaluate public health risk associated with DPR systems. They identified NoV as a pathogen of concern which may drive the risk in DPR systems given specific treatment processes. Also, results indicated that FAT systems require either high doses of UV disinfection or blending upstream of drinking water treatment facility to achieve the benchmark risk of infection due to exposure to NoV. Likewise, it was suggested that treatment trains which do not employ RO in advanced treatment processes, needs to either provide advanced oxidation process with high doses of UV or blending upstream of drinking water treatment facility to achieve the benchmark risk of infection due to exposure to *Cryptosporidium*.

Chaudhary et al. (2017) evaluated microbial risk associated with IPR and DPR systems using a QMRA approach. The study indicated that DPR systems generally pose lower risk of infection than *de facto* reuse system and that potable reuse systems which utilized surface water as a discharge/blending point for advanced treated wastewater resulted in similar risk than *de facto* reuse systems. This showed that concentration of pathogens in upstream surface water was the dominant factor in estimating risk of infection.

The dynamic disease transmission model was first designed and implemented by Eisenberg et al., 1996 which included different epidemiological states of the disease. Soller et al. (2003) performed the QMRA dynamic model in the City of Stockton, California to evaluate the beneficial effects on public health implementing an additional wastewater treatment during winter when discharge of secondary treated effluent into the San Joauin River can cause health risk associated to recreation events. The level of viral gastroenteritis was used to compare the effect of the

17

additional filtration process. Other dynamic QMRA studies are utilized in Newport Bay, Orange County, California (Soller et al., 2006) and in Mamala Bay, Hawaii (Cooper et al., 1996) to evaluate the public health risk associated to recreational exposure. Eisenberg et al. (1996) employed a dynamic disease transmission model to evaluate the risk of giardiasis by swimming in the recreational reservoirs which were augmented by reclaimed water. Several studies performed dynamic QMRA to evaluate cryptosporidiosis outbreak in Milwaukee (Eisenberg et al., 1998; Eisenberg et al., 2005; Brookhart et al., 2002; Soller and Eisenberg, 2008). Eisenberg et al. (2004) evaluated microbial health risks associated with exposure to biosolids-amended soil which demonstrated that secondary transmission of disease play an important role in disease incidence. The incidence of disease increases at higher rates of secondary transmission.

2.6   System Dynamics

System dynamics (SD) models are important tools to analyze the structure and behavior of the complex systems and to evaluate the effect of different policies on management of the problem (Pejic Bach & Ceric, 2007). System dynamics models need to be developed in several steps. First, the problem and its importance are identified. Spatial scale, temporal scale, and key variables and concepts must be defined (Stermen, 2000; Park, 2014). During the second step, initial hypothesis is generated, feedback processes is discovered, and cause and effect relationships between different system elements are represented using causal loop diagrams (Stermen, 2000; Park, 2014). In the third step, a computer simulation model is developed based on the relationships between the system's components, initial conditions, and estimation of parameters. In the fourth step, the model is tested to compare the temporal behavior of the system with the recorded behavior of the system. Other evaluation tests are also conducted such as extreme condition tests (to evaluate the robustness of the model), sensitivity analysis (to

18

evaluate the behavior of the model with uncertainty in parameters and initial conditions), integration error, etc. (Pejic Bach & Ceric, 2007; Stermen, 2000; Park, 2014). In the last step, the behavior of the system is analyzed under different scenarios and policy options that may arise in the future to compare the effect of different policies and to find out whether there is any interaction between them (Stermen, 2000; Park, 2014). System dynamics is a mathematical simulation methodology that describes the complex effects of the system elements and their inter-relationships using stocks, flows, convertors, and arrows. Different modeling software is being used for system dynamic methodology such as Vensim, STELLA, DYNAMO, Analytica, Powersim, etc (Park et al., 2014; Simonovic & Rajasekaram, 2004). The concept of SD is first propounded by Forrester (1958) to analyze the behavior of an industrial organization and to improve management control. More recently, SD has also been applied for environmental problems such as water resources management including reservoir operations and flood predictions and managements (Ahmad and Simonovic 2000; 2001; 2004; 2006), wastewater treatment and reuse (Park et al., 2014), various water applications (Tamaddun et al., 2018; Chen et al., 2017; Ahmad 2016; Mirchi et al., 2012), environmental management applications (Amoueyan et al., 2017; Venkatesan et al., 2011a,b; Rusuli et al., 2015), water resources problems in Lake Mead and the Las Vegas water supply system (Stave 2003; Nussbaum et al., 2015), effects of climate change on water resources (Dawadi et al., 2012, 2013; Zhang et al., 2016), water resources vulnerability and water allocations (Wu et al., 2013; Qaiser et al., 2011, 2013), carbon footprint of water projects (Shrestha et al., 2011, 2012), water and land availability and usage for solar systems (Bukhary et al., 2017), water conservation (Ahmad and Prashar 2010) and energy planning (Moumoni et al. 2014). Other examples in this field include: the *CanadaWater* model developed by Simonovic & Rajasekaram (2004) which deals with water

19

resource problems in Canada that takes into consideration the available water resources, wastewater treatment, economic and population growth, energy generation and food production; and application of the SD methodology using LINGO as a linear programming procedure for sustainable development of water resources in China focusing on water recycling by Xiang et al. (2013).

3 Quantifying Pathogen Risks Associated with Potable Reuse: A Risk Assessment Case Study for *Cryptosporidium*

ERFANEH AMOUEYAN[1], SAJJAD AHMAD[1], JOSEPH N.S. EISENBERG[2], BRIAN PECSON[3], DANIEL GERRITY[1]*

[1]Department of Civil and Environmental Engineering and Construction, University of Nevada, Las Vegas, Box 454015, 4505 S. Maryland Parkway, Las Vegas, NV 89154-4015, United States
[2]Department of Epidemiology, School of Public Health, University of Michigan, Ann Arbor, Michigan, United States
[3]Trussell Technologies, Inc., Pasadena, California, United States

*Corresponding author. Mailing address: Department of Civil and Environmental Engineering and Construction, University of Nevada, Las Vegas, Box 454015, 4505 S. Maryland Parkway, Las Vegas, NV 89154-4015, United States. Phone: (702) 895-3955. Fax: (702) 895-3936. Email: Daniel.Gerrity@unlv.edu.

3.1 Abstract

This study evaluated the reliability and equivalency of three different potable reuse paradigms: (1) surface water augmentation via *de facto* reuse with conventional wastewater treatment; (2) surface water augmentation via planned indirect potable reuse (IPR) with ultrafiltration, pre-ozone, biological activated carbon (BAC), and post-ozone; and (3) direct potable reuse (DPR) with ultrafiltration, ozone, BAC, and UV disinfection. A quantitative microbial risk assessment (QMRA) was performed to (1) quantify the risk of infection from *Cryptosporidium* oocysts; (2) compare the risks associated with different potable reuse systems under optimal and sub-optimal conditions; and (3) identify critical model/operational parameters based on sensitivity analyses. The annual risks of infection associated with the *de facto* and planned IPR systems were generally consistent with those of conventional drinking water systems [mean of $(9.4\pm0.3)\times10^{-5}$ to $(4.5\pm0.1)\times10^{-4}$], while DPR was clearly superior [mean of $(6.1\pm67)\times10^{-9}$ during sub-optimal operation]. Because the advanced treatment train in the planned IPR system was highly effective in reducing *Cryptosporidium* concentrations, the associated risks were generally dominated by the pathogen loading already present in the surface water. As a result, risks generally decreased with higher recycled water contributions (RWCs). Advanced treatment failures were generally inconsequential either due to the robustness of the advanced treatment train (i.e., DPR) or resiliency provided by the environmental buffer (i.e., planned IPR). Storage time in the environmental buffer was important for the *de facto* reuse system, and the model indicated a critical storage time of approximately 105 days. Storage times shorter than the critical value resulted in significant increases in risk. The conclusions from this study can be used to inform regulatory decision making and aid in the development of design or operational criteria for IPR and DPR systems.

Keywords: Quantitative microbial risk assessment (QMRA); *Cryptosporidium*; potable reuse; *de facto* reuse; ozone; ultraviolet (UV) disinfection; environmental buffer

3.2 Introduction

In recent years, indirect potable reuse (IPR) and direct potable reuse (DPR) have become more common due to population growth and increased water demand, especially in communities with limited or variable water resources. A historically common form of IPR is known as unplanned or *de facto* reuse (Rice et al., 2013; Rice et al., 2015), in which the source water for a drinking water treatment plant (DWTP) is impacted by treated wastewater effluent from an upstream community. These systems may not have permits specifically addressing augmentation of source water with treated wastewater (Cotruvo & Bell, 2014), and they may not satisfy recent potable reuse guidelines/regulations addressing the chemical and microbial risks posed by this practice. Planned IPR and DPR systems explicitly acknowledge these risks and, as a result, generally employ advanced water and/or wastewater treatment processes to ensure adequate protection of public health.

The primary distinction between IPR and DPR is that IPR incorporates an environmental buffer as a discharge and blending point (USEPA, 2012). The environmental buffer provides natural treatment barriers and is also used as a psychological barrier to improve public perception (Khan, 2013). DPR replaces the environmental buffer with additional treatment, monitoring, and/or the inclusion of an engineered storage buffer (Leverenz et al., 2011; Tchobanoglous et al., 2015). The engineered storage buffer is intended to provide response retention time to react to failures in the advanced treatment train, which are identified by monitoring critical control points (Tchobanoglous et al., 2011; NWRI, 2016a). Although advanced treatment may be adequate to deliver purified water directly into a drinking water distribution system, a recent study indicates that blending with raw water upstream of a conventional drinking water treatment plant may still offer significant reductions in public health risks (Soller et al., 2016).

24

Existing regulatory frameworks for IPR or DPR require specific treatment trains and/or compliance with stringent water quality metrics. For example, the California Division of Drinking Water (DDW) requires "full advanced treatment" (FAT) consisting of reverse osmosis (RO) and an advanced oxidation process (AOP) for planned IPR systems that directly inject recycled water into local aquifers (CDPH, 2014) or rely on surface water augmentation (NWRI, 2016b). Many other IPR projects throughout the world (e.g., Arizona, Singapore, and Australia) also employ RO and UV or UV/H_2O_2 to ensure adequate protection of public health (Gerrity et al., 2013). This treatment train has been shown to be effective in addressing known public health risks (Trussell et al., 2016) and is assumed to be sufficiently robust to mitigate unknown public health risks (CDPH, 2014), at least from a microbial standpoint. RO-based treatment trains can also achieve very low concentrations of total dissolved solids (TDS) and total organic carbon (TOC), which is important for achieving 0.5 mg/L of wastewater-derived TOC in California (CDPH, 2014). Due to sustainability concerns with RO (Gerrity et al., 2014), some communities are already employing or exploring the feasibility of ozone-biofiltration (Gerrity et al., 2013), as this treatment combination is equally capable of satisfying most public health criteria (Trussell et al., 2016). Ozone-biofiltration is unable to remove TDS without the use of RO or significant blending ratios, but some systems with low-TDS source waters may not require TDS reduction— even in DPR applications. However, the public health risks associated with ozone-biofiltration need to be better characterized and communicated to overcome the perception (or reality) of RO as a superior treatment process.

One of the primary drivers for the design of potable reuse treatment trains is mitigating risks associated with water-borne pathogens. Based on literature compiled in Trussell et al. (2013), a panel of public health experts recommended 12-10-9-log reduction of viruses,

25

Cryptosporidium, and total coliform bacteria, respectively, for potable reuse systems targeting annual risks of infection of 10^{-4} (NWRI, 2013). These recommendations are also consistent with the California DDW's 12-10-10-log reduction requirements for viruses, *Cryptosporidium*, and *Giardia*, respectively (CDPH, 2014). Many potable reuse treatment trains are capable of satisfying these pathogen requirements during periods of optimal performance. However, there is always the possibility of a failure in one or more treatment barriers that could affect the performance of downstream processes (i.e., a 'domino effect') and the overall log removals in a treatment train. With the widespread implementation of potable reuse, it is important to fully understand the "reliability" (Pecson et al., 2015) and "equivalency" (Trussell et al., 2016) of the various treatment paradigms and to identify critical operational conditions.

One way to achieve this goal is to perform a quantitative microbial risk assessment (QMRA), in which experimental data can be combined with mathematical models and statistical probabilities to estimate the risk of infection associated with a particular microbial hazard (Haas & Rose, 1995). The results of the QMRA can be used to characterize overall public health risks, identify adverse outcomes, and ultimately aid in risk management, risk communication, and decision making (Beaudequin et al., 2015; Petterson and Ashbolt, 2016). Both static (time-invariant) and dynamic (time-variant) QMRAs have been used to facilitate decision making in municipal, recreational, and agricultural applications (Soller et al., 2006; Olivieri et al., 2014a; Olivieri et al., 2014b). QMRAs have also been used to evaluate risks associated with *de facto* reuse along the Trinity River (Wu, 2015; Lim et al., 2016), hypothetical IPR scenarios (NRC, 2012), and even DPR (Forss & Ander, 2011; Soller et al., 2016).

The current study expands the QMRA knowledge base for potable reuse through the use of a system dynamics platform. System dynamics is a non-linear, mathematical simulation of

complex, interrelated system elements, which are represented as 'stocks', 'flows', 'convertors', and 'arrows' (Text S7; Forrester, 1958). This non-linear approach has been used to model water resources management and water quality scenarios (Stave, 2003; Venkatesan et al., 2011a; Dawadi & Ahmad, 2013; Rehan et al., 2013; Wu et al., 2013a); climate change impacts on water resources (Dawadi & Ahmad, 2012; Zhang et al., 2016; Simonovic & Rajasekaram, 2004); the water-energy nexus (Shrestha et al., 2011; 2012); and even recycled water applications (Venkatesan et al., 2011b; Qaiser et al., 2013; Xiang et al., 2013). Winz et al. (2009) and Mirchi et al. (2012) provide detailed reviews of system dynamics applications related to water resources.

System dynamics can also be used to model temporal variability in potable reuse applications, including changes in population structure, water quality, and treatment process performance. As such, the main objective of this study was to develop a system dynamics model to quantify the risk of cryptosporidiosis from ingestion of drinking water and to compare the risks associated with three different potable reuse systems: (1) surface water augmentation via *de facto* reuse with conventional wastewater treatment; (2) surface water augmentation via planned IPR with ultrafiltration, pre-ozone, BAC, and post-ozone; and (3) DPR with ultrafiltration, ozone, BAC, and UV disinfection. This model focused on quantifying and comparing baseline risks, determining critical values for some design/operational parameters (e.g., reservoir storage time), and evaluating sensitivity to water quality, operational conditions, and treatment failure. Three different scenarios encompassing a range of bin classifications were considered for the *de facto* reuse and planned IPR systems, and two different scenarios (or treatment objectives) were considered for the UV disinfection process in the DPR system: *Cryptosporidium* inactivation and NDMA attenuation. This model also serves as the foundation for future dynamic models

27

incorporating disease transmission and secondary exposure pathways, thereby closing the loop between finished drinking water and raw wastewater.

3.3 Methodology

3.3.1 Risk Calculations

Cryptosporidium was identified as the hazard for this QMRA. Exposure to *Cryptosporidium* was limited to primary pathways (i.e., ingestion via drinking water) and did not consider secondary exposure to infected individuals or fomites. The final concentration of *Cryptosporidium* was calculated based on initial concentrations in raw wastewater and log reduction estimates for engineered treatment processes and the environmental buffer (when applicable). An exponential dose response model (Eq. 3.1) was used to estimate the daily probability of infection due to ingestion of treated drinking water (Teunis et al., 1997; Zhang et al., 2012).

$$P_{inf,d} = 1 - e^{-rCw} \qquad \text{(Eq. 3.1)}$$

where, $P_{inf,d}$ = daily probability of infection

r = dose response (infectivity) parameter, oocysts^{-1}

C = oocyst concentration in ingested drinking water, oocysts/L

w = daily water consumption rate, L.

In this study, a daily water consumption rate of 2 L/day was assumed (USEPA, 2004; WHO, 2008), although the USEPA recently increased its default drinking water consumption rate to 2.4 L/day based on community ingestion at the 90th percentile (USEPA, 2015a).

A value of 0.00419 oocysts^{-1} (Barbeau et al., 2000; Zhang et al., 2012) was selected as the dose response parameter for the current study, but a range of values has been reported in the literature: 0.0022 oocysts^{-1} (Messner & Berger, 2016); 0.0572 oocysts^{-1} (Messner et al., 2001);

and 0.09 oocysts^{-1} (USEPA, 2006c). The current study addressed this uncertainty by assessing

the sensitivity of the model to this published range. It should also be noted that alternative

Cryptosporidium dose response models (e.g., fractional Poisson, beta-Poisson, exponential with

immunity) were recently proposed by Messner & Berger (2016), but these were not considered

in the current study.

The annual risk of infection was then calculated using Eq. 3.2 (Karavarsamis &

Hamilton, 2010).

$$P_{inf,a} = 1 - \prod_{i=1}^{365}(1 - P_{inf,d})_i \qquad \text{(Eq. 3.2)}$$

where, $P_{inf,a}$ = annual probability of infection.

Several different frameworks were used to compare the risks posed by the different

potable reuse systems. An annual risk of 10^{-4} has been used as a benchmark in previous studies

(Regli et al., 1991; Ryu et al., 2007; NWRI, 2013; Trussell et al., 2013; CDPH, 2014; Soller et

al., 2016), but it is not the formal basis for federal drinking water regulations for

Cryptosporidium in the United States (U.S.). Instead, the Long Term 2 Enhanced Surface Water

Treatment Rule (LT2) classifies source waters into different categories, or bins, based on their

average *Cryptosporidium* concentrations. Drinking water utilities must then achieve the

Cryptosporidium log reductions required by their bin classifications (USEPA, 2010a). This study

compared the annual risks of infection calculated by Eq. 2 against the risks associated with

compliance with LT2. A summary of baseline LT2 risk estimates is included in the

Supplementary Information (SI) in Figure S1.

The experimental treatment trains were also evaluated against the WHO guidelines for

drinking water quality, which are based on disease burden and disability adjusted life years

(DALYs). WHO recommends a target of 10^{-6} DALYs/person-year (WHO, 2008). The disease

burden for *Cryptosporidium* was calculated according to Eqs. 3.3 and 3.4 (Zhang et al., 2012; Health Canada, 2012).

$$R = P_{inf,a} \times S \times I \qquad \text{(Eq. 3.3)}$$

$$D = R \times \omega \qquad \text{(Eq. 3.4)}$$

where, R = risk of illness per year for an individual

$P_{inf,a}$ = probability of infection per year (see Eq. 3.2)

S = proportion of population susceptible to infection

I = proportion of population that develops symptomatic illness after infection

D = disease burden, DALYs/person-year

ω = health burden, DALYs/case

In addition to the LT2 and WHO frameworks, this study also considered the 10-log reduction target for *Cryptosporidium* (NWRI, 2013; CDPH, 2014) in determining appropriate operational conditions for the treatment trains described later. The constants used in the aforementioned equations are summarized in Table 3.1.

3.3.2 System Dynamics Model

A general description of system dynamics is provided in the SI in Text S7. Probabilities of infection were based on daily simulations of a STELLA 10.1 (ISEE Systems, Lebanon, NH) system dynamics model over a duration of 365 days. Statistical analyses were based on the results of 10,000 model iterations (Barreto & Howland, 2005; Martorell et al., 2008). For the *de facto* reuse and planned IPR systems, typical *Cryptosporidium* concentrations were assumed to be present in the upstream surface water feeding the community (described later), and these systems were also augmented with treated wastewater discharges from within the community. This is slightly different from the original definition of *de facto* reuse (i.e., upstream community

30

impacting a downstream community), but it allows for simplification of the model while still

maintaining the principal element of *de facto* reuse (i.e., limited treatment prior to environmental

discharge).

Table 3-1. Summary of the parameters and values used in the system dynamics model

Parameter		Description	Value	Units	Reference
Risk calculations	I	Proportion of symptomatic illness	0.7	unitless	Zhang et al. (2012)
	S	Susceptible proportion of population	100%	unitless	Zhang et al. (2012)
	ω	Health burden of *Cryptosporidium*	0.0017	DALYs/case	Health Canada (2012)
	r	Infectivity parameter	0.00419	oocysts^{-1}	Barbeau et al. (2000); (Ryu, Alum, Mena, & Abbaszadegan, 2007)
	w	Daily water consumption rate	2	L/per-day	WHO (2008)
Wastewater	C_c	Influent oocyst concentration	Lognormal (78, 112)[3]	oocysts/L	Rose et al. (2005)
Pre-ozone[1]	O_3/TOC	O_3/TOC ratio	1.1	mgO$_3$/mgC	Gerrity et al. (2014)
	TOC$_{WW}$	TOC concentration in 2° effluent	7.2	mgC/L	Gamage et al. (2013)
	TOC$_{UF}$	TOC concentration in UF filtrate	6.3	mgC/L	Trussell et al. (2016)
	O_3	Applied ozone dose	6.9	mg/L	Calculated
	IOD	Instantaneous ozone demand	4.0	mg/L	Text S3
	k_{O_3}	First order ozone decay rate constant	0.54	min^{-1}	Text S3
	t_{O_3}	Ozone contact time	5	min	Text S3
	T	Temperature	25	°C	Assumed
	CT	Ozone CT	5.0	mg-min/L	Text S3
Post-ozone[1]	O_3 CT	Ozone CT	10	mg-min/L	Text S3
	O_3	Applied ozone dose	5.1	mg/L	Calculated (based on target O_3 CT)
	t_{O_3}	Ozone contact time	30	min	Assumed (complete ozone decay)
	T	Temperature	25	°C	Assumed
Environmental buffer	$k_{4°C}$	Oocyst decay rate constant at 4°C	0.0093	day^{-1}	Peng et al. (2008)
	λ	Dimensionless temperature modifier	0.095	unitless	Peng et al. (2008)
	T_{sw}	Temperature of surface water			
		Baseline condition	20	°C	Assumed [based on Peng et al. (2008)]
		Critical condition	10	°C	Assumed (based on sensitivity analysis)
	RWC	Recycled water contribution	20%	unitless	Assumed [based on Rice et al. (2013)]
	t_{sw}	Storage time			
		Baseline condition	270	days	(Wu, 2015)
		Critical condition	105	days	Assumed (based on sensitivity analysis)
UV[2]	I_0	UV incident (maximum) intensity	25	mW/cm^2	Assumed (based on commercial system)
	I_{AVG}	UV average intensity	11.4	mJ/cm^2	Calculated (Eq. 13)
	x	UV path length	10	cm	Assumed [based on Lee et al. (2016)]
	k_A	UV absorbance of ozonated UF effluent	0.080	cm^{-1}	Text S5
	D	UV dose	80	mJ/cm^2	NWRI (2012)
	t_{UV}	UV exposure time	7.0	seconds	Calculated (Eq. 14)
	k_{UV}	Oocyst inactivation rate constant	0.243	(mJ/cm^2)$^{-1}$	Hijnen et al. (2006)

[1]Additional details in Text S2-S4; [2]Additional details in Text S5-S6; [3](Mean, Standard Deviation) with μ = 3.80 and σ = 1.06

The additional *Cryptosporidium* from the treated wastewater was determined from typical

raw wastewater concentrations (see Table 3.1) combined with output (i.e., treatment

performance, failure mode, etc.) from the model simulation. In the *de facto* reuse and planned

IPR systems, the degree of treatment incorporated into each scenario differed based on LT2 bin

31

classification requirements (described later). For the DPR system, there was no upstream surface water so all drinking water was provided by the advanced treated recycled water from within the community. The various water systems are depicted in Figure 3.1, and the unit processes used in each treatment train are depicted in Fig 3.2.
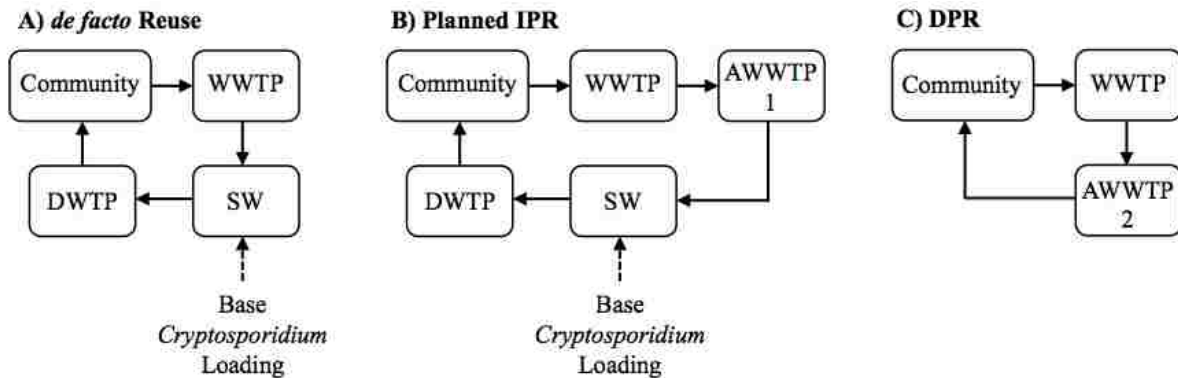
Figure 3-1. Potable reuse systems considered in this study (A) *de facto* reuse with upstream base loading of *Cryptosporidium*, (B) planned IPR with upstream base loading of *Cryptosporidium*, and (C) 'closed-loop' DPR. The wastewater-derived loadings of *Cryptosporidium* in (A) and (B) were modeled based on recycled water contributions, and the upstream base loadings of *Cryptosporidium* were modeled with three hypothetical scenarios (see Table 3.2). The AWWTPs differ based on the order of the unit processes and the final disinfection step: ozone for IPR and UV for DPR (see Figure 3.2). *WWTP = conventional wastewater treatment plant, SW = surface water, DWTP = conventional drinking water treatment plant, AWWTP = advanced wastewater treatment plant
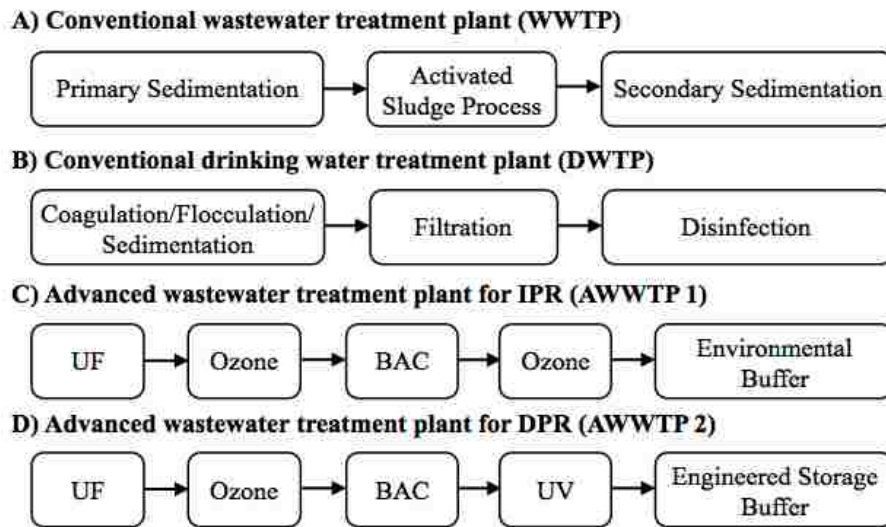
Figure 3-2. The treatment processes included in each sector of the system dynamics model (A) conventional wastewater treatment plant, (B) conventional drinking water treatment plant, (C) advanced wastewater treatment plant for the planned IPR system, and (D) advanced wastewater treatment plant for the DPR system. The operational conditions and expected performance of each unit process is summarized in Table 3.1.

32

The STELLA model included five different interconnected 'sectors' representing the major model components: (1) a conventional and advanced (if applicable) wastewater treatment plant; (2) a conventional drinking water treatment plant (for the IPR systems only); (3) the probability of infection calculated from the final *Cryptosporidium* concentration in the finished drinking water; (4) the bin classification, which was used to define the log removal credit for the conventional drinking water treatment plant in accordance with the LT2; and (5) the risk of infection and disease burden. Concentrations of *Cryptosporidium* in raw sewage and upstream surface water were modeled as probability distributions, the advanced treatment processes (e.g., pre-ozonation, post-ozonation, and UV disinfection) were modeled with dynamic algorithms (described later), and the remaining parameters and treatment processes were modeled using equations and output from the model or as point estimates when relevant data were not available in the literature. The system dynamics model was validated based on suggestions in Sterman (2000). These tests included structure assessment, dimensional consistency, parameter assessment, integration error (numerical integration method), behavior reproduction, and sensitivity analyses.

3.3.2.1 Conventional Wastewater Treatment Plant

Each of the potable reuse systems was modeled with a sector representing a conventional wastewater treatment plant (WWTP), which was assumed to include primary sedimentation, an activated sludge process, and secondary sedimentation (Figure 3.2A). Disinfection was omitted to make the model applicable to facilities that do not employ final disinfection or facilities that employ disinfection achieving minimal inactivation of *Cryptosporidium* oocysts (e.g., chlorination or chloramination). The concentration of *Cryptosporidium* in the raw wastewater was estimated as a lognormal distribution with a mean of 78 oocysts/L and a standard deviation

33

of 112 oocysts/L ($\mu = 3.80$ and $\sigma = 1.06$) (Rose et al., 2005). To account for reports of higher *Cryptosporidium* concentrations [e.g., mean of 242 oocysts/L in Robertson et al. (2006)], the current study included a sensitivity analysis on this parameter (described later).

Some recent studies recommend no *Cryptosporidium* credit for conventional WWTPs due to the lack of published data describing possible correlations between removal/inactivation of *Cryptosporidium* and secondary effluent water quality (Tchobanoglous et al., 2015). However, in this study, a constant 1-log removal credit was used as a conservative point estimate for WWTP removal (Rose et al., 2005).

3.3.2.2 *Planned Indirect Potable Reuse – Advanced Wastewater Treatment Plant #1*

In addition to the conventional WWTP sector, the planned IPR system included a sector representing an advanced WWTP employing ultrafiltration (UF), pre-ozonation, BAC, and post-ozonation (Figure 3.2C). This treatment train may be considered unsuitable for DPR because it may not consistently achieve the recommended 10-log reduction for *Cryptosporidium* unless high ozone CT values are achieved in both ozone steps—likely resulting in elevated bromate concentrations.

UF is considered a reliable barrier against nearly all pathogens, particularly larger microbes such as *Cryptosporidium* (Jacangelo et al., 1995), and current regulatory frameworks award 4-log removal for microfiltration (MF) or UF (Tchobanoglous et al., 2015). Ozonation has been shown to be highly effective in converting complex bulk organic matter into simpler, more biodegradable compounds, which improves overall TOC removal during subsequent biofiltration processes (Snyder et al., 2014). Ozone is also effective in destroying a wide range of trace organic compounds (TOrCs) (Lee et al., 2013). Therefore, pre-ozonation is often employed for these treatment objectives, and disinfection is an ancillary benefit. Although BAC has not been

34

shown to play an important role in pathogen attenuation, it has significant impacts on TOC

reduction (Reungoat et al., 2010; Trussell et al., 2016), attenuation of *N*-nitrosodimethylamine

(NDMA) (Gerrity et al., 2015; Trussell et al., 2016), and TOrC removal (Reungoat et al., 2010;

Gerrity et al., 2011). In contrast with the pre-ozonation step, post-ozonation for final disinfection

is typically controlled and monitored based on disinfection objectives.

For pre-ozonation, ozone dosing was based on O_3/TOC ratio because this parameter

achieves similar relative treatment efficacy in diverse wastewater qualities (Lee et al., 2013). To

extend this concept to disinfection efficacy, particularly for *Cryptosporidium*, it was necessary to

develop estimates for instantaneous ozone demand (IOD) and the ozone decay rate constant as a

function of O_3/TOC ratio. These parameters were then coupled with contact time and wastewater

temperature to estimate ozone CT and log inactivation. The IOD and the ozone decay rate

constant were determined according to Eqs. 3.5 and 3.6, respectively. These equations were

developed based on previous bench-scale ozone experiments in five different secondary effluents

(Gamage et al., 2013; Snyder et al., 2014). Additional details are provided in the SI in Text S2

and Text S3.

$$IOD = TOC \times 0.6025 \times \left(\frac{O_3}{TOC}\right)^{0.6679} \qquad R^2 = 0.93 \quad \text{(Eq. 3.5)}$$

where, IOD = instantaneous ozone demand, mg/L

$$\frac{O_3}{TOC} \leq 0.25 \qquad k_{O_3} = not\ defined \qquad \text{(Eq. 3.6a)}$$

$$\frac{O_3}{TOC} > 0.25 \qquad k_{O_3} = TOC \times 0.1001 \times \left(\frac{O_3}{TOC}\right)^{-1.605} \quad R^2 = 0.71 \ \text{(Eq. 3.6b)}$$

where, k_{O_3} = first order ozone decay rate constant, min^{-1}.

The ozone residual was modeled according to Eq. 3.7 using the wastewater-specific

operational and kinetic parameters from Eqs. 3.5 and 3.6.

$$O_3 \text{ residual } = \left[\left(\frac{O_3}{TOC}\right) \times TOC - IOD\right] \times e^{-k_{o_3}t} \tag{Eq. 3.7}$$

where, t = contact time, min.

The ozone CT was then calculated using Eq. 3.8 (based on integration of Eq. 3.7).

$$O_3 \text{ } CT = \frac{\left[\left(\frac{O_3}{TOC}\right) \times TOC - IOD\right]}{k_{O_3}} \times \left(1 - e^{-k_{o_3}t}\right) \tag{Eq. 3.8}$$

where, $O_3 \text{ } CT$ = product of ozone residual and contact time, mg-min/L.

Finally, *Cryptosporidium* log removal was calculated using the ozone dose response relationship described in Eq. 3.9 (USEPA, 2010a). This assumes that drinking water models for ozone disinfection are also applicable to wastewater treatment applications.

$$\textit{Cryptosporidium} \text{ Log Credit} = 0.0397 \times 1.09757^{T} \times O_3 \text{ } CT \tag{Eq. 3.9}$$

where, T = water temperature, ℃ (between 0.5℃ and 25℃) (USEPA, 2010a).

In contrast with the pre-ozonation step, the primary objective of post-ozonation is disinfection. As such, a potable reuse facility will likely operate the post-ozone step to achieve a specific ozone CT value. Instead of using the O₃/TOC approach described above, an ozone CT value of 10 mg-min/L (Text S3) and temperature of 25°C were assumed, and Eq. 3.9 was used to calculate the corresponding *Cryptosporidium* log credit for post-ozonation. Other ozone dosing parameters were then calculated using the equations described previously. Additional details related to ozone efficacy during normal and failure modes are provided in the SI in Text S3 and Text S4, and a schematic diagram of the advanced wastewater treatment plant is shown in Figure S9 in Text S7. Model parameters used for the baseline condition (e.g., TOC, O₃/TOC, contact time) are summarized in Table 3.1.

3.3.2.3 *Conventional Drinking Water Treatment Train*

The conventional drinking water treatment plant was included for the *de facto* reuse and planned IPR systems. In these systems, *Cryptosporidium* oocysts at the drinking water intake

36

originated in (1) the upstream surface water and (2) the local wastewater discharge. The final

concentration of *Cryptosporidium* oocysts at the drinking water intake accounted for both

dilution of the treated wastewater in the surface water and *Cryptosporidium* die-off during

storage. The *Cryptosporidium* concentration in the upstream surface water—typically linked to

upstream wastewater discharges, livestock operations, etc.—was assumed to be one of three

uniform distributions based on published data for 66 surface water treatment plants in the U.S.

(Table 3.2; LeChevallier et al., 1991). These were assumed to represent the concentrations

detected at the drinking water intake when no local wastewater was discharged into the source

water.

Table 3-2. Surface water *Cryptosporidium* concentrations and associated bin classifications.

Scenario	*Cryptosporidium* concentrations assumed for this study (oocysts/L)[1]	Bin classification (*Cryptosporidium* concentration in oocysts/L)[2]	Baseline treatment credit[3]	Additional treatment requirement[3]
1	Uniform Distribution [0.002,0.075]	Bin 1 (<0.075)	3 logs	0 log
2	Uniform Distribution [0.075,1]	Bin 2 (≥0.075 and <1)	3 logs	1 log
3	Uniform Distribution [3,112.75]	Bin 4 (≥3)	3 logs	2.5 logs

[1]LeChevallier et al. (1991) and [min, max]; [2]USEPA (2010a); [3]Assumes conventional filtration

For the local-wastewater-derived *Cryptosporidium* loadings, the *de facto* reuse and

planned IPR models allowed for varying percent contributions of treated wastewater into the

local surface water (i.e., the recycled water contribution or RWC). The extent of wastewater

influence in U.S. surface waters has been shown to vary considerably over time (Rice et al.,

2013). In 1980, the U.S EPA determined that the 25 most impacted municipal water utilities

received wastewater contributions ranging from 2% to 16% of their overall supply (USEPA,

1980). More recently, Rice et al. (2013) reported increases in *de facto* reuse for 17 of those 25

cities, with an average RWC of 68% and a maximum of 100% during extended periods of dry

weather. Moreover, California is likely to require a dilution ratio of at least 1:10 or 1:100,

depending on log credits awarded to the engineered treatment trains, for surface water

37

augmentation (NWRI, 2016b). To account for these ranges, a slider bar was added to the STELLA model to allow for user-specified RWC values from 0% to 100%. The baseline condition (i.e., RWC of 20%) was selected based on Rice et al. (2015), in which six of nine drinking water systems had RWCs of at least 20% under low flow conditions.

To evaluate the impact of retention time in the environmental buffer on pathogen die-off, a slider bar was added to the model to allow for changes in mean storage time from 0-365 days. For the current study, the baseline condition was assumed to be a mean storage time of 270 days to coincide with a case study of the Trinity River in Texas (Wu, 2015), although a 'critical' condition of 105 days was also evaluated (described later). According to California DDW's recommended design criteria for surface water augmentation, retention times should not be less than 2-4 months in order to allow for sufficient response time for operational upsets (NWRI, 2016b). Currently, there is a paucity of published literature documenting actual hydraulic retention times of wastewater-impacted drinking water reservoirs. Once additional tracer study and/or hydrodynamic modeling data are available, the mean retention time approach could be replaced with a more representative retention time distribution.

Die-off in the reservoir was quantified using a *Cryptosporidium* decay rate constant calculated with Eq. 3.10. The temperature correction is valid from 4ºC to 37ºC, which is the typical temperature range for most aquatic environments (Peng et al., 2008). Because *Cryptosporidium* is a large protozoan parasite, settling may lead to significant reductions in oocyst concentrations during long storage periods. However, settling was not specifically addressed in this study because of the site-specific nature of this removal mechanism, including velocity profiles, intake elevations, etc.

$$k_T = k_{4°C}e^{\lambda(T_{sw}-4)} \qquad \text{(Eq. 3.10)}$$

38

where, k_T = first order die-off rate constant for *Cryptosporidium* at temperature T_{sw}, day^{-1}

$k_{4°C}$ = first order die-off rate constant for *Cryptosporidium* at 4ºC, day^{-1}

λ = dimensionless modifier of temperature

T_{sw} = Temperature of the surface water, ºC.

The temperature-specific rate constant was then used in conjunction with Eq. 3.11 to determine the concentration of infectious, local-wastewater-derived *Cryptosporidium* remaining at the end of the storage period (Brookes et al., 2004).

$$C_{decay} = C_{eff} \times e^{-k_T t_{sw}} \qquad \text{(Eq. 3.11)}$$

where, C_{decay} = concentration of local-wastewater-derived *Cryptosporidium* after die-off, oocysts/L

C_{eff} = concentration of *Cryptosporidium* in treated wastewater, oocysts/L

t_{sw} = storage time in the surface water, days.

The upstream loading of *Cryptosporidium* was not affected by storage time in the model because it was assumed that the storage time was already reflected in the concentration previously detected at the intake prior to the discharge of locally treated wastewater. Therefore, the final concentration of *Cryptosporidium* detected at the intake was determined based on a mass balance approach assuming complete mixing (Wu, 2015; Eq. 3.12).

$$C_{intake} = C_{decay} \times RWC + C_{SW} \times (1 - RWC) \qquad \text{(Eq. 3.12)}$$

where, C_{intake} = concentration of *Cryptosporidium* at drinking water intake, oocysts/L

C_{SW} = concentration of *Cryptosporidium* from upstream surface water, oocysts/L

RWC = recycled water contribution.

The log removal of *Cryptosporidium* oocysts during conventional drinking water treatment was then determined in accordance with LT2 (Table 3.2), which resulted in the final

39

concentration in the finished drinking water consumed by the public. The conventional filtration process was credited with 3.0-log removal (USEPA, 2010a), and any additional log credits required by the LT2 bin classification were assumed to be achieved by a disinfection process. The corresponding bin classifications and treatment requirements, as described by the LT2, are summarized in Table 3.2. A schematic diagram of the conventional drinking water treatment plant is shown in Figure S10 in Text S7.

3.3.2.4   Direct Potable Reuse – Advanced Wastewater Treatment Plant #2

The DPR system (i.e., no surface water inputs) included UF, O_3, BAC, and UV (Figure 3.2D). This treatment train has been identified in the literature as a viable option for DPR (Trussell et al., 2016). UV is included for final disinfection in the DPR system because it is considered more robust when targeting *Cryptosporidium* inactivation. High dose UV is also effective as a final polishing step for NDMA photolysis and can be used for the attenuation of other trace organic contaminants (Lee et al., 2016). Chlorination would presumably be used for residual disinfection and to prevent pathogen regrowth in distribution systems, but residual chlorination was assumed to have no impact on *Cryptosporidium* concentrations. Therefore, no log removal credits were attributed to the engineered storage buffer.

The UF and BAC systems were modeled in a similar fashion to the planned IPR system, and the ozone process was modeled consistent with the aforementioned pre-ozonation step. Therefore, only UV was unique to the DPR treatment train. Major operational parameters for UV disinfection include incident UV intensity, path length, and absorptivity of the water matrix, which collectively affect the average UV intensity in the reactor. The values assumed for this study are summarized in Table 3.1. For the absorptivity of the water matrix, typical values were assumed for a nitrified effluent (i.e., after conventional wastewater treatment) and a filtered

40

nitrified effluent (i.e., after UF). The reduction in UV absorbance achieved by pre-ozonation (Gerrity et al., 2012) was also considered in the model and is described in greater detail in Text S5. The treatment objective for the UV disinfection process was set to either *Cryptosporidium* inactivation (baseline condition) or NDMA photolysis (NDMA scenario) (described later).

Average UV intensity in the reactor was determined by Eq. 3.13 (Chen et al., 2006), the UV dose was calculated by Eq. 3.14, and the corresponding log inactivation was calculated with Eq. 3.15, assuming first order kinetics (Hijnen et al., 2006). Relevant assumptions and constants are summarized in Table 3.1.

$$I_{avg} = I_0 \times \frac{\left(1-e^{-k'_A x}\right)}{k'_A x} = I_0 \times \frac{\left(1-10^{-k_A x}\right)}{2.303 \times k_A x} \qquad \text{(Eq. 3.13)}$$

where, I_{avg} = average UV_{254} intensity in the system, mW/cm^2

I_0 = incident (maximum) UV_{254} intensity, mW/cm^2

k'_A = base e absorptivity of the water matrix at 254 nm, cm^{-1}

k_A = base 10 absorptivity of the water matrix at 254 nm, cm^{-1}

x = reactor path length, cm.

$$D = I_{avg} \times t_{UV} \qquad \text{(Eq. 3.14)}$$

$$Cryptosporidium \text{ Log Credit} = -log\left(\frac{N}{N_0}\right) = k_{UV} \times D \qquad \text{(Eq. 3.15)}$$

where, D = UV_{254} dose, mJ/cm^2

t_{UV} = exposure time, s

k_{UV} = UV_{254} inactivation rate constant, (mJ/cm^2)$^{-1}$.

With respect to public health, additional water quality parameters, specifically disinfection byproducts, must be considered in a DPR system and might impact the operational conditions in the treatment facility. For this particular DPR treatment train, problematic

41

disinfection byproducts might include bromate formed during pre-ozonation, NDMA formed in the presence of chloramine (e.g., to control UF biofouling) or ozone, and trihalomethanes and haloacetic acids formed after exposure to chlorine in the engineered storage buffer and distribution system. Because of the pathogen focus of this study, these were not considered in the model (with the exception of NDMA).

Either *Cryptosporidium* or NDMA can be targeted by the UV process in the model by changing a control switch. With the *Cryptosporidium* treatment objective (baseline condition), the model assumed a target UV dose of 80 mJ/cm^2 (NWRI, 2012). With respect to NDMA, recent studies suggest that NDMA formation during ozonation may be problematic in some wastewater matrices (Gerrity et al., 2015). A downstream BAC process may achieve significant attenuation (Gerrity et al., 2015; Trussell et al., 2016), but high-dose UV photolysis (i.e., >100 mJ/cm^2) might still be warranted (Lee et al., 2016; Gerrity et al., 2016). For the NDMA scenario, the model assumed an NDMA concentration of 50 ng/L and a target reduction of 90% to achieve the California notification level of <10 ng/L (CDPH, 2014) with a 5-ng/L buffer, thereby requiring a UV dose of 512 mJ/cm^2 (Lee et al., 2016). For these target UV doses (i.e., 80 mJ/cm^2 or 512 mJ/cm^2), corresponding exposure times (7 sec and 45 sec, respectively) were calculated using Eqs. 13-14 and the UV-specific parameters listed in Table 3.1. Finally, the log credit for UV was limited to 6 logs regardless of the treatment objective and theoretical log reductions (Table S8), as required by CDPH (2014). Additional details related to UV disinfection efficacy during normal and failure modes are provided in Text S6. A schematic diagram of the DPR treatment train is shown in Figure S11 in Text S7.

3.3.2.5 *Advanced Treatment Failure Framework*

Assuming the various treatment processes are operating as intended, one can estimate the log removal/inactivation credits expected for each potable reuse system, as summarized in Table 3.3. The planned IPR and DPR treatment trains can theoretically achieve the 10-log reduction requirement without the environmental buffer, while the *de facto* reuse system is highly sensitive to the efficacy of the environmental buffer. However, failures during advanced treatment may have a significant detrimental impact on the total log removal in Table 3.3. To address this issue, the potential impacts of process failures were incorporated into the model to evaluate whether the treatment trains were sufficiently robust to adequately protect public health during sub-optimal operation.

Table 3-3. Assumed or calculated *Cryptosporidium* log removal credits for the baseline condition under optimal operational conditions (i.e., no failures).

Process	*de facto* Reuse		Planned IPR		DPR	
1	WWTP	1.0^2	WWTP	1.0^2	WWTP	1.0^2
2	EB	TBD^3	UF	4.0^4	UF	4.0^4
3	DWTP	$3.0\text{-}5.5^1$	O_3	2.0^5	O_3	2.0^5
4			BAC	0^6	BAC	0^6
5			O_3	4.1^7	UV	6.0^8
6			EB	TBD^3	ESB	0^9
7			DWTP	$3.0\text{-}5.5^1$		
Baseline Total[10]	**4.0 – 6.5**		**14.1 – 16.6**		**13.0**	

[1]Based on LT2 and corresponding bin classification for a drinking water treatment plant with conventional filtration (Table 3.2); [2]Rose et al, 2004; [3]Credit for environmental buffer determined by die off calculation (Eq. 11) and dilution (Eq. 12); [4]4-log credit awarded assuming satisfactory pressure decay test (Tchobanoglous et al., 2015); [5]Determined based on Eq. 9; [6]No credit granted to BAC (Tchobanoglous et al., 2015); [7]Determined based on Eq. 9; [8]Assumes UV dose of 80 mJ/cm^2 (NWRI, 2012) but limited to a maximum credit of 6 logs (CDPH, 2014); [9]No credit awarded for engineered storage buffer assuming chlorine as residual disinfectant; [10]Excludes environmental buffer

Table 3.4 summarizes the expected log credits during ideal operation and the modified log removal credits during failure mode for the critical unit processes in this study. The probabilities of failure for the UF and pre-ozone processes were based on a fault tree analysis and historical data from the DPR system in Namibia (Forss & Ander, 2011). The probability of failure for the post-ozonation process was based on a statistical distribution of historical ozone

43

CT values in Burns (2015) (Text S4). Due to a lack of failure data in the literature, an arbitrary

failure probability of 0.01 was assumed for UV (Text S6), and BAC failures were not

considered. Also, the model assumed a worst-case scenario (i.e., 0-log credit) for individual

process failures.

Table 3-4. *Cryptosporidium* reduction efficacy and probabilities of failure in different treatment processes.

Treatment Process	Log Removal during Ideal Operation	Probability of Failure	Log Removal Credit during Specified Failure(s)[6]				
			UF failure	Pre-O_3 failure	UF+Pre-O_3 failure	Post-O_3 failure	UV Failure
UF	4.0[1]	0.0028[2]	0	4.0	0	4.0	4.0
Pre-O_3	2.0	0.0021[2]	1.4	0	0	2.0	2.0
Post-O_3	4.1	0.000325[3]	2.7	1.0	0.6	0	N/A
UV	6.0[4]	0.01[5]	6.0[4]	6.0[4]	6.0[4]	N/A	0

[1]Tchobanoglous et al. (2015); [2]Forss & Ander (2011); [3]Burns (2015) and Text S4; [4]Assumed maximum credit (CDPH, 2014); [5]Arbitrary value due to lack of data but a sensitivity analysis was performed to evaluate the significance of this value (Text S6); [6]Text S4 and S6

Table 3.4 also summarizes the effects of compound failures, as described in Text S4-S6.

For example, UF failures not only eliminated the 4-log removal credit for UF, but they also

decreased the efficacy of the pre- and post-ozone processes in the planned IPR system and the

pre-ozone and UV processes in the DPR system. Specifically, UF failures caused increases in

TOC concentration in the UF filtrate. Assuming constant applied ozone doses, this led to

decreased O_3/TOC ratios for pre-ozonation (IPR and DPR) and post-ozonation (IPR only).

Moreover, this led to lower ozone CT values (IPR and DPR) and lower UV doses due to the

increase in UV_{254} absorbance of the water matrix (DPR). The model also considered the

possibility of simultaneous failures of UF and pre-ozonation, for example, which led to a

decrease in log inactivation from 4.1 (no failure scenario) to 0.6 (UF and pre-ozone failure) for

the post-ozonation process. Even with simultaneous failures of the upstream UF and ozone

44

processes, the UV process in the DPR system was still able to achieve greater than 6-log inactivation based on the calculated UV doses during failure modes (30 mJ/cm^2 and 194 mJ/cm^2), although NDMA attenuation decreased significantly (Tables S7-S8). Higher turbidities (e.g., due to UF failure) can also affect UV performance by scattering UV light and shielding target pathogens, but turbidity spikes were not considered in the model.

3.3.3 Sensitivity Analyses

To evaluate the significance of the various treatment processes, operational conditions, and parameter uncertainty, sensitivity analyses were performed on a subset of model inputs: (i) wastewater loading of *Cryptosporidium*, (ii) treatment process failures, (iii) reservoir storage time, (iv) recycled water contribution, (v) the temperature of the surface water, and (vi) the dose response parameter. Factor sensitivity (FS) values were calculated according to Eq. 3.16 to provide direct quantitative comparisons for the sensitivity analyses (Zwietering and Van Gerwen, 2000). FS values indicate the $\log_{10}$ ratio of the revised model output versus the baseline condition: large negative values (e.g., less than -0.3) indicate notable decreases in risk, large positive values (e.g., greater than 0.3) indicate notable increases in risk, and small values indicate minimal changes in risk.

$$FS = log_{10}\left(\frac{P_x}{P_{BL}}\right) \qquad \text{(Eq. 3.16)}$$

where, P_x = risk of infection for the modified condition

P_{BL} = risk of infection for the baseline condition.

45

3.4 Results and Discussion

3.4.1 Quantification of *Cryptosporidium* Oocysts for the Baseline Condition

Six different water qualities were characterized for the baseline condition: (1) raw sewage; (2) conventionally treated wastewater; (3) finished drinking water in the *de facto* reuse system; 4) finished drinking water in the IPR system; 5) advanced treated wastewater in the IPR system (i.e., before blending); and 6) finished drinking water in DPR system. Figure 3.3 compares the concentrations of *Cryptosporidium* oocysts for these water qualities using scenario 1 (bin 1 surface water) as an example. The analysis of variance (ANOVA) test followed by multiple comparison analysis test (Tukey-Kramer post hoc test) indicated that the concentrations of *Cryptosporidium* oocysts in the various waters were significantly different ($p<0.05$), except for the finished drinking waters in the *de facto* reuse and planned IPR systems. The environmental buffer clearly improved the quality of the conventionally treated wastewater as a result of pathogen die-off and dilution, thereby improving the finished drinking water quality in the *de facto* reuse system. However, the environmental buffer led to a significant deterioration in water quality for planned IPR. The occurrence of *Cryptosporidium* in the upstream surface water controlled the risk calculation in both IPR systems.

46
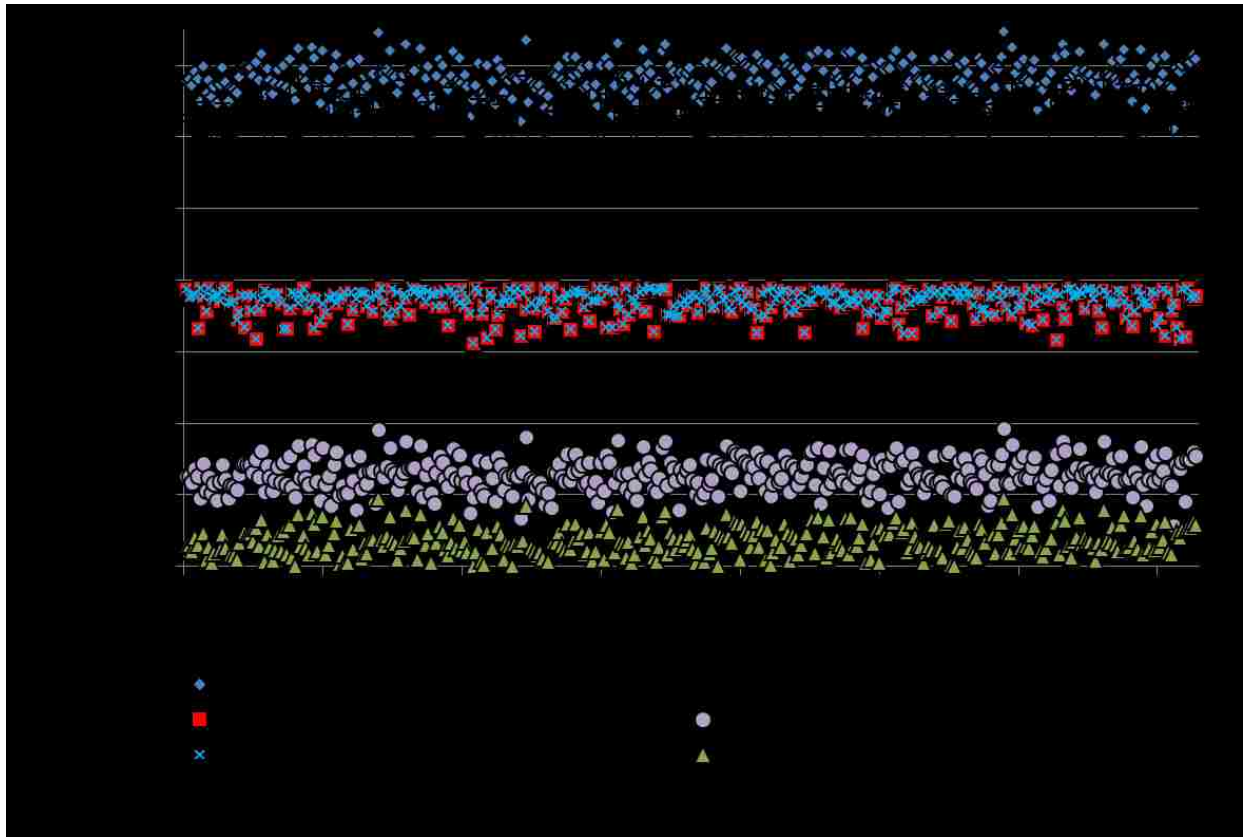
Figure 3-3. Concentration of *Cryptosporidium* oocysts in raw wastewater and the finished water from different treatment trains for the baseline condition (storage time of 270 days at a temperature of 20°C).

The model proved to be highly sensitive to storage time because pathogen die-off offset the limited reduction of *Cryptosporidium* in the *de facto* reuse system, and pathogen die-off also offset potential spikes in *Cryptosporidium* during failures in the planned IPR system. Despite higher concentrations of *Cryptosporidium* in the upstream surface water in scenarios 2 (Figure S12) and 3 (Figure S13), similar outcomes were observed. These results support the previous National Research Council suggestion that some engineered potable reuse systems might achieve similar or superior water quality compared to traditional systems incorporating environmental buffers (NRC, 2012).

3.4.2 Quantification of Public Health Risk for the Baseline Condition

The annual probabilities of infection and DALYs for both optimal and sub-optimal conditions are presented in Table 3.5. Because the model did not consider failures in conventional wastewater or drinking water treatment, there are no results for sub-optimal operation for *de facto* reuse. Blending the *de facto* and planned IPR product waters with upstream surface water resulted in nearly identical annual risks of infection (mean of 9.4×10^{-5} - 4.5×10^{-4}) and DALYs (mean of 1.1×10^{-7} - 5.3×10^{-7}), with the ranges representing results for the three bin scenarios. The small confidence levels in Table 3.5 also indicate that daily fluctuations in wastewater loadings had minimal impact on risk. Figure 3.4 illustrates how the modeled risks for the potable reuse scenarios under sub-optimal operation compare to the LT2 framework for conventional drinking water applications. The model suggests that under baseline conditions, the risks associated with *de facto* reuse and planned IPR are consistent with traditional bin 1, bin 2, or bin 4 drinking water systems. It is important to emphasize that the risks associated with planned IPR are elevated due to mixing with upstream surface water and not due to inadequate treatment or wastewater influence from within the community. Because of the dominance of the upstream surface water, advanced treatment failures were inconsequential for the planned IPR system, resulting in nearly identical annual risks of infection and DALYs for optimal and sub-optimal performance (Table 3.5). Although the impacts of process failure were more apparent for the DPR system, the overall risks for DPR were still at least three orders of magnitude lower than the LT2 framework and the 10^{-4} benchmark during sub-optimal operation.

Table 3-5. Statistical analysis of probability of infection per year and disease burden for optimal (i.e., no failures) and sub-optimal operation for the baseline condition. Values are based on the results from 10,000 model iterations.

Optimal operation

Statistics	*de facto* (Unplanned Indirect Potable Reuse)			Planned Indirect Potable Reuse			Direct Potable Reuse
$P_{inf,y}$	Scenario 1[2]	Scenario 2	Scenario 3	Scenario 1	Scenario 2	Scenario 3	
Mean	9.4E-05	1.3E-04	4.5E-04	9.4E-05	1.3E-04	4.5E-04	2.2E-11
St. Dev.	2.7E-06	3.4E-06	1.3E-05	2.7E-06	3.4E-06	1.3E-05	1.8E-12
95% Confidence ($\pm$)	5.3E-08	6.8E-08	2.5E-07	5.3E-08	6.7E-08	2.5E-07	3.5E-14
Minimum	8.4E-05	1.2E-04	4.0E-04	8.3E-05	1.2E-04	4.0E-04	1.9E-11
5th Percentile	9.0E-05	1.3E-04	4.3E-04	9.0E-05	1.3E-04	4.3E-04	2.0E-11
50th Percentile	9.4E-05	1.3E-04	4.5E-04	9.4E-05	1.3E-04	4.5E-04	2.3E-11
95th Percentile	9.9E-05	1.4E-04	4.7E-04	9.9E-05	1.4E-04	4.7E-04	2.5E-11
Maximum	1.1E-04	1.5E-04	5.0E-04	1.0E-04	1.4E-04	5.0E-04	2.8E-11
Disease Burden[1]							
Mean	1.1E-07	1.6E-07	5.3E-07	1.1E-07	1.6E-07	5.3E-07	2.7E-16
St. Dev.	3.3E-09	4.0E-09	1.5E-08	3.2E-09	4.1E-09	1.5E-08	2.7E-15
95% Confidence ($\pm$)	6.4E-11	8.1E-11	3.0E-10	6.3E-11	8.0E-11	3.0E-10	5.3E-17

Sub-optimal operation

Statistics	*de facto* (Unplanned Indirect Potable Reuse)[3]			Planned Indirect Potable Reuse			Direct Potable Reuse
$P_{inf,y}$	Scenario 1	Scenario 2	Scenario 3	Scenario 1	Scenario 2	Scenario 3	
Mean	-	-	-	9.4E-05	1.3E-04	4.5E-04	6.1E-09
St. Dev.	-	-	-	2.7E-06	3.4E-06	1.3E-05	6.7E-08
95% Confidence ($\pm$)	-	-	-	5.3E-07	6.7E-07	2.5E-06	1.3E-09
Minimum	-	-	-	8.4E-05	1.2E-04	4.1E-04	2.2E-11
5th Percentile	-	-	-	9.0E-05	1.3E-04	4.3E-04	3.4E-11
50th Percentile	-	-	-	9.4E-05	1.3E-04	4.5E-04	3.3E-10
95th Percentile	-	-	-	9.9E-05	1.4E-04	4.7E-04	1.9E-08
Maximum	-	-	-	1.0E-04	1.5E-04	5.1E-04	5.0E-06
Disease Burden[1]							
Mean	-	-	-	1.1E-07	1.6E-07	5.3E-07	7.2E-12
St. Dev.	-	-	-	3.2E-09	4.1E-09	1.5E-08	7.9E-11
95% Confidence ($\pm$)	-	-	-	6.3E-10	8.0E-10	3.0E-09	1.6E-12

[1]Disease burden in DALYs per person per year

[2]Scenarios refer to bin classifications (see Table 3.2); scenarios do not apply to direct potable reuse because there is no surface water influence

[3]Model did not consider failures for conventional drinking water treatment or conventional wastewater treatment
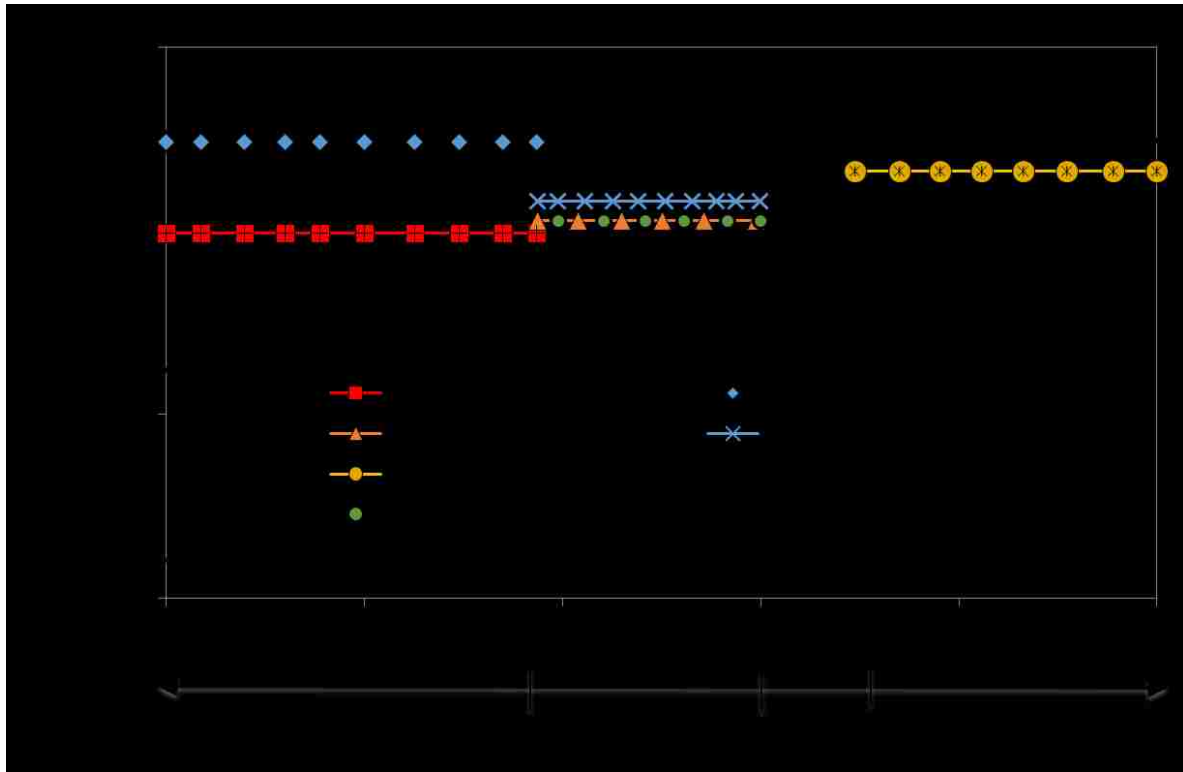
Figure 3-4. Comparison of annual risk of infection from the system dynamics model during sub-optimal operation with calculated risks based on the LT2 framework**.** The scenarios refer to the varying concentrations of *Cryptosporidium* in the upstream surface water (see Table 3.2), and the results are calculated for the baseline and critical conditions (see Table 3.1). Datasets denoted with an "a" reflect baseline conditions, and datasets denoted with a "b" reflect critical conditions (i.e., 105 days of storage time and a temperature of 10°C).

3.4.3   Water Resource Management and Policy Implications

Sensitivity analyses were performed to identify the most influential parameters in each treatment train and to assess the implications of various management and regulatory/policy measures. The results for the sensitivity analyses were then used to identify 'critical' conditions based on observed changes in model output.

3.4.3.1   *Effects of Increased Wastewater Loading of Cryptosporidium*

Variability in wastewater loading of *Cryptosporidium* was evaluated in the context of an outbreak scenario. This study defined an outbreak as a 1-log increase in the raw wastewater concentration. This assumption is supported by Haas & Rose (1995), who showed a 10-fold

50

increase in *Cryptosporidium* concentration in finished water during the 1993 Milwaukee

outbreak, and also by Trussell et al. (2013), who estimated 10-fold to 100-fold increases in raw

wastewater concentration during outbreak conditions. The 1-log increase also allows for

consideration of studies [e.g., Robertson et al. (2006)] reporting higher *Cryptosporidium*

concentrations than Rose et al. (2005). Even though higher concentrations of *Cryptosporidium* in

the raw wastewater were expected to result in higher risks of infection, model output for the IPR

systems indicated that at least 270 days of reservoir storage time at 20°C was sufficient to

completely buffer the effects of the outbreak. The outbreak condition increased the risk for DPR

by a factor of 10, but the final risk ($\approx 4 \times 10^{-8}$) was still well below the 10^{-4} benchmark. The

corresponding factor sensitivity values are summarized in Table 3.6.

Table 3-6. Summary of factor sensitivity (FS) values for the sensitivity analyses on wastewater *Cryptosporidium* concentrations (i.e., outbreak condition) and process failure. FS values indicate the $\log_{10}$ ratio of the revised model output versus the baseline condition: large negative values (e.g., less than -0.3) indicate notable decreases in risk, large positive values (e.g., greater than 0.3) indicate notable increases in risk, and small values (e.g., greater than -0.3 and less than 0.3) indicate minimal changes in risk. For example, an FS value of 0.3 indicates the risk has increased by a factor of 2 due to the change.

Revised Condition	*de facto* Reuse			Planned IPR			DPR
	Scenario 1	Scenario 2	Scenario 3	Scenario 1	Scenario 2	Scenario 3	
Outbreak	1.2E-02	1.2E-02	1.0E-03	1.2E-03	2.9E-03	2.8E-03	**1.5E+00**
UF Failure	N/A	N/A	N/A	1.2E-08	3.3E-10	0.0E+00	**4.6E+00**
Pre-O$_3$ Failure	N/A	N/A	N/A	2.0E-09	0.0E+00	0.0E+00	N/A
Post-O$_3$ Failure	N/A	N/A	N/A	0.0E+00	0.0E+00	0.0E+00	**2.0E+00**
UV Failure	N/A	N/A	N/A	N/A	N/A	N/A	**6.0E+00**

*Bold values indicate that the risk increased/decreased by more than a factor of 2 relative to the baseline condition.

**All FS values in this table are positive, which indicates increases in risk for all systems and for all scenarios.

3.4.3.2 *Effects of Failures during Advanced Treatment for Planned IPR and DPR*

The factor sensitivity values associated with specific process failures are summarized in

Table 3.6 for the three planned IPR systems and the DPR system. Planned IPR scenario 3, which

51

was classified as a bin 4 surface water system, had the highest risk of infection for the baseline condition but was completely insensitive to process failures. Again, the higher baseline risk was due to the higher upstream surface water loading of *Cryptosporidium*, and the system's lack of sensitivity to failure was due to increased resiliency linked to the environmental buffer and the greater removal requirements for the conventional drinking water treatment plant. Although extremely minor, UF failure had the greatest impact on risk for scenarios 1 and 2 because of the immediate reduction in log credits for UF and the 'domino effects' on downstream processes. Therefore, the effects of process failures in all planned IPR scenarios were negligible because the failures were sufficiently mitigated by the 270 days of storage in the environmental buffer. Because of the reduced resiliency of the DPR treatment train, process failures resulted in significant increases in annual risk, particularly during a UV failure. However, the DPR system had sufficient treatment redundancy to achieve the 10^{-4} annual risk benchmark even during process failures.

3.4.3.3 *Effects of Reservoir Storage Time*

Because of the high level of treatment provided by the planned IPR treatment train, reservoir storage time had a negligible impact on annual risk during normal operation. Because this was highly dependent on *Cryptosporidium* loadings in the upstream surface water, discharge to a 'pristine' source water would yield different results. For the *de facto* reuse system, storage times shorter than 270 days led to higher risks of infection (Figure 3.5). A 'critical' threshold (i.e., FS>0.3) occurred between 90 and 180 days of storage for surface water scenarios 1 and 2, but even zero days of storage had minimal impact on scenario 3 because of the high upstream surface water loading and robust treatment provided at the drinking water treatment plant. Therefore, 105 days was selected as the target storage time for the 'critical condition' analysis

52

(described later). It is important to note that the current model does not account for non-ideal flow conditions, such as short-circuiting, which could significantly reduce storage times for some parcels of water. Therefore, it is important to verify whether mean retention time is a reasonably accurate hydrodynamic representation of real-world systems.

Storage time (days)	0	30	60	90	120	150	180	210	240	270*	300	330	360
FS 1	**2.86E+00**	**2.31E+00**	**1.76E+00**	**1.23E+00**	7.37E-01	**3.50E-01**	1.27E-01	3.72E-02	8.41E-03	0.00	-2.38E-03	-3.04E-03	-3.23E-03
FS 2	**1.74E+00**	**1.21E+00**	7.17E-01	**3.38E-01**	1.23E-01	3.79E-02	1.07E-02	2.85E-03	6.25E-04	0.00	-1.75E-04	-2.23E-04	-2.37E-04
FS 3	1.81E-01	5.87E-02	1.72E-02	4.87E-03	1.36E-03	3.80E-04	1.04E-04	2.75E-05	6.00E-06	0.00	-1.67E-06	-2.14E-06	-2.27E-06
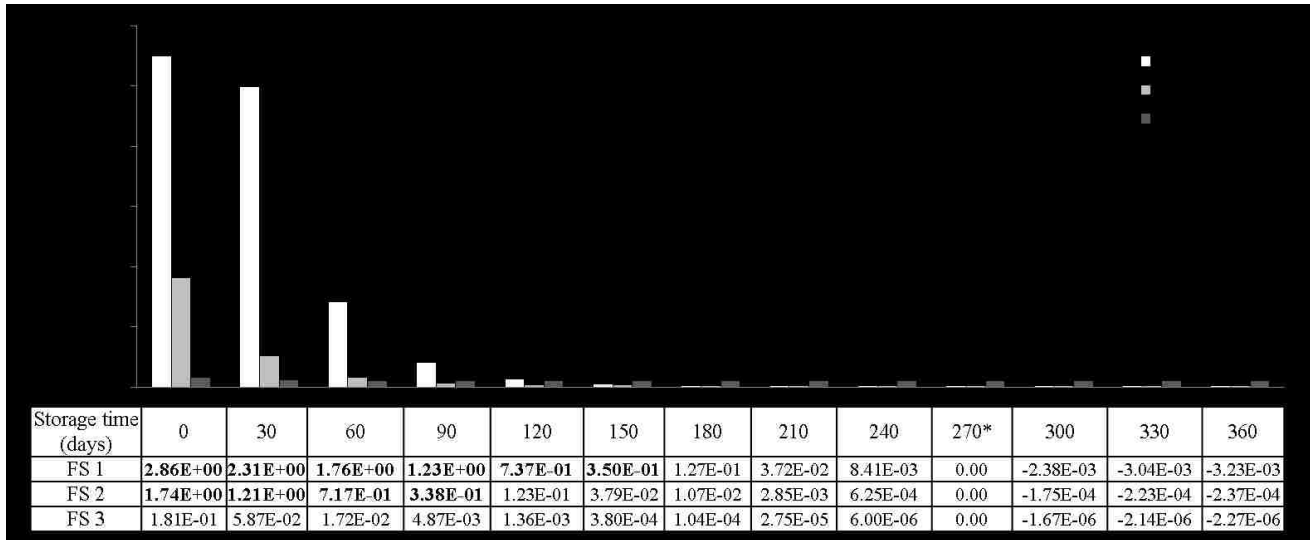
Figure 3-5. Sensitivity analysis on reservoir storage time for the three scenarios of the *de facto* reuse system (storage time had negligible impact on the planned IPR system). The asterisk indicates the reservoir storage time for the baseline condition (270 days). Bold values indicate that the risk increased/decreased by more than a factor of 2 relative to the baseline condition. FS = factor sensitivity value.

3.4.3.4 *Effects of Recycled Water Contribution*

Figure 3.6 illustrates the relationship between RWC and annual risk of infection for *de facto* reuse and planned IPR. For the planned IPR system, higher RWCs led to reduced annual risk of infection regardless of storage time—from a 25% reduction for a 40% RWC to a 75% reduction for an 80% RWC (Figure 3.6B). The same results were observed for *de facto* reuse with a storage time of 270 days, but results were significantly different for *de facto* reuse with a 105-day storage time (Figure 3.6A). For the less contaminated bin 1 surface water (scenario 1), the annual risk of infection increased by a factor of 1.2-1.6 for RWCs of 40-80%. On the other

www.manaraa.com

hand, the more contaminated surface waters in scenarios 2 and 3 were characterized by decreased risks of infection—actually lower than the risks for scenario 1—as the RWC increased to 80%. These results suggest that the relative impacts of RWC are highly dependent on other system variables, including storage time and bin classification.

RWC	20%*	40%	60%	80%
FS 1	0.00	7.33E-02	1.36E-01	1.91E-01
FS 2	0.00	-9.87E-02	-2.27E-01	**-4.09E-01**
FS 3	0.00	-1.25E-01	**-3.01E-01**	**-6.00E-01**

RWC	20%*	40%	60%	80%
FS 1	0.00	-1.25E-01	**-3.01E-01**	**-6.02E-01**
FS 2	0.00	-1.25E-01	**-3.01E-01**	**-6.02E-01**
FS 3	0.00	-1.25E-01	**-3.01E-01**	**-6.01E-01**
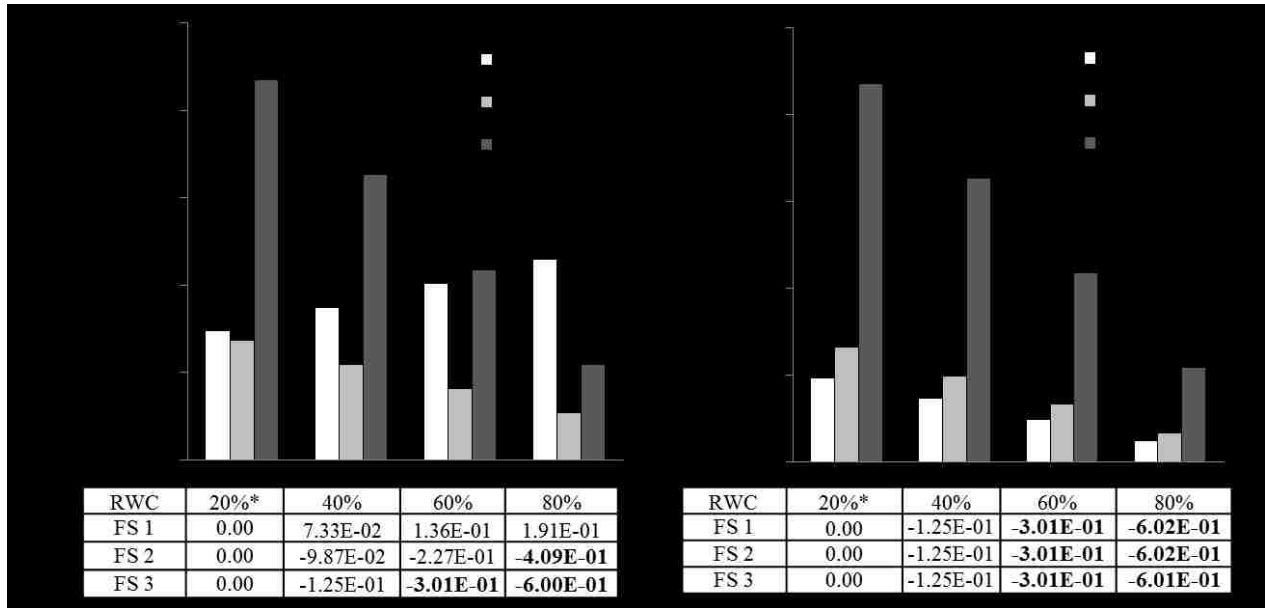
Figure 3-6. Sensitivity analysis on recycled water contribution
for (A) *de facto* reuse system with 105 days of storage time and (B) *de facto* reuse with 270 days of storage time or planned IPR with either 105 or 270 days of storage time. The asterisk indicates the RWC for the baseline condition (20%). Bold values indicate that the risk increased/decreased by more than a factor of 2 relative to the baseline condition. FS = factor sensitivity value.

3.4.3.5 *Effects of Temperature in the Environmental Buffer*

Because the planned IPR system was insensitive to operational changes in the environmental buffer, changes in reservoir temperature had no significant impacts on annual risk. Figure 3.7 illustrates the results of the sensitivity analysis for temperature in the *de facto* reuse system. The annual risk of infection was less sensitive to temperature changes when coupled with 270 days of storage time (Figure 3.7B) versus 105 days of storage time (Figure 3.7A). However, for both 105 days and 270 days, the annual risk of infection increased by a factor of 10 in scenario 1 (i.e., bin 1 surface water) when the temperature dropped from 20°C (baseline

condition) to 5°C. This is attributable to the reduction in die-off of wastewater-derived

Cryptosporidium at the lower reservoir temperature coupled with the lack of additional treatment

at the conventional drinking water treatment plant. The temperature effects were less pronounced

for scenarios 2 and 3, which included additional treatment at the drinking water treatment plant

in accordance with LT2. For scenario 1, notably higher risks were also observed for temperatures

of 10°C, but the risks decreased relative to the baseline condition for temperatures greater than

20°C. A temperature of 10°C was selected for the 'critical' condition analysis.
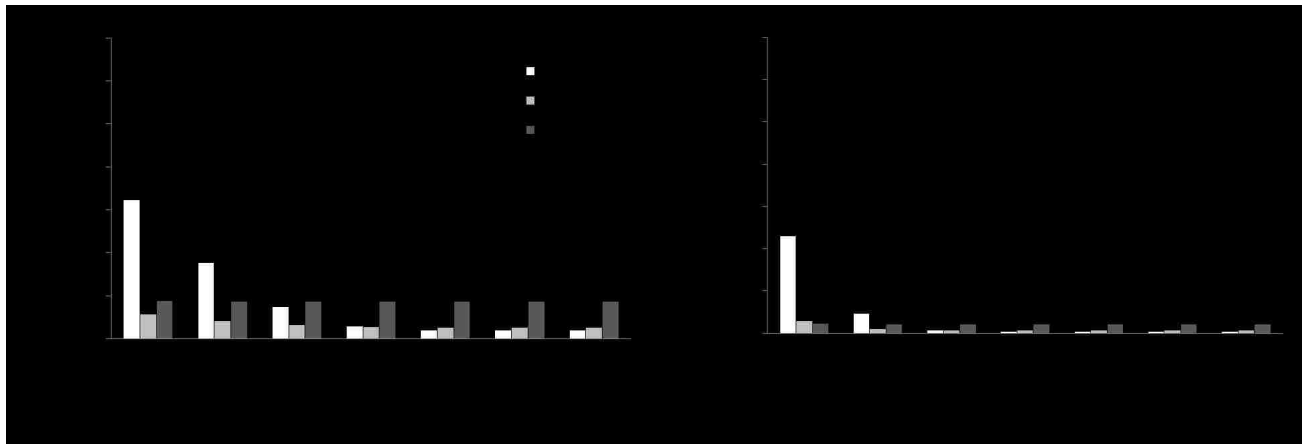
Figure 3-7. Sensitivity analysis on temperature in the environmental buffer for the *de facto* reuse system (A) 105 days of storage time and (B) 270 days of storage time. The asterisk indicates the reservoir temperature for the baseline condition (20°C). Bold values indicate that the risk increased/decreased by more than a factor of 2 relative to the baseline condition. FS = factor sensitivity value.

3.4.3.6 *Analysis of the Critical Condition*

Figure 3.8 illustrates the *Cryptosporidium* oocyst concentrations in the various water

matrices for the critical conditions, specifically a storage time of 105 days at a temperature of

10°C, for scenario 1. The corresponding data for scenarios 2 and 3 are provided in Figures S14

and S15. Because the IPR (before blending) and DPR product waters were not influenced by the

critical condition, their concentrations remained largely unchanged from the baseline condition

for all three scenarios. The final IPR drinking water (after blending) was also similar due to the

high quality of the advanced treated wastewater and the dominance of the upstream surface water. The final drinking water in the scenario 1 *de facto* reuse system exhibited the greatest change—an approximate 10-fold increase in *Cryptosporidium* concentration—due to the reduced buffering capacity of the reservoir and the lower level of treatment at the drinking water treatment plant. The additional log reduction credits for the drinking water treatment plant in scenarios 2 and 3 were able to compensate for the reduction in die-off in the environmental buffer. The corresponding annual risks of infection for the critical condition are illustrated and compared against the LT2 framework in Figure 3.4.
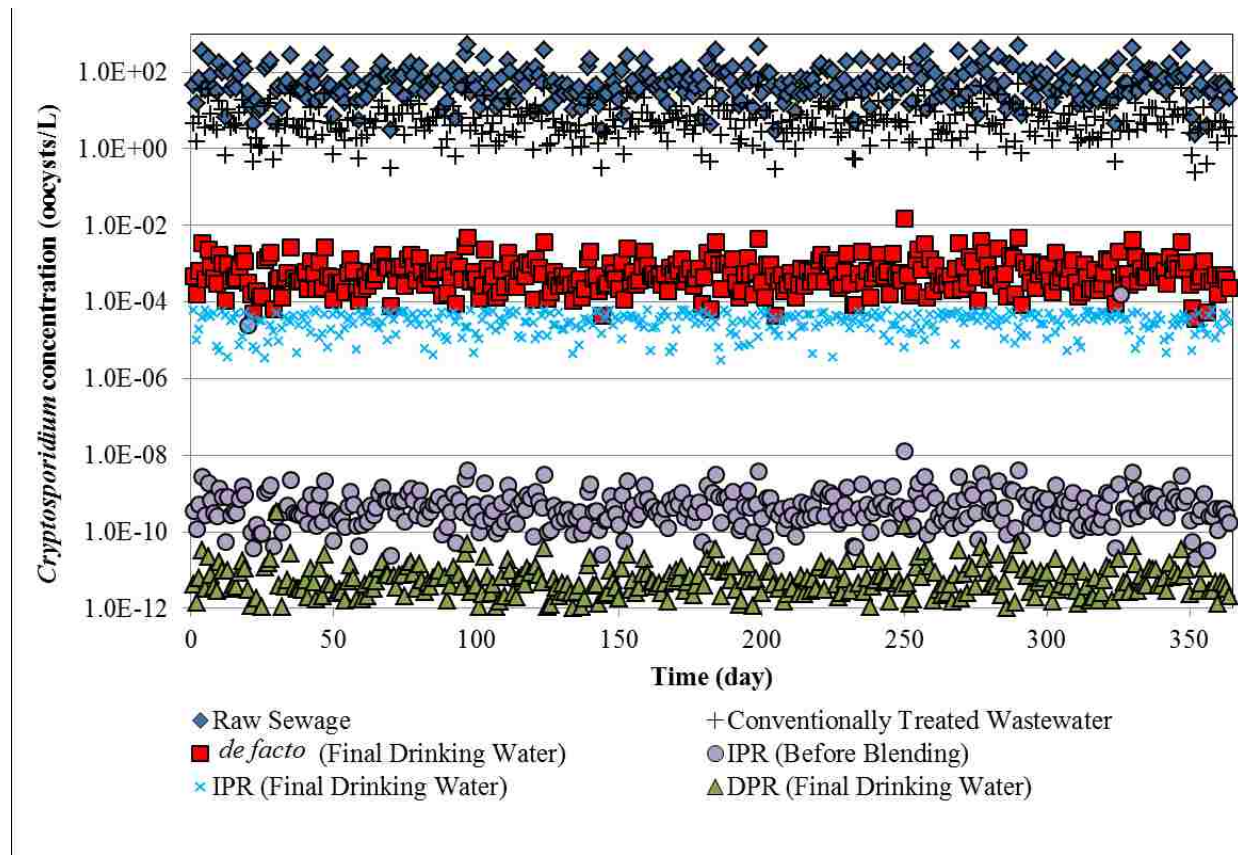
Figure 3-8. Concentration of *Cryptosporidium* oocysts in raw wastewater and the finished water from different treatment trains for the 'critical' condition
(storage time of 105 days at a temperature of 10°C).

3.4.4   Sensitivity Analysis on the Dose Response Parameter

Figure 3.9 illustrates the result of the sensitivity analysis on the *Cryptosporidium* dose response parameter for the baseline condition (i.e., temperature of 20°C and a storage time of 270 days under sub-optimal operation). As expected, higher dose response parameters resulted in higher annual risks of infection, and the increases were nearly proportional to the ratio of the modified and original r values for the low *Cryptosporidium* concentrations/doses expected in the finished drinking waters. For dose response parameters of 0.0572 and 0.09 oocysts^{-1}, the annual risks of infection for all IPR scenarios exceeded the 10^{-4} benchmark by at least one order of magnitude, but the annual risk for DPR ($\sim 9 \times 10^{-8}$) was still well below the 10^{-4} benchmark. Therefore, uncertainty in the dose response parameter did not necessarily impact relative differences between the potable reuse systems, but there was a significant impact on absolute risk values.
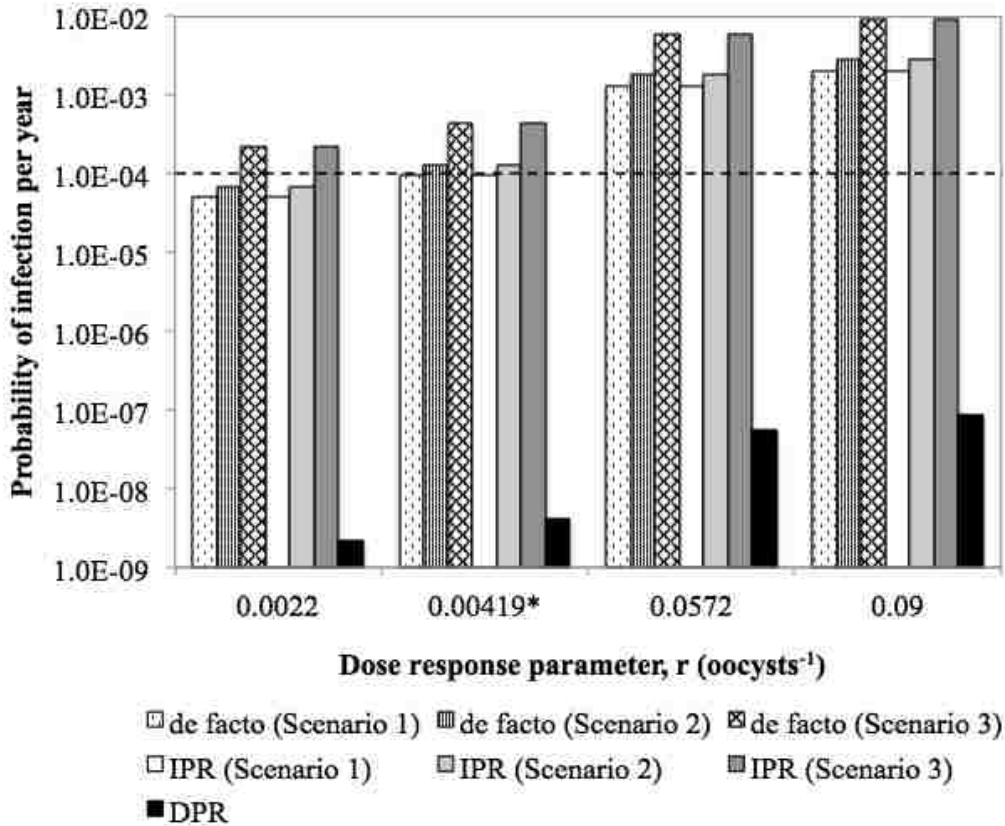
Figure 3-9. Sensitivity analysis on dose response parameter for the baseline condition (temperature of 20°C and storage time of 270 days). The asterisk indicates the baseline dose response parameter of 0.00419 oocysts^{-1}, and the dashed line represents the benchmark annual risk of 10^{-4}.

3.5   Conclusion

The risks associated with the *de facto* and planned IPR systems were generally consistent with those of conventional drinking water systems, while DPR was clearly superior. Because the advanced treatment train in the planned IPR system was highly effective in reducing *Cryptosporidium* concentrations, the associated risks were generally dominated by upstream surface water conditions. Moreover, risks generally decreased with higher recycled water contributions (RWCs), except for the bin 1 *de facto* reuse system with short reservoir storage times. Outbreak conditions and advanced treatment failures were generally inconsequential, at least with respect to *Cryptosporidium*, either due to the robustness of the advanced treatment

58

train (i.e., DPR) or resiliency provided by the environmental buffer (i.e., planned IPR). Storage time in the environmental buffer was important for the *de facto* reuse system, and the model indicated a critical storage time of approximately 105 days, although this was also temperature-dependent. A critical condition consisting of a 105-day storage time in the environmental buffer at a temperature of 10°C resulted in a significant difference between planned IPR and *de facto* reuse for a bin 1 system, with *de facto* reuse exhibiting a 10-fold higher annual risk of infection. This is attributable to the reduced treatment provided by the bin 1 drinking water treatment plant, which reduced the resiliency of the system. Therefore, the bin 2 and bin 4 *de facto* reuse systems generally exhibit higher risks of infection for storage times longer than 105 days, regardless of temperature, but bin 1 may exhibit higher risks when shorter storage times are coupled with colder temperatures.

The conclusions developed from the model output can be used by stakeholders to better understand the role of various operational parameters on public health risks in diverse potable reuse systems. Moreover, the data from this study can be used to inform regulatory decision making and aid in the development of design or operational criteria for IPR and DPR systems. Future modeling efforts would benefit from a more comprehensive characterization of temporal variability in advanced treatment process efficacy. Although failures in the planned IPR and DPR treatment trains were generally inconsequential for the overall *Cryptosporidium* risk calculations, model accuracy could be improved by incorporating statistical distributions of process efficacy rather than using 'absolute' failures (i.e., worst-case scenarios). Moreover, the implications of process failure—and other critical parameters—might change when modeling risks associated with other pathogens, such as norovirus. Finally, there is a need to better understand the hydrodynamics of drinking water reservoirs to allow for more accurate modeling

of the environmental buffer, particularly considering that storage time was a critical parameter for some potable reuse systems.

Acknowledgments

Supplementary Information Available

A Supplementary Information file with 15 figures and 8 tables is available which can be found in Appendix 1 of this dissertation.

4 Equivalency of Indirect and Direct Potable Reuse Paradigms in a Quantitative Microbial Risk Assessment Framework

ERFANEH AMOUEYAN[1], SAJJAD AHMAD[1], JOSEPH EISENBERG[2], DANIEL
GERRITY[1]*

[1]*Department of Civil and Environmental Engineering and Construction, University of Nevada,*

Las Vegas, Box 454015, 4505 S. Maryland Parkway, Las Vegas, NV 89154-4015, United States

[2]*Department of Epidemiology, School of Public Health, University of Michigan, Ann Arbor,*

Michigan, United States

[3]*Trussell Technologies, Inc., Pasadena, California, United States*

[*]Corresponding author. Mailing address: Department of Civil and Environmental Engineering
and Construction, University of Nevada, Las Vegas, Box 454015, 4505 S. Maryland Parkway,
Las Vegas, NV 89154-4015, United States. Phone: (702) 895-3955. Fax: (702) 895-3936. Email:
Daniel.Gerrity@unlv.edu.

4.1 Introduction

Evaluating the microbiological quality of drinking water is critically important for ensuring adequate public health protection, particularly in potable reuse applications. *Cryptosporidium*, norovirus (NoV), adenovirus (AdV), and *Salmonella*, all of which can be transmitted via the fecal-oral route, are some of the main etiological agents of gastroenteritis worldwide (National Research Council, 2012). NoV, AdV, and *Salmonella* are also listed on the United States (U.S.) Environmental Protection Agency's (EPA) Contaminant Candidate List (CCL4), thereby identifying these pathogens for priority research (USEPA, 2015b).

Despite the importance of these pathogens in the context of public health, the industry lacks information on their survival in the environment and attenuation through some treatment processes. For example, quantification of NoV infectivity has been elusive due to the ineffectiveness of conventional cell culture methods. Instead, studies have relied on MS2 (Lee & Ko, 2013), feline calicivirus (FCV) (Doultree et al., 1999; Duizer et al., 2004; Nuanualsuwan and Cliver, 2003; Thurston-Enriquez et al., 2005; Abbaszadegan et al., 2007) and murine norovirus (MNV) (Karst et al., 2003; Katayama et al., 2006; Lee et al., 2008; Lim et al., 2010; Wu, 2015) as viral surrogates, or used a probabilistic approach to estimate viral inactivation based on genome damage (Pecson et al., 2011). Recently, MNV has been identified as a valuable surrogate for evaluating NoV survival in the environment (Bae & Schwab, 2008; Cannon et al., 2006; Hirneisen & Kniel, 2013; Yi et al., 2016), but incomplete characterization still requires the use of other surrogates such as MS2 in some instances.

Because of the challenging nature of pathogen detection, particularly in highly treated water, the drinking water and potable reuse industries generally rely on log removal values (LRVs) to ensure adequate protection of public health (Pecson et al., 2015). For potable reuse,

62

the "12-10-10" LRV framework initially implemented in California is now being adopted by other states (EPA, 2017). An independent panel of public health experts also supported the adoption of this framework with two minor exceptions: they noted that satisfying the *Cryptosporidium* LRV would presumably satisfy the LRV for *Giardia*, which is generally more susceptible to treatment, and that a 9-log total coliform LRV might be warranted to address concerns related to *Salmonella*. Therefore, they proposed a "12-10-9" framework (NWRI, 2013) for viruses, *Cryptosporidium*, and total coliform bacteria as a surrogate for *Salmonella*. These log reductions are based on raw sewage as the source water, while the "8-5.5-6" framework for viruses, *Cryptosporidium*, and *Giardia* in Texas uses pathogen levels in the presumably more consistent secondary wastewater effluent as the basis for treatment train design (TWDB, 2015). Because they all target a 10^{-4} annual risk of infection, experts suggested that New Mexico could adopt any of these frameworks for future DPR projects (NWRI, 2016c). On the other hand, Australia and the World Health Organization (WHO) proposed a target of 10^{-6} disability adjusted life years (DALYs) per person per year, which corresponds with a 10^{-3} annual risk of infection and LRVs of 9.5-8-8.1 for viruses, *Cryptosporidium*, and *Campylobacter* in untreated wastewater (NRMMC-EPHC-NHMRC, 2008).

Previous studies have performed quantitative microbial risk assessments (QMRAs) to evaluate public health risks associated with indirect potable reuse (IPR) (Olivieri et al., 1999; Lim et al., 2017) and direct potable reuse (DPR) (Pecson et al., 2017; Soller et al., 2017), but there are few direct comparisons of IPR and DPR using the same QMRA framework (Chaudhry et al., 2017), particularly studies that simultaneously compare treatment trains in *de facto* reuse, planned IPR, and DPR applications (Amoueyan et al., 2017). Many studies emphasize treatment trains employing high-pressure membrane filtration [i.e., nanofiltration (NF) or reverse osmosis

(RO)] (Chaudhry et al., 2017), and some studies focus on alternative treatment trains relying on ozone-biofiltration (Amoueyan et al., 2017), while few studies include both (Soller et al., 2017). While most employ a stochastic Monte Carlo approach to address parameter variability, few studies have described the potential impacts of process failure (Pecson et al., 2017) and associated 'domino effects' (Amoueyan et al., 2017) on risk estimates.

Each study is characterized by various strengths and limitations, but, more importantly, the unique attributes of each QMRA approach allow one to reach important conclusions regarding the safety and reliability of potable reuse treatment train design. For example, Amoueyan et al. (2017) found that the upstream surface water concentration of *Cryptosporidium* oocysts was the dominant factor in IPR applications, assuming wastewater-derived *Cryptosporidium* was attenuated with sufficient storage time in the environmental buffer. The existing QMRA literature generally agrees that potable reuse treatment trains are adequately protective of public health, particularly when compared with conventional drinking water applications. However, it has also been demonstrated that a small number of daily risk spikes for certain pathogens may cause disproportionate increases in annual risk under certain conditions (e.g., low UV doses) or when using alternative dose response models (Soller et al., 2017). Therefore, additional QMRA studies are still warranted to characterize the relative impacts of parameter variability and uncertainty across a wide range of pathogens and treatment train scenarios.

As such, the main objective of this study was to perform a QMRA to estimate health risks associated with *Cryptosporidium*, NoV, AdV, and *Salmonella* that could potentially occur in the finished drinking water of *de facto* reuse, planned IPR, and DPR systems employing ozone-biofiltration or RO-based treatment trains. The stochastic nature of observed LRVs was captured

64

with a Monte Carlo approach and published statistical distributions of treatment process performance. Short-term failures and associated 'domino effects' were also incorporated into the model framework. Therefore, the results of this study allow for a comprehensive evaluation of treatment train 'equivalence' in the context of protozoan, viral, and bacterial pathogen exposure. Specifically, this study expands upon Amoueyan et al. (2017) by including additional pathogens and a direct comparison of 'full advanced treatment' (FAT) [i.e., treatment trains employing RO and an advanced oxidation process (AOP)] vs. ozone-biofiltration. This study will also aid in characterizing the relative risks posed by planned potable reuse vs. *de facto* reuse in the U.S., thereby allowing for a determination of the adequacy of current Safe Drinking Water Act (SDWA) safeguards given the ubiquity of wastewater-impacted source waters (Rice et al., 2013).

4.2 Methodology

4.2.1 Potable reuse systems and treatment trains

Figure 4.1 summarizes the seven *de facto* reuse, planned IPR, and DPR systems considered in this study. These were selected to encompass the spectrum of potable reuse systems currently in use, under design/construction, or under consideration for future projects. Potable reuse treatment trains with UV disinfection (i.e., TT2, TT4, TT5,TT6, TT7) were assumed to employ low-dose UV targeting disinfection. In addition to the unit processes listed in Figure 4.1, the IPR systems (TT1-TT4) accounted for the effects of dilution and storage time in their respective environmental buffers. The surface water augmentation/blending systems (TT1, TT3, TT4, and TT5) employed conventional drinking water treatment with chlorine disinfection prior to distribution, and the groundwater replenishment system (TT2) employed chlorination upon withdrawal from the aquifer. LRVs for the unit processes are described later.

65
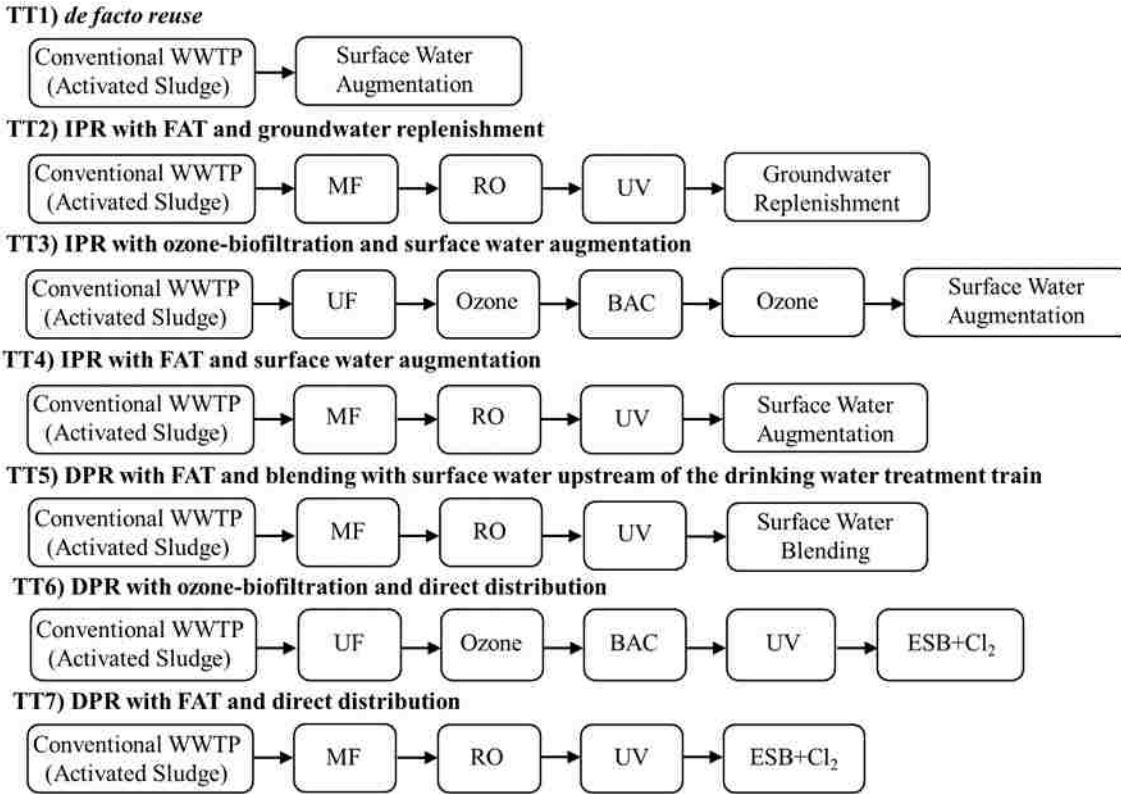
Figure 4-1. Treatment processes included in each potable reuse system.
The conventional WWTP included only secondary wastewater treatment. The surface water augmentation/blending treatment trains (TT1, TT3, TT4, TT5) employed a conventional drinking water treatment plant with chlorine disinfection prior to distribution. The groundwater replenishment treatment train (TT2) included chlorine disinfection upon withdrawal from the aquifer. MF = microfiltration, UF = ultrafiltration, RO = reverse osmosis, UV = ultraviolet disinfection, BAC = biological activated carbon, Cl_2 = free chlorine disinfection, ESB = engineered storage buffer.

4.2.2 Target pathogens and raw wastewater concentrations

Cryptosporidium, NoV, AdV, and *Salmonella* were selected as the target pathogens for the QMRA because they account for most of the waterborne gastroenteritis cases in the U.S. (Craun et al., 2006; National Research Council, 2012). *Cryptosporidium* and AdV are also common drivers for treatment train design due to their demonstrated resistance to oxidative (USEPA, 2006a) and UV disinfection processes (Gerba et al., 2002), respectively. Inclusion of disinfectant resistant pathogens in a QMRA is recommended to mitigate uncertainties by

66

addressing 'extreme' hazards (Gerba et al., 2018). *Salmonella* was also included in the current study based on the aforementioned recommendation of public health experts (NWRI, 2013).

Transmission of the target pathogens may occur either through direct contact with a host or through contaminated surfaces, food, or water (Rzeżutka & Cook, 2004), but this study addressed only the primary exposure route via contaminated drinking water. Historically, NoV infections have generally been transmitted through contaminated food (Percival et al., 2013), but a recent QMRA indicated that NoV may be a concern for potable reuse as well (Soller et al., 2018), thereby justifying its inclusion in the current study. *Salmonella* has also been associated with foodborne disease but is more frequently transmitted through contaminated water (Lemarchand & Lebaron, 2003; WHO, 2008). Data on pathogen occurrence in various water matrices was collected from the literature and described with best-fit probability distribution functions (PDFs), which are summarized in Table 4.1 and illustrated along with the corresponding cumulative distribution functions (CDFs) in Figures S1-S3. *Cryptosporidium* concentrations were based on immunomagnetic separation and immunofluorescence assay microscopy (i.e., U.S. EPA Method 1623) (Rose et al., 2005), NoV and AdV concentrations were based on genome copy data (described below), and *Salmonella* concentrations were based on most probable number (MPN) culture methods (Koivunen et al., 2003; Lemarchand & Lebaron, 2003).

Detection and quantification of NoV in different water matrices (e.g., sewage, surface water, and groundwater) is typically accomplished with quantitative polymerase chain reaction (qPCR), and concentrations are reported based on genome copies (gc) (Lodder & de Roda Husman, 2005; Borchardt et al., 2012; Eftim et al., 2017). Some studies suggest that using genomes copies as a surrogate for infectious viral particles may overestimate risk estimates when

67

performing a QMRA (Abel et al., 2017), but Gerba et al. (2018) recommended continued use of

qPCR-based data until a more appropriate alternative was developed. For culturable viruses,

genome copies may provide a relatively accurate estimate of infectious particles in early stages

of wastewater treatment, and some studies show that ratios of infectious particles to genome

copies can range from 1/700 for AdV 40/41 (McBride et al., 2013; Lim et al., 2015) to 1/7 for

AdV serotype 1 (Parker et al., 2017). Therefore, the use of genome copy data can be justified in

some contexts, particularly in the absence of infectivity data (e.g., NoV), when ratios of

infectious particles to genome copies are expected to be high (e.g., in raw sewage), or when

additional conservatism is preferred (e.g., potable reuse).

Table 4-1. Statistical distributions of pathogen occurrence in different water sources (WW = raw wastewater, SW = surface water, and GW = groundwater). The *Cryptosporidium* surface water distributions are provided for a bin 1 (S1), bin 2 (S2), and bin 4 (S3) surface water. The corresponding probability distribution functions and cumulative distribution functions are shown in Figures S1-S3.

Pathogen	Water	Concentration	Unit	Reference
Cryptosporidium	WW	Lognormal[a] ($10^{1.89}$, $10^{2.05}$)	oocysts/L	Rose et al. (2005)
	SW (S1)	Uniform[b] ($10^{-2.70}$,$10^{-1.12}$)		LeChevallier et al. (1991); USEPA (2010)
	SW (S2)	Uniform[b] ($10^{-1.12}$, $10^{0.00}$)		LeChevallier et al. (1991); USEPA (2010)
	SW (S3)	Uniform[b] ($10^{0.48}$, $10^{2.05}$)		LeChevallier et al. (1991); USEPA (2010)
	GW	0		Lodder & de Roda Husman (2005); Ogorzaly et al. (2010)
NoV	WW	Normal[c] ($10^{3.95}$, $10^{1.11}$)	gc/L	Eftim et al. (2017)
	SW	Lognormal[d] ($10^{2.95}$, $10^{3.22}$)		Lodder & de Roda Husman (2005)
	GW	Uniform[b] (0, $10^{-0.22}$)		Borchardt et al. (2012)
AdV	WW	Uniform[b] ($10^{3.25}$, $10^{8.62}$)	gc/L	Hewitt et al. (2011)
	SW	Uniform[b] ($10^{2.94}$, $10^{3.88}$)		Jiang et al. (2001)
	GW	Uniform[b] ($10^{-1.11}$, $10^{1.00}$)		Borchardt et al. (2012); Allard & Vantarakis (2017)
Salmonella	WW	Weibull[e] ($10^{-0.44}$, $10^{3.36}$)	MPN/L	Koivunen et al. (2003); Lemarchand & Lebaron (2003)
	SW	Uniform[b] ($10^{-0.22}$, $10^{2.63}$)		Lemarchand & Lebaron (2003)
	GW	0		Lodder & de Roda Husman (2005); Ogorzaly et al. (2010)

[a](mean, standard deviation) with $\mu = 3.80$ and $\sigma = 1.06$
[b](minimum, maximum)
[c](mean, standard deviation)
[d](mean, standard deviation) with $\mu = 6.04$ and $\sigma = 1.22$
[e](shape, scale)

Studies have reported mean NoV concentrations in raw wastewater as high as 7.70 $\log_{10}$ gc/L, but the corresponding sample sizes have been limited (Simmons et al., 2011) or based on small-scale applications such as a single office building (Jahne, 2017) (additional discussion in Text S1). With a more comprehensive review of the literature, Eftim et al. (2017) reported a mean concentration of 3.95 $\log_{10}$ gc/L and standard deviation of 1.10 $\log_{10}$ gc/L for pooled NoV genogroups (NoV GI and GII; Table 4.1). Although studies have reported infectivity data for AdV in wastewater (Hewitt et al., 2011; Hurst et al., 1988), few studies have reported infectivity data for source waters. To maintain consistency, genome copy data were used to describe AdV occurrence in raw wastewater, surface water, and groundwater (Table 4.1) (Jiang et al., 2001; Hewitt et al., 2011; Borchardt et al., 2012; Allard & Vantarakis, 2017).

4.2.3 Source water concentrations for target pathogens

4.2.3.1 Surface water

The *de facto* reuse system (TT1), the planned IPR systems with surface water augmentation (TT3 and TT4), and the DPR system with surface water blending (TT5) were all influenced by pathogen concentrations in the upstream surface water. Consistent with Amoueyan et al. (2017), the upstream surface water concentration of *Cryptosporidium* oocysts was based on the bin classification system established by the U.S. EPA's Long Term 2 Enhanced Surface Water Treatment Rule (LT2ESWTR) and occurrence data in LeChevallier et al. (1991). Using data for typical virus concentrations in surface water (Choi & Jiang, 2005; Haramoto et al., 2007; Jiang et al., 2001; Lodder & de Roda Husman, 2005; Katayama et al., 2017), a lognormal distribution was fit to NoV (Lodder & de Roda Husman, 2005), and a uniform distribution was fit to human AdV serotypes 40 and 41 (Jiang et al., 2001). A uniform distribution was also fit to published *Salmonella* concentrations in surface water (Byappanahalli et al., 2009; Haley et al.,

2009; Jyoti et al., 2010; Lemarchand & Lebaron, 2003; Levantesi et al., 2012). The distributions are summarized in Table 4.1, and the corresponding PDFs and CDFs are illustrated in Figure S2.

4.2.3.2 Groundwater

The planned IPR system employing groundwater replenishment was influenced by pathogen concentrations in the diluent groundwater. Although groundwater is less likely to be contaminated by bacteria and protozoa, albeit with some exceptions (Salvadori et al., 2009), groundwater systems are known to be susceptible to viral contamination (Ogorzaly et al., 2010; Rzeżutka & Cook, 2004). This is related to the longer survival of viral pathogens compared to fecal bacteria and the smaller sizes of viruses, which make them more likely to pass through the soil and reach the aquifer (Hijnen et al., 2005; Ogorzaly et al., 2010; Pang et al., 2005; Rzeżutka & Cook, 2004). In this study, uniform distributions were assumed for the diluent groundwater concentrations of NoV (Borchardt et al., 2012) and AdV (Borchardt et al., 2012; Allard & Vantarakis, 2017), while *Cryptosporidium* and *Salmonella* occurrence was assumed to be negligible. The distributions are summarized in Table 4.1, and the corresponding PDFs and CDFs are illustrated in Figure S3.

4.2.4 Pathogen log reduction values for the environmental buffer

This study focused on recycled water contribution (RWC), storage time, and temperature as the most important factors affecting pathogen dilution and die-off in the environmental buffer. All parameters related to pathogen dilution and die-off are summarized in Table 4.2. Surface water RWC was based on Rice et al. (2015), which evaluated nine source waters and found that six had RWCs of at least 20%, and a 270-day storage time was assumed for the surface water environmental buffer, consistent with the Trinity River in Texas (Wu, 2015). The groundwater RWC was based on data from Sloss et al. (1996), which indicated that the mean RWC for 66

70

groundwater replenishment sites at the Montebello Forebay was ~15% (Sloss et al., 1996; Text

S2). California requires no less than 2 months of storage in groundwater replenishment systems

(CDPH, 2014), so 2 months was also assumed for the baseline condition in the current study.

Table 4-2. Summary of model parameters for the environmental buffer baseline condition. All rate constants are base e.

Water	Parameter	Description	Value	Reference
GW	T_{GW}	Temperature	10°C	Nevecherya et al. (2005); Ogorzaly et al. (2010)
	RWC_{GW}	Recycled water contribution	15%	Calculated[a]
	t_{GW}	Storage time	2 months	CDPH (2014)
	$k_{Crypto,GW,10°C}$	Inactivation rate constant	0.014 d^{-1}	Calculated[b]
	$k_{NoV,GW,10°C}$	Inactivation rate constant	0.055 d^{-1}	Calculated[b]
	$k_{AdV,GW,10°C}$	Inactivation rate constant	0.029 d^{-1}	Calculated[b]
	$k_{Salmonella,GW,10°C}$	Inactivation rate constant	0.138 d^{-1}	Bitton et al. (1983)
SW	T_{SW}	Temperature	20°C	Peng et al. (2008)
	RWC_{SW}	Recycled water contribution	20%	Rice et al. (2015)
	t_{SW}	Storage time	270 days	Wu (2015)
	$k_{Crypto,SW,20°C}$	Inactivation rate constant	0.043 d^{-1}	Calculated[b]
	$k_{NoV,SW,20°C}$	Inactivation rate constant	0.875 d^{-1}	Calculated[b]
	$k_{AdV,SW,20°C}$	Inactivation rate constant	0.036 d^{-1}	Calculated[b]
	$k_{Salmonella,SW,20°C}$	Inactivation rate constant	0.349 d^{-1}	Calculated[b]

[a]Calculated based on Text S2; Sloss et al. (1996)
[b]Calculated with Eq. 2 and the parameters in Table 4.3

Several studies have evaluated survival (i.e., inactivation kinetics) of *Cryptosporidium*

(Peng et al., 2008), viruses (Yates & Gerba, 1983; Yates et al., 1985; Nevecherya et al., 2005;

Lee et al., 2008; Ogorzaly et al., 2010; Rigotto et al., 2011; Wu, 2015), and *Salmonella* (Bitton et

al., 1983; Nevecherya et al., 2005; Pachepsky et al., 2014; Sjorgen, 1994) in the environment.

Cryptosporidium is known to be highly persistent in the environment (Rzeżutka & Cook, 2004),

with base e inactivation rate constants of $k_{4°C} = 0.0051$ d^{-1} for groundwater and $k_{4°C} = 0.0093$ d^{-1}

for surface water (Peng et al., 2008). Inactivation rate constants for other temperatures can be

determined with Eq. 4.1 and dimensionless temperature modifiers of 0.158 for groundwater and

0.095 for surface water (Peng et al., 2008).

71

$$k_{Crypto,T} = k_{Crypto,4}e^{\lambda(T-4)} \qquad \text{(Eq. 4.1)}$$

where, $k_{Crypto,T}$ = base e *Cryptosporidium* inactivation rate constant at T°C (day^{-1}),

$k_{Crypto,4°C}$ = base e *Cryptosporidium* inactivation rate constant at 4°C (day^{-1}),

λ = dimensionless temperature modifier,

T = temperature of the surface water or groundwater (°C).

Data generated from Eq. 4.1 can be used in conjunction with Eq. 4.2 to calculate

activation energy and the Arrhenius equation constant, which can then be used as an alternative

approach for determining temperature-specific inactivation rate constants. This framework was

specifically needed for the other target pathogens but is also presented for *Cryptosporidium* in

Table 4.3.

Table 4-3. First order rate constants (base e) and associated Arrhenius equation parameters (Eq. 2) for *Cryptosporidium*, norovirus, adenovirus, and *Salmonella* inactivation (i.e., die-off) in groundwater and surface water.

Parameter	*Cryptosporidium*		Norovirus		Adenovirus		*Salmonella*	
	GW[a]	SW[a]	GW[b]	SW[c]	GW[d]	SW[e]	GW[f]	SW[g]
$k_{4°C}$ (d^{-1})	0.005	0.009	0.024	0.173	0.018	--	--	--
$k_{10°C}$ (d^{-1})	0.013	0.016	0.053	--	--	0.007	0.138	0.187
$k_{19°C}$ (d^{-1})	0.055	0.039	0.176	--	--	0.030	--	--
$k_{20°C}$ (d^{-1})	0.064	0.043	0.201	--	0.064	--	--	0.347
$k_{25°C}$ (d^{-1})	0.141	0.068	0.394	1.382	--	--	--	--
E_a (kJ/mole)[h]	108.22	65.07	91.94	67.96	54.85	111.94	N/A	42.66
C[h]	41.69	23.56	36.15	27.75	19.77	42.60	N/A	16.45

[a]Calculated with Eq. 1 (Peng et al., 2008)
[b]Calculated with Eq. 3 (Nevecherya et al., 2005) with MS2 as a surrogate
[c]Yang & Griffiths (2013) with MS2 as a surrogate
[d]Ogorzaly et al. (2010)
[e]Rigotto et al. (2011)
[f]Bitton et al. (1983)
[g]Pachepsky et al. (2014)
[h]Calculated with Eq. 3

The *Cryptosporidium* inactivation rate constants for the baseline conditions in the current study (i.e., 10°C for groundwater and 20°C for surface water) are summarized in Table 4.2.

$$ln\ k = \left(\frac{-E_a}{R}\right)\left(\frac{1}{T}\right) + C \qquad \text{(Eq. 4.2)}$$

where, k = base e inactivation rate constant (d^{-1}),

E_a = activation energy (kJ/mole),

R = universal gas constant = 0.008314 kJ/mole-K,

C = Arrhenius equation constant,

T = temperature (K).

Due to a lack of infectivity data, MS2 inactivation was used as a surrogate for NoV in the current study. Eq. 4.3 was proposed by Nevecherya et al. (2005) for determining the MS2 inactivation rate constant in groundwater as a function of temperature. Base e MS2 inactivation rate constants were also reported by Yang & Griffiths (2013) for surface water: 0.173 d^{-1} and 1.382 d^{-1} for temperatures of 4°C and 25°C, respectively. Published data for AdV inactivation are also summarized in Table 4.3 (Ogorzaly et al., 2010; Rigotto et al., 2011). These virus models and rate constants were then used in conjunction with Eq. 4.2 to determine the corresponding Arrhenius equation parameters and ultimately the inactivation rate constants for the baseline conditions in the current study, which are summarized in Table 4.2.

$$\log(1/k) = 1.862 - 0.0583 \times T \qquad \text{(Eq. 4.3)}$$

where, k = base e MS2 inactivation rate constant (assumed for NoV as well), day^{-1}

T = temperature of groundwater, °C (valid from 4-23°C)

As a point of comparison, California awards a 1-log virus credit for each month of storage/travel time in the aquifer. This is consistent with the MS2 inactivation rate constant determined with Eq. 3 for a temperature of ~13°C. However, when evaluating lower

73

temperatures or other viruses (e.g., AdV), the die-off rate may deviate from the California

framework, as illustrated in Figure 4.2.
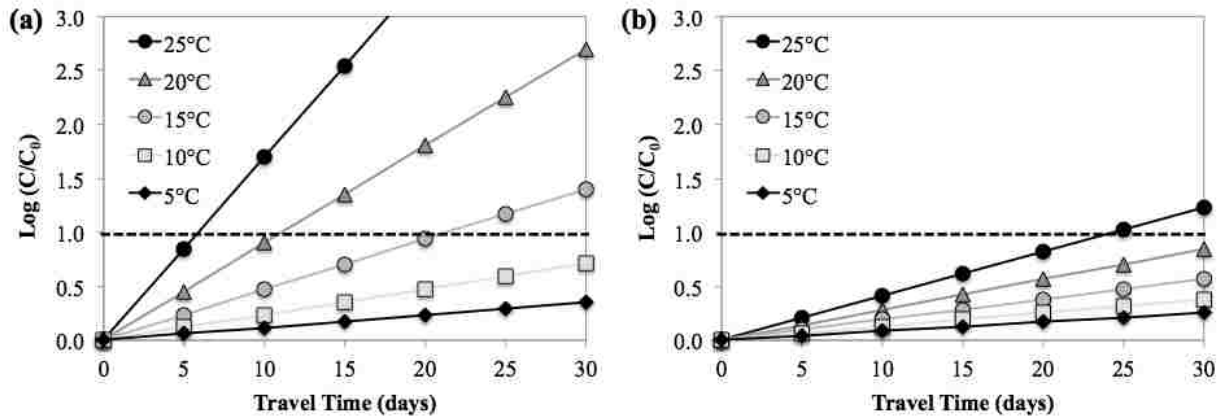
Figure 4-2. Estimated log reduction of (a) norovirus and (b) adenovirus in groundwater as a function of travel time and temperature

The following base e inactivation rate constants were reported for *Salmonella* in surface

water by Pachepsky et al. (2014): 0.187 d^{-1} and 0.347 d^{-1} for temperatures of 10°C and at 20°C,

respectively. On the other hand, there is a paucity of data describing *Salmonella* inactivation in

groundwater (Sjorgen, 1994; Gorden & Toze, 2003), and those existing studies may not be

representative and/or applicable to environmental survival according to John and Rose (2005).

Therefore, due to a lack of data, a base e inactivation rate constant of 0.138 day^{-1}, which was

determined for *Salmonella* in groundwater at temperatures ranging from 10-12°C (Bitton et al.,

1983), was assumed for this study.

4.2.5   Pathogen log reduction values for engineered treatment processes

When sufficient data were available in the literature, a probabilistic approach (i.e., a

statistical distribution on the LRV) was used to estimate pathogen removal/inactivation by each

engineered treatment process in the aforementioned treatment trains. In the case of insufficient

data for a particular pathogen, relevant surrogates were used, and in the case of limited data for

74

treatment reliability, point estimates were used for the expected LRV. These data, along with

typical probabilities of failure, are summarized in Table 4.4 and described in greater detail

below. Because the data in Table 4.4 represent observed treatment performance, they may differ

from the typical regulatory credit awarded to each treatment process. Regulatory credits are

summarized in Table S2 for comparison.

Table 4-4. Assumed pathogen log reduction values (LRVs) for engineered treatment processes for an assumed temperature of 25°C. N = normal distribution and U = uniform distribution.

Treatment process	Probability of failure	LRVs			
		Cryptosporidium	**Norovirus**	**Adenovirus**	*Salmonella*
WWTP CAS	--	N (1.58, 1.30)[e]	N (1.20, 0.78)[f]	N (2.34, 1.20)[g]	N (3.23, 0.76)[e]
DWTP Filter	--	3[r]	2[r]	2[r]	N/A
DWTP Cl₂	--	0[r]	2[q]	2[q]	U (2.30, 3.15)[p]
GW Cl₂	--	0[r]	4[r]	4[r]	U (2.30, 3.15)[p]
MF	0.0028[a]	N (4.60, 0.96)[h,n]	U (1.50, 3.30)[d]	U (2.40, 4.90)[d]	N (5.96, 1.47)[h,n]
UF	0.0028[a]	N (5.52, 0.51)[h,k]	N (4.00, 0.10)[h,i]	4.9[d,o]	N (4.80, 0.60)[h]
RO	0.00009[d]	N (4.50, 0.73)[h]	N (4.30, 0.34)[h,l]	U (2.70, 6.50)[d]	N (6.00, 0.60)[m]
BAC	--	U (0.00, 0.85)[d]	U (0.00, 1.00)[d]	U (0.00, 0.60)[d]	U (0.50, 2.00)[d]
Pre-O₃	0.0021[a]	Determined based on ozone CT (Eqs.4-6); O₃ CT= 5 (mg-min/L)[c]			
Post-O₃	0.000325[b,c]	Determined based on ozone CT (Eqs. 4-6); O₃ CT= 10 (mg-min/L)[c]			
UV	0.0002[d]	Determined based on UV dose (Eq. 7); UV dose = 80 (mJ/cm²)[s]			
ESB Cl₂	--	0[r]	6[t]	6[t]	U (2.30, 3.15)[p]

[a]Forss and Ander (2011); [b]Burns (2015); [c]Amoueyan et al. (2017); [d]Soller et al. (2017); [e]Ottoson et al. (2006) with *E. coli* as a surrogate for *Salmonella*; [f]Lodder et al. (2005); [g]Haramoto et al. (2007); [h]Chaudhary et al. (2017); [i]Matsushita et al. (2013); [k]Beauchamp et al. (2011); [l]Governal & Gerba (1999) with MS2 as a surrogate; [m]Gerba et al. (1997); [n]Hong et al. (2001); [o]Qui et al. (2015); [p]Francy et al. (2012); [q]USEPA (1991); [r]USEPA (2006a); [s]NWRI (2012); [t]Salveson et al. (2016)

4.2.5.1 *Conventional wastewater and drinking water treatment plant*

For the conventional wastewater treatment plant, normal distributions were assumed for

the LRVs for *Cryptosporidium* (Ottoson et al., 2006), NoV (Lodder et al., 2005), AdV

(Haramoto et al., 2007), and *Salmonella* (Ottoson et al., 2006) based on typical data for a

conventional activated sludge (CAS) process; no tertiary treatment was assumed.

For the conventional drinking water treatment plant, specifically conventional filtration, a

3-log credit was awarded for *Cryptosporidium* and a 2-log credit was awarded for NoV and AdV

75

for consistency with the U.S. EPA's Surface Water Treatment Rules (SWTRs) (USEPA, 1991). An additional 2-log credit was awarded for NoV and AdV for final disinfection with free chlorine to achieve the 4 total logs required by the U.S. EPA's SWTR. For TT2 with groundwater replenishment, free chlorine was assumed to achieve 4-log NoV and AdV inactivation consistent with the U.S. EPA's Ground Water Rule (USEPA, 2006a). For *Salmonella*, no LRV was awarded for conventional filtration, but inactivation by free chlorine was assumed to follow a uniform distribution (Francy et al., 2012).

4.2.5.2 *Low-pressure (MF/UF) and high-pressure (RO) membrane technologies*

According to WHO (2008), MF is expected to remove 3 to 4 logs of bacteria and protozoa but less than 1 log of viruses. More recent studies have reported 1.5 to 3.3-log removal of NoV with MF, 2.4 to 4.9-log removal of AdV with MF (Soller et al., 2017), up to 4.9-log removal of AdV with UF (Qui et al., 2015), and up to 9-log removal of *Salmonella* using MF (Chaudhry et al., 2017; Hong et al., 2001). During nominal operation, both MF and UF are capable of serving as absolute barriers for protozoan cysts (Hong et al., 2001; LeChevallier & Au, 2004; Reardon et al., 2005). Although the primary benefit of RO membranes is the removal of total dissolved solids (TDS), they are also capable of achieving significant pathogen attenuation, although the ability to demonstrate RO membrane integrity with suitable surrogate parameters often limits the corresponding regulatory LRV to ~2 logs (NRC, 2012). In practice, RO membranes are able to achieve up to 6.5-log removal of MS2 phage (Chaudhary et al., 2017; Governal & Gerba, 1999) and more than 6-log removal of bacteria (Gerba et al., 1997).

4.2.5.3 *Disinfection processes*

4.2.5.3.1 Ozonation

Log inactivation during ozonation was based on an ozone CT framework and assumed CT values of 5 mg-min/L and 10 mg-min/L for pre-ozone and post-ozone, respectively (Amoueyan et al., 2017). These CT values were used in conjunction with temperature-dependent equations for the inactivation of *Cryptosporidium* (Eq. 4.4) and viruses (Eq. 4.5) (USEPA, 2010). Thurston-Enriquez et al. (2005) indicated that 4-log inactivation of AdV and FCV (a surrogate for NoV) could be achieved at 5°C with ozone Ct values of 0.60 mg-min/L and 0.03 mg-min/L, respectively, which are much lower than the 1.2 mg-min/L required for generalized viruses at 5°C (Eq. 4.5; USEPA, 2010). Therefore, the U.S. EPA equations were assumed to represent a potentially conservative estimate of viral inactivation for this QMRA.

$$\textit{Cryptosporidium Log Credit} = 0.0397 \times (1.09757)^{\text{Temp}} \times \text{CT} \qquad \text{(Eq. 4.4)}$$

$$\text{Virus Log Credit} = 2.1744 \times (1.0726)^{\text{Temp}} \times \text{CT} \qquad \text{(Eq. 4.5)}$$

where, CT = product of ozone residual and contact time (mg-min/L),

Temp = temperature (°C)

Disinfection kinetics for *Salmonella* are poorly defined in the literature, thereby necessitating the use of bacterial surrogates such as *E. coli*. The Chick-Watson model (Eq. 4.6) was fit to ozone disinfection data for *E. coli* from Zuma et al. (2009), which resulted in a base e inactivation rate constant of 0.32 (mg-min/L)$^{-1}$. Temperature effects were not considered because studies have shown that temperature (0°C to 30°) does not have a significant impact on bacterial inactivation kinetics (Kinman & Rempel, 1975; Zuma et al., 2009). Additional details related to this calculation are provided in Text S4.

$$ln\frac{N}{N_0} = -k \times CT \qquad \text{(Eq. 4.6)}$$

77

where, k = base e Chick-Watson inactivation rate constant $[(\text{mg-min/L})^{-1}]$

CT = ozone CT value (mg-min/L)

Collectively, these CT values and models resulted in estimated *Cryptosporidium*, NoV, AdV, and *Salmonella* LRVs of 2, 6, 6, and 1.5 for pre-ozonation and 4.1, 6, 6, and 3.2 for post-ozonation, respectively, under nominal operating conditions and a wastewater temperature of 25°C.

4.2.5.3.2 *Chlorine*

Chlorination is known to be ineffective for *Cryptosporidium* inactivation so an LRV of 0 was assumed (USEPA, 2006a). The USEPA CT guideline (USEPA, 1991), which requires 3 mg-min/L at 20°C and 6 mg-min/L at 10°C for 4-log virus inactivation, was used as the basis for modeling viral LRVs with chlorination in surface water and groundwater, respectively. Also, for the engineered storage buffer (ESB) in the DPR systems, a conservative value of 18 mg-min/L was assumed for 6-log virus inactivation (Salveson et al., 2016). Francy et al. (2012) studied chlorination of secondary effluent at four wastewater treatment plants and observed a minimum log removal of 2.30 and a maximum log removal of 3.15 for *E. coli*. Due to lack of data on log inactivation of *Salmonella*, these values were used as a uniform distribution for *Salmonella* inactivation with free chlorine.

4.2.5.3.3 UV disinfection

Eq. 7 can be used in conjunction with the following base 10 rate constants to calculate expected LRVs for UV disinfection systems. *Cryptosporidium* [0.243 $(\text{mJ/cm}^2)^{-1}$; Hijnen et al., 2006] and *Salmonella* [0.515 $(\text{mJ/cm}^2)^{-1}$; Hijnen et al., 2006] are considered to be highly susceptible to UV inactivation, while AdV [0.024 $(\text{mJ/cm}^2)^{-1}$; Hijnen et al., 2006] is often the driver for the design of UV disinfection systems in drinking water applications. Although

78

reliable infectivity assays are not yet available for NoV, experiments with MNV [0.150

$(mJ/cm^2)^{-1}$; Text S5] indicate that NoV is likely highly susceptible to UV disinfection (Lee al.,

2008). As recommended by NWRI (2012), a target UV dose of 80 mJ/cm² was assumed in the

model, but pathogen removal was limited to 6 logs, in accordance with CDPH (2014). Although

some potable reuse systems employ UV doses aimed at NDMA photolysis (e.g., >100 mJ/cm²)

(Amoueyan et al. 2017), the 80-mJ/cm² disinfection dose was assumed for conservatism.

Moreover, treatment process failures and associated 'domino effects' were considered based on

changes in UV254 absorbance. Additional details related to this UV failure framework are

available in Amoueyan et al. (2017) and Text S6.

$$-log\left(\frac{N}{N_0}\right) = k_{UV} \times D \qquad \text{(Eq. 4.7)}$$

where, k_{UV} = base 10 UV$_{254}$ inactivation rate constant $(mJ/cm^2)^{-1}$,

D = UV$_{254}$ dose (mJ/cm^2).

4.2.6 Dose response models

Table 4.5 summarizes the various parameters used to estimate daily risk and DALYs per

illness assuming 2 L of daily drinking water consumption (USEPA, 2004; WHO, 2008). An

exponential dose response model was used for *Cryptosporidium* (Eq. 4.8; USEPA, 2006b) and

AdV (Eq. 4.8; Crabtree et al., 1997; Heerden et al., 2005), fractional Poisson was used for NoV

(Eq. 4.9; Messner et al., 2014), and beta Poisson was used for *Salmonella* (Eq. 10; Haas et al.,

1999; Soller et al., 2016). Estimating daily risk of AdV infection requires conversion of genome

copy data to an infectious dose using a tissue culture infective dose (TCID50) conversion factor

of 1/700 TCID50/gc (Lim et al., 2015; McBride et al., 2013).

Table 4-5. List of parameters used for dose response assessment and risk characterization calculations.

Description	Parameters	Unit	Reference
Dose-response parameters			
Cryptosporidium	r = 0.09	oocysts^{-1}	USEPA (2006b)
Norovirus	P = 0.722; μ = 1106	unitless; gc	Messner et al. (2014)
Adenovirus	r = 0.4172	unitless	Heerden et al. (2005); Haas et al. (1999)
Salmonella	α = 0.3126; β = 2884	unitless	Haas et al. (1999); Soller et al. (2016)
Adenovirus conversion factor	1/700	TCID50/gc	McBride et al. (2013); Lim et al. (2015)
Health Burden			
Cryptosporidium	0.0017	DALYs/case	Health Canada. (2012)
Norovirus	0.00095	DALYs/case	Kemmeren et al. (2006)
Adenovirus	0.0534	DALYs/case	Gaunt et al. (2011)
Salmonella	0.068	DALYs/case	Calculated[a]
Conditional probability of illness given an infection			
Cryptosporidium	$(P_{ill}|P_{inf})_{Crypto}$ = 0.7		Zhang et al. (2012)
Norovirus	η = 2.55×10^{-3}; $r_{ill,NoV}$ = 0.086		Teunis et al. (2008)
Adenovirus	$(P_{ill}|P_{inf})_{AdV}$ = 0.5		McBride et al. (2013); Lim et al. (2015)
Salmonella	$(P_{ill}|P_{inf})_{Salmonella}$ = 0.41		Jertborn et al. (1990); Calculated[b]

[a]Additional details in Text S7
[b]Based on symptomatic illness and total infection (Text S7)
gc= genome copies

It should also be noted that the AdV dose response model was developed based on AdV aerosol exposure through the inhalation route. Since there is a higher probability of infection through aerosols than ingestion, the use of an inhalation dose response model likely leads to a conservative risk estimate (USEPA, 2010b). The implications of using alternative dose response models [e.g., the fractional Poisson model for *Cryptosporidium* (Eq. 4.9) proposed by Messner et al. (2016)] was evaluated through sensitivity analysis.

$$P_{inf,d} = 1 - e^{-r \times Dose} \tag{Eq. 4.8}$$

where, $P_{inf,d}$ = daily probability of infection,

 r = dose response parameter,

 Dose = pathogen dose (oocysts for *Cryptosporidium* or TCID50 for AdV)

$$P_{inf,d} = P \times (1 - e^{-\frac{Dose}{\mu}}) \tag{Eq. 4.9}$$

where, P = fraction of susceptibles (P = 0.722 for NoV and 0.737 for *Cryptosporidium*)

μ = mean aggregate size (μ = 1106 for NoV and 1 for *Cryptosporidium*)

$$P_{inf,d} = 1 - (1 + \frac{Dose}{\beta})^{-\alpha} \qquad \text{(Eq. 4.10)}$$

where, α and β = beta Poisson dose response parameters

4.2.7 Risk characterization

The outcomes of this study for pathogen-specific annual risk (risk due to exposure to each target pathogen individually) (Eq. 4.11) and the combined annual risk (cumulative risk due to exposure to all pathogens) (Eq. 4.12) were compared against the benchmark risk of 10^{-4} infection per person per year and the WHO guideline for disease burden of 10^{-6} DALYs per person per year. All parameters used in the dose response assessment and risk calculations are summarized in Table 4.5.

$$P_{inf,a} = 1 - \prod_{i=1}^{365}(1 - P_{inf,d})_i \qquad \text{(Eq. 4.11)}$$

where, $P_{inf,a}$ = annual probability of infection.

$$P_{overall,\ inf,a} = 1 - (\prod_{i=1}^{365}[1 - P_{Cryp-inf,d}]_i \times \prod_{i=1}^{365}[1 - P_{NoV-inf,d}]_i \times \prod_{i=1}^{365}[1 -$$

$$P_{AdV-inf,d}]_i \times \prod_{i=1}^{365}[1 - P_{Salmoenlla-inf,d}]_i) \qquad \text{(Eq. 4.12)}$$

Disease burden (Eq. 4.13) was computed based on annual risk of illness and published health burdens for the target pathogens when available (Health Canada, 2012; Gaunt et al., 2011; Kemmeren et al., 2006), as summarized in Table 4.5.

$$DB = P_{ill,a} \times HB \qquad \text{(Eq. 4.13)}$$

where, DB = disease burden (DALYs/person-year),

$P_{ill,a}$ = annual risk of illness for an individual,

HB = health burden (DALY/case).

Annual risk of illness can be defined as the proportion of infectious individuals who develop symptomatic infection (Eq. 4.14).

$$P_{ill} = P_{inf} \times \left(P_{ill}|P_{inf}\right) \qquad \text{(Eq. 4.14)}$$

where, $(P_{ill}|P_{inf})$ = conditional probability of illness given an infection.

The conditional probability of illness given an infection has been reported as a point estimate for *Cryptosporidium* and adenovirus (Lim et al., 2015) and as a function of intake dose for norovirus (Teunis et al., 1999; Teunis et al., 2008), as described in Eq. 4.15.

$$P_{ill,NoV}|P_{inf,NoV} = 1 - (1 + \eta \times C_{NoV}w)^{-r_{ill,NoV}} \qquad \text{(Eq. 4.15)}$$

where, η and $r_{ill,NoV}$ = parameters of the distribution for the duration of infection,

C_{NoV} = concentration of norovirus in ingested drinking water (gc/L),

w = daily water consumption rate (L).

The health burden and conditional probability of illness given an infection due to exposure to *Salmonella* was not available in the literature so Eq. 4.16 was used in conjunction with published information for relevant parameters (Jertborn et al., 1990; Health Canada, 2012) (Text S7).

$$HB = YLD + LYL \qquad \text{(Eq. 4.16)}$$

where,　YLD = years lived with disability

LYL = life years lost due to mortality

4.2.8　Model platform and simulation approach

The STELLA 10.1 (ISEE Systems, Lebanon, NH) system dynamics platform was used to develop the model. The model was simulated with a Monte Carlo approach over 365 days and with 10,000 iterations. To evaluate parameter uncertainty, sensitivity analyses were conducted on the following parameters: (1) wastewater loading of pathogens (i.e., an outbreak condition), (2)

82

water temperature in the environmental buffer, (3) storage time in the environmental buffer, (4) recycled water contribution (RWC), and (5) dose-response model (i.e., *Cryptosporidium*). Factor sensitivity (FS) was used to quantify sensitivity (Zwietering and Van Gerwen, 2000; Amoueyan et al., 2017), according to Eq. 4.17. FS values greater than 0.3 and less than -0.3 indicated significant changes in risk.

$$FS = log_{10}\left(\frac{P_x}{P_{BL}}\right) \qquad \text{(Eq. 4.17)}$$

where, P_x = risk of infection for the modified condition

P_{BL} = risk of infection for the baseline condition.

4.3   Results and discussion

4.3.1   Comparison of public health risk for different potable reuse treatment trains

Pathogen LRV probability distribution functions for all potable reuse systems (assuming no failures) are shown in Figure 4.3. Under these 'optimal' conditions, all planned IPR and DPR treatment train achieved the 12-10-9-log reduction of viruses, *Cryptosporidium*, and bacteria, respectively, recommended by NWRI (2013). However, the LRV in the *de facto* reuse system was not compared with NWRI requirement since this treatment train was not 'officially' recognized as a reuse project. The impact of environmental buffers in attenuation of pathogens was not included in Figure 4.3.

The annual risk of infection was calculated for each of the target pathogens separately and also for the combined effect of all pathogens under both optimal and sub-optimal operation. The results for optimal operation are provided in Table S9, and the results for sub-optimal operation are summarized in Figure 4.4 and Table 4.6. A direct comparison of optimal and sub-optimal operation are shown in Figure S6. Infection risks for DPR treatment trains (TT6 and TT7) or IPR with FAT and groundwater replenishment (TT2) were typically less than the

83

benchmark risk of 10^{-4} for each individual pathogens and also for the combined risk of all pathogens. The only exception was for the maximum annual risk for AdV in TT7 (max = 7.3×10^{-04}), which was due to AdV's resistance to UV disinfection. Although TT6 also employed UV disinfection but UF and pre-ozonation prior to UV could sufficiently attenuate AdV concentration in TT6. TT2 was shown to be very effective for mitigating risks associated with *Cryptosporidium* and *Salmonella*, which is consistent with NRC (2012). TT2 was also effective for NoV and AdV, but MF process could achieve higher LRV of AdV compared to NoV. Therefore, the annual risk of infection due to AdV was less than NoV for this treatment train (mean= 7.8×10^{-6} and SD= 2.5×10^{-7} for AdV; mean = 1.2×10^{-5} and SD = 3.7×10^{-7} for NoV). Except for TT2, the risk associated with AdV was greater than for NoV. This was due to the higher concentrations of AdV in the water matrices and AdV's greater resistance to natural die-off and UV disinfection.

Table 4-6. Summary of infection risk and disease burden due to exposure to target pathogens in each treatment train during sub-optimal operation.

Pathogen	Annual Risk of Infection					Disease Burden				
	min	P5	median	P95	max	min	P5	median	P95	max
TT1, TT3, TT4, TT5 (surface water discharge or blending)										
Crypto (S1)	1.8E-03	1.9E-03	2.0E-03	2.1E-03	2.2E-03	2.2E-06	2.3E-06	2.4E-06	2.5E-06	2.6E-06
Crypto (S2)	2.6E-03	2.7E-03	2.8E-03	2.9E-03	3.1E-03	3.0E-06	3.2E-06	3.4E-06	3.5E-06	3.6E-06
Crypto (S3)	8.7E-03	9.1E-03	9.6E-03	1.0E-02	1.1E-02	1.0E-05	1.1E-05	1.1E-05	1.2E-05	1.3E-05
NoV	2.6E-04	2.9E-04	3.4E-04	4.0E-04	4.5E-04	7.6E-14	1.3E-13	2.2E-13	4.9E-13	1.7E-12
AdV	1.1E-03	1.2E-03	1.2E-03	1.3E-03	1.3E-03	3.0E-05	3.1E-05	3.3E-05	3.4E-05	3.5E-05
Salmonella	8.0E-04	8.7E-04	1.0E-03	1.2E-03	1.3E-03	2.2E-05	2.4E-05	2.8E-05	3.2E-05	3.6E-05
Combined	5.0E-03	5.2E-03	5.4E-03	5.6E-03	5.7E-03	-	-	-	-	-
TT2 (FAT with groundwater replenishment)										
Crypto	4.0E-14	3.9E-13	3.6E-12	9.9E-11	6.3E-7	4.7E-17	4.6E-16	4.3E-15	1.2E-13	7.5E-10
NoV	1.1E-05	1.2E-05	1.2E-05	1.3E-05	1.3E-05	1.2E-16	1.3E-16	1.4E-16	1.5E-16	1.6E-16
AdV	5.0E-06	5.3E-06	5.6E-06	6.3E-06	5.5E-05	1.3E-07	1.4E-07	1.5E-07	1.7E-07	1.5E-06
Salmonella	0.0E+00	0.0E+00	0.0E+00	0.0E+00	0.0E+00	0.0E+00	0.0E+00	0.0E+00	0.0E+00	0.0E+00
Combined	1.6E-05	1.7E-05	1.8E-05	1.9E-05	6.7E-05	-	-	-	-	-
TT6 (DPR with ozone-BAC and direct distribution)										
Crypto	1.4E-11	2.2E-11	8.5E-10	2.6E-07	3.6E-06	1.7E-14	2.6E-14	1.0E-12	3.1E-10	4.2E-09
NoV	0.0E+00	0.0E+00	8.2E-14	9.5E-12	1.3E-06	0.0E+00	0.0E+00	0.0E+00	0.0E+00	0.0E+00
AdV	2.7E-11	4.6E-11	1.8E-08	4.4E-06	6.7E-05	0.0E+00	1.2E-12	4.7E-10	1.2E-07	1.8E-06
Salmonella	0.0E+00	0.0E+00	0.0E+00	2.4E-13	1.4E-10	0.0E+00	0.0E+00	0.0E+00	6.8E-15	4.0E-12
Combined	6.0E-11	1.0E-10	5.4E-08	4.4E-06	6.7E-05	-	-	-	-	-
TT7 (DPR with FAT and direct distribution)										
Crypto	4.5E-12	8.6E-12	3.7E-11	2.5E-09	7.7E-05	5.4E-15	1.0E-14	4.4E-14	3.0E-12	9.1E-08
NoV	0.0	1.0E-12	1.4E-12	3.1E-11	1.0E-07	0.0E+00	0.0E+00	0.0E+00	0.0E+00	0.0E+00
AdV	1.5E-07	4.5E-07	1.2E-06	1.5E-05	7.3E-04	4.0E-09	1.2E-08	3.3E-08	4.1E-07	1.9E-05
Salmonella	0.0E+00	0.0E+00	0.0E+00	0.0E+00	5.4E-14	0.0E+00	0.0E+00	0.0E+00	0.0E+00	1.5E-15
Combined	1.5E-07	4.5E-07	1.2E-06	1.5E-05	7.3E-04	-	-	-	-	-

85

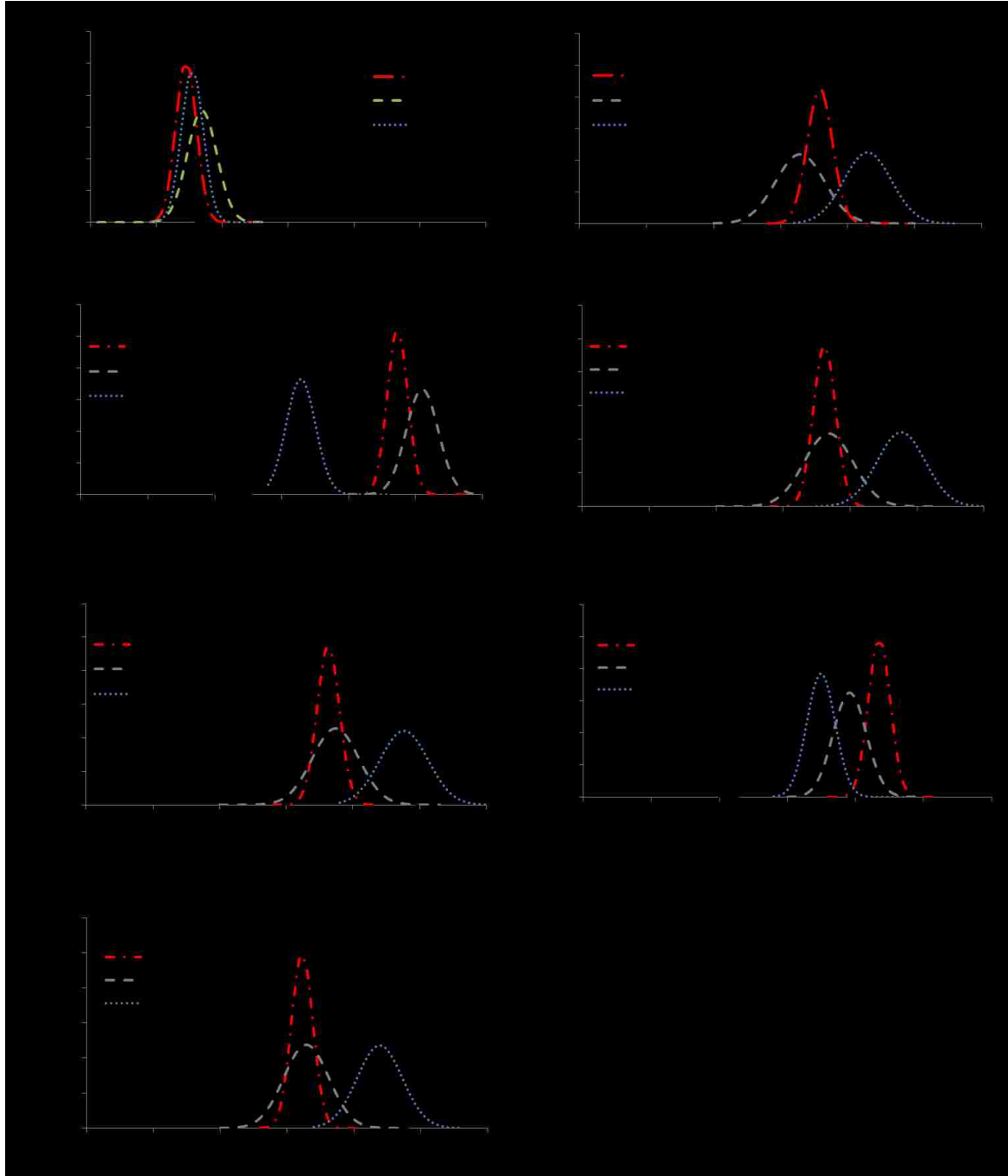**Figure 4.3.** Log reduction of target pathogens in potable reuse treatment trains during optimal operation (i.e., no failure). Pathogen attenuation in environmental buffers was not calculated in LRV. The LRVs for *de facto* reuse was shown as a comparison with other treatment trains. However, it was not compared with the recommended 12-10-9 LRVs since it is not officially recognized as a reuse project.

86

Figure 4.4. Annual risk of infection due to exposure to (A) *Cryptosporidium*, (B) norovirus, (C) adenovirus, and (D) *Salmonella* during sub-optimal operation. The risk for *Salmonella* with TT2 was below what could be assessed by the model and was calculated as zero. Also, the "+" for TT6 and TT7 indicates the maximum risk for *Salmonella*; the corresponding min, 25th, 50th, and 75th percentiles ranged from 0 to 8.4×10^{-15}).

All of the treatment trains employing either surface water discharge (IPR: TT1, TT3, and TT4) or blending (DPR: TT5), exhibited identical results for annual risk for all pathogens, with values exceeding the 10^{-4} annual risk benchmark. This indicates that the risks for these treatment trains were dominated by pathogen concentrations in the upstream surface water. Previous studies reported similar results (Amoueyan et al., 2017; Chaudhary et al., 2017). On the other hand, risks associated with the DPR systems with direct distribution (TT6 and TT7) were up to 10 orders of magnitudes lower than the surface water systems for all pathogens.

The results of combined risk for all pathogens (Table 4.6) showed that TT2 (IPR with FAT and groundwater replenishment) and TT6 (DPR with ozone-biofiltration and direct distribution) were below the 10^{-4} benchmark at all times, while the combined risk for TT7 complied with the 10^{-4} benchmark at the 95th percentile but exceeded the benchmark with its

87

maximum value. However, TT7 was still more reliable than the surface water IPR systems. TT6 was superior to all other treatment trains with combined annual risk ranging from 6.0×10^{-11} to 6.7×10^{-5}.

Figure 4.5 illustrates the calculated disease burdens for each of the treatment trains and for each target pathogen. When the infection risks of NoV were translated to disease burdens, they all fell below the WHO's recommended threshold of 10^{-6} DALYs per person per year. In contrast, the disease burdens of *Cryptosporidium*, AdV, and *Salmonella* for the surface water treatment trains (TT1, TT3, TT4 and TT5) all exceeded the recommended threshold. The disease burdens were the lowest in the DPR systems with direct distribution (TT6 and TT7) and IPR with groundwater replenishment (TT2) although the maximum values for AdV still exceeded the 10^{-6} benchmark.

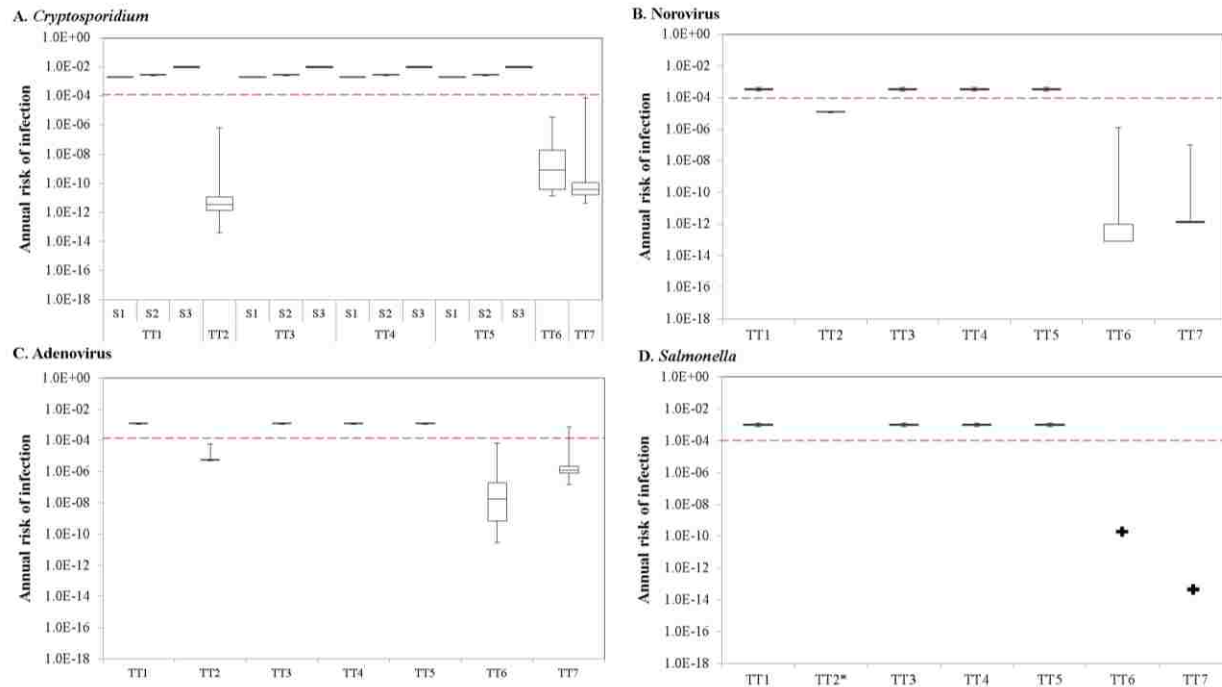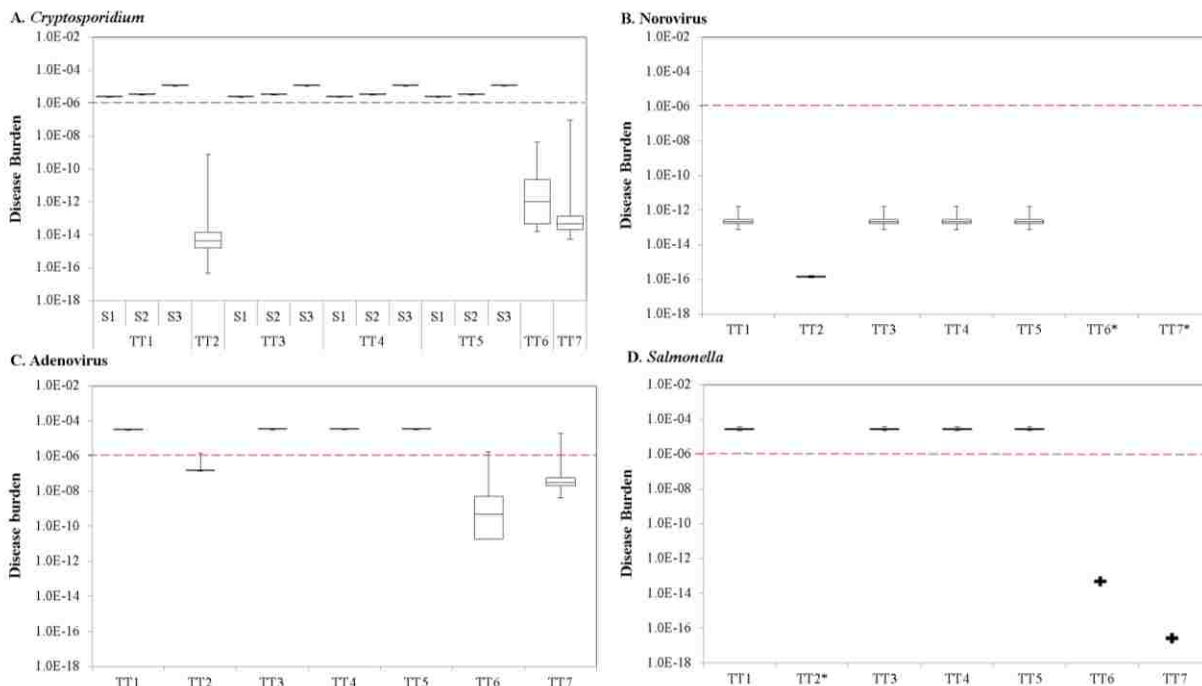**Figure 4-5.** Disease burden due to exposure to (A) *Cryptosporidium*, (B) norovirus, (C) adenovirus, and (D) *Salmonella* during sub-optimal operation.
Disease burdens for *Salmonella* with TT2 and norovirus with TT6 and TT7 were below what could be assessed by the model and was calculated as zero. Also, the "+" for TT6 and TT7 indicates the maximum disease burden for *Salmonella*; the corresponding min, 25th, 50th, and 75th percentiles ranged from 0 to 2.3×10^{-16}).

88

4.3.2 Results of sensitivity analyses

4.3.2.1 Impact of wastewater loading of pathogens (outbreak conditions)

With respect to *Cryptosporidium*, outbreak conditions have previously been defined as a

1-log increase in the raw wastewater concentration, in accordance with published data for the

1993 Milwaukee outbreak (Haas and Rose, 1995). The results for the IPR systems (TT1-TT4)

showed that with sufficient storage time (i.e., at least 270 days at 20ºC in surface water and 2

months at 10°C in groundwater), the impacts of higher wastewater loadings could be entirely

mitigated (Figure S7). DPR systems with direct distribution (TT6 and TT7) were significantly

impacted by an increase in *Cryptosporidium* concentration, and the risks increased proportionally

by a factor of 10. Nevertheless, the final risks for the DPR systems (6.7×10^{-10} and 7.7×10^{-10} for

TT6 and TT7, respectively) were still several orders of magnitude lower than the benchmark risk

(Table 4.7). DPR with blending upstream of the drinking water treatment facility (TT5) achieved

similar results as IPR systems with surface water augmentation.

Table 4-7. Impact of wastewater loading (outbreak conditions) on annual risk of infection during sub-optimal operation. Corresponding graphs are shown in Figure S7-S10.

Train	*Cryptosporidium*		Norovirus		Adenovirus[b]		*Salmonella*	
	Normal	Outbreak	Normal	Outbreak	Normal	Outbreak	Normal	Outbreak
TT1	NS	NS	NS	NS	1.2E-03	8.0E-02[b]	NS	NS
TT2	NS	NS	NS	NS	5.5E-06	4.5E-04[b]	NS	NS
TT6	6.7E-11	6.7E-10	1.5E-09	2.5E-08	1.3E-10	1.3E-06[b]	0.0E+00	2.2E-10[d]
TT7	7.6E-11	7.7E-10	2.8E-10	1.9E-07	1.1E-06	1.1E-04[c]	NS	NS

Note: TT3, TT4, and TT5 were not impacted by outbreak conditions and therefore are not included in this table.
[a]NS = not significant
[b]These results are for 4-log increase in adenovirus concentration in wastewater.
[c] These results are for 2-log increase in adenovirus concentration in wastewater which resulted in a risk above 10^{-4} benchmark.
[d] These results are for 5-log increase in *Salmonella* concentration in wastewater.

With respect to NoV, outbreaks have been linked to 5-log increases in wastewater

concentrations (Barker et al., 2013). This simulated increase resulted in only a 1-log increase in

risk for TT6 (DPR with ozone-BAC and direct distribution) and a 3-log increase for TT7 (DPR

89

with FAT and direct distribution) (Table 4.7). Similar to *Cryptosporidium*, the IPR systems (TT1-TT4) and the DPR system with blending (TT5) were not significantly impacted by higher concentrations of NoV.

Due to a lack of data on AdV outbreaks, wastewater concentrations were increased by 1 to 5 logs for consistency with *Cryptosporidium* and NoV, respectively. The results showed that the DPR systems with direct distribution (TT6 and TT7) were impacted the most by an AdV outbreak (Table 4.7 and Figure S9). With only a 2-log increase in AdV concentration in wastewater, the risk of infection in TT7 ($\approx 1.1 \times 10^{-04}$) exceeded the benchmark risk. This was due to the high level of resistance of AdV to UV disinfection. However, in TT6, UF and pre-ozonation prior to UV could sufficiently attenuate AdV concentration. Similar results were obtained for TT2 (IPR with FAT and groundwater replenishment) when the concentration of adenovirus increased by 4 logs. The greater robustness of TT2 compared to TT7 was due to the additional attenuation achieved by inactivation in the environmental buffer. However, the benchmark risk was still exceeded with the 4-log increase in AdV concentration because AdV is more stable in the environment than other viruses, as shown previously in Figure 4.2. Also, although TT1 (*de facto* reuse) was significantly impacted by a 3-log increase in AdV concentration, the other IPR systems (TT3 and TT4) and the DPR system with surface water blending (TT5) were not impacted by the outbreak, even with a 5-log increase in AdV concentration. However, it should be noted that the risk for AdV in TT1, TT3, TT4, and TT5 had already exceeded the 10^{-4} benchmark risk for the baseline condition (i.e., in the absence of an outbreak). Thus, it can be concluded that TT6 was the most robust treatment train during an outbreak of AdV.

90

Similar to AdV, outbreaks of *Salmonella* have resulted in a wide range of published wastewater concentrations (Blaser et al., 1982; Teunis et al., 2010). Therefore, *Salmonella* risk during an outbreak was also modeled based on 1 to 5-log increases in wastewater concentration (Figure S10). The results showed that only TT6 was significantly impacted by increases in *Salmonella* concentration (i.e., 4-log increase in annual risk for a 5-log increase in *Salmonella* concentration). The exclusivity of the effect to TT6 was due to lower LRVs for the ozone-biofiltration treatment train (as compared with FAT) coupled with the absence of an environmental buffer (as compared with IPR) to compensate for the higher *Salmonella* concentrations. Nevertheless, the final *Salmonella* risk for all treatment trains, including TT6, was still well below the 10^{-4} benchmark risk.

4.3.2.2 *Impact of storage time in environmental buffer*

Among treatment trains that utilized an environmental buffer (either surface water or groundwater), TT1 (S1) (i.e., *de facto* reuse with the lowest concentration of *Cryptosporidium*) and TT1 (S2) (*de facto* reuse with a moderate concentration of *Cryptosporidium*) were the most sensitive treatment trains to changes in storage time when targeting *Cryptosporidium*. The annual risk of infection started to increase significantly when storage time decreased from 270 days to 120 days and 60 days for S1 and S2, respectively (Figure 4.6a). In other words, storage time is a significant factor when conventionally treated wastewater is discharged into relatively high quality surface water supplies. These results are slightly different from Amoueyan et al. (2017), which identified 150 days and 90 days as critical storage times for S1 and S2, respectively. This is because an exponential dose response parameter of 0.09 was used in the current study vs. 0.00419 in Amoueyan et al. (2017).

The annual risk of infection for *Cryptosporidium* was also sensitive to storage time for TT2 (IPR with FAT and groundwater replenishment), albeit to a lesser extent. The change became significant when storage time in the groundwater decreased from the baseline value of two months to one month (Figure 4.6b). However, the final risk for TT2 was still well below the 10^{-4} benchmark regardless of storage time. This was related to the efficacy of FAT in attenuating *Cryptosporidium* and the assumption that *Cryptosporidium* was not present in diluent groundwater. The other planned IPR systems (TT3-TT5) were not significantly impacted by changes in storage time because of the low *Cryptosporidium* concentrations in the advanced treated wastewater, which made the *Cryptosporidium* concentration in the upstream surface water the dominant factor. AdV was also sensitive to storage time because of its resistance to environmental stress. The results of the sensitivity analysis (Figure 4.6c) indicated that storage times less than 150 days for TT1 (*de facto* reuse) led to significantly higher risk of infection. Similar to *Cryptosporidium*, the risk of adenovirus in the planned IPR systems (TT2-TT4) were not impacted by changes in storage time due to the very low AdV concentrations in the advanced treated wastewater.

With respect to NoV and *Salmonella*, storage time was not a significant parameter.

Figure 4-6. Sensitivity analysis on storage time in environmental buffer a) TT1 (de facto reuse) targeting *Cryptosporidium* for scenario 1 and 2, b) TT2 (IPR with groundwater replenishment) targeting *Cryptosporidium*, and c) TT1 (de facto reuse) targeting adenovirus. (Asterisk * indicates the baseline conditions). FS values greater than 0.3 and less than -0.3 indicates significant changes in risk. For example, an FS value of 0.3 indicates the risk has increased by a factor of 2 due to the changes in storage time.

4.3.2.3 *Impact of recycled water contribution in the environmental buffer*

With respect to *Cryptosporidium,* annual risk of infection was inversely related to RWC

in IPR systems with surface water augmentation and the baseline storage time of 270 days

(Figure 4.7a). When RWC increased to 40% and 80%, annual risks of infection in the IPR

systems with surface water augmentation (TT1, TT3, and TT4) decreased by 25% and 75%,

respectively. However, these results may vary with shorter storage times, as explained previously
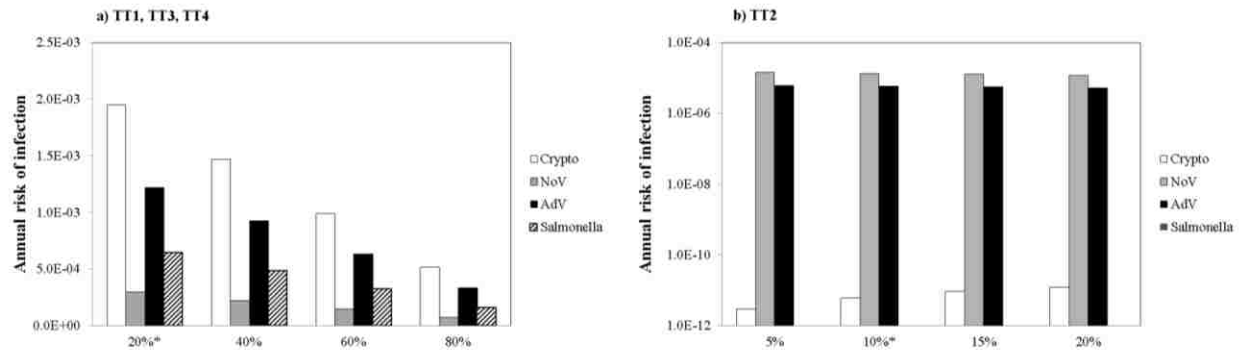
in Amoueyan et al. (2017).

93

Figure 4-7. Sensitivity analysis on RWC for a) TT1, TT3, and TT4 (IPR with surface water augmentation at storage time of 270 days and temperature of 20°C) and b) TT2 (IPR with groundwater replenishment at storage time of 60 days and temperature of 10°C). These results may vary with shorter storage times, as explained previously in Amoueyan et al. (2017). (Asterisk * indicates the baseline conditions)

Similar results were obtained for NoV, AdV, and *Salmonella* in the IPR systems with surface water augmentation. However, the results were different for TT2 (IPR with FAT and groundwater replenishment), for which higher RWCs led to slightly higher risk of infection for *Cryptosporidium* (Figure 4.7b). When RWC increased from 15% to 20%, the annual risk of infection increased by 34%. Also, decreasing the RWC from the baseline value of 10% to 5% resulted in a 68% reduction in risk. This is due to the assumption that *Cryptosporidium* was not present in the diluent groundwater. For NoV and AdV, there were no significant changes in annual risk of infection with higher RWCs. Also, the *Salmonella* risk for TT2 was below the level that could be assessed by the model.

4.3.2.4 *Impact of water temperature in the environmental buffer*

Similar to the storage time, *Cryptosporidium* risk was impacted the most by varying water temperature in the environmental buffer for TT1 (S1 and S2) and TT2. Temperature changes did not significantly impact TT1 at scenario 3 (ie., with the highest concentration of *Cryptosporidium* in surface water) due to robust treatment provided at the drinking water treatment plant. The risk of infection increased 4-fold in TT1 (S1) and 0.3-fold in TT1 (S2) when temperature dropped from 20°C to 10°C. This was due to slower inactivation kinetics at lower

94

temperatures and the lower level of treatment employed for S1 at the conventional drinking water treatment plant (consistent with LT2). Also, the risk significantly increased for TT2 when the temperature of the groundwater dropped from 10ºC to 5ºC, which again was attributed to slower inactivation kinetics. The other planned IPR systems (TT3 and TT4) were insensitive to temperature changes in the environmental buffer. With respect to AdV, surface water temperatures lower than 20ºC resulted in up to 2 orders of magnitude higher risks than the baseline condition, while no significant reduction in risk was observed at temperatures higher than 20ºC. Temperatures changes were insignificant for NoV and *Salmonella*.

4.3.2.5 *Impact of treatment process failure*

No significant differences in risk were observed in the event of treatment process failures for the planned IPR systems with surface water augmentation (TT3 and TT4) or the DPR system with surface water blending (TT5). Therefore, only the results for TT2 (IPR with FAT and groundwater replenishment), TT6 (DPR with ozone-BAC and direct distribution), and TT7 (DPR with FAT and direct distribution) were impacted by failures (Table 4.8).

Table 4-8- Sensitivity analysis on treatment process failures

Pathogens	Planned IPR			Ozone-based DPR			FAT-based DPR		
	MF	RO	UV	UF	pre-O3	UV	MF	RO	UV
Crypto	3.17	3.58	**6.00**	**5.86**	1.92	**6.00**	4.02	4.11	**6.00**
NoV	0.00	0.00	0.00	N/A	N/A	N/A	0.65	**4.25**	**6.08**
AdV	1.05	2.27	0.22	**5.34**	**6.89**	1.92	3.55	4.63	1.92
Salmonella	N/A	N/A	N/A	2.78	0.00	**4.56**	2.15	**3.29**	**3.40**

Note: N/A indicates the risk for *Salmonella* was below the limits that could be assessed by the model

Although AdV was less impacted by UV failure due to its inherent resistance to UV, failures during UV disinfection were particularly important for *Cryptosporidium*, NoV (in FAT-based DPR), and *Salmonella* (in both DPR systems) because their overall LRVs decreased by up to 6 logs. Therefore, even though DPR systems with direct distribution achieved a lower risk of

95

infection compared to the planned IPR systems (except TT2), the planned IPR systems were more robust in the event of treatment process failure due to the effects of the environmental buffer. Generally, UF and UV were identified as critical processes for *Cryptosporidium* attenuation; RO and UV as critical processes for norovirus and *Salmonella* attenuation; and pre-ozonation and UF were identified as critical processes for adenovirus attenuation.

4.3.2.6 *Impact of dose-response model*

The fractional Poisson model was also used as an alternative dose response model for *Cryptosporidium*, as suggested by Messner et al. (2016). The results showed that by using fractional Poisson, the final risk due to exposure to *Cryptosporidium* in all treatment trains increased about 7-fold. Previous studies on fractional Poisson dose response model for *Cryptosporidium* showed similar results (Soller et al., 2016). However, in DPR systems with direct distribution (TT6 and TT7) and planned IPR system with groundwater replenishment (TT2) the risk was still well below the benchmark of 10^{-4}. While, in the IPR systems with surface water augmentation (TT1, TT3, and TT4) and DPR with blending (TT5), employing fractional Poisson model instead of exponential model increased the risk up to 7.3×10^{-2}.

4.4 Conclusion

All potable reuse treatment trains evaluated in this study could achieve the 12-10-9-log reduction of viruses, *Cryptosporidium*, and bacteria, respectively, recommended by NWRI (2013). However, potable reuse treatment trains with surface water utilization (IPRs with surface water augmentation and DPR with blending upstream of the drinking water treatment facility) resulted in similar risks which all exceeded the benchmark of 10^{-4} for each individual pathogen and for the combined effect of all pathogens. This indicated that the risks for these treatment trains were dominated by concentration of pathogens in the upstream surface water. DPR

96

treatment trains with direct distribution and planned IPR system with groundwater replenishment typically resulted in risk of infection less than the benchmark of 10^{-4}. Although the combined risk of all pathogens in TT7 (DPR with FAT and direct distribution) exceeded the 10^{-4} benchmark at the maximum value (7.3×10^{-4}) but the 95th percentile was below the benchmark (1.5×10^{-5}) and this treatment train was still more reliable than the IPR systems with surface water augmentation. TT6 led to the lowest combined risk among all other treatment trains ranging from 6.0×10^{-11} to 6.7×10^{-5} annual risk of infection per person per year.

Although DPR systems resulted in lower risk than IPR systems with surface water augmentation, the performance of DPR systems were significantly impacted during outbreak conditions. The results of this study indicated that, risk of infection from *Cryptosporidium* during outbreak conditions increased by a factor of 10 in DPR systems while, IPR systems could sufficiently mitigate the higher wastewater loading, if at least 270 days at 20ºC and 2 month of storage time at 10°C could be provided in surface water and groundwater, respectively. Nevertheless, the final risks for the DPR systems (6.7×10^{-10} and 7.7×10^{-10} for TT6 and TT7, respectively) were still several orders of magnitude lower than the benchmark risk. With respect to AdV, this study suggested TT6 was the most robust treatment train during the outbreak conditions.

The study also identified 120 days and 150 days as the critical storage times in surface water in the *de facto* reuse systems when targeting *Cryptosporidium* and AdV, respectively. Also, when temperature in surface water dropped from 20°C to 10°C, risk of *Cryptosporidium* and adenovirus increased up to 4-fold and 20-fold, respectively. This was due to slower inactivation kinetics at lower temperatures especially for AdV. With respect to NoV and *Salmonella*, storage time and temperature were not significant parameters.

97

Also, the results identified UV disinfection as a significant treatment process in the DPR systems when targeting *Cryptosporidium* and norovirus. However, no significance impact was observed in planned IPR systems with surface water augmentation (TT3 and TT4) or the DPR system with surface water blending (TT5) in the event of treatment process failures.

The conclusions from this model can be used to better characterize public health risk associated with different waterborne pathogens in potable reuse applications and to better understand the critical parameters and operational conditions that could significantly impact the performance of potable reuse systems.

Acknowledgements

Supplementary Information

Supplementary data related to this article can be found in Appendix 2 of this dissertation.

5 A Dynamic Quantitative Microbial Risk Assessment for Norovirus Exposure in Potable Reuse Systems

ERFANEH AMOUEYAN[1], SAJJAD AHMAD[1], JOSEPH EISENBERG[2], DANIEL

GERRITY[1]*

[1]Department of Civil and Environmental Engineering and Construction, University of Nevada,

Las Vegas, Box 454015, 4505 S. Maryland Parkway, Las Vegas, NV 89154-4015, United States

[2]Department of Epidemiology, School of Public Health, University of Michigan, Ann Arbor,

Michigan, United States

*Corresponding author. Mailing address: Department of Civil and Environmental Engineering

and Construction, University of Nevada, Las Vegas, Box 454015, 4505 S. Maryland Parkway,

Las Vegas, NV 89154-4015, United States. Phone: (702) 895-3955. Fax: (702) 895-3936. Email:

Daniel.Gerrity@unlv.edu.

5.1   Introduction

In 1996, the Pathogen Risk Assessment Working Group of the International Life Sciences Institute (ILSI) collaborated with the United States (U.S.) Environmental Protection Agency (EPA) to develop a revised framework for quantitative microbial risk assessment (QMRA). Specifically, the working group emphasized the need for inclusion of secondary transmission and immunity to improve risk estimates for waterborne disease (ILSI, 1996). Soon thereafter, Eisenberg et al. (1996) described the first dynamic model for waterborne disease, and then Eisenberg et al. (2002; 2004) expanded the model to account for the unique properties of target pathogens, including asymptomatic vs. symptomatic infection rates; the duration of incubation, infection, and immunity; and shedding rate (Eisenberg et al., 2002; 2004).

Most QMRAs for waterborne pathogens involve static models, in which the probability of infection is calculated as a single exposure event. However, outbreaks caused by highly contagious pathogens (e.g., norovirus; NoV) often involve a significant number of 'secondary' cases (Zelner et al., 2010). Most static models do not capture the effects of secondary transmission, thereby underestimating the true risk of waterborne disease within a community. In contrast, dynamic QMRAs allow for differentiation of major pathogen sources, waterborne vs. foodborne exposure, primary vs. secondary transmission, etc. A typical dynamic framework with various epidemiological states [susceptible (S), exposed (E), carrier state 1 (C1), diseased (D), carrier state 2 (C2), and post-infection (P)] is illustrated in Figure 5.1. Dynamic disease transmission models have been used to characterize risk due to recreational exposures to *Giardia* (Eisenberg et al., 1996), the Milwaukee cryptosporidiosis outbreak (Eisenberg et al., 1998; Eisenberg et al., 2005; Brookhart et al., 2002), risks due to exposure to biosolids-amended soils

100

(Eisenberg et al., 2004); parsimony for static vs. dynamic modeling frameworks (Soller and

Eisenberg, 2008); and the duration of post-infection immunity to NoV (Simmons et al., 2013).
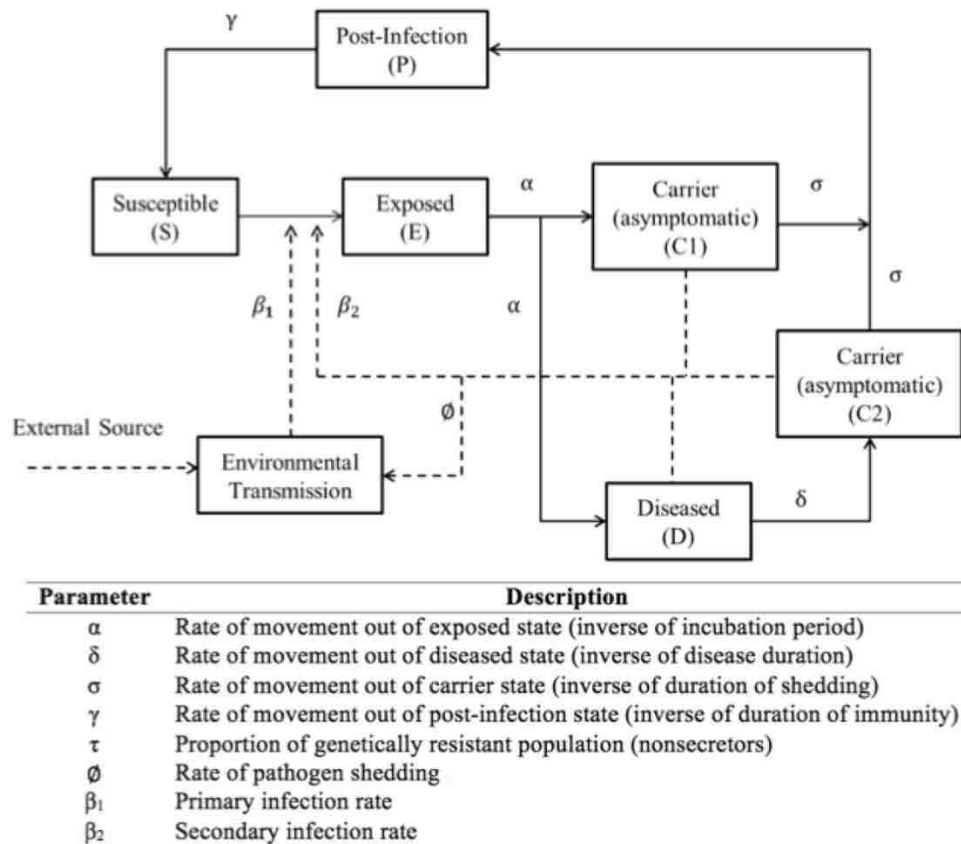

Parameter	Description
α	Rate of movement out of exposed state (inverse of incubation period)
δ	Rate of movement out of diseased state (inverse of disease duration)
σ	Rate of movement out of carrier state (inverse of duration of shedding)
γ	Rate of movement out of post-infection state (inverse of duration of immunity)
τ	Proportion of genetically resistant population (nonsecretors)
Ø	Rate of pathogen shedding
β_1	Primary infection rate
β_2	Secondary infection rate

Figure 5-1. Graphical depiction of the dynamic disease transmission model.
The movement of individuals from one state to another is represented with solid lines, and
pathogen transmission routes are represented by dashed lines.

NoV is the most common cause of acute gastroenteritis in the U.S., with approximately

20 million cases annually that affect up to 5% of the population (Hall et al., 2013a). NoV has

been implicated in several waterborne outbreaks linked to contaminated well water or

recreational water (Anderson et al., 2003; Parshionikar et al., 2003), but NoV is generally

transmitted through contaminated food, accounting for up to 50% of all foodborne outbreaks in

the U.S. (CDC, 2009-2011). Therefore, it is important to characterize the relative significance of

101

waterborne vs. foodborne NoV outbreaks to aid in developing effective and cost-efficient interventions.

Several studies have presented QMRAs on indirect potable reuse (IPR) and direct potable reuse (DPR) systems for a wide variety of waterborne pathogens (Olivieri et al., 1999; Amoueyan et al., 2017; Chaudhry et al., 2017; Lim et al., 2017; Pecson et al., 2017; Soller et al., 2017). However, these models generally involve a static framework that does not account for the impacts of alternative exposure routes (e.g., consumption of contaminated food), secondary transmission, or the duration of post-infection immunity. Recent studies have also implicated NoV as a major driver of risk in potable reuse systems (Soller et al., 2018; Soller et al., 2017), thereby warranting further study.

The objective of this study was to develop a dynamic QMRA to evaluate the efficacy of different potable reuse treatment trains in adequately mitigating risk of acquiring NoV-associated gastroenteritis. This study not only characterizes the reliability of potable reuse treatment trains in achieving relevant public health benchmarks under nominal conditions, but it also evaluates the significance of treatment train failures, disease states and duration, endemic disease within the community, alternative exposure routes (i.e., a foodborne outbreak), and secondary transmission to identify the most influential model components, parameters, and assumptions. Finally, this model allows for a direct comparison with Amoueyan et al. (*in preparation*; Chapter 3), which presented a static QMRA of NoV risk in potable reuse systems.

5.2   Methodology

A conceptual comparison of a static QMRA (Amoueyan et al., 2017) and the current dynamic QMRA, which focuses on NoV as the primary hazard, is illustrated in Figure 5.2. In the current study, a Monte Carlo simulation was used to capture stochastic variability in model

102

parameters (e.g., pathogen concentrations, treatment process performance) based on assigned probability distributions. The dynamic QMRA assumed susceptible individuals could contract NoV through exposure to contaminated drinking water or food (i.e., primary transmission) or contact with infected individuals, surfaces, or fomites (i.e., secondary transmission) (CDC, 2014; Hall et al., 2012; Simmons et al., 2013). The model then simulated pathogen shedding into the wastewater and pathogen attenuation during natural or engineered treatment in IPR and DPR systems. Each of these model components is described in greater detail in the following sections.
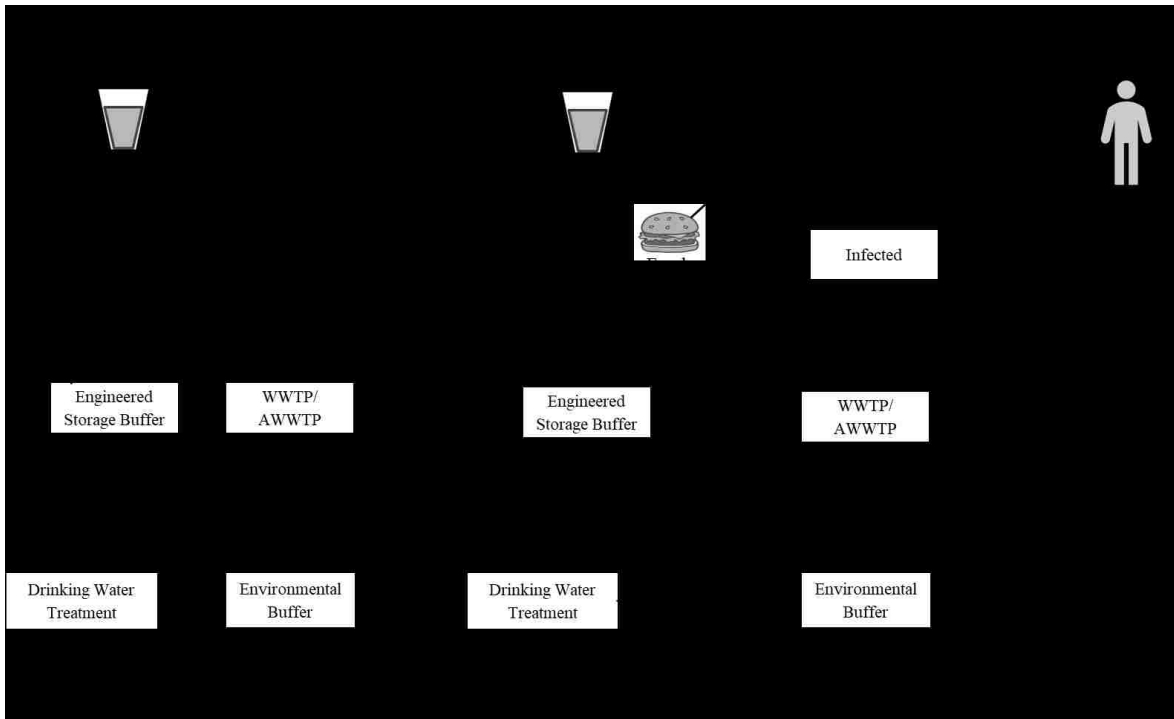

Figure 5-2. Conceptual comparison of (A) static and (B) dynamic risk assessment frameworks. The static framework represents the structure of the QMRA in Amoueyan et al. (2017; 2018), and the dynamic framework represents the structure of the current QMRA. Transmission rate constants are defined as follows: β_1 = primary transmission rate constant for drinking water, β_2 = secondary transmission rate constant, β_3 = primary transmission rate constant for food. The solid lines represent travel of water through an IPR system, and dashed lines represent travel of water through a DPR system. The dynamic model also uses a 'distributed delay' approach (Eisenberg et al. 2004) to accurately capture time/duration effects.

5.2.1 Norovirus epidemiology

Susceptibility to NoV is dependent upon the presence of histo-blood group antigens (HBGAs) within the human gut, and fucosyltransferase 2 enzyme (FUT2) is required for secretion of these HBGAs. In "nonsecretors", inactivation of FUT2 prevents those individuals from contracting a NoV infection (Currier et al., 2015; Nordgren et al., 2016). In the current study, non-secretors were assumed to comprise 20% of the total population (Currier et al., 2015; Simmons et al., 2013). Although these individuals were not at risk of developing or transmitting NoV infections, they were still considered in the overall population-based risk calculation.

For the susceptible fraction of the population, the daily risk (i.e., β_1) was based on NoV concentration in the finished drinking water, an assumed water ingestion rate of 2 L/day (USEPA, 2004; WHO, 2008), and a fractional Poisson dose response model (Eq. 5.1; Messner et al., 2014).

$$P_{inf,d} = P \times (1 - e^{-\frac{Dose}{\mu}})$$ (Eq. 5.1)

where, $P_{inf,d}$ = daily probability of infection

P = fraction of susceptible subjects = 0.722 for NoV,

Dose = number of NoV 'particles' consumed (genome copies),

μ = mean aggregate size = 1106 genome copies for NoV.

The average incubation period for NoV (i.e., duration from exposure to infection) was assumed to be follow a uniform distribution ranging from 12 to 48 hours (CDC, 2014), and the duration of disease was assumed to follow a uniform distribution ranging from 1 to 3 days (CDC, 2014; Aoki et al., 2009). The infected population was also divided into symptomatic (69%) and asymptomatic (31%) infections (Teunis et al., 2015; Zhang et al., 2011), with symptomatic individuals shedding at a rate of 250×10^9 genome copies/g feces and asymptomatic individuals

104

shedding at a rate of 12×10^9 genome copies/g feces (Amar et al., 2007; Atmar et al., 2008). Studies have shown that shedding can last for 2 to 3 weeks post-infection (Okhuysen et al., 1995; Atmar et al., 2008), and post-symptomatic individuals sometimes shed at rates similar to when they were symptomatic (Milbrath et al., 2013). Therefore, the shedding period was assumed to follow a uniform distribution ranging 2 to 21 days. During this time, secondary transmission is likely, with rates following a uniform distribution from 0.08 to 0.24 secondary infections per shedding individual per day (Zelner et al. 2010). The acquired immunity that develops post-infection 'wanes' during the recovery period until the individual returns to the fully susceptible state. Previously, the NoV post-infection period (i.e., duration of immunity) was suggested to be at least 6 months (Johnson et al., 1990), but Simmons et al. (2013) proposed a longer immunity period, which was modeled as a uniform distribution ranging from 3.2 to 5.1 years of immunity. These values are all summarized in Table 5.1.

5.2.2   Model scenarios

Amoueyan et al. (2018) previously described a static QMRA for NoV in a *de facto* reuse system, three planned IPR systems, and three DPR systems. Similar to the current dynamic model, log removal of NoV was achieved through dilution, natural die-off in the environmental buffer (i.e., surface water reservoir or groundwater aquifer), and inactivation/removal by engineered water and wastewater treatment processes.

Amoueyan et al. (2018) demonstrated that planned potable reuse systems that utilize surface water discharge (i.e., IPR) or blending (i.e. DPR) achieve similar annual NoV risks as *de facto* reuse systems due to the dominance of upstream NoV concentrations. Therefore, this dynamic QMRA focused on (1) a *de facto* reuse system, which was assumed to be representative of each of the aforementioned surface water systems; (2) a planned IPR system with full

105

advanced treatment (FAT) consisting of microfiltration (MF), reverse osmosis (RO), high-dose UV disinfection, direct injection into the local aquifer, and final disinfection with free chlorine; (3) a DPR system with ultrafiltration (UF), ozone (O_3), biological activated carbon (BAC), UV disinfection, an engineered storage buffer (ESB) with free chlorine disinfection, and direct distribution to the consumer; and (4) a DPR system with FAT, an ESB with free chlorine disinfection, and direct distribution to the consumer. A summary of the treatment trains is shown in Figure 5.3.

Table 5-1. Summary of dynamic QMRA model parameters and values.

Parameter	Unit	Value	Reference
NoV shedding rate ($\emptyset$)			
Symptomatic individuals	gc/g-feces	250×10^9	Atmar et al. (2008)
Asymptomatic individuals	gc/g-feces	12×10^9	Atmar et al. (2008)
Feces production rate	g-feces/person	Uniform (200, 750)[a]	Barker et al. (2013); Rao (2006)
Wastewater generation rate	gallons/person-day	Uniform (50, 70)	USEPA (2002)
Community			
Large community	persons	1,000,000	Assumed
Small community	persons	1,000	Assumed
Initial latent population	percent	0% or 5%	Eisenberg et al. (2005)
Birth rate	day^{-1}	3.4×10^{-5}	National Center for Health Statistics (2018)
Death rate	day^{-1}	2.3×10^{-5}	National Center for Health Statistics (2018)
Probability of symptomatic response	percent	69%	Teunis et al. (2015); Zhang et al. (2011)
Latency period ($1/\alpha$)	hours	Uniform (12, 48)	CDC (2014)
Duration of disease ($1/\delta$)	days	1-3	CDC (2014); Aoki et al. (2009)
Duration of shedding ($1/\sigma$)	days	Uniform (2, 21)[a]	Atmar et al. (2008); Aoki et al. (2009)
Duration of immunity ($1/\gamma$)	years	Uniform (3.2, 5.1)	Simmons et al. (2013)
Proportion of nonsecretors (τ)	percent	20%	Simmons et al. (2013); Currier et al. (2015)
β_1 (primary transmission through water)	infections/person-day	Table 5.2[b]	Amoueyan et al. (2018)
β_2 (secondary transmission)	infections/person-day	Uniform (0.08, 0.24)[a]	Zelner et al. (2010)
β_3 (primary transmission through food)	day^{-1}	7×10^{-6}[c]	Hall et al. (2012); CDC (2009-2011)
NoV dose response model (Eq. 1 in main text)			
Fraction of susceptible subjects (P)	-	0.722	Messner et al. (2014)
Mean aggregate size (μ)	-	1106	Messner et al. (2014)
NoV Occurrence			
WW at time 0	gc/L	Normal (8913, 13)[d]	Eftim et al. (2017)
SW (prior to blending)	gc/L	Lognormal (888, 1643)[e]	Lodder & de Roda Husman. (2005)
SW RWC/storage time	percent and days	20% and 270	Rice et al. (2015); Wu, 2015
GW (prior to blending)	gc/L	Uniform (0, 0.6)[a]	Borchardt et al. (2012)
GW RWC/storage time	percent and days	15% and 60	Sloss et al. (1996); CDPH (2014)

[a](minimum, maximum); [b]Initial conditions for β_1 are summarized in Table 5.2 and were based on a previous static QMRA model (Amoueyan et al., 2018); [c] The number is based on 35 people per 1,000,000 people per year which was applied over a 5-day time period to simulate a foodborne outbreak; [d](mean, standard deviation); [e](mean, standard deviation) with $\mu = 6.04$ and $\sigma = 1.22$
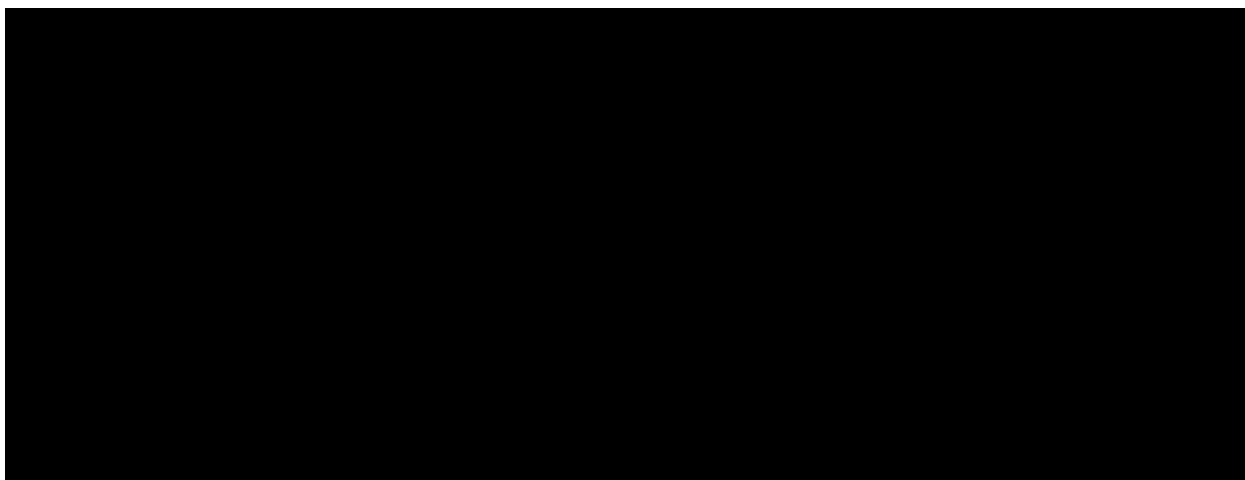
Figure 5-3. Potable reuse treatment trains included in the dynamic QMRA.
The conventional wastewater treatment plant (WWTP) included only secondary wastewater treatment. The drinking water treatment plant (DWTP) represented a conventional filtration system with final disinfection and was assumed to be compliant with the U.S. EPA Surface Water Treatment Rules. The chlorination step following groundwater replenishment was assumed to be compliant with the U.S. EPA Ground Water Rule. The chlorination step included in the engineered storage buffer (ESB) was assumed to be compliant with guidelines for ESBs in DPR systems (Salveson et al., 2016). MF = microfiltration, UF = ultrafiltration, RO = reverse osmosis, UV = ultraviolet disinfection, BAC = biological activated carbon.

Pathogen attenuation was modeled with probability distributions for the expected log removal values (LRVs) for the engineered treatment processes, which also accounted for unit process failure and associated 'domino effects' (Amoueyan et al., 2017; Amoueyan et al., 2018). In the IPR systems, pathogen attenuation was also achieved with dilution and natural die-off based on recycled water contribution (RWC) [20% for surface water (Rice et al., 2015) and 15% for groundwater (Sloss et al., 1996)], die-off rate (Amoueyan et al., 2018), and estimated storage time in the environmental buffer [270 days for surface water (Wu, 2015) and 60 days for groundwater (CDPH, 2014)].

5.2.3 **Scenario 1: Simultaneous evaluation of primary and secondary transmission**

In this scenario, exposure to NoV occurred through contaminated drinking water (i.e., primary transmission; β_1) or through contact with shedding individuals (i.e., secondary transmission; β_2). Primary exposure through food was not considered in this scenario (i.e., $\beta_3 =$

107

0). The initial conditions for β_1 for each treatment train were determined previously in Amoueyan et al. (2018) and are summarized as the mean annual risks for the static model in Table 5.2. Once susceptible individuals were infected, they potentially infected other susceptible individuals and also shed pathogens to the wastewater, thereby allowing for calculation of time-dependent raw wastewater concentrations based on the parameters in Table 5.1. The primary risk due to exposure to contaminated drinking water then varied over time based on the stochastic performance of the engineered treatment trains and environmental buffer (when applicable). In other words, the daily risk (i.e., β_1) was recalculated for each day of the simulation using the simulated concentration of NoV in the finished drinking water.

5.2.4 **Scenario 2: Relative significance of secondary transmission**

This scenario focused on the relative contribution of secondary transmission (i.e., β_2; Table 5.1) to overall disease incidence in the community. In this scenario, the pathogen shedding rate was set to zero, but primary transmission could still occur due to a baseline level of NoV in local drinking water. In other words, β_1 was held constant at the static risk values shown in Table 5.1.

5.2.5 **Scenario 3: Relative significance of time-dependent primary transmission**

This scenario focused on the relative contribution of dynamic primary transmission to overall disease incidence in the community. Because secondary transmission (i.e., β_2) was set to zero, the risk estimates in this scenario were expected to be approximately similar to the static model, in which drinking water was the only source of NoV. However, the post-infection immunity period considered in the dynamic model was also expected to reduce estimated risks relative to the static model.

108

5.2.6 **Scenario 4: Relative significance of foodborne transmission**

This scenario expanded the framework of Scenario 1 by including primary transmission through contaminated food (i.e., β_3) as an additional NoV exposure route. In addition to evaluating the relative significance of a foodborne outbreak to overall risk in the community, this scenario also allowed for an evaluation of potable reuse treatment train reliability through robustness (Pecson et al., 2015) in the event of an outbreak condition. The additional primary transmission route was applied to the model over a five-day period to simulate a foodborne outbreak at a local food preparation center (e.g., a restaurant). The transmission rate constant (i.e., $\beta_3 = 7\times10^{-6}$ day^{-1}) was based on data for reported illnesses associated with foodborne NoV outbreak in the U.S. from 2001 to 2008 (Hall et al., 2012).

5.3 **Simulation approach and initial conditions**

The dynamic model was developed in STELLA 10.1 (ISEE Systems, Lebanon, NH). The movement of individuals through the various epidemiological states was modeled using a series of ordinary differential equations (ODEs) (Text S1; Eisenberg et al., 1998; Soller & Eisenberg, 2008) and the parameters summarized in Tables 5.1.

Two different population sizes—a small community of 1,000 and a large community of 1,000,000 people—were considered to evaluate the role of population size in propagating disease throughout the community. As suggested by previous studies (Eisenberg et al., 1996; Simmons et al., 2013), birth (3.4×10^{-5} day^{-1}) and death (2.3×10^{-5} day^{-1}) rates were also included (National Center for Health Statistics, 2018). The birth rate was applied to the total population but only added individuals to the susceptible state, and the death rate was applied to all epidemiological states (S, E, C1, D, C2, and P). Each model scenario was simulated based on two initial latent conditions: (1) an endemic scenario in which 5% of the community was 'exposed' at time zero

109

(Eisenberg et al., 2005) and (2) a scenario in which all secretors were in the susceptible state at time zero (i.e., no initial latent population). The 5% latency scenario allowed for a simulation of real-world conditions, and the 0% latency scenario allowed for a direct comparison with the static model in Amoueyan et al. (2018). There were no further distinctions for sex, age, or immunocompromised individuals.

All states except the susceptible state (S) were characterized as distributed delays and described by gamma distributions with a shape parameter of 4 (Soller & Eisenberg, 2008; Zelner et al., 2010), as shown in Figure 5.4.
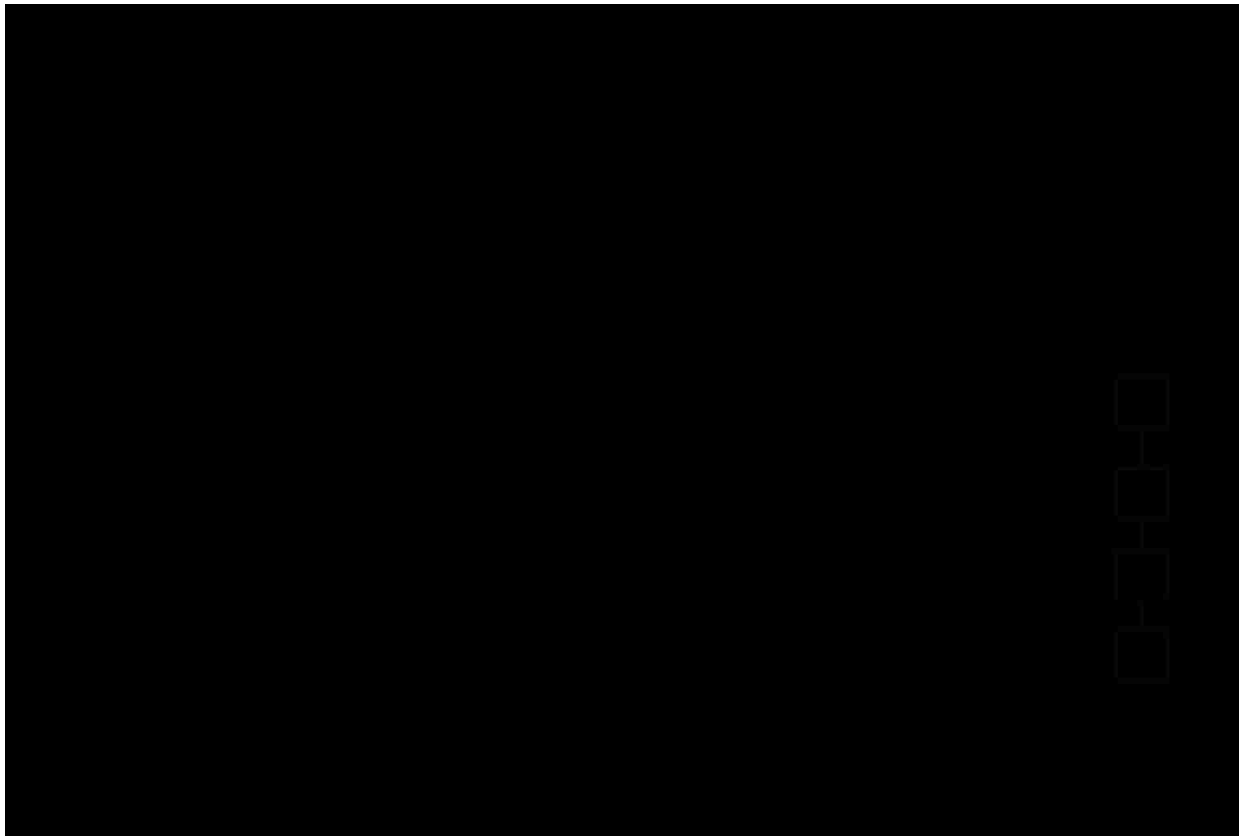

Figure 5-4. Dynamic disease transmission model used to simultaneously evaluate the impacts of primary and secondary transmission.

To incorporate waning immunity, it was assumed that the level of protection during the immunity period (1/γ) decreased linearly from full protection to no protection (Eisenberg et al.,

www.manaraa.com

2004). Four different compartments with different levels of immunity were used to simulate the
post-infection state (P1, P2, P3, and P4), with P1 representing full protection and P4 representing
the least protection. Therefore, individuals in P2, P3, and P4 could theoretically move to the
exposed state (E) through primary or secondary NoV exposure, or ultimately return to the
susceptible state with no protection. Eq. 5.2 was used to define the rate constant of movement
from P2, P3, and P4 to the exposed state (E) (Soller & Eisenberg, 2008).

$$\beta_{ji} = \frac{\beta_j(i-1)}{n} \qquad \text{(Eq. 5.2)}$$

where, $j = 1$ for primary transmission or 2 for secondary transmission,

$i = 1$, 2, 3, or 4 depending on the protected state,

n = total number of compartments in the protected state = 4.

5.4   Risk Calculation

Annual cumulative incidence (CI) was used as the principal measure of risk and was
calculated as the number of individuals who entered either the diseased state (D) or the
asymptomatic carrier state (C_1) during each simulated year divided by the total population for
that year (Eisenberg et al., 2004; Soller and Eisenberg, 2008). Therefore, CI can also be
described as the annual risk of infection per person for the dynamic QMRA. Because the model
simulated true travel times for each 'parcel' of water and for movement of individuals between
epidemiological states, a typical 365-day simulation would not have been adequate to achieve
steady state conditions (Eisenberg et al., 2004). Instead, each model iteration simulated 10 years,
and the results were based on 1,000 model iterations.

5.5 Model Validation

The model was validated as suggested by Sterman (2000). These tests included structure assessment, dimensional consistency, behavior reproduction, integration error, extreme conditions, and sensitivity analysis. Moreover, to ensure consistency between the previous static model (Amoueyan et al., 2018) and the current dynamic model, the following model validation scenario was also evaluated: no secondary transmission ($\beta_2 = 0$) and no post-infection immunity ($1/\gamma = 0$). These conditions provided a more direct comparison with the static model than Scenario 3 because the significant time lag associated with post-infection immunity was eliminated. Different 'delta time' (DT) values (i.e., the time interval simulated by each model calculation) were also evaluated to identify the DT with the most accurate simulation of movement between the various epidemiological states. The optimal DT value was determined to be 1/16 which means calculations were done 16 times per time unit. Time unit in this simulation was considered as one day.

5.6 Sensitivity Analysis

Sensitivity analyses were conducted to evaluate the relative impact of various model inputs and to identify the most influential parameters. Sensitivity analyses were performed on pathogen shedding rate ($\emptyset$), secondary transmission rate constant (β_2), the duration of latency ($1/\alpha$), the duration of disease ($1/\delta$), the duration of shedding in either carrier state ($1/\sigma$), and the duration of post-infection immunity ($1/\gamma$). The Morris method (Eq. 5.3) was used to define the relative sensitivity of the final risk to different model inputs (Wu et al., 2013b). Parameters with higher relative sensitivity parameters were considered to be more influential for estimating disease incidence.

$$\text{Relative sensitivity} = \frac{\Delta CI/CI_0}{\Delta P/P_0} \qquad \text{(Eq. 5.3)}$$

112

where, $\Delta CI/CI_0$ = relative changes in cumulative incidence,

$\Delta P/P_0$ = relative changes in the input parameter.

5.7   Results

5.7.1   Scenario 1: Simultaneous evaluation of primary and secondary transmission

Cumulative incidence (CI) was calculated for each year of the model simulation for initial latent populations of 0% and 5% (i.e., endemic). The mean cumulative incidence for each treatment train in the endemic setting was slightly higher than those of the 0% initial latent population (Table 5.2). The percent differences ranged from 19% for *de facto* reuse to 30% for FAT-based DPR, although the DPR systems achieved the lowest overall CIs for each latent condition. The increase in CI for the endemic condition was simply due to the baseline level of disease at time zero, which then propagated through the community.

Table 5-2. Comparison of mean annual risk of norovirus infection for the previous static model (Amoueyan et al., 2018) and the current dynamic model under different scenarios. The static model risks for each treatment train were used as the initial conditions ($\beta 1$,time=0) for the dynamic model.

Condition	Static Model		Dynamic Scenario 1		Dynamic Scenario 2		Dynamic Scenario 3		Dynamic Scenario 4	
β_1	N/A		Dynamic		Static		Dynamic		Dynamic	
β_2	N/A		Uniform[a]		Uniform[a]		0		Uniform[a]	
β_3	N/A		0		0		0		Point[a]	
Latent = 0%	**Mean[b]**	**SD**	**Mean[c]**	**SD**	**Mean[c]**	**SD**	**Mean[c]**	**SD**	**Mean[c]**	**SD**
A. *de facto* reuse	3.4E-04	3.1E-05	5.8E-02	4.5E-02	5.8E-02	4.5E-02	2.6E-04	5.7E-06	1.6E-01	2.2E-03
B. Planned IPR	1.2E-05	3.7E-07	5.5E-02	6.6E-02	5.5E-02	6.6E-02	9.6E-06	2.0E-07	6.1E-02	4.5E-04
C. O$_3$-based DPR	1.5E-09	4.1E-08	4.4E-02	7.3E-02	4.4E-02	7.3E-02	2.3E-11	6.5E-11	4.7E-02	3.2E-04
D. FAT-based DPR	2.8E-10	3.7E-09	4.4E-02	7.1E-02	4.4E-02	7.1E-02	4.1E-11	9.5E-11	4.6E-02	3.2E-04
Latent = 5%	**Mean**	**SD**	**Mean[c]**	**SD**	**Mean[c]**	**SD**	**Mean[c]**	**SD**	**Mean[c]**	**SD**
A. *de facto* reuse	N/A	N/A	6.9E-02	9.6E-02	6.9E-02	9.6E-02	2.9E-03	7.8E-03	3.4E-01	5E-03
B. Planned IPR	N/A	N/A	6.8E-02	1.0E-01	6.8E-02	1.0E-01	2.6E-03	7.8E-03	3.4E-01	5E-03
C. O$_3$-based DPR	N/A	N/A	5.6E-02	1.1E-01	5.6E-02	1.1E-01	2.6E-03	7.8E-03	3.4E-01	5E-03
D. FAT-based DPR	N/A	N/A	5.7E-02	1.1E-01	5.7E-02	1.1E-01	2.7E-03	7.9E-03	3.4E-01	5E-03

[a]Defined in Table 5.1; [b]These values (after conversion to daily risk) served as initial conditions for β_1 in the dynamic primary transmission scenarios; [c]These values represent cumulative incidence

113

The maximum CI for scenario 1 ranged from 0.18 for the DPR treatment trains to 0.23 for the IPR treatment trains (Table S2), which are consistent with Phillips et al. (2010) (annual incidence per person = 0.19) and Simmons et al. (2013) (annual incidence per person = 0.21). The maximum CIs in the current study were associated either with the first year of the endemic condition or with infections resulting from secondary transmission. Scallan et al. (2011) noted that total acute gastroenteritis in the U.S. amounted to 0.65 cases/person-year, which is higher than the current study, and that acute gastroenteritis linked to water was approximately 0.05 cases/person-year, which is lower than the current study. Therefore, secondary transmission may explain the discrepancy between the current study and the water-specific values in Scallan et al. (2011), and the lack of foodborne exposure in scenario 1 may explain the discrepancy between the current study and the higher overall value in Scallan et al. (2011). The results showed that including secondary transmission increased the risk of the dynamic model significantly compared to the static model and none of the treatment trains could achieve the 10^{-4} benchmark. There was no noticeable impact of community size on CI.

Based on a comparison of the static risks from Amoueyan et al. (2018) and the dynamic risks for Scenario 1 (Table 5.2: Latent = 0%), the dynamic model resulted in notably higher risks. In fact, estimated risks for the de facto reuse system increased by two orders of magnitude, and risks in the FAT-based DPR system increased by eight orders of magnitude. The major differences in model structure included (1) varying primary transmission based on disease incidence within the community; (2) secondary transmission, which was expected to increase risk; and (2) the distributed delays associated with the epidemiological states, which were expected to decrease risk. Therefore, changes in primary transmission (focus of scenario 3) or secondary transmission (focus of scenario 2) appeared to be driving the risk in the dynamic

114

model. These results can potentially be explained based on observations in Phillips et al. (2010) and predicted data in Simmons et al. (2013), both of which studied age-specific annual incidence of NoV-associated gastroenteritis. Both studies noted that disease incidence was highest in younger age groups, particularly among children less than 5 years old who were characterized by higher rates of secondary transmission.

5.7.2 Scenario 2: Relative significance of secondary transmission

To further elucidate the role of secondary transmission, the primary transmission rate was held constant in scenario 2. The results of this scenario are summarized in Table 5.2. The mean risks in Table 5.2 were nearly identical for scenarios 1 and 2, which suggested that varying primary transmission (i.e., scenario 1) had a negligible impact on CI and that secondary transmission was primarily driving risk in the potable reuse systems. Particularly when considering the 0% latent population condition, the risk posed by the baseline level of NoV in any of the potable reuse systems was still sufficient to drive the secondary transmission pathway. These results were consistent data from the national outbreak reporting system, which identified secondary transmission as primary exposure route for acute gastroenteritis caused by NoV (66.1% of all NoV cases in the U.S. from 2009-2010) (Hall et al., 2013b).

5.7.3 Scenario 3: Relative significance of time-dependent primary transmission

This scenario highlighted the potential role of varying primary transmission on CI by eliminating the secondary transmission route. As expected based on the results from the previous scenarios, the CI values were considerably lower in scenario 3 (Table 5.2). Moreover, the dynamic risk values for scenario 3 were slightly lower than the static risk values from Amoueyan et al. (2018), which could be explained either by long-term NoV attenuation within the potable reuse systems or more likely the distributed delay structure of the dynamic model.

115

Nevertheless, it is still important for potable reuse systems to achieve the recommended benchmark risk of 10^{-4}. If attenuation through the potable reuse treatment trains is inadequate, the impact of the person-environment-person pathway (i.e., shedding to wastewater) may become more significant. In the dynamic model, the CI in the *de facto* reuse with a 0% latent population was 2.6×10^{-4}, which is slightly higher than the 10^{-4} benchmark, but the planned IPR and DPR systems were all well below the 10^{-4} benchmark. Brunkard et al. (2011) reported that only 0.11% of waterborne disease outbreak in the U.S. between 2007 and 2008 were related to NoV which resulted in 265 infectious cases (annual risk of 9.0×10^{-7} per person).

5.7.4   Scenario 4: Relative significance of foodborne transmission

The national outbreak reporting system identified foodborne transmission as the second most important NoV exposure route (second only to person-person transmission) (Hall et al., 2013b). Foodborne transmission accounted for 25.9% of all NoV-associated gastroenteritis cases in the U.S. between 2009 and 2010 (Hall et al., 2013b). The results of this scenario are summarized in Table 5.2. Relative increase in cumulative incidence in scenario 4 was attributed to the combined effect of secondary transmission and primary exposure to drinking water. To evaluate robustness of the treatment trains as a result of pathogen shedding into wastewater due to outbreak event, primary transmission through drinking water (β_1) was calculated for each of the treatment trains during both normal and outbreak conditions and shown in Fig. 5.5. As illustrated in Figure 5.5A, the additional cases of gastroenteritis caused by contaminated food had no noticeable impact on primary transmission through drinking water at 5% initial latent population. However, the primary risk was higher compared to Fig. 5.5B due to the initial level of disease within the community. However, when not 'masked' by the initial latent population, the foodborne outbreak resulted in a considerable increase in primary risk through drinking water

116

(up to 5 orders of magnitude) for the DPR systems, although the overall annual risk of infection

was still well below the 10^{-4} benchmark (maximum of 9.5×10^{-7}). On the other hand, neither IPR

system was impacted by the foodborne outbreak due to the robustness of the advanced treatment

train and/or environmental buffer. Additional simulations indicated that the foodborne outbreak

had significant impact on CI in the *de facto* reuse system when the storage time decreased to less

than ~10 days (Figure S1). The planned IPR system was sufficiently robust to mitigate the

impacts of a foodborne outbreak regardless of storage/travel time in the aquifer (Figure S2).

Therefore, it may be concluded that the planned IPR system with FAT and groundwater

replenishment was the most robust treatment train in the case of outbreak conditions. Again, the

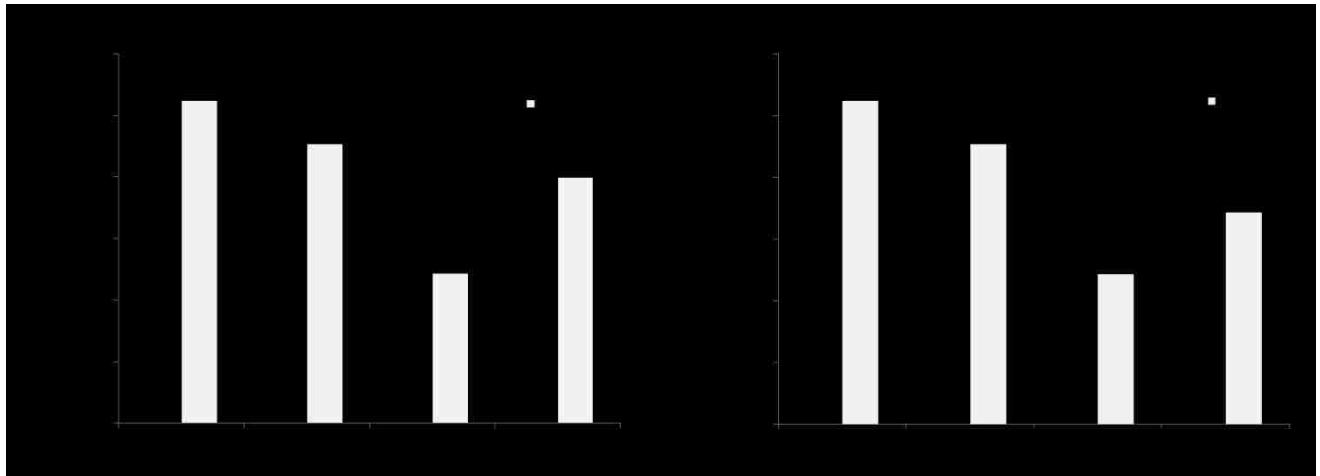size of the community had no apparent impact on CI.

Figure 5-5. Summary of results for dynamic scenario 4, specifically the relative impact of foodborne transmission on primary transmission through drinking water (β_1).
The normal condition referred to $\beta_3 = 0$, and the outbreak condition referred to $\beta_3 = 7 \times 10^{-6}$ day^{-1} which was applied over a 5-day period). The results represent risk of infection in one year of simulation in which outbreak occurs.

5.7.5   Model validation

5.7.5.1   *Comparison with static model*

To ensure consistency between the previous static model (Amoueyan et al., 2018) and the

current dynamic model, the model was adjusted to eliminate secondary transmission ($\beta_2 = 0$) and

117

post-infection immunity ($1/\gamma = 0$). As noted earlier, these conditions provided a more direct comparison with the static model than the aforementioned conditions for Scenario 3. The results summarized in Table S1 indicate that there is consistency between the static model and the dynamic model when the distinguishing model components are deactivated, thereby validating the dynamic QMRA.

5.7.5.2 *Extreme condition tests*

Test 1: $\beta_1 = \beta_2 = \beta_3 = 0$. This scenario simulated the condition in which there was no primary exposure to NoV from contaminated drinking water ($\beta_1 = 0$) or food ($\beta_3 = 0$), and there was also no secondary exposure to infected individuals ($\beta_{12} = 0$). Therefore, assuming a 0% initial latent population, there should have been no incidence of disease within the community. Assuming a 5% initial latent population, there should have been an initial spike in disease incidence as the latent individuals progressed to the diseased or carrier states, but the number of infectious individuals was then expected to remain at zero once those individuals recovered. The results shown in Figure 5.6 are consistent with these expectations. The peak value in the graph was consistent with a 5% initial latent population (i.e., 5% × 80% × 1,000,000 = 40,000). Also, since the maximum duration of exposed (E), diseased (D), and shedding (C1 or C2) was estimated to be 2 days, 3 days, and 21 days, respectively (Table 5.1), infectious individuals were expected to recover after a maximum of 26 days, as demonstrated in Figure 5.6.
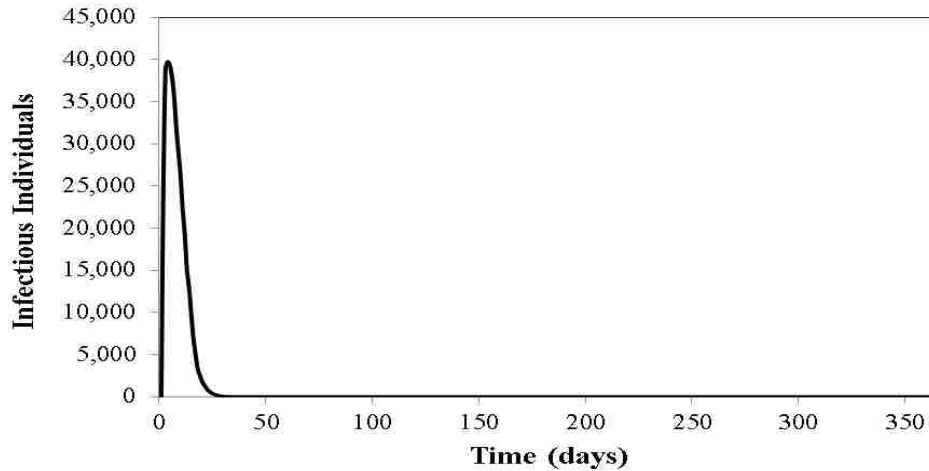
118

Figure 5-6. Extreme condition test (test 1): $\beta_1 = \beta_2 = \beta_3 = 0$. Number of infectious individuals were estimated based on endemic setting with 5% initial latent population.

Test 2: $1/\gamma = 0$. Assuming no protection from disease (i.e., duration of immunity = $1/\gamma = 0$), infectious individuals return to the susceptible state immediately after leaving either carrier states. Therefore, in the presence of primary and secondary transmission routes, it was expected that the number of infectious individuals increase over time (Figure 5.7). The variations in the number of infectious people were due to probability distributions assigned to each of the model parameters. Also, as expected the results showed significantly higher number of infections compared to the normal condition with immunity levels included. The number of infectious individuals at both "immunity" and "no immunity" models are shown in Fig. 5.7. As expected, in both models the number of infectious individuals increased until all initially latent population went through the epidemiological states and became infectious. Meanwhile, the infectious individuals spread the virus which could transmit the disease to other susceptible population and therefore the number of infectious individuals was amplified due to secondary transmission. In "no immunity" model, soon after infectious individuals left the carrier states, they became susceptible and could get infected again by both symptomatically and asymptomatically infectious persons.

119

The cumulative incidence was about two orders of magnitude higher for the 'no immunity' dynamic model than the 'immunity' dynamic model for each of the potable reuse systems (Table S3). Thus, including immunity in the model resulted in a lower cumulative incidence of disease, which is consistent with Simmons et al. (2013) and Phillips et al. (2010).
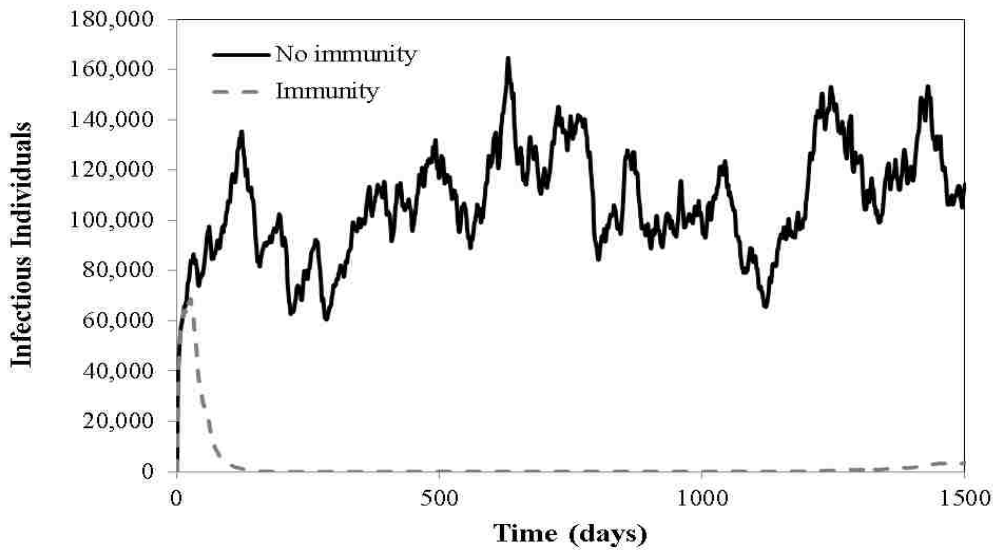

Figure 5-7. Extreme condition test (test 2): $1/\gamma = 0$. Number of infectious individuals were estimated based on endemic setting with 5% initial latent population.

5.7.6   Sensitivity analysis

The sensitivity analyses identified the rate of secondary transmission, duration of immunity, and duration of shedding as the most significant parameters affecting the risk estimates. Also, sensitivity analysis on storage time in environmental buffer during outbreak conditions was addressed earlier in section 3.4.

5.7.6.1   *Secondary transmission (β_2)*

Secondary transmission was previously identified as the most important component contributing to disease incidence in the dynamic model. Fig. 5.8 illustrates cumulative incidence as a function of secondary transmission rate ($\beta_2 = 0$ to 0.5 infections/person-day based on profile likelihood of NoV outbreak by Zelner et al. (2010)) during normal condition (no outbreak, $\beta_3=0$)

120

where all other parameters set to the values in Table 5.1. As expected, a higher rate of secondary transmission led to higher CI within the community.
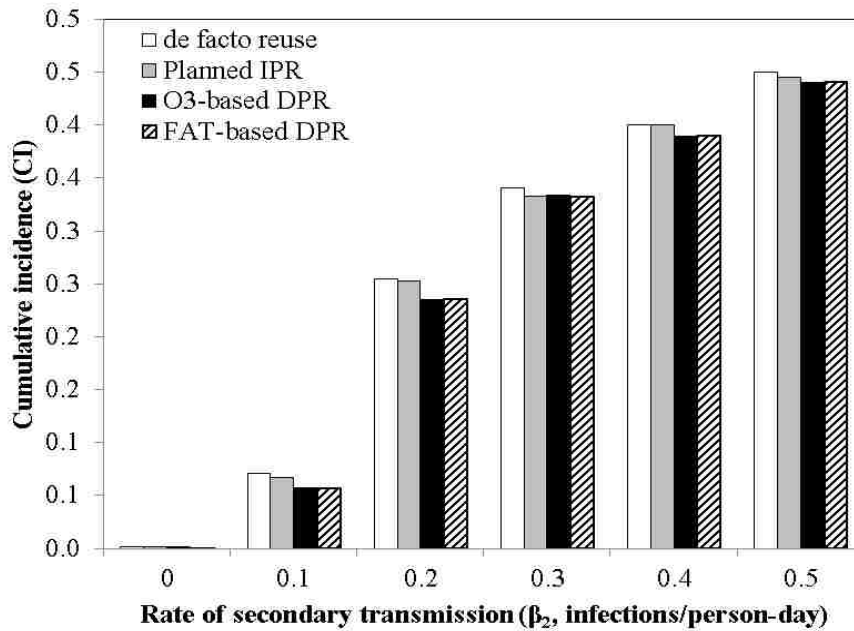

Figure 5-8. Cumulative incidence as a function of secondary transmission rate at 5% initial latent population. $B_2=0$ refers to scenario 3 in which the only source of NoV is from primary exposure through drinking water.

As shown in Fig. 5.8, relative sensitivity of disease incidence to secondary transmission rate decreased as the secondary transmission rate increased. For example, when secondary transmission rate increased from zero to 0.1, disease incidence increased by a factor of 2.5×10^1 while, increasing secondary transmission rate from 0.4 to 0.5 increased the disease incidence by a factor of 1.2×10^{-1}. This result was consistent with Eisenberg et al. (2004) which showed lower relative sensitivity at higher rates of secondary transmission compared to the lower rates of secondary transmission due to exposure to enteroviruses. The importance of secondary transmission for NoV infections can be illustrated with observed data for schools and child care facilities in which young children with higher rates of disease incidence (annual risk of 1.22×10^{-1} per person among children who attended daycare in their first year of age; Hullegie et al. 2016),

121

make up most of the population, or in other 'high contact' areas, such as nursing homes, hospitals, or cruise ships. According to national outbreak reporting systems, approximately 3,500 outbreaks occurred from 2009-2012, of which 63% were related to health care facilities, 22% to restaurants or banquet facilities, and 6% to schools or daycare facilities. Studies have reported that the highest prevalence of NoV occurs in healthcare settings, with risk of illness ranging from 9-78% (Iturriza-Gómara and Lopman, 2014; Kambhampti et al., 2015; Weinstein et al., 2008).

5.7.6.2 *Duration of immunity (1/γ)*

Disease incidence was inversely related to the duration of immunity (Figure 5.9). A longer duration of protection effectively led to larger portions of the population with some level of protection at any given time, thereby limiting the number of new infections in any given year. With a duration of immunity of at least one year, CI decreased dramatically. Therefore, it could be suggested that if a vaccine could achieve a 1-year protection from NoV infection, especially in children less than 5 years old, it could be significantly beneficial for public health protection. However, Simmons et al. (2013) recommended development of NoV vaccine to provide protection for a duration of 5 years for greater cost and health benefits per person vaccinated.
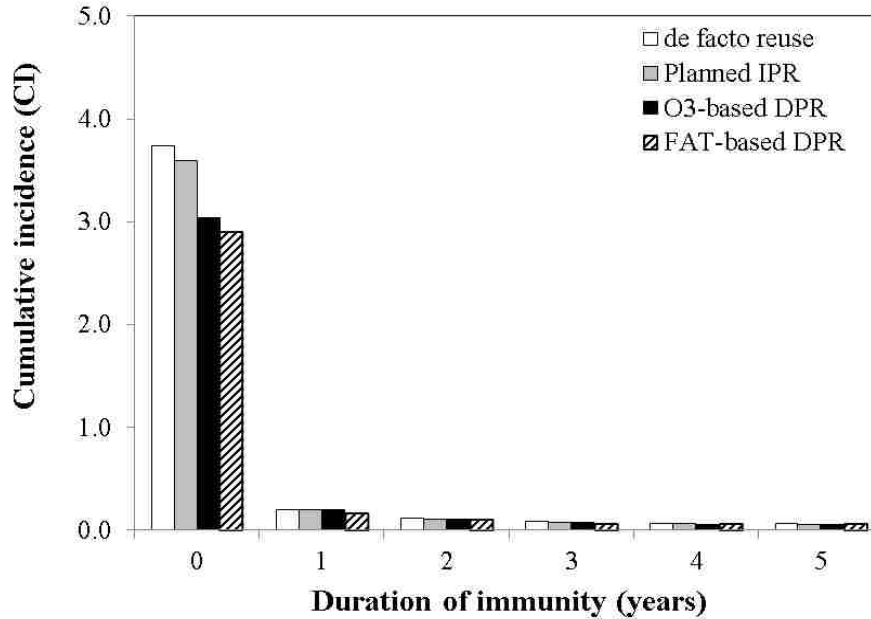
Figure 5-9. Cumulative incidence of disease as a function of duration of immunity. The results are based on one simulation at 5% initial latent population and β1 and β2 were set as listed in Table 5.1.

5.7.6.3 *Duration of shedding (1/σ)*

Studies have reported different NoV shedding rates ranging from several hundred viruses per gram of feces to more than 10^{11} genome copies per gram of feces (Aoki et al., 2010; Atmar et al., 2008; Teunis et al., 2015). Although a higher shedding rate was expected to result in higher NoV concentrations in the raw wastewater and consequently the finished drinking water, the results indicated that shedding rate (varied from 10^3 to 10^{13} gc/g feces for both symptomatic and asymptomatic infections) did not significantly impact cumulative incidence (relative sensitivity ≈0). This was due to the robustness of the engineered treatment processes and/or natural die off and dilution. For example, when die-off rate in the surface water was set to zero for the *de facto* reuse scenario, the cumulative incidence increased by one order of magnitude for the higher pathogen shedding rate (i.e., 3-orders of magnitude higher pathogen shedding than normal rate listed in Table 5.1). On the other hand, the duration of shedding was demonstrated to have a significant impact on cumulative incidence of disease (Figure 5.10). This was presumably linked

123

to the importance of secondary transmission. When the duration of shedding increased from 2 days (minimum duration of shedding) to 21 days (maximum duration of shedding), cumulative incidence increased about 9-orders of magnitude (depending on the treatment train) with *de facto* reuse system resulted in highest incidence (Figure 5.10). Similar to duration of immunity, relative sensitivity of disease incidence to duration of shedding decreased at higher duration of shedding (relative sensitivity= $1.5\times10^{+8}$, and 5.9×10^{-1} when duration of shedding increased from 2 days to 21 days and from 21 days to 40 days, respectively).
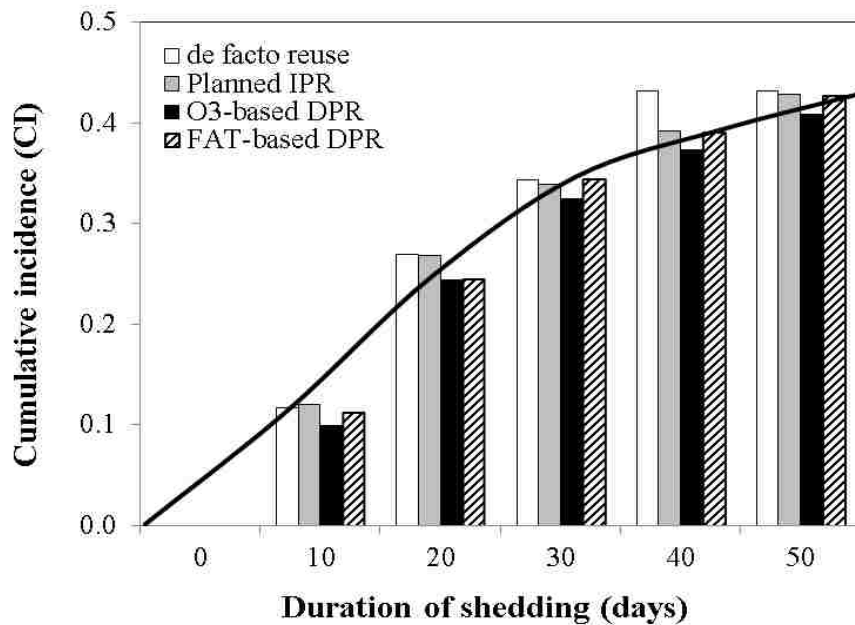

Figure 5-10. Cumulative incidence of disease as a function of duration of shedding.
The results are based on one simulation at 5% initial latent population and $\beta1$ and $\beta2$ were set as listed in Table 5.1.

5.8   Conclusion

The main goal of this study was to evaluate performance of different potable reuse treatment trains in case of NoV infection, outbreak conditions, and significance of secondary transmission and immunity in NoV transmission through potable reuse systems. Results suggested that incidence of NoV disease was mainly attributed to secondary transmission and that primary

124

www.manaraa.com

transmission through drinking water did not play a significant role in NoV infections. However, it is important to provide the recommended benchmark risk of 10^{-4} in potable reuse systems to limit the risk of infection associated with drinking water exposure pathway. Results of the study indicated that the *de facto* reuse and planned IPR systems were sufficiently robust to handle the impact of outbreak in the community. Increased number of infectious cases when employing these treatment trains was mainly associated to secondary transmission pathway.

However, with less storage time in the environmental buffer, pathogen shedding into the local wastewater became more important. For example, decreasing storage time in the *de facto* reuse system from 270 days to 10 days resulted in more than 2-orders of magnitude increase in primary transmission through drinking water during an outbreak event. On the other hand, with planned IPR system, even very short storage times could sufficiently mitigate the effects of a NoV outbreak. This was due to a lower concentration of NoV in the groundwater prior to blending and the robustness of the advanced treatment train. Therefore, among the treatment trains evaluated in this study, the planned IPR system suggested as the most robust treatment train especially in case of outbreak conditions. This result may change if other planned IPR (i.e., ozone-based treatment trains with surface water augmentation) or DPR (i.e., FAT-based with blending upstream of drinking water treatment facility) would also be considered in this dynamic model.

The results of the sensitivity analyses indicated that secondary transmission, duration of immunity, and duration of shedding were the most significant parameters in the dynamic transmission model. Potable reuse treatment trains were able to adequately attenuate NoV concentration in the raw wastewater through natural die-off, dilution, or advanced treatment processes even when infectious individuals excreted as much as 10^{13} gc/g of feces into the

125

wastewater which is higher than normally expected concentrations. However, since secondary transmission drives the risk of NoV, longer duration of shedding or infectiousness increased the incidence of disease through secondary transmission. Similarly, higher rates of secondary transmission led to higher incidence within the community. Longer duration of immunity led to lower disease incidence. Increasing the duration of protection from 0 (no protection) to one year significantly impacted the cumulative incidence within the community. Therefore, it could be concluded that if the potable reuse treatment trains could achieve the recommended benchmark risk of 10^{-4} and if the secondary transmission pathway could be limited by developing a NoV vaccine that could provide at least 1-year protection against the virus, the incidence of disease within the community could be significantly reduced.

Acknowledgements

Supplementary Information

A Supplementary Information file for this article can be found in Appendix 3 of this dissertation.

6   Conclusion

6.1   Findings from current study that support previous literature

- A previous study by Chaudhary et al. (2017) reported that in potable reuse systems that utilize surface water as a discharge or blending point, the concentration of pathogens in the upstream surface water dominates the risk calculation. The results of the QMRAs in the current study provided further support for this statement. Two IPR systems (i.e., ozone-based and FAT-based) with surface water augmentation and one DPR system (FAT-based) with surface water blending resulted in similar risks as a *de facto* reuse system. The DPR systems with direct distribution and the planned IPR system with groundwater replenishment achieved lower risks of infection for all pathogens due to the robustness of the treatment trains and minimal/no pathogen contributions from the source water. These results also confirm the statement by the National Research Council suggesting that environmental buffers may not always be necessary to provide adequate public health protection and that some engineered systems might achieve similar or superior water quality than traditional systems incorporating environmental buffers (NRC, 2012).

- Potable reuse systems that employ surface water discharge or blending are more likely to exceed the 10^{-4} annual risk benchmark for each pathogen or for the combination of all target pathogens. Again, this is because of pathogen occurrence in upstream source waters and not necessarily because of the inadequacy of the engineered treatment trains. The DPR systems with direct distribution (both ozone-based and FAT-based) and the planned IPR system with groundwater replenishment were generally able to achieve the recommended benchmark. The only exception was adenovirus in the FAT-based DPR

www.manaraa.com

system with direct distribution, although the benchmark risk was only exceeded by the absolute maximum risk simulated for that treatment train. In other words, the 95th percentile annual risk was still less than the 10^{-4} benchmark. This was due to adenovirus resistance to UV disinfection. These findings support Chaudhary et al. (2017), which suggested that *de facto* reuse resulted in higher risks of *Cryptosporidium*, norovirus, and combined pathogen risk than DPR systems.

- Although Soller et al. (2017) and Soller et al. (2018) suggested that norovirus drives the risk in DPR systems, the results of the current study indicated that *Cryptosporidium* and adenovirus resulted in higher risks of infection in both IPR and DPR treatment trains. Only in the IPR system with groundwater replenishment did norovirus result in a higher risk than *Cryptosporidium*, although the risk was still lower than the 10^{-4} benchmark. The results of the current study are consistent with Forss and Ander (2011), which involved a QMRA on the DPR system in Windhoek, Namibia. They identified *Cryptosporidium* as the most critical pathogen (as opposed to *Giardia* and norovirus). The results of the current study also confirm statistics from the national reporting outbreak system. Specifically, the data suggest a low rate of primary transmission of NoV through drinking water (annual risk of infection of 9.0×10^{-7} per person in the U.S. between 2007 and 2008) (Brunkard et al., 2011).

- According to this study, potable reuse treatment trains employing ozone-biofiltration are generally equivalent to RO-based treatment trains on the basis of public health, which is consistent with the findings of Trussell et al. (2016). Gerrity et al. (2014) also evaluated the applicability of ozone-biofiltration systems and concluded that ozone-based treatment trains can provide adequate public health protection while also saving up to $51 million

128

in capital costs and up to $4 million in O&M costs compared to FAT in a 10 MGD potable reuse facility.

- With respect to *Cryptosporidium*, the results of the current study showed that potable reuse treatment trains that employ UV disinfection are superior to other treatment trains and generally achieve annual risks that are several orders of magnitude lower than the 10^{-4} annual benchmark. The only exception was the DPR system with blending upstream of a conventional drinking water treatment facility, for which the risk was dominated by *Cryptosporidium* in the upstream surface water. Also, UF and UV were found to be important treatment processes for *Cryptosporidium* removal/inactivation, which is consistent with Forss and Ander (2011).

- The results of this QMRA indicated that all of the potable reuse treatment trains evaluated in the current study could reliably achieve the required 12-10-9-log reductions of viruses, *Cryptosporidium*, and *Salmonella* that are recommended by the California Division of Drinking Water (DDW) and NWRI (2013). However, potable reuse treatment trains with surface water utilization (IPRs with surface water augmentation and DPR with blending upstream of the drinking water treatment facility) resulted in similar risks which all exceeded the benchmark of 10^{-4} for each individual pathogen and for the combined effect of all pathogens. While, DPR treatment trains with direct distribution and planned IPR system with groundwater replenishment typically resulted in risk of infection less than the benchmark of 10^{-4}.

- Evaluating the significance of different norovirus transmission suggested that person-person transmission (i.e., secondary transmission) dominated the risk calculation, followed by foodborne transmission and then waterborne transmission. These findings

129

are confirmed by the national outbreak reporting system, which attributed 66% of all norovirus infectious cases to secondary transmission pathway, 26% to foodborne transmission, and only 0.2% to waterborne transmission in the U.S. between 2009 and 2010 (Hall et al., 2013b).

- The results of the dynamic QMRA indicated a maximum cumulative incidence of 0.18 for the DPR treatment trains (both ozone-based and FAT based) and 0.23 for the *de facto* reuse and planned IPR system with groundwater replenishment, although these risks were dominated by secondary transmission. These results are consistent with Phillips et al. (2010) (annual incidence per person = 0.19) and Simmons et al. (2013) (annual incidence per person = 0.21). Eliminating the impact of secondary transmission resulted in several orders of magnitude lower risk ranging from 2.6×10^{-04} to 4.1×10^{-11} (depending on the treatment train) which supported the statement that the risk was dominated by secondary transmission and not the drinking water.

- The most important factors in the norovirus dynamic disease transmission model were the secondary transmission rate constant, the duration of immunity, and the duration of shedding. These results are consistent with the disease transmission model for enterovirus performed by Eisenberg et al. (2004). Both studies also showed higher cumulative incidence for higher secondary transmission and for shorter durations of immunity.

6.2 Novelty and findings specific to this study

Previous studies primarily focused on static QMRAs to evaluate risks associated with IPR systems (Olivieri et al., 1999; Lim et al., 2017) and DPR systems (Pecson et al., 2017; Soller et al., 2017; Soller et al., 2018). A few studies provided a QMRA framework for direct comparison of IPR and DPR (Chaudhary et al., 2017) and for evaluating the potential impact of

130

treatment process failure (Pecson et al., 2017). The current study provided a QMRA framework for direct comparison of *de facto*, IPR, and DPR systems, while also incorporating the impact of treatment process failures and the associated 'domino effects'. This study also provided a framework to compare the efficacy of both ozone-biofiltration and RO-based treatment trains, the impacts of extreme conditions (e.g., outbreaks), and the most critical parameters/operational conditions in potable reuse systems in a static and dynamic context.

Findings specific to the static QMRA

- With respect to *Cryptosporidium*, this study found that storage time and temperature in the environmental buffer were the most significant operational conditions affecting risk in planned IPR systems. The study initially identified a storage time of approximately 105 days and a surface water temperature of 10°C as being critical conditions for *Cryptosporidium*. These results were based on an exponential dose response model for *Cryptosporidium* with a dose response parameter of 0.00419 (Barbeau et al., 2000). However, use of a different dose response parameter ($r = 0.09$; USEPA, 2006b) resulted in a revised critical storage time of 120 days at 10°C. Storage times shorter than these critical values resulted in significant increases in risk. With respect to adenovirus, which exhibits greater resistance to environmental stress than other viruses, a critical storage time of 150 days was identified in *de facto* reuse systems. Storage time and temperature were not significant parameters in other planned IPR systems with surface water augmentation and also with respect to NoV and *Salmonella*, storage time and temperature were not significant parameters.

- Although surface water was not important for norovirus or *Salmonella* risk, a temperature of 20°C was identified as a critical condition for adenovirus. Temperature lower than

131

20ºC resulted in up to 2 orders of magnitude higher risk for adenovirus compared to the baseline condition because of this virus' slower inactivation kinetics in the environment.

- This study identified pre-ozonation and UF as critical processes for adenovirus attenuation; RO and UV as critical processes for norovirus and *Salmonella* attenuation; and UF and UV as critical treatment processes for *Cryptosporidium*.

- The results of the static QMRA indicated that advanced treatment failures were generally insignificant either due to the robustness of the advanced treatment train (i.e., DPR) or resiliency provided by the environmental buffer (i.e., planned IPR).

Findings specific to the dynamic QMRA

- In general, the results suggested that all potable reuse treatment trains were sufficiently robust to handle spikes in norovirus concentration from an outbreak, although IPR systems exhibited greater robustness than DPR systems. However, a storage time of at least 10 days in surface water for the *de facto* reuse systems was critical for preventing a foodborne outbreak of NoV from further propagating through the community via drinking water.

- Planned IPR with FAT and groundwater replenishment was identified as the most robust treatment train which could sufficiently attenuate norovirus concentration in the event of an outbreak even with very short storage time in groundwater (<5 days). However, planned IPR systems with surface water augmentation and DPR systems with FAT and blending were not considered in the dynamic framework. Including these treatment trains may impact this conclusion.

- The current study suggested that a duration of immunity to norovirus of at least one year could dramatically decrease the cumulative incidence of disease within the community.

132

Therefore, developing a vaccine that could provide at least 1 year of protection, especially in children younger than 5 years old who are more prone to secondary transmission, would be very beneficial to public health. This was consistent with reported results by Simmons et al. (2013).

These findings could ultimately have implication for more widespread implementation of potable reuse, thereby increasing water resource security by expanding water portfolios throughout the United States in a sustainable manner. The conclusions developed from these QMRA models can be used in the development of regulatory frameworks to aid in identifying critical targets, such as storage time in the environmental buffer and overall reliability of the advanced treatment trains. The research identified the components and operational conditions that were most critical to minimizing public health risks due to exposure to different pathogens in potable reuse systems in order to improve the decision-making processes in development and operational designs of potable reuse systems.

The main sources of uncertainties in this study was related to failure in the treatment processes and occurrence of pathogens in raw water sources, especially viruses. As suggested by Forss and Ander (2011) employing methods such as a Fault Tree Analysis to calculate the actual failure in all treatment processes improved the results of the QMRA. Also, information on infectivity of norovirus and dose response model for norovirus could be beneficial to estimate more accurate risk of infection for norovirus.

6.3   Recommendations

According to this study, *de facto* reuse systems were the less reliable treatment trains on the basis of public health protection with the highest sensitivity to operational changes such as contribution of wastewater effluent, storage time, and temperature in environmental buffers. Since many of the nation's water systems utilizes *de facto* reuse as a source of drinking water specially during drought or under low-flow conditions it is important to fully characterize the quality of water in upstream source water and the performance of *de facto* reuse systems under various operational conditions to ensure adequate public health protection. For example, for surface waters with higher concentrations of pathogens than treated wastewater (e.g., bin 2, 3, and 4 for *Cryptosporidium*) higher contribution of wastewater effluent is recommended to decrease the final risk.

Higher risk of infection in potable reuse systems with environmental buffers (i.e., IPR) than those with no environmental buffers (i.e., DPR) may suggest that even though "indirect" reuse has a connotation that is safer than "direct" reuse, these are not correlated to the quality of the final product water and therefore, may not be a good representative of adverse impact on public health from a technical perspective.

This study can be expanded by including other pathogens, such as *giardia*, *E. coli*, and rotavirus. Also, other potable reuse treatment trains could be developed and simulated in both static and dynamic frameworks. Even though studies are under evaluation to estimate NoV infectivity to be utilized in dose-response assessments, in case of potable reuse applications, NoV was not identified as an important pathogen in risk assessment. Therefore, it is recommended to better characterize the risk associated with pathogens such as *Cryptosporidium* and AdV which drive the risk in potable reuse applications by performing the dynamic QMRA

134

and evaluating the impact of secondary transmission of these pathogens in public health risk estimation.

Appendix 1

Text S1. Annual risk of infection by *Cryptosporidium* in the context of the LT2 framework

      Annual risk of infection by *Cryptosporidium* was calculated assuming 2 liters of daily water consumption and an exponential dose response parameter of 0.00419 oocysts^{-1}. These risks assume compliance with LT2 for conventional filtration (i.e., 3-log credit via filtration + bin requirement) and direct filtration (i.e., 2.5-log credit via filtration + bin requirement). As illustrated in Figure S1, conventional filtration and direct filtration are equivalent for influent concentrations greater than 0.075 oocysts/L. The dashed line denotes the annual risk benchmark of 10^{-4}.
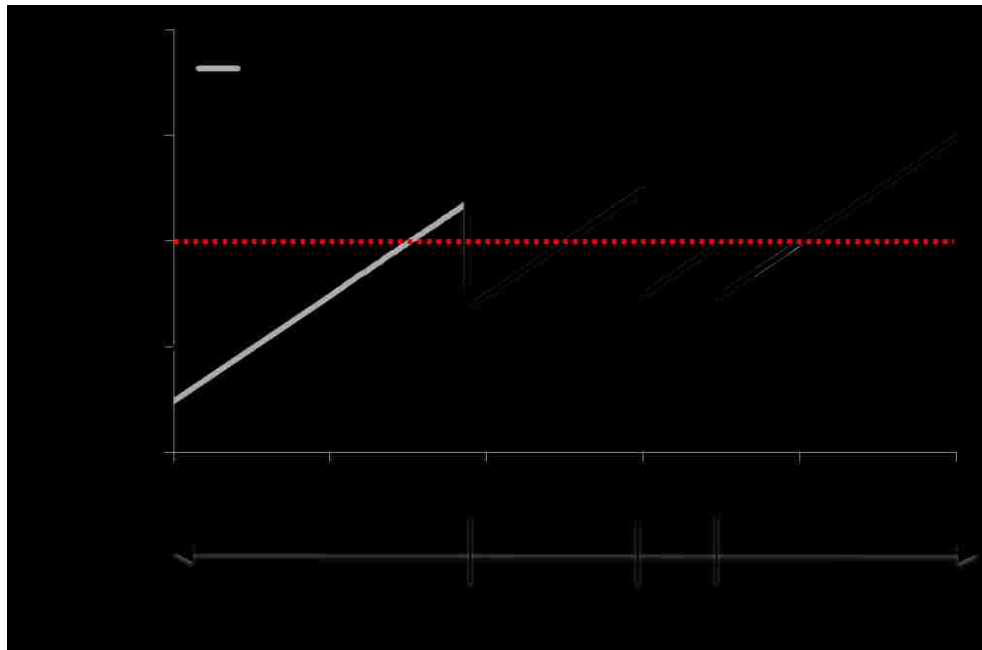

Figure S1. Annual risk of infection by *Cryptosporidium* in the context of the LT2 framework.

Text S2. Determination of instantaneous ozone demand and ozone decay rate constant

Figure S2 illustrates data generated from ozone demand/decay testing of five different secondary wastewater effluents (Snyder et al., 2014). The graph illustrates the relationship between instantaneous ozone demand (IOD), which is standardized to total organic carbon (TOC) concentration, and O_3/TOC ratio at 25°C.
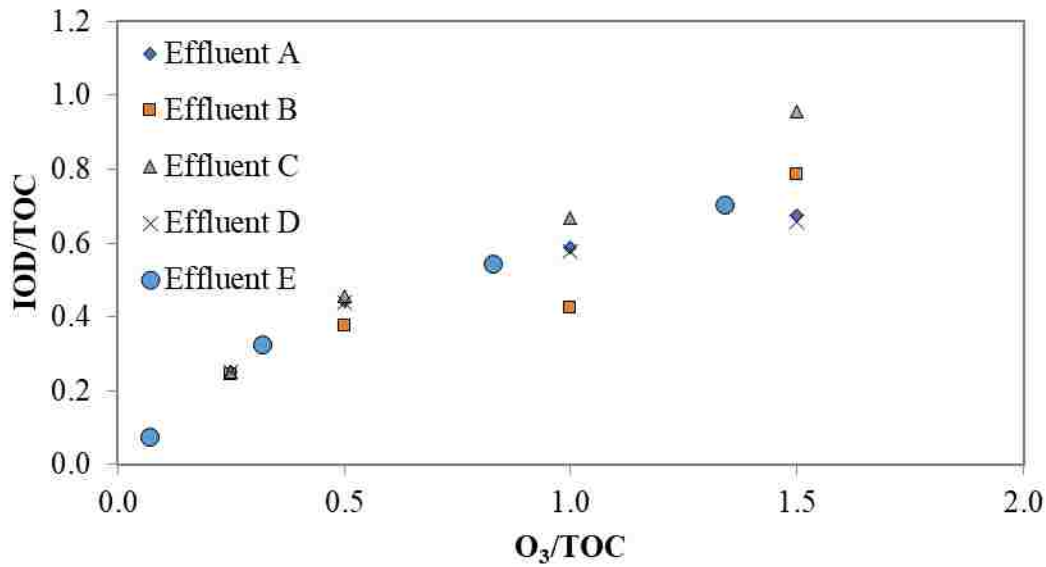

Figure S2. Relationship between IOD/TOC and O_3/TOC for ozonated secondary effluents.

After aggregating all of the data from the five secondary effluents, a regression model was developed to estimate the IOD/TOC ratio (Eq. S1) and the IOD (Eq. S2). A similar approach was used to develop a regression model to estimate the TOC-standardized first order ozone decay rate constant (Eq. S3) and the first order ozone decay rate constant (Eq. S4). The corresponding regression models are illustrated in Figure S3 and Figure S4, respectively.

Instantaneous ozone demand (at 25•C):

$$\frac{IOD}{TOC} = 0.6025 \times \left(\frac{O_3}{TOC}\right)^{0.6679} \tag{Eq. S1}$$

$$IOD = TOC \times 0.6025 \times \left(\frac{O_3}{TOC}\right)^{0.6679} \tag{Eq. S2}$$

138

First order ozone decay rate constant (at 25•C):

$$\frac{k_{O_3}}{TOC} = 0.1001 \times \left(\frac{O_3}{TOC}\right)^{-1.605} \tag{Eq. S3}$$

$$k_{O_3} = TOC \times 0.1001 \times \left(\frac{O_3}{TOC}\right)^{-1.605} \tag{Eq. S4}$$
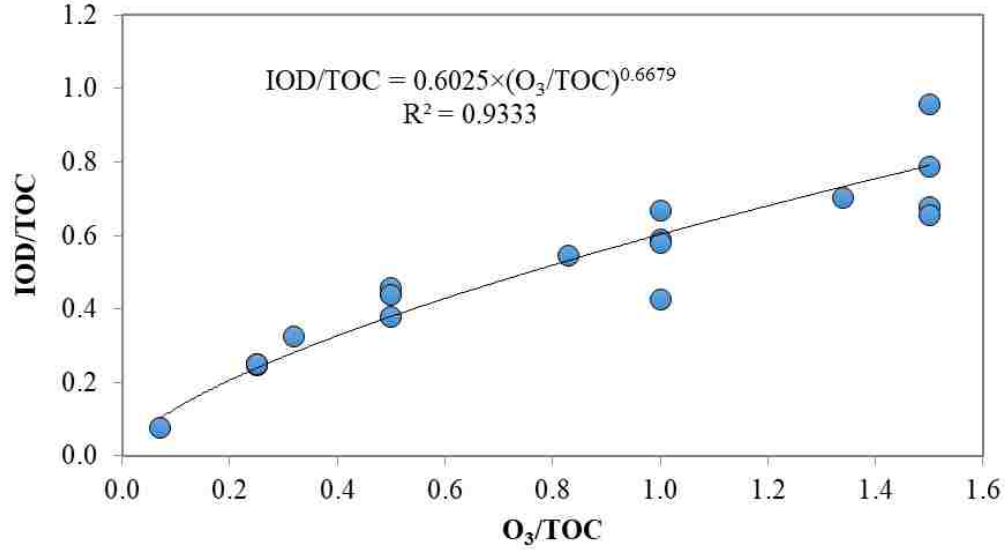

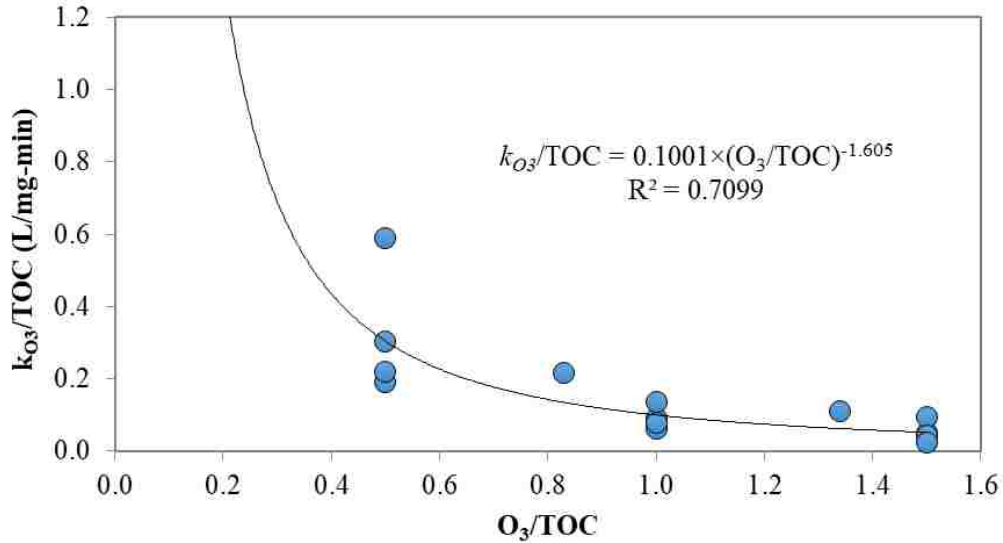**Figure S3.** Regression model for instantaneous ozone demand (at 25°C).

Figure S4. Regression model for first order ozone decay rate constant (at 25°C).

Because of practical limitations of batch ozone demand/decay testing with the indigo trisulfonate method, it is not possible to accurately characterize ozone residual kinetics for $O_3/TOC < 0.25$ unless a quench-flow approach is employed. As a result, the ozone decay rate constant model was separated into two different equations (Eq. S5 and Eq. S6) with a threshold O_3/TOC of 0.25. For $O_3/TOC < 0.25$, the IOD is assumed to be equal to the applied ozone dose, thereby negating the need for a corresponding ozone decay rate constant. In the context of disinfection, the model assumes O_3/TOC values less than 0.25 result in an ozone 'CT' value of 0 mg-min/L.

$$\frac{O_3}{TOC} \leq 0.25 \qquad k_{O_3} = not\ defined \qquad\qquad (Eq.\ S5)$$

$$\frac{O_3}{TOC} > 0.25 \qquad k_{O_3} = TOC \times 0.1001 \times (\frac{O_3}{TOC})^{-1.605} \qquad (Eq.\ S6)$$

Text S3. *Cryptosporidium* log inactivation for pre-ozonation and post-ozonation

Pre-ozonation process:

Because the main objectives of the pre-ozonation process are typically bulk organic matter transformation and TOrC oxidation, the O_3/TOC ratio is a highly useful parameter. However, it is still necessary to estimate the corresponding IOD and k_{O_3} for a particular O_3/TOC ratio because ozone "CT" still provides a more accurate estimate of *Cryptosporidium* inactivation. The corresponding parameters for the baseline scenario in the system dynamics model are summarized in Eq. S7-S10.

$$IOD = TOC \times 0.6025 \times (\tfrac{O_3}{TOC})^{0.6679} \qquad\qquad \text{(Eq. S7)}$$

$$k_{o_3} = TOC \times 0.1001 \times (\tfrac{O_3}{TOC})^{-1.605} \qquad\qquad \text{(Eq. S8)}$$

In Gamage et al. (2013), the median TOC concentration of the five secondary effluents was 7.2 mgC/L. Assuming a 13% reduction in TOC by UF (Trussell et al., 2016), the TOC concentration in the UF filtrate/pre-ozone feed would be 6.3 mgC/L. Using this value and an O_3/TOC ratio of 1.1 mgO₃/mgC, the corresponding applied ozone dose, IOD, and ozone decay rate constant would be 6.9 mg/L, 4.0 mg/L, and 0.54 min^{-1}, respectively. Assuming an ozone contact time of 5 minutes, Eqs. S9-S11 can be used to calculate the corresponding ozone residual (0.19 mg/L) and ozone CT (5.0 mg-min/L) in the pre-ozone effluent. An O_3/TOC of 1.1 mgO₃/mgC is assumed to be adequate to achieve significant oxidation of a wide range of TOrCs (Gerrity et al., 2014), including the 69% destruction of 1,4-dioxane (Snyder et al., 2014) required by the CA DDW potable reuse regulations (CDPH, 2014). A 5-minute contact time was selected to achieve nearly complete ozone decay and also achieve 2-log inactivation of *Cryptosporidium* based on the resulting ozone CT of 5.0 mg-min/L (Eq. S12).

141

$$O_3 \text{ residual } = \left[\left(\frac{O_3}{TOC}\right) \times TOC - IOD\right] \times e^{-k_{o_3}t} \qquad \text{(Eq. S9)}$$

$$O_3 \text{ } CT = \int_0^t \left[\left(\frac{O_3}{TOC}\right) \times TOC - IOD\right] \times e^{-k_{o_3}t} dt \qquad \text{(Eq. S10)}$$

Ozone CT can be calculated with an analytical solution to Eq. S10, as shown in Eq. S11, or estimated as the area under the curve of ozone residual versus contact time, as shown in Figure S5.

$$O_3 \text{ } CT = \frac{\left[\left(\frac{O_3}{TOC}\right) \times TOC - IOD\right]}{k_{o_3}} \times \left(1 - e^{-k_{o_3}t}\right) \qquad \text{(Eq. S11)}$$

According to the LT2 guidance manual (USEPA, 2010), *Cryptosporidium* inactivation with ozone can be estimated according to Eq. S12, in which T is the temperature in °C.

$$Cryptosporidium \text{ Log Credit} = 0.0397 \times 1.09757^T \times \text{Ozone } CT \qquad \text{(Eq. S12)}$$

For the computed O_3 CT of 5.0 mg-min/L and an assumed water temperature of 25°C, the corresponding *Cryptosporidium* log removal would be 2.0.
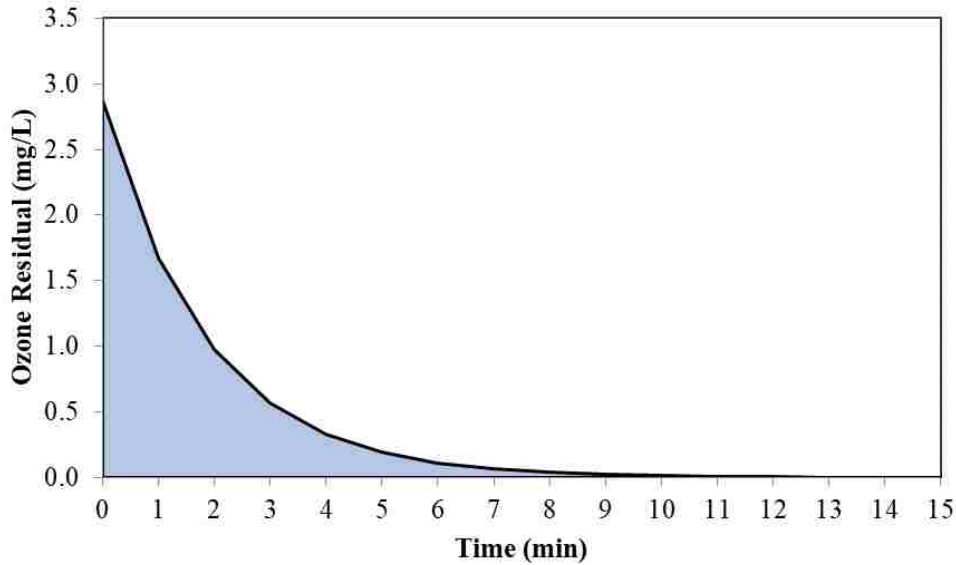

Figure S5. Ozone residual as a function of contact time.

142

Post-ozonation process:

Since the post-ozonation process is primarily used for disinfection purposes, it was assumed that the process would be operated and monitored to achieve a target ozone CT value. Considering the calculated/estimated removal and inactivation of *Cryptosporidium* prior to post-ozonation (7.0 logs; Table 3.3), an additional 3-log inactivation would be sufficient to meet the 10-log target established by the CA DDW and NWRI. Therefore, an ozone CT of 10 mg-min/L was assumed based on the published data by Korich et al. (1990) and LeChevallier and Au (2004), which demonstrated that constant exposure to 1 mg/L of ozone for 10 minutes could achieve this 3-log target. In fact, an ozone CT of 10 mg-min/L and an assumed water temperature of 25°C yields a *Cryptosporidium* log inactivation of 4.1 based on Eq. 12.

It is important to note that it will likely be acceptable to achieve the 10-log target in California by combining log credits from the advanced wastewater treatment plant and the conventional drinking water treatment plant (NWRI, 2016b), which will reduce burden on the advanced treatment processes. In other words, it may be possible to decrease the target CT value for post-ozone and still achieve the 10-log benchmark in the planned IPR system. This could result in a series of benefits, including reduced cost, energy consumption, and bromate formation. However, the proposed surface water augmentation regulations in California also require a minimum hydraulic retention time of 2-4 months and a minimum dilution ratio of 100:1 (or 10:1 if an additional 1-log credit is demonstrated somewhere in the treatment train). Instead of incorporating these requirements into the model, the higher post-ozone CT value was used as an alternative source of conservatism.

Text S4. Impact of process failures on ozone efficacy

Impact of UF and pre-ozonation on post-ozonation:

Ozone demand/decay and ozone disinfection efficacy are influenced by various water quality parameters, particularly turbidity and bulk organic matter composition and concentration. This model focuses exclusively on the effects of TOC in estimating the impacts of process failures on ozone efficacy. While UF generally achieves a nominal reduction in TOC, the combination of ozone and BAC can achieve significant reductions in TOC in potable reuse applications. For this study, a 13% reduction in TOC was assumed for UF, and a 40% reduction was assumed for O_3-BAC (Trussell et al., 2016). A failure in the UF process was assumed to result in 0% TOC reduction, and a failure in the pre-ozone process (i.e., minimal bulk organic matter transformation) was assumed to result in a 5% TOC reduction after BAC. These operational scenarios and the resulting water qualities are shown in Table S1.

Table S1. Failure scenarios for UF-O_3-BAC and the effects on TOC concentration

Scenario	UF		O3-BAC	
	Reduction	**TOC (mg/L)[3]**	**Reduction**	**TOC (mg/L)[4]**
Normal (no failure)	13%[1]	6.3	40%[1]	3.8
UF failure	0%	7.2	40%[1]	4.3
Pre-O_3 failure	13%[1]	6.3	5%[2]	6.0
UF and pre-O_3 failure	0%	7.2	5%[2]	6.8

[1] Trussell et al. (2016)

[2] Minimal reduction by BAC assumed during ozone failure (unpublished data)

[3] TOC for O_3-BAC feed; initial TOC concentration assumed to be 7.2 mgC/L (Gamage et al., 2013)

[4] TOC for post-ozone feed

For the baseline condition, the ozone CT for pre-ozonation (5.0 mg-min/L) was calculated based on an initial TOC concentration of 6.3 mgC/L, an O_3/TOC ratio of 1.10, and the equations described in Text S2. These operating conditions result in an applied ozone dose of 6.9 mg/L.

For post-ozonation, an ozone CT of 10 mg-min/L was specifically targeted to achieve adequate *Cryptosporidium* reduction across the entire treatment train. By reversing the approach described in Text S2, it is possible to determine that the applied ozone dose in the post-ozonation process is 5.1 mg/L, assuming the ozone is allowed to decay completely (i.e., contact time > 30 minutes based on the aforementioned demand/decay model).

Failures in the treatment train will have significant effects on ozone disinfection efficacy. For example, a UF failure will result in an increase in TOC in the pre-ozone feed. Assuming the applied ozone dose remains constant (i.e., constant ozone generator power and feed gas flow rate) during a UF failure, the resulting O_3/TOC ratio will decrease, thereby resulting in a lower ozone CT value and less *Cryptosporidium* inactivation. A similar effect would be observed in the post-ozonation process during a failure in pre-ozonation or a simultaneous failure in UF and pre-ozonation. The effects of these failure scenarios on TOC concentrations were summarized in Table S1, and the effects on ozone CT and the corresponding levels of *Cryptosporidium* inactivation are summarized in Tables S2-S3.

Table S2. Pre-ozonation CT values and log inactivation during process failures (at 25°C).

Scenario	TOC (mg/L)	O3/TOC[1]	Ozone CT (mg-min/L)	Inactivation (logs)
Normal (no failure)	6.3	1.1	5.0	2.0
UF failure	7.2	1.0	3.4	1.4
Pre-O_3 failure	N/A	0	0	0
UF and pre-O_3 failure	N/A	0	0	0

[1] Applied ozone dose assumed to be constant at 6.9 mg/L

Table S3. Post-ozonation CT values and log inactivation during process failures (at 25°C).

Scenario	TOC (mg/L)	O3/TOC[1]	Ozone CT (mg-min/L)	Inactivation (logs)
Normal (no failure)	3.8	1.4	10	4.1
UF failure	4.3	1.2	6.6	2.7
Pre-O_3 failure	6.0	0.9	2.4	1.0
UF and pre-O_3 failure	6.8	0.7	1.6	0.6
Post-O_3 failure	N/A	0	0	0

[1] Applied ozone dose assumed to be constant at 5.1 mg/L

145

Failure in the post-ozonation process:

Burns (2015) reported historical ozone CT values for a full-scale water recycling facility in Australia. Table S4 summarizes the statistical distribution of these ozone CT values.

Table S4. Statistical distribution of observed ozone CT values in Burns (2015)

Parameter	Post-Ozone
P5	3.4
P50	5.1
P95	7.0
P99	8.3
Max.	9.8
N	8,579

Assuming a normal distribution with the given 5th and 95th percentiles, the mean and standard deviation were estimated using a system of equations. Specifically, the corresponding Z values for the 5th and 95th percentiles are -1.645 and 1.645, respectively. Coupled with the historical ozone CT data, for which the 5th and 95th percentiles were 3.4 mg-min/L and 7.0 mg-min/L, the mean and standard deviation can be calculated as shown in Eqs. S13 and S14. Using this approach, the mean (μ) and standard deviation (σ) were determined to be 5.2 mg-min/L and 1.09 mg-min/L, respectively. The corresponding distribution is shown in Figure S6.

$$Z = \frac{x - \mu}{\sigma} \qquad\qquad \text{(Eq. S13)}$$

$$\begin{cases} -1.645 = \frac{3.4 - \mu}{\sigma} \\ 1.645 = \frac{7 - \mu}{\sigma} \end{cases} \qquad\qquad \text{(Eq. S14)}$$
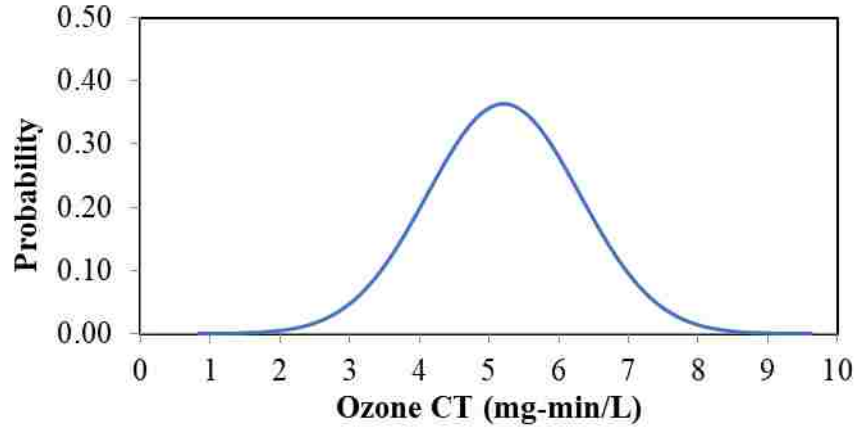
Figure S6. Normal distribution of post-ozonation CT values.

According to Burns (2015), the primary objective of the post-ozonation process at the full-scale facility was disinfection, specifically 0.6-log inactivation of *Cryptosporidium*. According to Eq. S12, for a temperature of 25℃ and a log inactivation target of 0.6, the corresponding ozone CT would be 1.5 mg-min/L. Assuming this is the treatment objective for Burns (2015), failure can be described as any observed ozone CT < 1.5 mg-min/L. According to the statistical distribution above, the corresponding probability of post-ozonation failure is 0.000325. This value was used as the probability of failure for the post-ozonation process in the current study (Table 3.4 in main text).

147

Text S5. Impact of ozonation on UV absorbance

Microbial inactivation with germicidal UV light is highly dependent on water quality and the performance of preceding treatment units, particularly unit processes that address turbidity and UV transmittance (UVT). Water matrices with high levels of suspended solids may result in significant shielding of target microbes, and water matrices with high absorptivity (i.e., low transmissivity) within the action spectrum of the UV lamp will exhibit low inactivation efficiencies. One way of estimating the expected level of microbial inactivation is to calculate the average UV dose within a reactor. This UV dose is a function of the average UV intensity and the exposure time. For this study, hydraulic inefficiencies were not considered (i.e., exposure times remained constant), but the model did account for water quality changes, specifically related to UV_{254} absorbance. The main text demonstrates how the incident intensity of a low-pressure (i.e., 254 nm light) UV disinfection system can be adjusted based on path length and the UV_{254} absorbance of the water matrix to determine the average UV intensity.

Table S5 summarizes typical UV_{254} absorbance values (k_A) for various wastewater qualities. This study assumed values for nitrified secondary effluents ($k_A = 0.25$ cm^{-1}) and filtered nitrified secondary effluents ($k_A = 0.175$ cm^{-1}) for modeling of the DPR advanced wastewater treatment train. When the preceding UF system exhibits normal operation, the feed to the ozone system is assigned a $k_A = 0.175$ cm^{-1}, but when the UF system is in failure mode, the feed to the ozone system is assigned a $k_A = 0.25$ cm^{-1}. The subsequent effect of ozonation on UV_{254} absorbance was determined according to correlations developed in Gerrity et al. (2012). These correlations describe the percent reduction in UV_{254} absorbance, which relates to the increase in UV_{254} transmittance, as a function of O_3/TOC ratio, as described in Eq. S15.

148

Although BAC achieves significant reductions in TOC in O_3-BAC systems, BAC was assumed to have no significant effect on UV_{254} absorbance.

Table S5. Typical base 10 UV_{254} absorbance values (k_A) for various wastewater qualities.

Wastewater	Metcalf & Eddy (2007)	Chen et al. (2006)	This study
Secondary effluent	0.15-0.35	0.17-0.50	--
Filtered effluent	--	0.20-0.40	--
Nitrified effluent	0.10-0.25	0.25-0.45	0.25
Filtered nitrified effluent	0.10-0.25	--	0.175

$$\Delta UV_{254}(\%) = 100 \times 0.51 \times \left(\frac{O_3}{TOC}\right)^{0.63} \tag{Eq. S15}$$

Once the final UV_{254} absorbance is known, the expected UV dose can be adjusted to account for water quality effects. The current study assumed a typical O_3/TOC ratio of 1.1 for bulk organic matter transformation and trace organic contaminant destruction, which would result in a 54% reduction in UV_{254} absorbance during normal operation. Therefore, the final UV_{254} absorbance under normal operational conditions (i.e., fully functioning UF and O_3) would be 0.080 cm^{-1}. In the event of a UF failure, the feed to the ozone system would have a UV_{254} absorbance of 0.25 cm^{-1}, and the O_3/TOC ratio of 1.1 would achieve a UV_{254} absorbance of 0.115 cm^{-1}. In the event of ozone failure, the water quality would be equivalent to a filtered nitrified effluent with a UV_{254} absorbance of 0.175 cm^{-1}. Finally, simultaneous failures in the UF and ozone systems would result in a UV_{254} absorbance of 0.25 cm^{-1}. These scenarios are summarized in Table S6.

Table S6. UV_{254} absorbance values for different modeling scenarios.

Operational Scenario	UV_{254} absorbance or k_A (cm^{-1})
Normal (no failure)	0.080
UF failure (with O_3)	0.115
O_3 failure (with UF)	0.175
UF and O_3 failure	0.25

149

Text S6. Model framework for UV disinfection

As described in the main text, the UV process in the DPR system can be modeled with two different approaches. In the first approach, the primary treatment objective is disinfection, and the target UV dose is 80 mJ/cm^2, which is the minimum recommended dose according to the National Water Research Institute's UV disinfection guidelines (NWRI, 2012). In the second approach, the primary treatment objective is NDMA photolysis. The model assumes an NDMA concentration of 50 ng/L in the UV feed and a treatment objective of 5 ng/L, which is intended to reliably achieve the 10-ng/L notification level in California (CPDH, 2014).

Given the parameters listed in Table 3.1 in the main text (i.e., $I_0 = 25$ mW/cm^2 and path length = 10 cm), one can use the UV$_{254}$ absorbance values in Table S6 to determine the I_{avg} for the system and the required hydraulic residence time in the UV reactor to achieve the target UV doses in each scenario. Again, the hydraulic residence times are calculated based on the 'no failure' scenario, and the hydraulic residence times remain constant during the various failure scenarios, thereby reducing the UV dose. The UV doses for the various scenarios were calculated using Eqs. 13-15 in the main text and are summarized in Table S7. The UV-dose-based photolysis rate constant for NDMA was assumed to be 4.5×10^{-3} (mJ/cm^2)$^{-1}$ (Lee et al., 2016). The effects on *Cryptosporidium* inactivation and NDMA destruction are summarized in Table S8.

Table S7. UV$_{254}$ absorbance values and UV doses for different modeling scenarios.

Operational Scenario	UV$_{254}$ absorbance or k_A (cm^{-1})	UV Dose in Disinfection Scenario (mJ/cm^2)	UV Dose in NDMA Scenario (mJ/cm^2)
Normal (no failure)	0.0802	80	512
UF failure (with O$_3$)	0.1146	62	395
O$_3$ failure (with UF)	0.175	43	274
UF and O$_3$ failure	0.25	30	194

150

Disinfection scenario:

Normal (no failure): $I_{avg} = I_0 \times \frac{\left(1-10^{-k_A x}\right)}{2.303 \times k_A x} = 25 \times \frac{(1-10^{-0.0802 \times 10})}{2.303 \times 0.0802 \times 10} = 11.4$ mJ/cm^2

Target UV Dose = 80 mJ/cm^2 = $I_{avg} \times$ t = 11.4 mJ/cm$^2 \times$ t → t = 7.0 seconds (constant)

NDMA scenario:

ln (C/C$_0$) = -$k_{NDMA,UV} \times$ UV Dose → ln (5/50) = -4.5×10^{-3} (mJ/cm^2)$^{-1}$ × UV Dose

Target UV Dose = 512 mJ/cm^2 = $I_{avg} \times$ t = 11.4 mJ/cm$^2 \times$ t → t = 45 seconds (constant)

Table S8. UV_{254} absorbance values and theoretical treatment efficacy. The log inactivation values assume linear extrapolation of published UV dose response curves for *Cryptosporidium*. These estimated values are significantly higher than the values actually observed in experimental samples and are assumed to be unreasonably high. Therefore, log inactivation credits are typically capped according to regulatory frameworks (e.g., 6 logs in California) or based on maximum observed inactivation levels in practice or experiments.

Operational Scenario	Disinfection Scenario		NDMA Photolysis Scenario	
	Log Inactivation of *Cryptosporidium*[1]	Percent Reduction in NDMA	Log Inactivation of *Cryptosporidium*[1]	Percent Reduction in NDMA
Normal (no failure)	19	30%	124	90%
UF failure (with O_3)	15	24%	96	83%
O_3 failure (with UF)	10	18%	66	71%
UF and O_3 failure	7	13%	47	58%

[1]*Cryptosporidium* log credit limited to 6.0 in model (CDPH, 2014)

As described in the main text, an arbitrary failure probability of 0.01 was assumed for UV due to a lack of failure data in the literature. The significance of this value was then evaluated using a sensitivity analysis. The results of the sensitivity analysis for a range of failure probabilities (0.0001-0.1) are shown in Figure S7. The results illustrated that probabilities of failure less than 0.01 did not have a significant impact on the final risk of infection, but a probability of failure of 0.1 caused the risk of infection to increase by 6 orders of magnitude. Because a 10% failure rate (i.e., once every 10 days) is likely overly conservative, a value of 0.01 was deemed appropriate for the baseline condition.

Figure S7. Sensitivity analysis on probability of failure of UV disinfection.
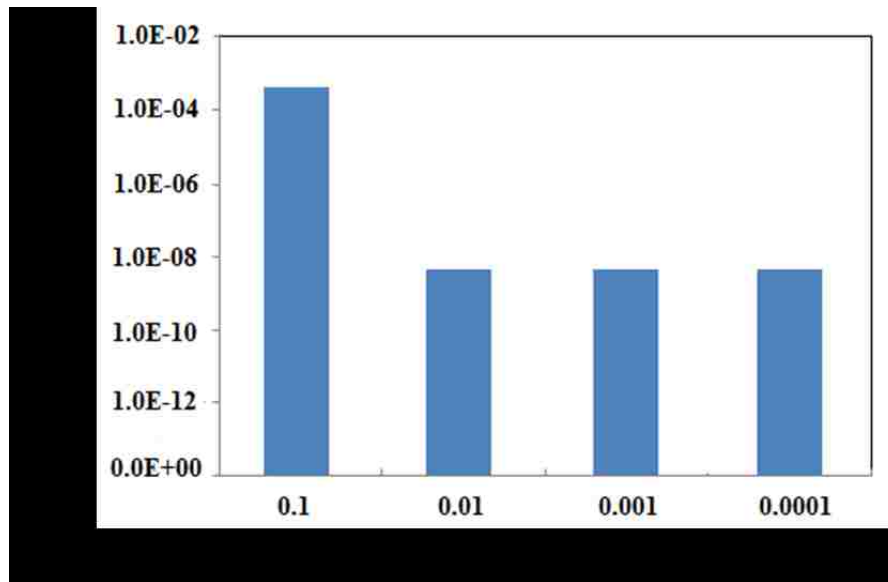
System dynamics is a non-linear, mathematical simulation of complex, interrelated system elements, which are represented as stocks, flows, convertors, and arrows (Forrester, 1958). Figure S7 illustrates how these key features are represented in the STELLA software platform. For the current study, the system dynamics model was used to predict the concentration of *Cryptosporidium* oocysts at each point in the potable reuse system. In this stock-and-flow structure, each stock represents an engineered or environmental barrier, and the flows represent the wastewater that passes through each component of the system. Each of the three potable reuse systems modeled in this study (i.e., *de facto*, planned IPR, and DPR) incorporates different sectors, as illustrated in Figures S8-S11 below.
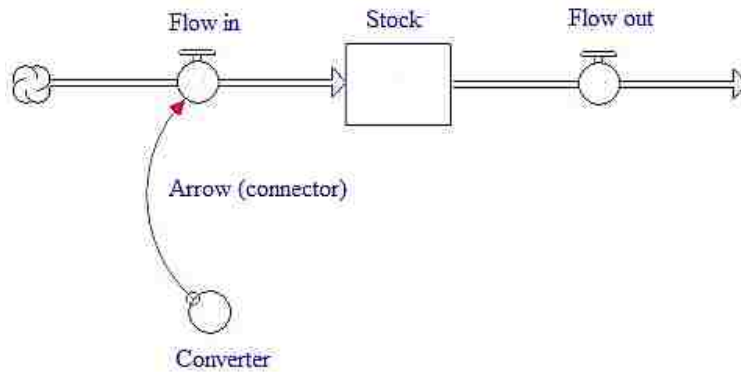

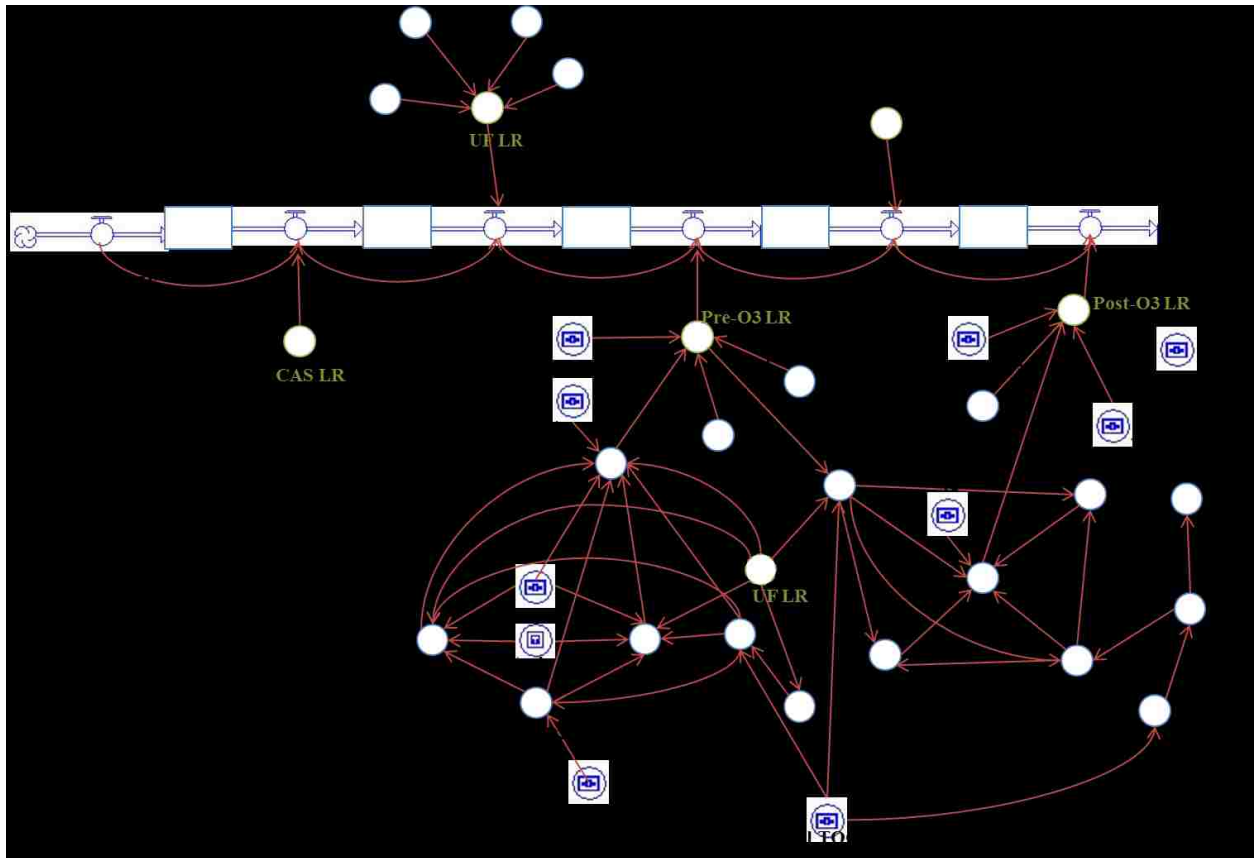**Figure S8**. A schematic diagram of the key features of system dynamics STELLA

154

Figure S9. Schematic diagram of the flows and converters used in the advanced wastewater treatment train sector in the planned IPR system. The schematic is adapted from the STELLA system dynamics software program.
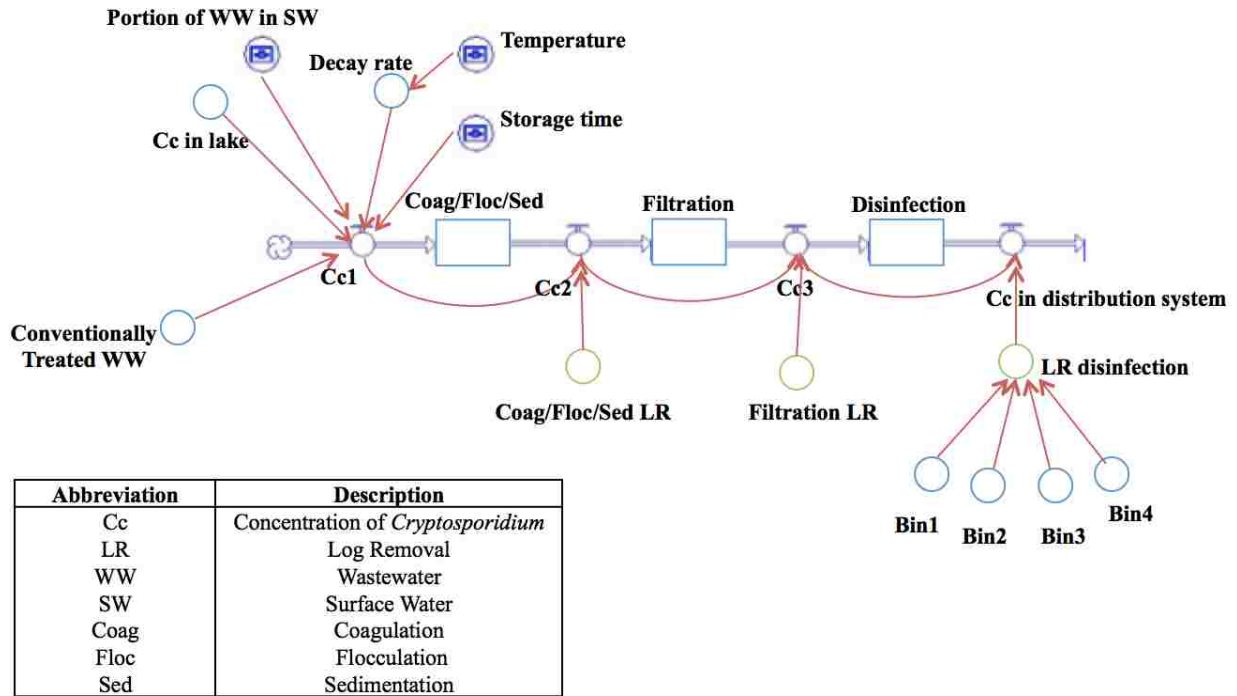
Figure S10. Schematic diagram of the flows and converters used in the conventional drinking water treatment plant sector. The schematic is adapted from the STELLA system dynamics software program.
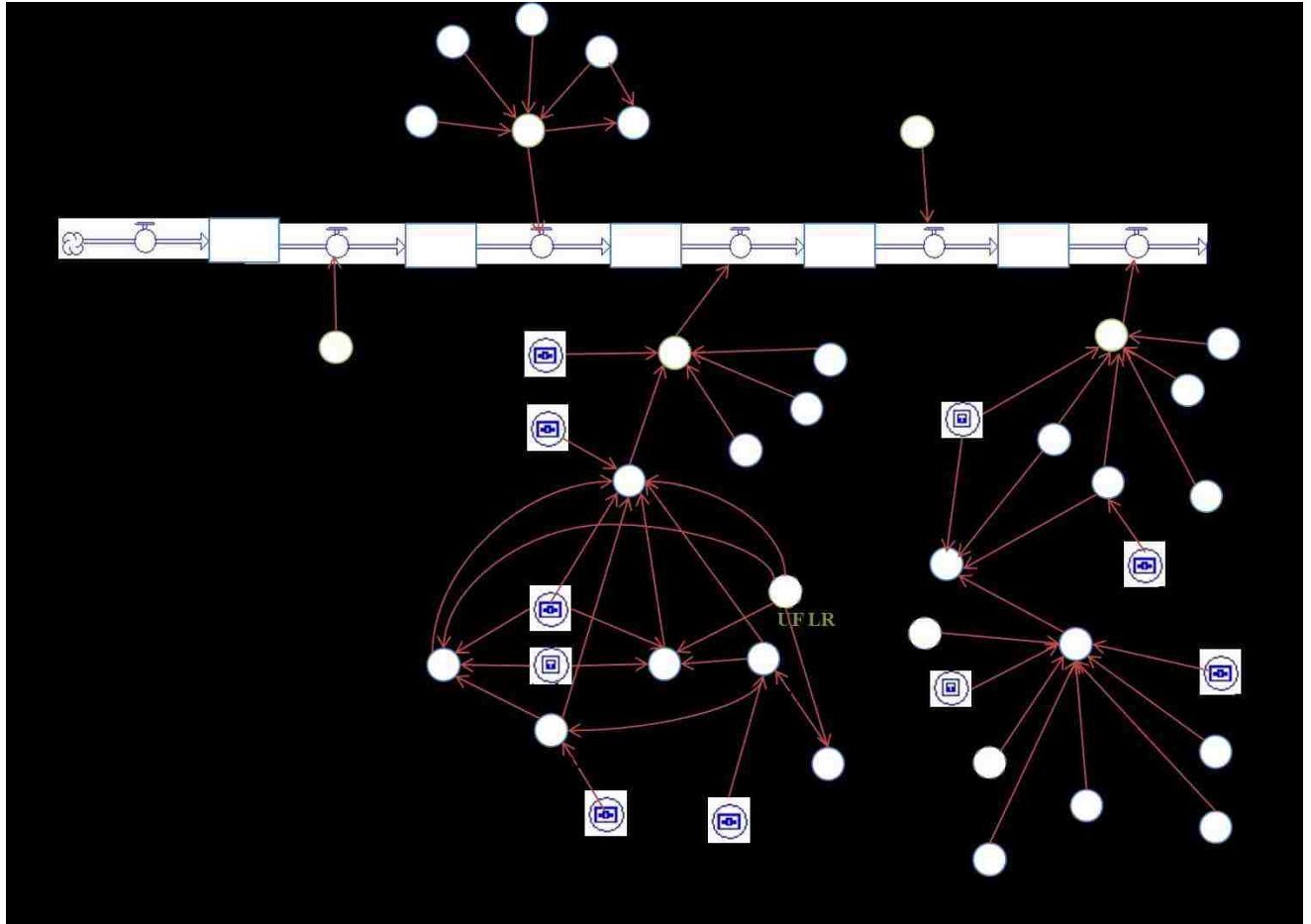
Figure S11. Schematic diagram of the flows and converters used in the advanced wastewater treatment train sector in the DPR system. The schematic is adapted from the STELLA system dynamics software program.
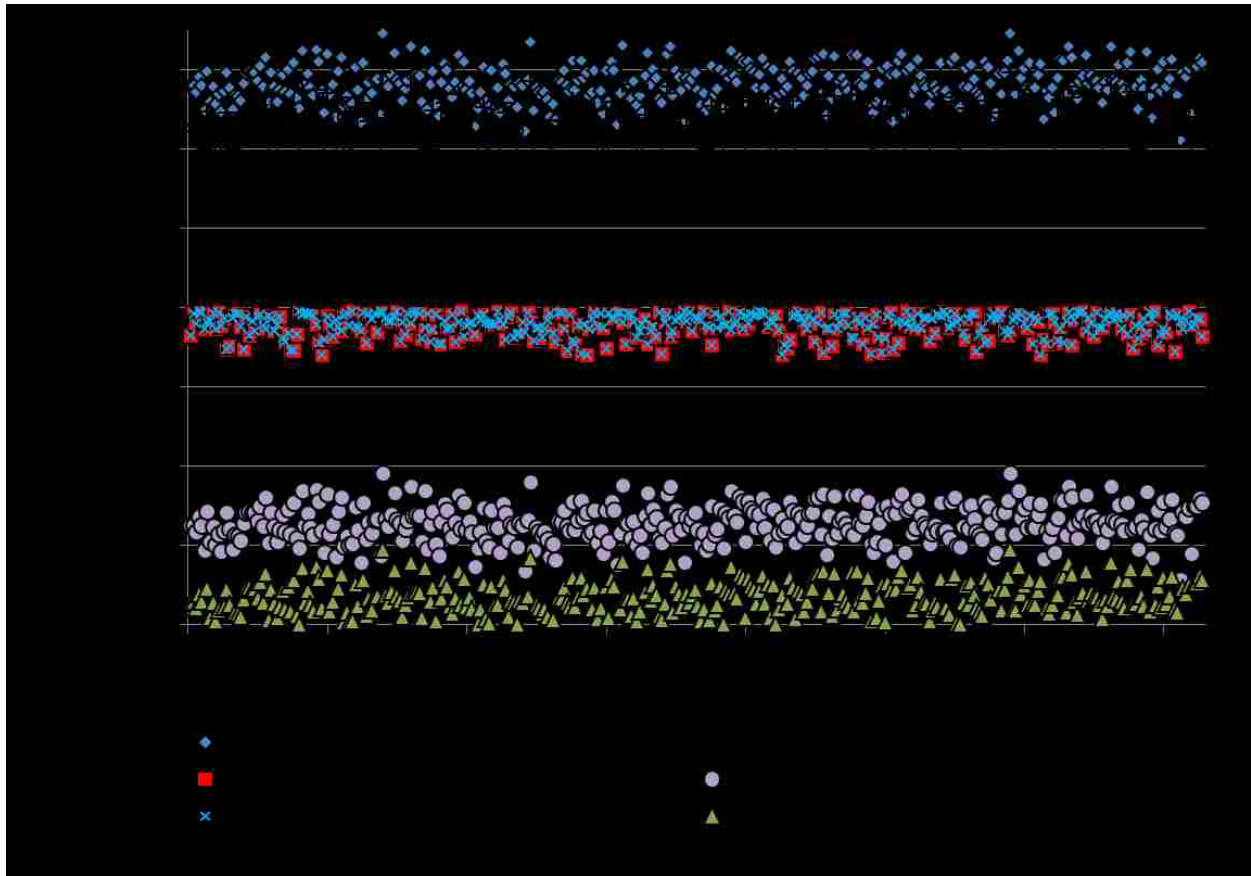
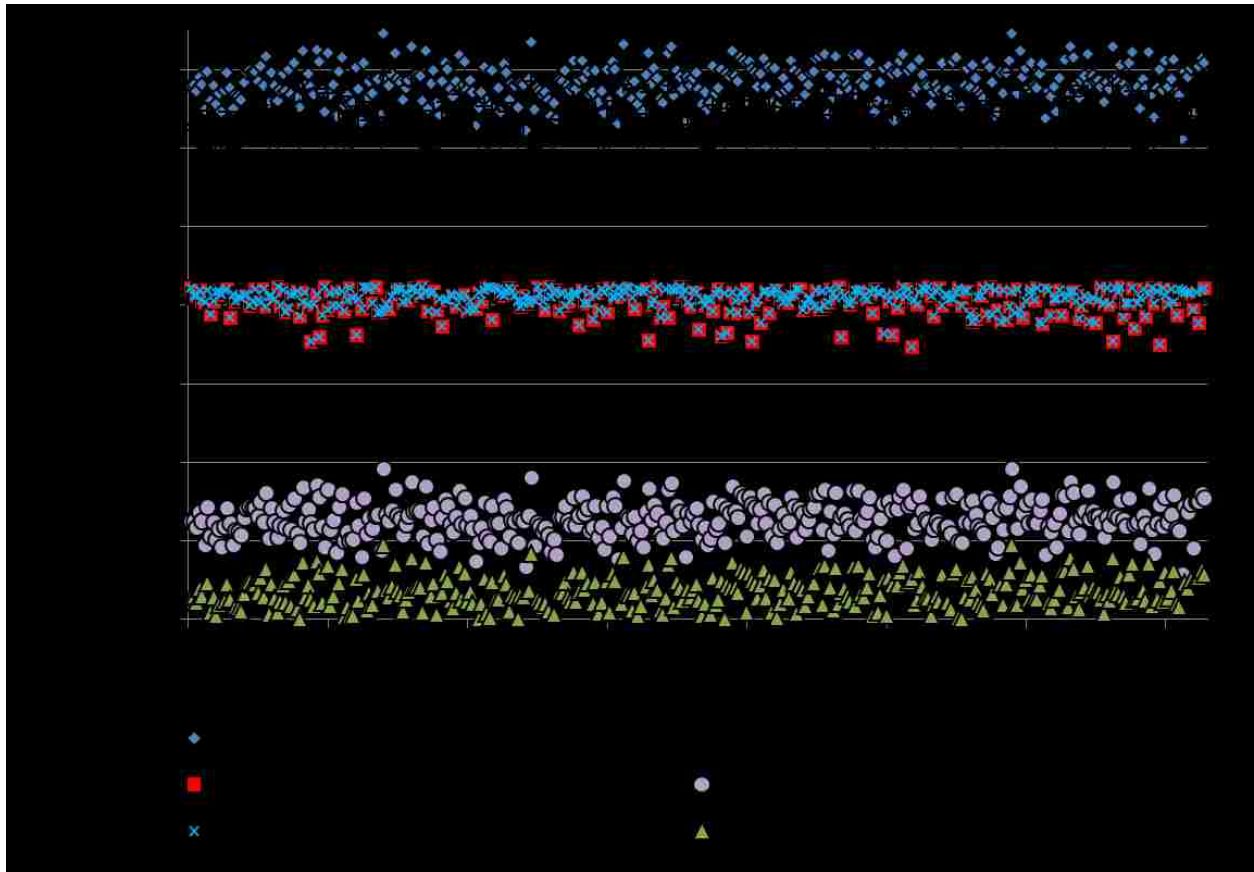**Figure S12**. *Cryptosporidium* concentrations for the scenario 2 baseline condition.

158

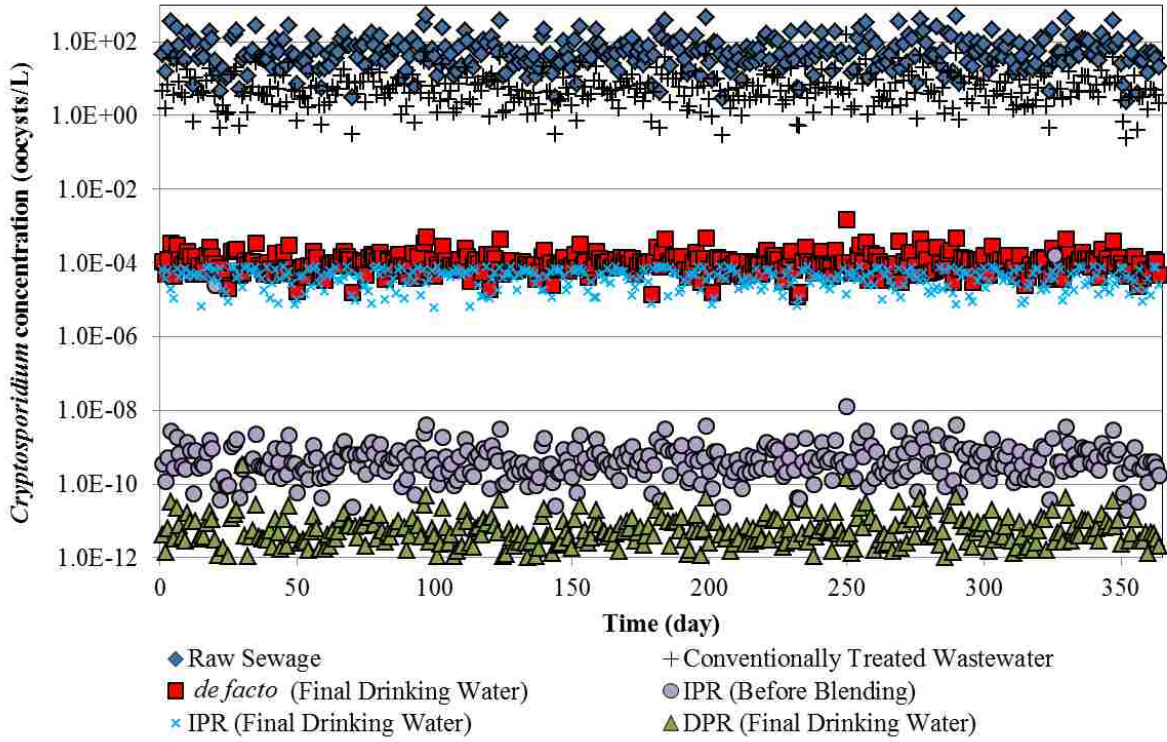**Figure S13**. *Cryptosporidium* concentrations for the scenario 3 baseline condition.

Figure S14. *Cryptosporidium* concentrations for the scenario 2 critical condition.
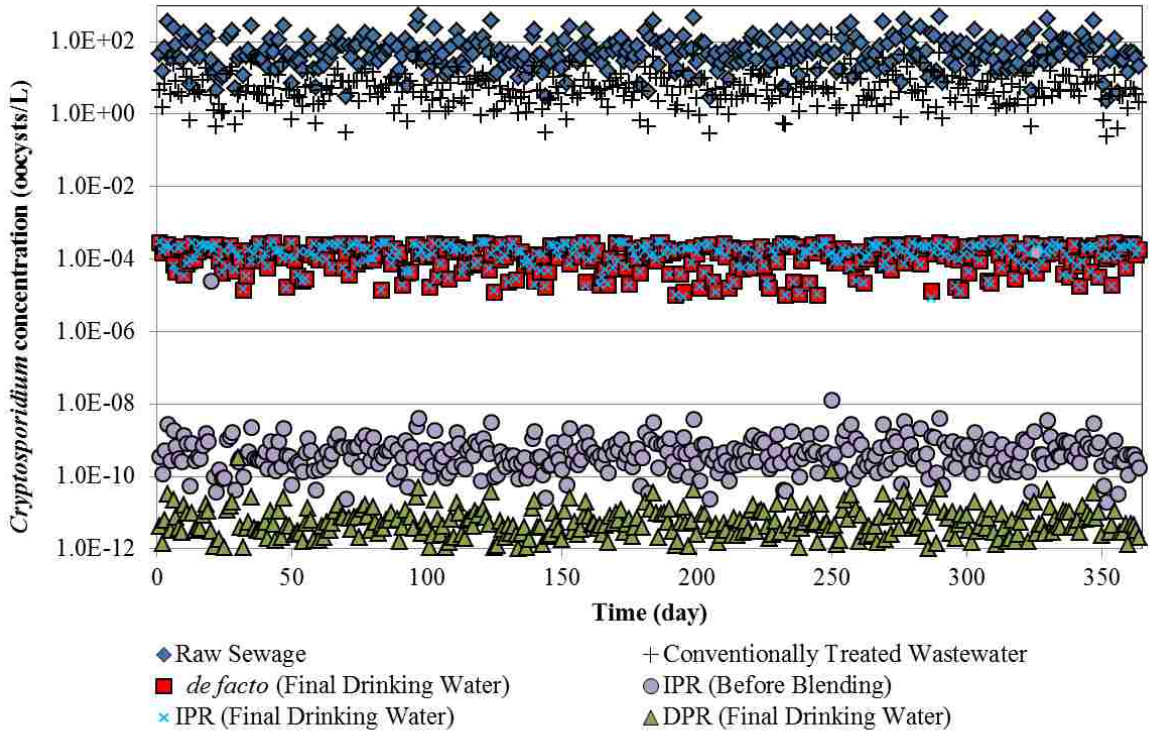
Figure S15. *Cryptosporidium* concentrations for the scenario 3 critical condition.

Appendix 2

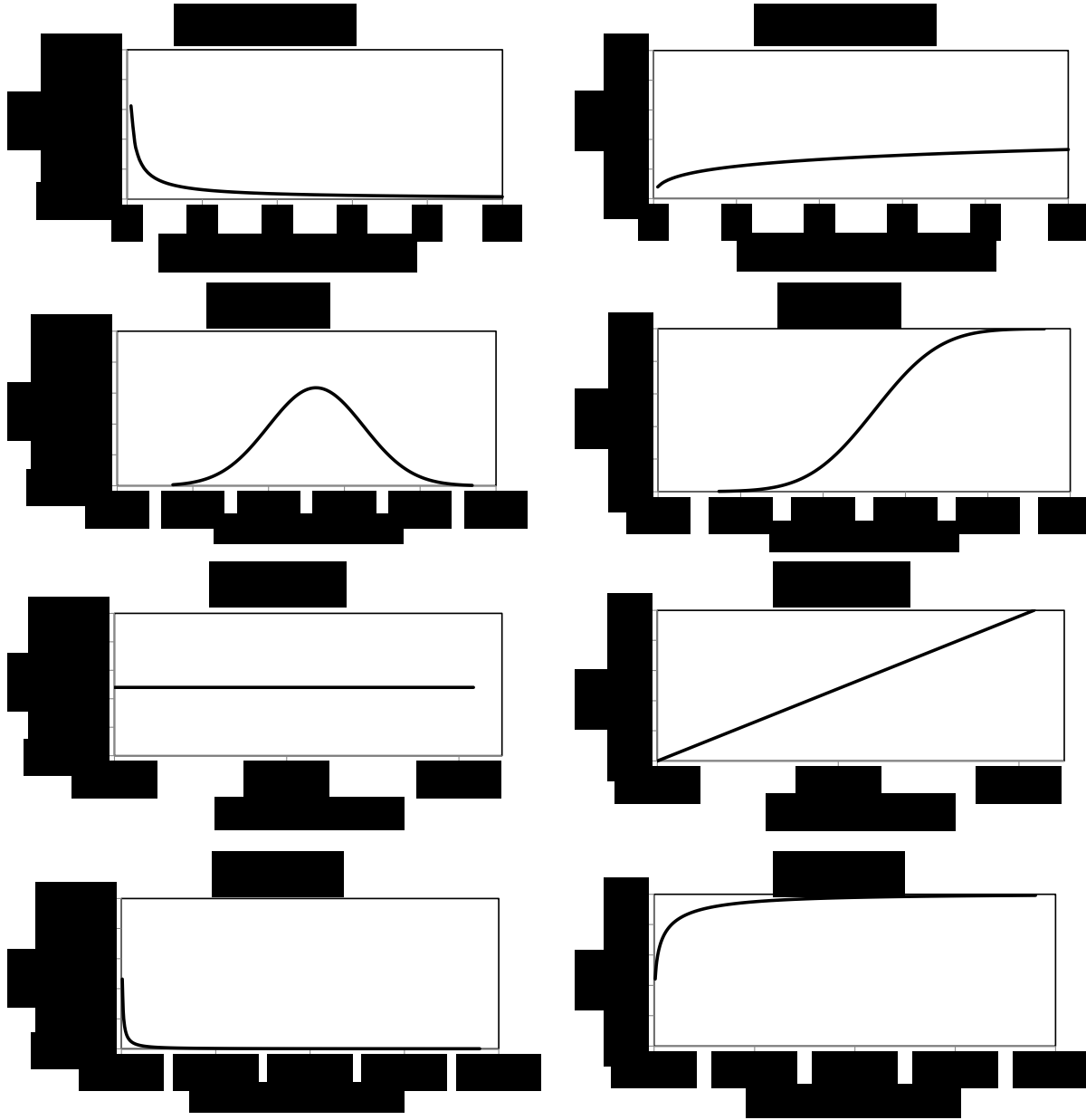**Text S1**. Pathogen probability (PDFs) and cumulative distribution functions (CDFs)

Figure S1. PDFs and CDFs of pathogen concentrations in raw wastewater.

Additional discussion related to NoV concentrations in raw wastewater:

Jahne (2017) reported NoV concentrations in wastewater from a single office building, with a maximum of $7.5\log_{10}$ gc/L, but this may overestimate the levels that are expected in a blended municipal wastewater from the larger community. The values in Jahne (2017) may be appropriate when evaluating small-scale DPR systems—a single office building, for example—but may not be appropriate at larger scale.

Simmons et al. (2011) reported a mean concentration of 7.7 $\log_{10}$ gc/L in eight samples from a single wastewater treatment plant, although this value was inflated due to an extreme spike in a sample collected in January. Seasonal effects were also observed for NoV in Eftim et al. (2017). Excluding the maximum value from Simmons et al. (2011), the median concentration was 5.8 $\log_{10}$ in the remaining 7 samples from that wastewater treatment plant.

Due to the small sample sizes in these studies, the more comprehensive review in Eftim et al. (2017) was used as the basis for NoV concentrations in raw wastewater in the current study. However, this highlights the importance of local pathogen characterization when assessing public health risk.
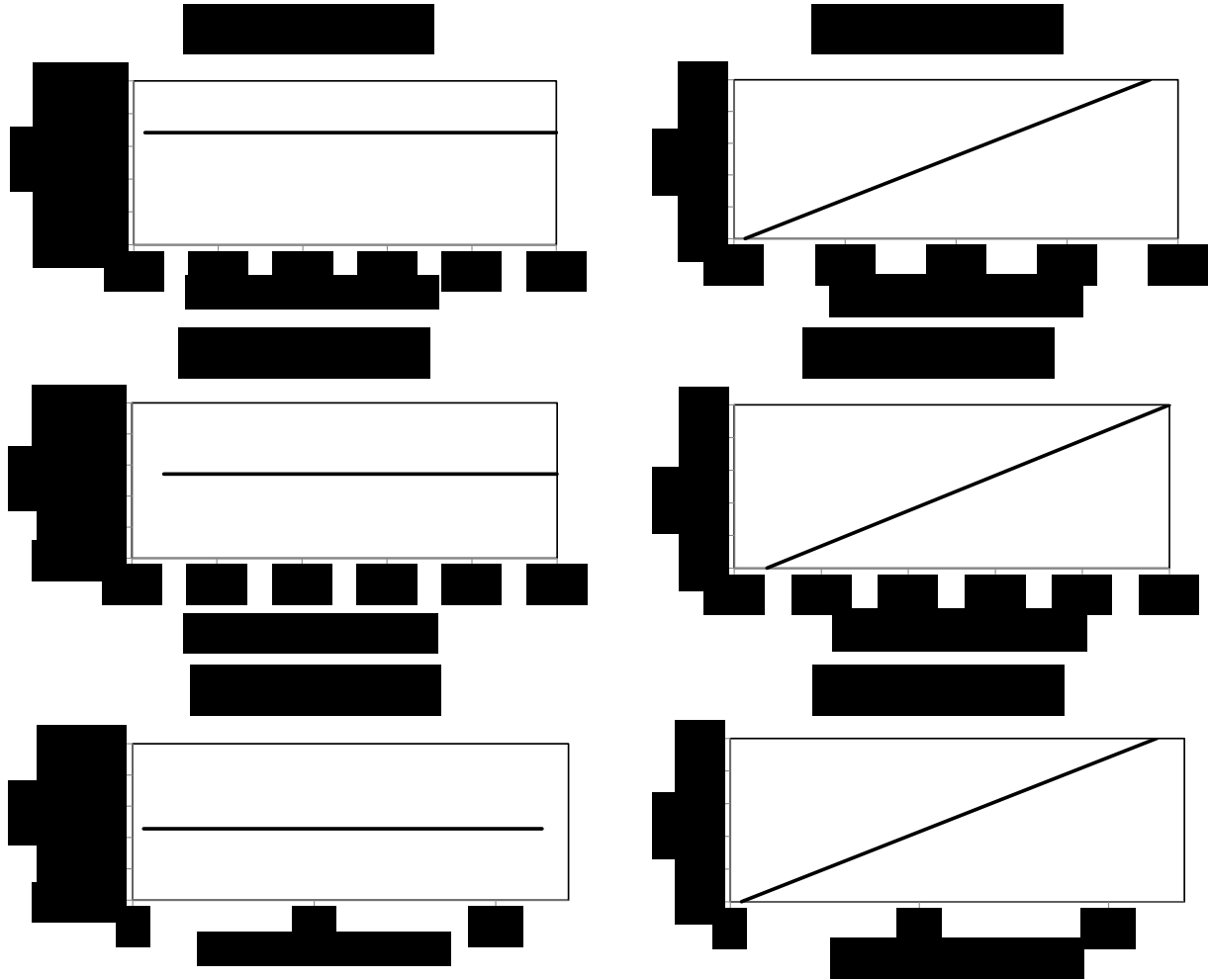
Figure S2. PDFs and CDFs of pathogen concentrations in surface water. For Cryptosporidium, S1 = Bin 1 surface water, S2 = Bin 2 surface water, and S3 = Bin 4 surface water, in accordance with the LT2ESWTR and LeChevallier et al. (1991).

Figure S2 (continued). PDFs and CDFs of pathogen concentrations in surface water.

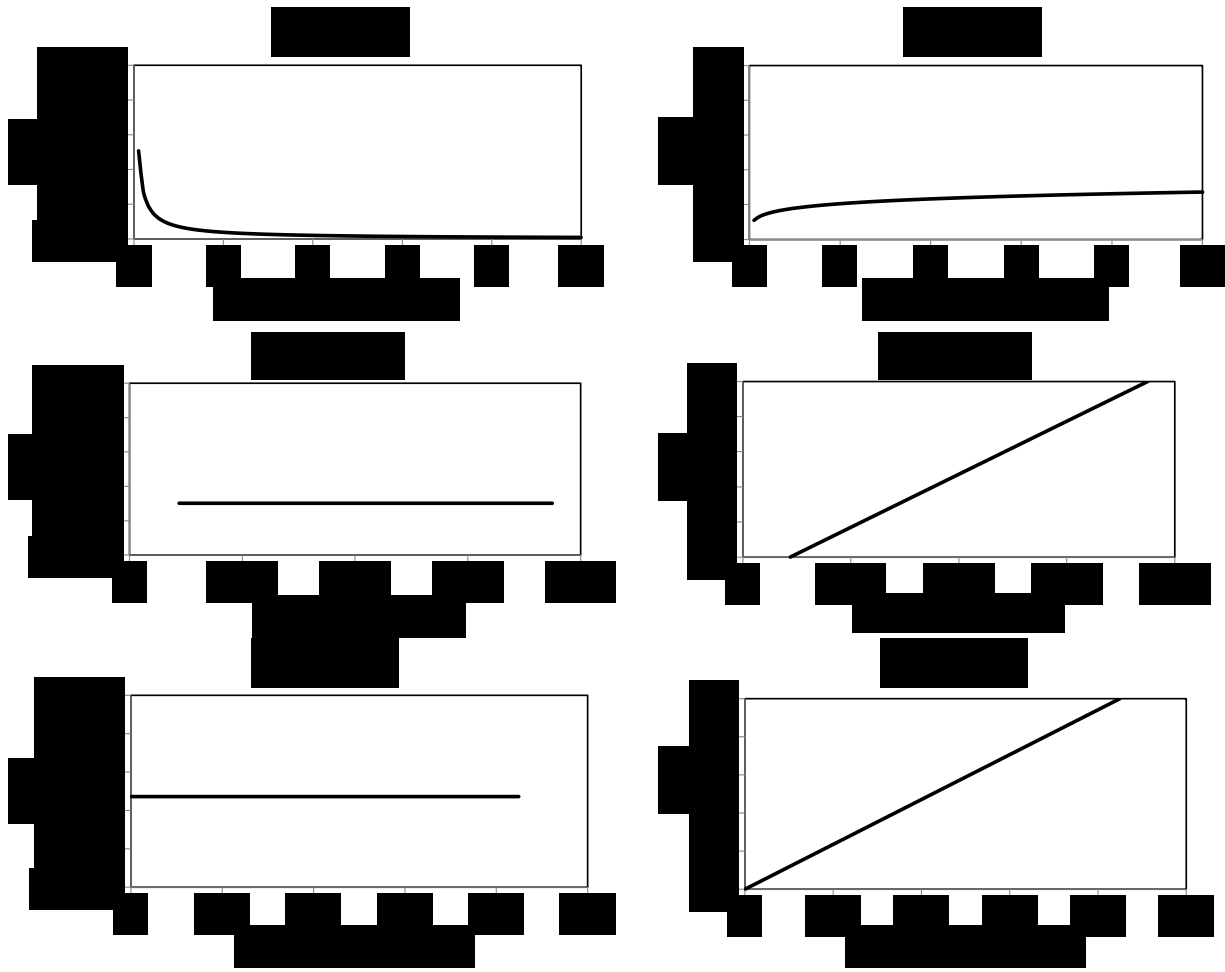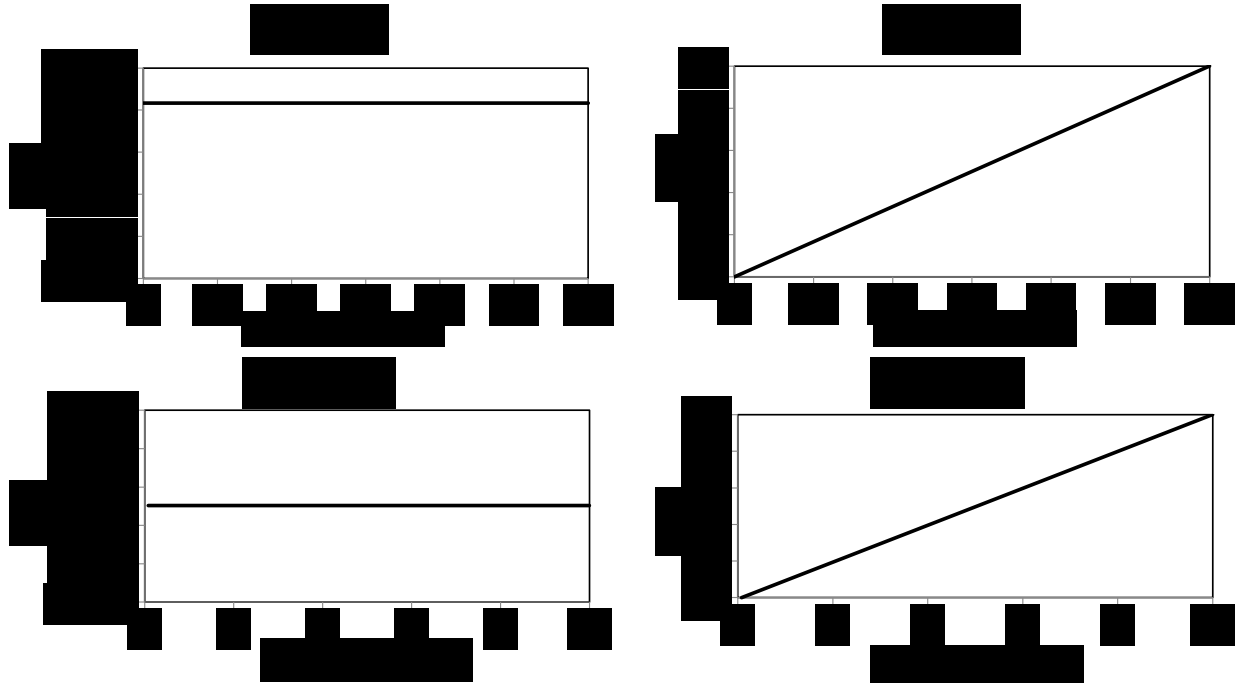**Figure S3.** PDFs and CDFs of pathogen concentrations in groundwater. The *Cryptosporidium* oocyst and *Salmonella* concentrations were assumed to be 0.

Text S2. Recycled water contribution in groundwater replenishment projects

Table S1 summarizes the recycled water contribution (RWC) at 66 groundwater replenishment sites in the Montebello Forebay (from 1960 to 1991) (Sloss et al., 1996). The average RWC was determined to be 14% (and rounded up to 15% for the current study) according to Eq. S1.

Table S1. RWCs in the Montebello Forebay (Sloss et al., 1996).

Number of service areas (f)	RWC (%)	m	f × m
8	0	0	0
14	1-4	2.5	35
19	5-19	12	228
25	20-31	25.5	637.5

$$\overline{x_g} = \frac{\sum f \times m}{n} = \frac{900.5}{66} = 14\% \qquad \text{(Eq. S1)}$$

where, $\overline{x_g}$ = mean of the frequency distribution data

f = frequency

m = midpoint of each group

n = total frequency

168

Text S3. Regulatory log removal value (LRV) framework

Because the data in Table 3.4 in the main text represent observed treatment performance, they may differ from the typical regulatory credit awarded to each treatment process. The regulatory credits summarized in Table S2 are provided as a basis for comparison.

Table S2. Typical pathogen regulatory log credits for engineered treatment processes.

Treatment Process	*Cryptosporidium*	Norovirus	Adenovirus	*Salmonella*
CAS[a]	NC[h]	1[g]	1[g]	NC
Conventional Filtration[b]	3	2	2	NC[c]
MF[a,i]	4	0	0	4
UF[a,g,i]	4	1	1	4
RO[a,g]	1.5-2.0	1.5-2.0	1.5-2.0	1.5-2.0
BAC[a,g]	0	0	0	0
Ozone[g]	1	6	6	4
UV[a,h]	6	6	6[a,d]	6
Chlorine				
DWTP	0[a]	2[b]	2[b]	4[f]
ESB	0[a]	6[a,e]	6[a,e]	4[f]

[a]Tchobanoglous et al. (2015)
[b]USEPA (2006b)
[c]LT2 does not provide direct guideline on log reduction of *Salmonella*
[d]At a minimum UV dose of 235 mJ/cm^2
[e]based on maintaining a minimum free residual of 0.4 mg/L over 24 hour storage time
[f]NRC (2012)
[g]Trussell et al. (2016)
[h]NC = no credit
[i]CDPH (2011)

Text S4. Ozone inactivation of *E. coli* as a surrogate for *Salmonella*

Because *Salmonella* disinfection kinetics are poorly defined in the literature, data describing *E. coli* inactivation with ozone (Table S3; Zuma et al., 2009) were used as a surrogate. The corresponding log inactivation and ozone CT values are summarized in Table S4 and Figure S4.

**Table S3.** Kinetics of E. coli inactivation with ozone (Zuma et al., 2009)

Time (min)	O_3 Concentration (mg/L)				
	0.91	1.78	2.78	3.44	4.72
	Log CFU/mL				
0	8.28	8.29	8.23	8.10	8.13
1	7.78	7.59	7.50	7.13	6.39
2	7.02	6.73	6.51	6.10	5.22
3	6.28	5.76	5.56	4.60	4.05
4	5.70	4.90	4.60	3.89	3.00
5	5.20	4.06	3.71	2.99	-
6	4.70	3.49	2.78	2.40	-

Table S4. CT table (mg-min/L) for log inactivation of E. coli

CT	Log Removal	CT	Log Removal	CT	Log Removal
0	0.00	9.44	2.91	18.88	4.08
0.91	0.50	2.73	2.00	4.55	3.08
1.78	0.70	5.34	2.53	8.90	4.23
2.78	0.73	8.34	2.67	13.9	4.52
3.44	0.97	10.32	3.50	17.2	5.11
4.72	1.74	14.16	4.08	5.46	3.58
1.82	1.26	3.64	2.58	10.68	4.80
3.56	1.56	7.12	3.39	16.68	5.45
5.56	1.72	11.12	3.63	20.64	5.70
6.88	2.00	13.76	4.21		

*CT values were calculated based on data from Table S3.

Figure S4. Inactivation of E. coli as a function of ozone CT. Adapted from Zuma et al. (2009).

171
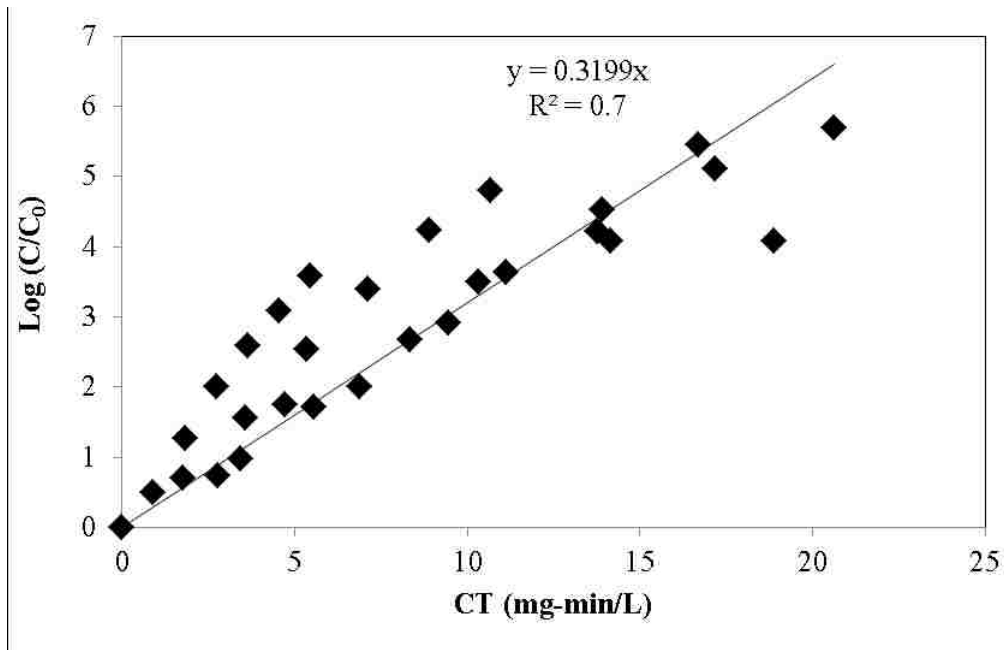
Text S5. Inactivation of norovirus by UV disinfection

Due to lack of information, MNV was used as a viral surrogate to evaluate the
effectiveness of UV disinfection for NoV inactivation (Lee et al., 2008). The MNV log
inactivation data from Lee et al. (2008) are summarized in Table S5 and plotted in Figure S5.
Based on linear regression, the first order inactivation rate constant was determined to be 0.15
$(mJ/cm^2)^{-1}$.

Table S5. Log inactivation of MNV as a function of UV dose (Lee et al., 2008).

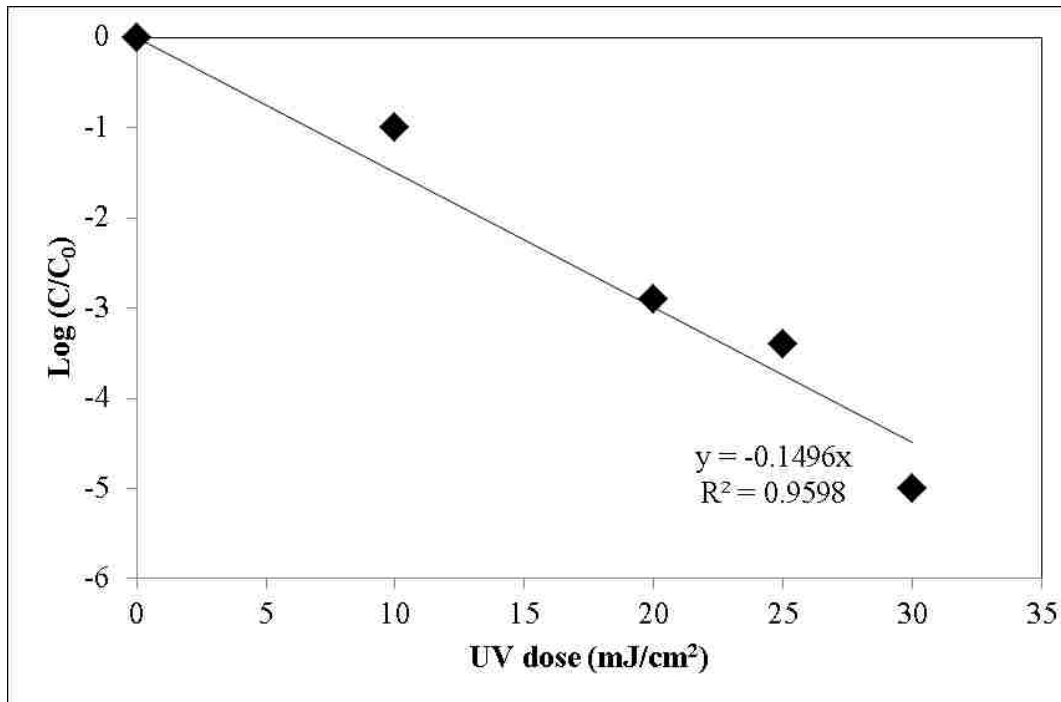| UV dose (mJ/cm^2)	Log reduction
0	0
10	-1.0
20	-2.9
25	-3.4
30	-5.0

Figure S5. Log inactivation of MNV as a function of UV dose (Lee et al., 2008).

172

Text S6. UV$_{254}$ absorbance values for different wastewater qualities

Table S6. Typical base 10 UV$_{254}$ absorbance values (k_A) for various wastewater qualities.

Wastewater	Metcalf & Eddy (2007)	Chen et al. (2006)	This study
Secondary effluent	0.15-0.35	0.17-0.50	--
Filtered effluent	--	0.20-0.40	--
Nitrified effluent	0.10-0.25	0.25-0.45	0.25
Filtered nitrified effluent	0.10-0.25	--	0.175
MF filtrate	0.04-0.10	0.158-0.3	0.17
RO permeate	0.01-0.05	0.05-0.2	0.10

Table S7. UV$_{254}$ absorbance values for different modeling scenarios.

Operational Scenario	UV$_{254}$ absorbance or k_A (cm^{-1})
Normal (no failure)	0.08 (O$_3$-based)
	0.10 (RO-based)
MF failure (with RO)	0.10
RO failure (with MF)	0.17
MF and RO failure	0.25
UF failure (with O$_3$)	0.115
O$_3$ failure (with UF)	0.175
UF and O$_3$ failure	0.25

173

Table S8. Health burden calculation for Salmonella.

	Health outcome	Outcome fraction	Duration of illness	Severity weight	DALYs/case
Morbidity	Mild diarrhea	0.9984	0.01918 years (7 days)[b]	0.067[d]	1.29×10^{-3}
Mortality	Death	0.0016[a]	Life expectancy/age at death[c]	1	0.0666
Health Burden					0.068

[a]Calculated based on Ao et al. (2010) (93 million infections and 155,000 diarrheal death each year)
[b]Health Canada. (2010)
[c]U.S. life expectancy = 78.7 years (World Bank, 2015); Age at death (the mean weighted age of the population assuming no difference in fatality rates) = 36.88 (Health Canada, 2010)
[d]Based on mild diarrhea from *Cryptosporidium*, *Giardia*, and rotavirus

YLD= (outcome fraction × duration of illness × severity weight) for health outcome contributing to morbidity

LYL= ([life expectancy – age at death] × severity weight) for health outcome contributing to mortality

Conditional probability of illness given an infection: According to Jertborn et al. (1990), the

number of cases that developed symptomatic disease after infection was 7 out of 17 cases.

Asymptomatic disease of *Salmonella* is not considered to be an illness (Mangen et al., 2013).

$$\left(P_{ill}\middle|P_{inf}\right) = \frac{Symptomatic\ Salmonellosis}{Symptomatic+\ Asymptomatic} = \frac{7}{17} = 0.41 \qquad \text{(Eq. S2)}$$

Table S9. Annual risk of infection during optimal operation.

| Pathogen	Annual Risk of Infection					Disease Burden				
	min	P5	median	P95	max	min	P5	median	P95	max
TT1, TT3, TT4, TT5										
Crypto (S1)	1.8E-03	1.9E-03	2.0E-03	2.1E-03	2.2E-03	2.2E-06	2.3E-06	2.4E-06	2.5E-06	2.6E-06
Crypto (S2)	2.6E-03	2.7E-03	2.8E-03	2.9E-03	3.1E-03	3.0E-06	3.2E-06	3.4E-06	3.5E-06	3.6E-06
Crypto (S3)	8.7E-03	9.1E-03	9.6E-03	1.0E-02	1.1E-02	1.0E-05	1.1E-05	1.1E-05	1.2E-05	1.3E-05
NoV	2.6E-04	2.9E-04	3.4E-04	4.0E-04	4.5E-04	7.6E-14	1.3E-13	2.2E-13	4.9E-13	1.7E-12
AdV	1.1E-03	1.2E-03	1.2E-03	1.3E-03	1.3E-03	3.0E-05	3.1E-05	3.3E-05	3.4E-05	3.5E-05
Salmonella	8.0E-04	8.7E-04	1.0E-03	1.2E-03	1.3E-03	2.2E-05	2.4E-05	2.8E-05	3.2E-05	3.6E-05
TT2										
Crypto	0.0E+00	9.5E-14	5.7E-13	2.9E-12	6.8E-11	0.0E+00	1.1E-16	6.8E-16	3.4E-15	8.1E-14
NoV	1.1E-05	1.2E-05	1.2E-05	1.3E-05	1.3E-05	9.7E-17	1.1E-16	1.2E-16	1.3E-16	1.3E-16
AdV	5.0E-06	5.3E-06	5.6E-06	5.9E-06	6.0E-06	1.3E-07	1.4E-07	1.5E-07	1.6E-07	1.6E-07
Salmonella	0.0E+00	0.0E+00	0.0E+00	0.0E+00	0.0E+00	0.0E+00	0.0E+00	0.0E+00	0.0E+00	0.0E+00
TT6										
Crypto	1.2E-11	1.8E-11	2.9E-11	5.2E-11	1.4E-10	1.4E-14	2.2E-14	3.5E-14	6.2E-14	1.6E-13
NoV	0.0E+00	0.0E+00	0.0E+00	0.0E+00	0.0E+00	0.0E+00	0.0E+00	0.0E+00	0.0E+00	0.0E+00
AdV	2.7E-11	3.7E-11	5.1E-11	6.8E-11	8.4E-11	0.0E+00	9.8E-13	1.4E-12	1.8E-12	2.3E-12
Salmonella	0.0E+00	0.0E+00	0.0E+00	0.0E+00	8.2E-14	0.0E+00	0.0E+00	0.0E+00	0.0E+00	2.3E-15
TT7										
Crypto	2.8E-12	7.1E-12	1.9E-11	9.2E-11	6.2E-10	3.3E-15	8.4E-15	2.3E-14	1.1E-13	7.4E-13
NoV	0.0E+00	1.2E-12	1.4E-12	1.5E-12	1.0E-11	0.0E+00	0.0E+00	0.0E+00	0.0E+00	0.0E+00
AdV	1.5E-07	4.0E-07	1.0E-06	2.8E-06	5.7E-06	4.0E-09	1.1E-08	2.7E-08	7.5E-08	1.5E-07
Salmonella	0.0E+00	0.0E+00	0.0E+00	0.0E+00	0.0E+00	0.0E+00	0.0E+00	0.0E+00	0.0E+00	0.0E+00
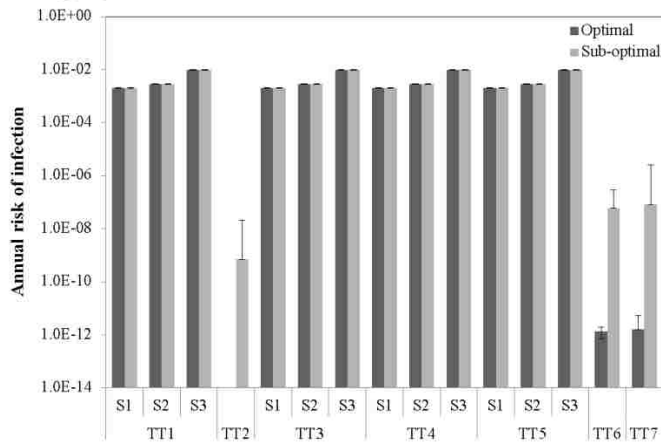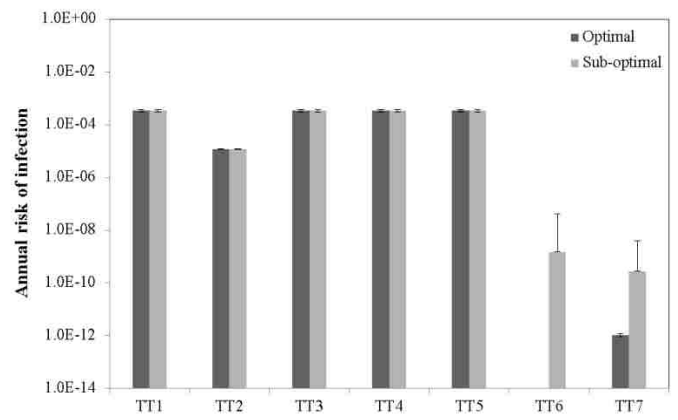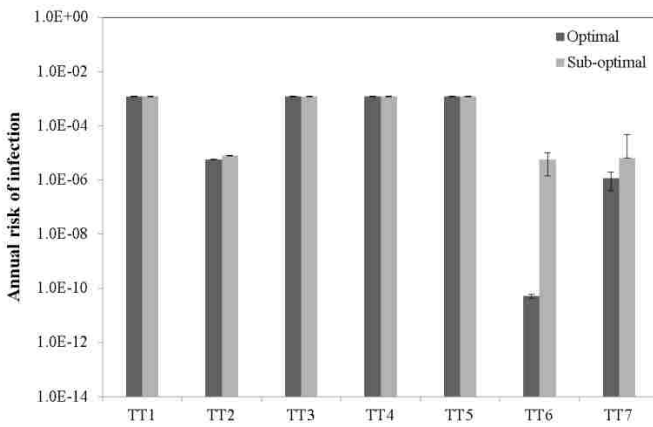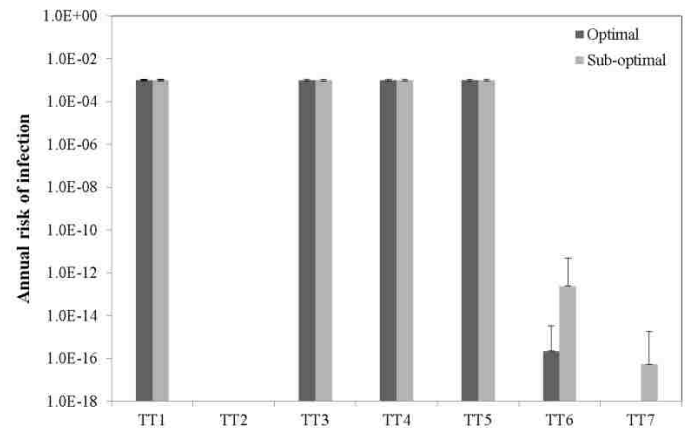
Figure S6. Comparison of annual risk of infection during optimal and sub-optimal operations.
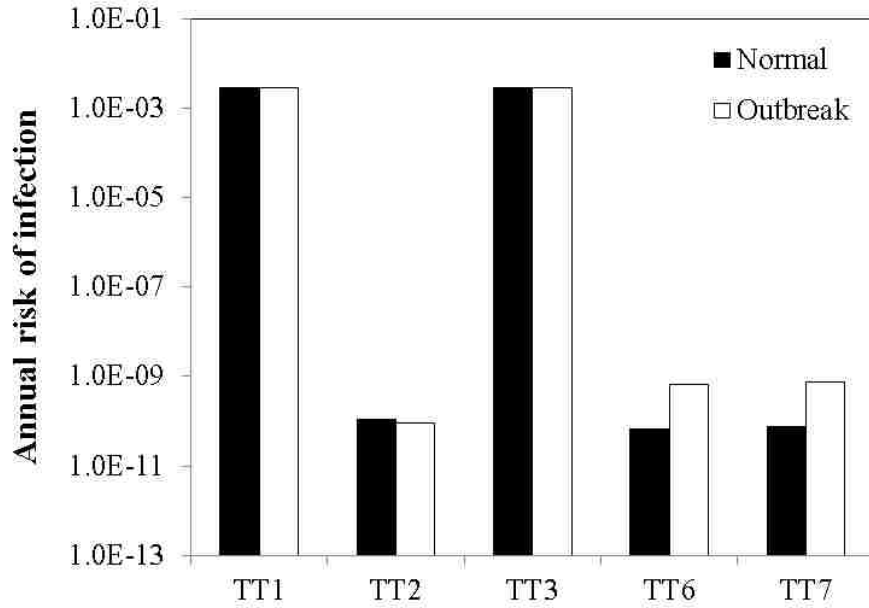
Figure S7. Impact of *Cryptosporidium* outbreak on annual risk of infection during sub-optimal operations. The results of TT4 (IPR with FAT and surface water augmentation) and TT5 (DPR with FAT and blending upstream of the drinking water treatment facility) were similar to TT3 and therefore not shown in the Figure.

177
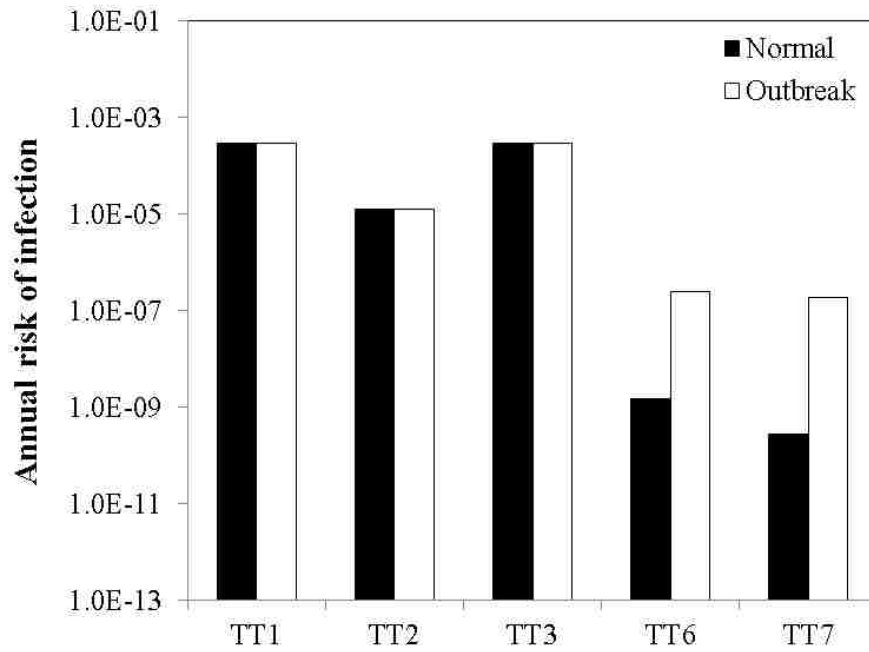
Figure S8. Impact of norovirus outbreak on annual risk of infection during sub-optimal operations. The results of TT4 (IPR with FAT and surface water augmentation) and TT5 (DPR with FAT and blending upstream of the drinking water treatment facility) were similar to TT3 and therefore not shown in the Figure.

178

www.manaraa.com

Figure S9. Impact of AdV outbreak on annual risk of infection during sub-optimal operations. The results of TT4 (IPR with FAT and surface water augmentation) and TT5 (DPR with FAT and blending upstream of the drinking water treatment facility) were similar to TT3 and therefore not shown in the Figure.

179

Figure S10. Impact of *Salmonella* outbreak on annual risk of infection during sub-optimal operations. The results of TT4 (IPR with FAT and surface water augmentation) and TT5 (DPR with FAT and blending upstream of the drinking water treatment facility) were similar to TT3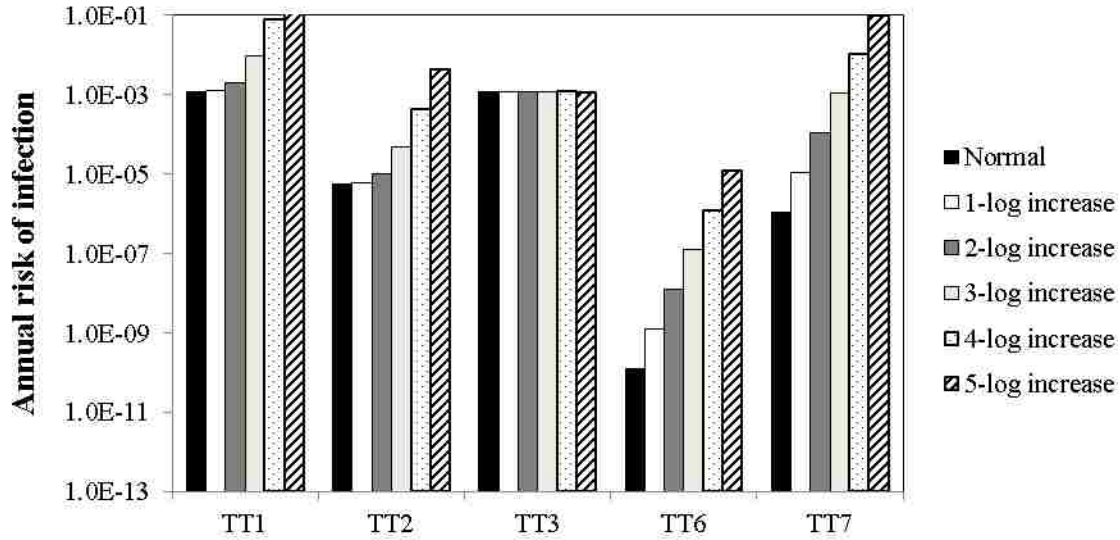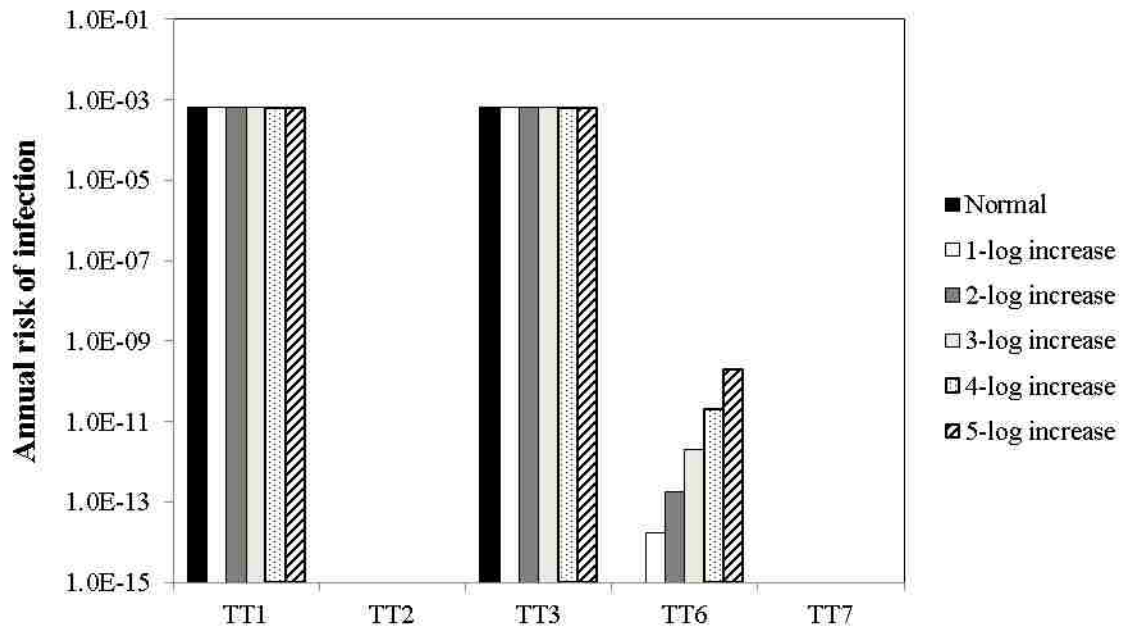 and therefore not shown in the Figure. The risk with TT2 and TT7 was below what could be assessed by the model and was calculated as zero

Appendix 3

Text S1. Ordinary differential equations used in dynamic QMRA.

$$\frac{dE_1}{dt} = \beta_2 S(D + C_1 + C_2) + \beta_1 S + \beta_2\left(\frac{1}{4}\right)P_2(D + C_1 + C_2) + \beta_1(\frac{1}{4})P_2 + \beta_2\left(\frac{2}{4}\right)P_3(D + C_1 + C_2) + \beta_1(\frac{2}{4})P_3$$
$$+ \beta_2\left(\frac{3}{4}\right)P_4(D + C_1 + C_2) + \beta_1(\frac{3}{4})P_4 - \alpha E_1$$

$$\frac{dE_2}{dt} = \alpha E_1 - \alpha E_2$$

$$\frac{dE_3}{dt} = \alpha E_2 - \alpha E_3$$

$$\frac{dE_4}{dt} = \alpha E_3 - \alpha E_4$$

$$\frac{dS}{dt} = -\beta_2 S(D + C_1 + C_2)/N - \beta_1 S + \gamma P_4$$

$$\frac{dP_1}{dt} = \sigma_1 C_{14} + \sigma_2 C_{24} - \gamma P_1$$

$$\frac{dP_2}{dt} = \gamma P_1 - \gamma P_2 - \beta_2\left(\frac{1}{4}\right)P_2(D + C_1 + C_2)/N - \beta_1(\frac{1}{4})P_2$$

$$\frac{dP_3}{dt} = \gamma P_2 - \gamma P_3 - \beta_2\left(\frac{2}{4}\right)P_3(D + C_1 + C_2)/N - \beta_1(\frac{2}{4})P_3$$

$$\frac{dP_4}{dt} = \gamma P_3 - \gamma P_4 - \beta_2\left(\frac{3}{4}\right)P_4(D + C_1 + C_2)/N - \beta_1(\frac{3}{4})P_4$$

$$\frac{dD_1}{dt} = P_{sym}\,\alpha E_4 - \delta D_1$$

$$\frac{dD_2}{dt} = \delta D_1 - \delta D_2$$

$$\frac{dD_3}{dt} = \delta D_2 - \delta D_3$$

$$\frac{dD_4}{dt} = \delta D_3 - \delta D_4$$

$$\frac{dC_{21}}{dt} = \delta D_4 - \sigma_2 C_{21}$$

$$\frac{dC_{22}}{dt} = \sigma_2 C_{21} - \sigma_2 C_{22}$$

$$\frac{dC_{23}}{dt} = \sigma_2 C_{22} - \sigma_2 C_{23}$$

$$\frac{dC_{24}}{dt} = \sigma_2 C_{23} - \sigma_2 C_{24}$$

$$\frac{dC_{11}}{dt} = \left(1 - P_{sym}\right)\sigma E_4 - \sigma_1 C_{11}$$

$$\frac{dC_{12}}{dt} = \sigma_1 C_{11} - \sigma_1 C_{12}$$

$$\frac{dC_{13}}{dt} = \sigma_1 C_{12} - \sigma_1 C_{13}$$

182

$$\frac{dC_{14}}{dt} = \sigma_1 C_{13} - \sigma_1 C_{14}$$

Table S1. Model validation: comparison of the static and dynamic risk. The results of the dynamic model were based on 0% initial latent population, no primary transmission due to contaminated food ($\beta_3 = 0$), no secondary transmission ($\beta_2 = 0$), and no duration of immunity ($1/\gamma = 0$) to allow for a direct comparison with the static model. The minor differences in the models were due to the distributed delays for the remaining epidemiological states (i.e., exposed, diseased, and carrier) in the dynamic model.

Treatment trains	Static		Dynamic	
	Mean	**SD**	**Mean**	**SD**
A. *de facto* reuse	3.4E-04	3.1E-05	3.4E-04	1.7E-06
B. IPR (FAT+GW replenishment)	1.2E-05	3.7E-07	1.0E-05	3.1E-08
C. DPR (O$_3$-biofiltration)	0.0E+00	0.0E+00	0.0E+00	0.0E+00
D. DPR (FAT)	1.1E-12	1.6E-13	9.0E-13	2.1E-15

Table S2. Annual risk of infection calculated by the static model and cumulative incidence calculated by the dynamic model. The results of the dynamic model were based on 0% initial latent. The dynamic model includes secondary transmission which makes the risks higher than the static model.

Treatment trains	Static Model[a]			Dynamic Model[b]		
	min	median	max	min	median	max
A. *de facto* reuse	2.6E-04	3.4E-04	4.5E-04	6.4E-03	3.7E-02	2.3E-01
B. Planned IPR	1.1E-05	1.2E-05	1.3E-05	5.5E-04	2.7E-02	2.3E-01
C. O$_3$-based DPR	0.0E+00	8.2E-14	1.3E-06	8.9E-08	7.0E-03	1.8E-01
D. FAT-based DPR	0.0E+00	1.4E-12	1.0E-07	3.0E-08	7.4E-03	1.8E-01

[a]These values represent annual risk of infection
[b]These values represent cumulative incidence

Table S3. Comparison of the cumulative incidence calculated by dynamic model including secondary transmission with and without immunity. The results are based on 5% initial latent population.

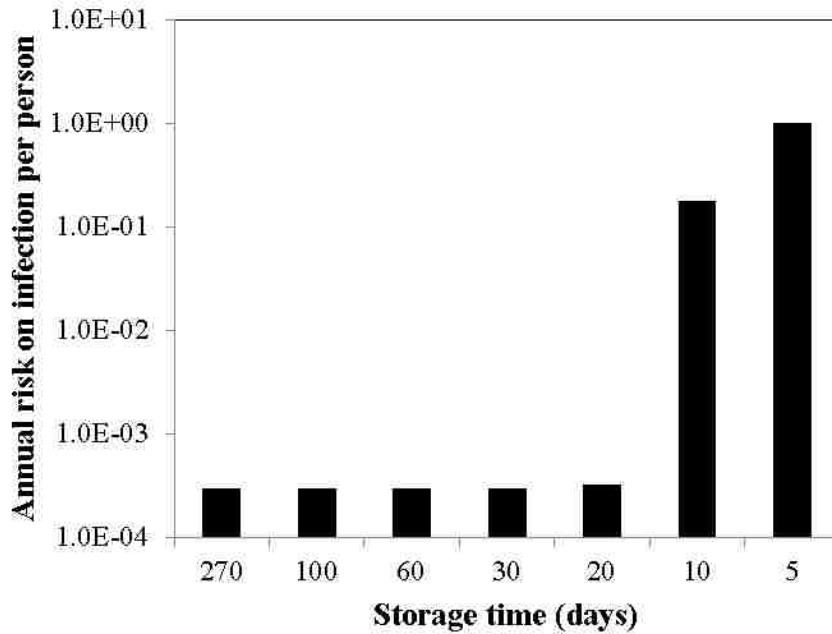| Treatment trains	Dynamic with Immunity		Dynamic with No Immunity	
	Mean	SD	Mean	SD
A. *de facto* reuse	6.9E-02	9.6E-02	3.7E+00	1.1E+00
B. IPR (FAT+GW replenishment)	6.8E-02	1.0E-01	3.6E+00	1.2E+00
C. DPR (O$_3$-biofiltration)	5.6E-02	1.1E-01	3.0E+00	1.7E+00
D. DPR (FAT)	5.7E-02	1.1E-01	2.9E+00	1.8E+00

Figure S1. Annual risk of infection for the *de facto* reuse system for scenario 4 (i.e., foodborne outbreak) as a function of storage time in the environmental buffer. The base e inactivation rate constant for NoV in surface water with a temperature of 20°C was assumed to be 0.875 day^{-1} (Amoueyan et al., 2018; Yang & Griffiths, 2013).
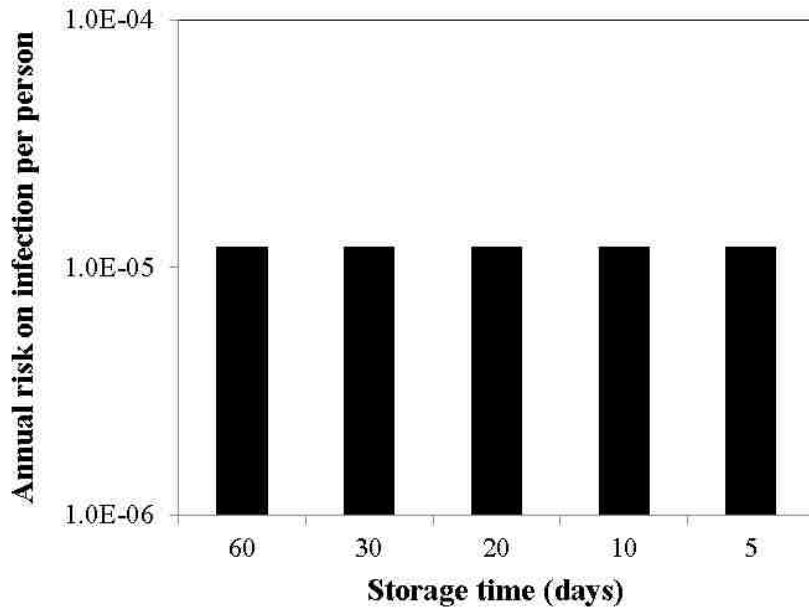
184

Figure S2. Annual risk of infection for the planned IPR system for scenario 4 (i.e., foodborne outbreak) as a function of storage/travel time in the aquifer. The base e inactivation rate constant for NoV in groundwater with a temperature of 10°C was assumed to be 0.055 day^{-1} (Amoueyan et al., 2018; Nevecherya et al., 2005).

185

www.manaraa.com

References

Abbaszadegan, M., Mayer, B. K., Ryu, H., & Nwachuku, N., 2007. Efficacy of removal of CCL viruses under enhanced coagulation conditions. Environmental Science & Technology, 41(3), 971-977.

Abel, N., Schoen, M. E., Kissel, J. C., & Meschke, J. S., 2017. Comparison of risk predicted by multiple norovirus dose–response models and implications for quantitative microbial risk assessment. Risk Analysis, 37(2), 245-264.

Ahmad, S., 2016. Managing Water Demands for a Rapidly Growing City in Semi-Arid Environment: Study of Las Vegas, Nevada. International Journal of Water Resources and Arid Environment, 5(1), 35-42.

Ahmad, S., & Prashar, D., 2010. Evaluating Municipal Water Conservation Policies Using Dynamic Simulation Model Water Resources Management, 24(13), 3371-3395.

Ahmad, S., & Simonovic, S. P., 2000. System dynamics modeling of reservoir operations for flood management. Journal of Computing in Civil Engineering, 14(3), 190–198.

Ahmad, S., & Simonovic, S. P., 2001. Modeling Dynamic Processes in Space and Time--A Spatial System Dynamics Approach. World Water and Environmental Resources Congress. Orlando, FL. May 20-24, 2001. pp. 1-20. https://doi.org/10.1061/40569(2001)88

Ahmad, S., Simonovic, S.P., 2004. Spatial system dynamics: new approach for simulation of water resources systems. Journal of Computing in Civil Engineering, 18 (4), 331-340.

Ahmad, S., Simonovic, S.P., 2006. An intelligent decision support system for management of floods. Water Resources Management, 20 (3), 391-410.

Allard, A. and Vantarakis, A., 2017. Adenoviruses. In: J.B. Rose and B. Jiménez-Cisneros, Global Water Pathogens Project.

186

Amar, C., East, C., Gray, J., Iturriza-Gomara, M., Maclure, E., & McLauchlin, J., 2007. Detection by PCR of eight groups of enteric pathogens in 4,627 faecal samples: Re-examination of the english case-control infectious intestinal disease study (1993–1996). European Journal of Clinical Microbiology & Infectious Diseases, 26(5), 311-323.

Ames, D. P., Quinn, N. W., & Rizzoli, A. E., 2014. Applications of quantitative microbial risk assessment (QMRA) to regulatory decision making.

Amoueyan, E., Ahmad, S., Eisenberg, J. N., Pecson, B., & Gerrity, D., 2017. Quantifying pathogen risks associated with potable reuse: A risk assessment case study for cryptosporidium. Water Research, 119, 252-266.

Anderson, A. D., Heryford, A. G., Sarisky, J. P., Higgins, C., Monroe, S. S., Beard, R. S., & Seys, S. A., 2003. A waterborne outbreak of Norwalk-like virus among snowmobilers—Wyoming, 2001. The Journal of Infectious Diseases, 187(2), 303-306.

Aoki, Y., Suto, A., Mizuta, K., Ahiko, T., Osaka, K., & Matsuzaki, Y., 2010. Duration of norovirus excretion and the longitudinal course of viral load in norovirus-infected elderly patients. The Journal of Hospital Infection, 75(1), 42-46.

Asano, T., Burton, F.L., Leverenz, H.L., Tsuchihashi, R. & Tchobanoglous, G., 2007 Water Reuse: Issues, Technologies, and Applications. McGraw-Hill, New York.

Atmar, R. L., Opekun, A. R., Gilger, M. A., Estes, M. K., Crawford, S. E., Neill, F. H., et al., 2008. Norwalk virus shedding after experimental human infection. Emerging Infectious Diseases, 14(10), 1553-1557.

Bae, J., & Schwab, K. J., 2008. Evaluation of murine norovirus, feline calicivirus, poliovirus, and MS2 as surrogates for human norovirus in a model of viral persistence in surface water and groundwater. Applied and Environmental Microbioly, 74(2), 477-484.

Barbeau, B., Payment, P., Cle, B., & Pre, M., 2000. Evaluating the risk of infection from the presence of *Giardia* and *Cryptosporidium* in drinking water. Quantitative Microbioly, 2(1), 37-54.

Barker, S. F., Packer, M., Scales, P. J., Gray, S., Snape, I., & Hamilton, A. J., 2013. Pathogen reduction requirements for direct potable reuse in Antarctica: evaluating human health risks in small communities. Science of the Total Environment, 461, 723-733.

Barreto, H., & Howland, F. M., 2005. Introductory econometrics: Using Monte Carlo simulation with Microsoft excel. Cambridge University Press: Cambridge, United Kingdom.

Beauchamp, N., Bouchard, C., & Lence, B. J., 2011. QMRA-based reliability analysis to assess the performance of an ultrafiltration plant. Journal of Water Supply: Research and Technology-Aqua, 60(2), 89-100.

Beaudequin, D., Harden, F., Roiko, A., Stratton, H., Lemckert, C., & Mengersen, K., 2015. Modelling microbial health risk of wastewater reuse: A systems perspective. Environmental International, 84, 131-141.

Bitton, G., Farrah, S.R., Puskin, R.H., Butner. J., & Chou. Y. J., 1983. Survial of Patogenic and Indicator Organisms in Ground Water. Ground Water, 21 (4), 405–408.

Blaser, M. J., & Newman, L. S., 1982. A review of human salmonellosis: I. Infective dose. Reviews of Infectious Diseases, 4(6), 1096-1106.

Borchardt, M. A., Spencer, S. K., Kieke, B. A., Lambertini, E., & Loge, F. J., 2012. Viruses in nondisinfected drinking water from municipal wells and community incidence of acute gastrointestinal illness. Environmental Health Perspectives, 120(9), 1272-1279.

Brookes, J. D., Antenucci, J., Hipsey, M., Burch, M. D., Ashbolt, N. J., & Ferguson, C., 2004. Fate and transport of pathogens in lakes and reservoirs. Environmental International, 30(5), 741-759.

Brookhart, M. A., Hubbard, A. E., Van Der Laan, M. J., Colford, J. M., & Eisenberg, J. N., 2002. Statistical estimation of parameters in a disease transmission model: analysis of a Cryptosporidium outbreak. Statistics in Medicine, 21(23), 3627-3638.

Brunkard, J. M., Ailes, E., Roberts, V. A., Hill, V., Hilborn, E. D., Craun, G. F., & Carpenter, J., 2011. Surveillance for waterborne disease outbreaks associated with drinking water—United States, 2007–2008. MMWR Surveillance Summaries, 60(12), 38-68.

Bukhary, S., Ahmad, S., & Batista, J., 2017. Analyzing land and water requirements for solar deployment in the Southwestern United States. Renewable & Sustainable Energy Reviews, 82, 3288–3305.

Burns, N., 2015. Ozone & biofiltration treatment for the production of high quality recycled water. Water Environment Federation (WEF) webinar series. The role of ozone in high level disinfection and other application. July 15, 2015.

Byappanahalli, M. N., Sawdey, R., Ishii, S., Shively, D. A., Ferguson, J. A., Whitman, R. L., & Sadowsky, M. J., 2009. Seasonal stability of cladophora-associated salmonella in lake michigan watersheds. Water Research, 43(3), 806-814.

Cannon, J. L., Papafragkou, E., Park, G. W., Osborne, J., Jaykus, L., & Vinjé, J., 2006. Surrogates for the study of norovirus stability and inactivation in the environment: A comparison of murine norovirus and feline calicivirus. Journal of Food Protection, 69(11), 2761-2765.

189

Centers for Disease Control and Prevention. 2009. Surveillance for foodborne disease

outbreaks—United States, 2006. MMWR Morbidity Mortality Weekly Report, 58, 609–15.

Centers for Disease Control and Prevention. 2010. Surveillance for foodborne disease

outbreaks—United States, 2007. MMWR Morbidity Mortality Weekly Report, 59, 973–9.

Centers for Disease Control and Prevention. 2011. Surveillance for foodborne

disease outbreaks—United States, 2008. MMWR Morbidity Mortality Weekly Report, 60,

1197–202.

Centers for Disease Control and Prevention. 2014. Vital signs: Foodborne norovirus outbreaks—

United States, 2009-2012. MMWR Morbidity Mortality Weekly Report, 63(22), 491-495.

CDPH, 2014. Groundwater Replenishment Reuse FINAL Regulations. California Department of

Public Health: Sacramento, CA.

Chaudhry, R. M., Hamilton, K. A., Haas, C. N., & Nelson, K. L., 2017. Drivers of microbial risk

for direct potable reuse and de facto reuse treatment schemes: The impacts of source water

quality and blending. International Journal of Environmental Research and Public Health,

14(6), 635.

Chen, C., Ahmad, S., Kalra, A., & Xu, Z., 2017. A dynamic model for exploring water resource

management scenarios in an inland arid area: Shanshan County, Northwestern China.

Journal of Mountain Science, 14(6), 1039-1057

Chen, J. P., Yang, L., Wang, L. K., & Zhang, B., 2006. Ultraviolet radiation for disinfection.

Advanced Physicochemical Treatment Processes. 4, 317-366. Humana Press: New York,

NY.

Choi, S., & Jiang, S. C., 2005. Real-time PCR quantification of human adenoviruses in urban rivers indicates genome prevalence but low infectivity. Applied & Environmental Microbiology, 71(11), 7426-7433.

Crabtree, K.D., Gerba, C.P., Rose, J.B., and Haas, C.N., 1997. Waterborne adenovirus: a risk assessment. Water Science & Technology, 35(11-12), 1-6.

Cooper, R.C. & Olivieri, A.W., 1996. Mamala Bay Infectious Disease Public Health Risk Assessment, Mamala Bay Study Commission Final Report, April 1996.

Cotruvo, J. A., & Bell, K. Y., 2014. Need for direct and indirect potable water reuse specifications. Journal of American Water Works Association, 106(2), 28-30.

Crabtree, K. D., Gerba, C. P., Rose, J. B., & Haas, C. N., 1997. Waterborne adenovirus: a risk assessment. Water Science & Technology, 35(11-12), 1-6.

Craun, M. F., Craun, G. F., Calderon, R. L., & Beach, M. J., 2006. Waterborne outbreaks reported in the united states. Journal of Water and Health, 4(S2), 19-30.

Currier, R. L., Payne, D. C., Staat, M. A., Selvarangan, R., Shirley, S. H., Halasa, N., et al., 2015. Innate susceptibility to norovirus infections influenced by FUT2 genotype in a united states pediatric population. Clinical Infectious Diseases, 60(11), 1631-1638.

Dawadi, S., & Ahmad, S., 2013. Evaluating the impact of demand-side management on water resources under changing climatic conditions and increasing population. Journal of Environmental Management, 114, 261-275.

Dawadi, S., & Ahmad, S., 2012. Changing climatic conditions in the Colorado River Basin: Implications for water resources management. Journal of Hydrology, 430-431, 127-141.

Doultree, J., Druce, J., Birch, C., Bowden, D., & Marshall, J., 1999. Inactivation of feline calicivirus, a norwalk virus surrogate. Journal of Hospital Infection, 41(1), 51-57.

191

Duizer, E., Bijkerk, P., Rockx, B., De Groot, A., Twisk, F., & Koopmans, M., 2004. Inactivation of caliciviruses. Applied & Environmental Microbiology, 70(8), 4538-4543.

Eftim, S. E., Hong, T., Soller, J., Boehm, A., Warren, I., Ichida, A., & Nappier, S. P., 2017. Occurrence of norovirus in raw sewage–A systematic literature review and meta-analysis. Water Research, 111, 366-374.

Eisenberg, J. N., Seto, E. Y., Olivieri, A. W., & Spear, R. C., 1996. Quantifying water pathogen risk in an epidemiological framework. Risk Analysis, 16(4), 549-563.

Eisenberg, J. N., Seto, E. Y., Colford Jr, J. M., Olivieri, A., & Spear, R. C., 1998. An analysis of the Milwaukee cryptosporidiosis outbreak based on a dynamic model of the infection process. Epidemiology, 255-263.

Eisenberg, J. N., Brookhart, M. A., Rice, G., Brown, M., & Colford, J. M.,Jr., 2002. Disease transmission models for public health decision making: Analysis of epidemic and endemic conditions caused by waterborne pathogens. Environmental Health Perspectives, 110(8), 783-790.

Eisenberg, J. N., Soller, J. A., Scott, J., Eisenberg, D. M., & Colford, J. M., 2004. A dynamic model to assess microbial health risks associated with beneficial uses of biosolids. Risk Analysis, 24(1), 221-236.

Eisenberg, J. N., Lei, X., Hubbard, A. H., Brookhart, M. A., & Colford Jr, J. M., 2005. The role of disease transmission and conferred immunity in outbreaks: Analysis of the 1993 cryptosporidium outbreak in Milwaukee, Wisconsin. American Journal of Epidemiology, 161(1), 62-72.

Forrester, J. W., 1958. Industrial dynamics: A major breakthrough for decision makers. Harvard Business Review, 36(4), 37-66.

Forss, M., & Ander, H., 2011. Microbiological risk assessment of the water reclamation plant in Windhoek, Namibia. Thesis in the Master's Program Geo and Water Engineering. Department of Civil and Environmental Engineering. Chalmers University of Technology.

Francy, D. S., Stelzer, E. A., Bushon, R. N., Brady, A. M., Williston, A. G., Riddell, K. R., Gellner, T. M., 2012. Comparative effectiveness of membrane bioreactors, conventional secondary treatment, and chlorine and UV disinfection to remove microorganisms from municipal wastewaters. Water Research, 46(13), 4164-4178.

Gamage, S., Gerrity, D., Pisarenko, A. N., Wert, E. C., & Snyder, S. A., 2013. Evaluation of process control alternatives for the inactivation of Escherichia coli, MS2 bacteriophage, and Bacillus subtilis spores during wastewater ozonation. Ozone Science & Engineering, 35(6), 501-513.

Gaunt, E., Harvala, H., McIntyre, C., Templeton, K., & Simmonds, P., 2011. Disease burden of the most commonly detected respiratory viruses in hospitalized patients calculated using the disability adjusted life year (DALY) model. J. Clinical Virology, 52(3), 215-221.

Gerba, C. P., Naranjo, J. E., & Hansan, M. N., 1997. Evaluation of a combined portable reverse osmosis and iodine resin drinking water treatment system for control of enteric waterborne pathogens. Journal of Environmental Science and Health, Part A, 32(8), 2337-2354.

Gerba, C.P, Gramos, D.M and Nwachuku, N., 2002. Comparative inactivation of enteroviruses and adenovirus 2 by UV light. Applied & Environmental Microbiology, 68, pp. 5167–9.

Gerba, C. P., Betancourt, W. Q., Kitajima, M., & Rock, C. M., 2018. Reducing uncertainty in estimating virus reduction by advanced water treatment processes. Water research, 133, 282-288.

Gerrity, D., Gamage, S., Holady, J. C., Mawhinney, D. B., Quiñones, O., Trenholm, R. A., & Snyder, S. A., 2011. Pilot-scale evaluation of ozone and biological activated carbon for trace organic contaminant mitigation and disinfection. Water Research, 45(5), 2155-2165.

Gerrity, D., Gamage, S., Jones, D., Korshin, G. V., Lee, Y., Pisarenko, A., Trenholm, R. A., Von Gunten, U., Wert, E. C., & Snyder, S. A., 2012. Development of surrogate correlation models to predict trace organic contaminant oxidation and microbial inactivation during ozonation. Water Research, 46(19), 6257-6272.

Gerrity, D., Pecson, B., Trussell, R. S., & Trussell, R. R., 2013. Potable reuse treatment trains throughout the world. J. Water Supply Research and Technology, AQUA, 62(6), 321-338.

Gerrity, D., Owens-Bennett, E., Venezia, T., Stanford, B. D., Plumlee, M. H., Debroux, J., & Trussell, R. S., 2014. Applicability of ozone and biological activated carbon for potable reuse. Ozone Science and Engineering, 36(2), 123-137.

Gerrity, D., Pisarenko, A. N., Marti, E., Trenholm, R. A., Gerringer, F., Reungoat, J., & Dickenson, E., 2015. Nitrosamines in pilot-scale and full-scale wastewater treatment plants with ozonation. Water Research, 72, 251-261.

Gerrity, D., Lee, Y., Gamage, S., Lee, M., Pisarenko, A. N., Trenholm, R. A., & Snyder, S. A., 2016. Emerging investigators series: Prediction of trace organic contaminant abatement with UV/H_2O_2: Development and validation of semi-empirical models for municipal wastewater effluents. Environmental Science: Water Research & Technology, 2(3), 460-473.

Gordon, C., & Toze, S., 2003. Influence of groundwater characteristics on the survival of enteric viruses. Journal of Applied Microbiology, 95(3), 536-544.

Governal, R., & Gerba, C., 1999. Removal of MS-2 and PRD-1 bacteriophages from an ultrapure water system. Journal of Industrial Microbiology & Biotechnology, 23(3), 166-172.

194

Haas, C. N., 2015. Microbial dose response modeling: past, present, and future. Environmental
Science & Technology, 49(3), 1245-1259.

Haas, C. N., & Rose, J. B., 1995. Developing an action level for *Cryptosporidium*. Journal of
American Water Works Association, 87(9), 81-84.

Haas, C. N., Rose, J. B., & Gerba, C. P., 1999. Conducting the Dose–Response assessment.
Quantitative Microbial Risk Assessment, Second Edition, 267-321.

Haley, B. J., Cole, D. J., & Lipp, E. K., 2009. Distribution, diversity, and seasonality of
waterborne salmonellae in a rural watershed. Applied & Environmental Microbiology,
75(5), 1248-1255.

Hall AJ, Lopman BA, Payne DC, et al. 2013a. Norovirus disease in the United States. Emerging
Infectious Diseases, 19, 1198–1205.

Hall, A. J., Lopman, B. A., Payne, D. C., Patel, M. M., Gastañaduy, P. A., Vinjé, J., & Parashar,
U. D., 2013b. Norovirus disease in the United States. Emerging Infectious Diseases, 19(8),
1198.

Hall, A. J., Eisenbart, V. G., Etingue, A. L., Gould, L. H., Lopman, B. A., & Parashar, U. D.,
2012. Epidemiology of foodborne norovirus outbreaks, united states, 2001-2008. Emerging
Infectious Diseases, 18(10), 1566-1573.

Haramoto, E., Katayama, H., Oguma, K., & Ohgaki, S. (2007). Quantitative analysis of human
enteric adenoviruses in aquatic environments. Journal of Applied Microbiology, 103(6),
2153-2159.

Health Canada, 2012. Guidelines for Canadian Drinking Water Quality: Guideline Technical
Document—Enteric Protozoa: Giardia and Cryptosporidium. Catalogue No. H129-

23/2013E-PDF. Water, Air and Climate Change Bureau, Healthy Environments and Consumer Safety Branch, Health Canada: Ottawa, Ontario.

Heerden, J., Ehlers, M., Vivier, J., & Grabow, W., 2005. Risk assessment of adenoviruses detected in treated drinking water and recreational water. Journal of Applied Microbiology, 99(4), 926-933.

Hewitt, J., Leonard, M., Greening, G. E., & Lewis, G. D., 2011. Influence of wastewater treatment process and the population size on human virus profiles in wastewater. Water Research, 45(18), 6267-6276.

Hijnen, W., Beerendonk, E., & Medema, G. J., 2006. Inactivation credit of UV radiation for viruses, bacteria and protozoan (oo)cysts in water: A review. Water Research, 40(1), 3-22.

Hijnen, W. A., Brouwer-Hanzens, A. J., Charles, K. J., & Medema, G. J., 2005. Transport of MS2 phage, escherichia coli, clostridium perfringens, cryptosporidium parvum, and giardia intestinalis in a gravel and a sandy soil. Environmental Science & Technology, 39(20), 7860-7868.

Hirneisen, K. A., & Kniel, K. E., 2013. Comparing human norovirus surrogates: Murine norovirus and tulane virus. Journal of Food Protection, 76(1), 139-143.

Hong, S., Miller, F., & Taylor, J., 2001. Assessing pathogen removal efficiency of microfiltration by monitoring membrane integrity. Water Science and Technology: Water Supply, 1(4), 43-48.

Hullegie, S., Bruijning-Verhagen, P., Uiterwaal, C. S., van der Ent, C. K., Smit, H. A., & de Hoog, M. L., 2016. First-year Daycare and Incidence of Acute Gastroenteritis. Pediatrics, e20153356.

196

Hurst, C. J., McClellan, K. A., & Benton, W. H., 1988. Comparison of cytopathogenicity, immunofluorescence and in situ DNA hybridization as methods for the detection of adenoviruses. Water Research, 22(12), 1547-1552.

ILSI. 1996. A conceptual framework to assess the risks of human disease following exposure to pathogens. Risk Analysis, 16, 841-848.

Iturriza-Gómara, M., & Lopman, B., 2014. Norovirus in healthcare settings. Current Opinion in Infectious Diseases, 27(5), 437.

Jacangelo, J. G., Adham, S. S., & Laîné, J., 1995. Mechanism of *Cryptosporidium*, *Giardia*, and MS2 virus removal by MF and UF. Journal of American Water Works Association, 87(9), 107-121.

Jahne, M., 2017. Risk-based guidance for decentralized non-potable water systems. USEPA. Office of Research and Development.

Jertborn, M., Haglind, P., Iwarson, S., & Svennerholm, A., 1990. Estimation of symptomatic and asymptomatic salmonella infections. Scandinavian Journal of Infectious Diseases, 22(4), 451-455.

Jiang, S., Noble, R., & Chu, W., 2001. Human adenoviruses and coliphages in urban runoff-impacted coastal waters of southern California. Applied & Environmental Microbiology, 67(1), 179-184.

Johnson PC, Mathewson JJ, DuPont HL, Greenberg HB., 1990. Multiple challenge study of host susceptibility to Norwalk gastroenteritis in US adults. Journal of Infectious Diseases, 161, 18–21.

Jyoti, A., Ram, S., Vajpayee, P., Singh, G., Dwivedi, P. D., Jain, S. K., & Shanker, R., 2010. Contamination of surface and potable water in south Asia by salmonellae: Culture-

independent quantification with molecular beacon real-time PCR. Science of the Total Environment, 408(6), 1256-1263.

Kambhampati, A., Koopmans, M., & Lopman, B. A., 2015. Burden of norovirus in healthcare facilities and strategies for outbreak control. Journal of Hospital Infection, 89(4), 296-301.

Karavarsamis, N., & Hamilton, A., 2010. Estimators of annual probability of infection for quantitative microbial risk assessment. Journal of Water Health, 8(2), 365-373.

Karst, S. M., Wobus, C. E., Lay, M., Davidson, J., & Virgin, H. W., 2003. STAT1-dependent innate immunity to a norwalk-like virus. Science (New York, N.Y.), 299(5612), 1575-1578.

Katayama, K., Hansman, G., Oka, T., Ogawa, S., & Takeda, N., 2006. Investigation of norovirus replication in a human cell line. Archives of Virology, 151(7), 1291-1308.

Katayama, H. and Vinjé, J., 2017. Norovirus and other Calicivirus. In: J.B. Rose and B. Jiménez-Cisneros, (eds) Global Water Pathogens Project.

Khan, S., 2013. Drinking water through recycling: The benefits and costs of supplying direct to the distribution system. Australian Academy of Technology Sciences and Engineering.

Kemmeren, J. M., Mangen, M., Van Duynhoven, Y., & Havelaar, A., 2006. Priority setting of foodborne pathogens: Disease burden and costs of selected enteric pathogens.

Kinman, R. N., & Rempel, G., 1975. Water and wastewater disinfection with ozone: A critical review. Critical Reviews in Environmental Science & Technology, 5(1), 141-152.

Koivunen, J., Siitonen, A., & Heinonen-Tanski, H., 2003. Elimination of enteric bacteria in biological–chemical wastewater treatment and tertiary filtration units. Water Research, 37(3), 690-698.

LeChevallier, M. W., & Au, K., 2004. Water treatment and pathogen control IWA Publishing.

198

LeChevallier, M. W., Norton, W. D., & Lee, R. G., 1991. Occurrence of *giardia* and *Cryptosporidium* spp. in surface water supplies. Applied & Environmental Microbiology, 57(9), 2610-2616.

Lee, J., Zoh, K., & Ko, G., 2008. Inactivation and UV disinfection of murine norovirus with TiO2 under various environmental conditions. Applied & Environmental Microbiology, 74(7), 2111-2117.

Lee, Y., Gerrity, D., Lee, M., Bogeat, A. E., Salhi, E., Gamage, S., Trenholm, R. A., Wert, E. C., Snyder, S. A., & von Gunten, U., 2013. Prediction of micropollutant elimination during ozonation of municipal wastewater effluents: Use of kinetic and water specific information. Environmental Science & Technology, 47(11), 5872-5881.

Lee, J. E., & Ko, G., 2013. Norovirus and MS2 inactivation kinetics of UV-A and UV-B with and without TiO 2. Water Research, 47(15), 5607-5613.

Lee, Y., Gerrity, D., Lee, M., Gamage, S., Pisarenko, A., Trenholm, R. A., Canonica, S., Snyder, S. A., & von Gunten, U., 2016. Organic contaminant abatement in reclaimed water by UV/H$_2$O$_2$ and a combined process consisting of O$_3$/H$_2$O$_2$ followed by UV/H$_2$O$_2$: Prediction of abatement efficiency, energy consumption, and byproduct formation. Environnemental Science & Technology, 50(7), 3809-3819.

Lemarchand, K., & Lebaron, P., 2003. Occurrence of salmonella spp. and cryptosporidium spp. in a french coastal watershed: Relationship with fecal indicators. FEMS Microbiology Letters, 218(1), 203-209.

Levantesi, C., Bonadonna, L., Briancesco, R., Grohmann, E., Toze, S., & Tandoi, V., 2012. *Salmonella* in surface and drinking water: Occurrence and water-mediated transmission. Food Research International, 45(2), 587-602.

Leverenz, H. L., Tchobanoglous, G., & Asano, T., 2011. Direct potable reuse: A future imperative. J. Water Reuse & Desalination, 1(1), 2-10.

Lim, M. Y., Kim, J. M., Lee, J. E., & Ko, G., 2010. Characterization of ozone disinfection of murine norovirus. Applied & Environmental Microbiology, 76(4), 1120-1124.

Lim, K., Hamilton, A. J., & Jiang, S. C., 2015. Assessment of public health risk associated with viral contamination in harvested urban stormwater for domestic applications. Science of the Total Environment, 523, 95-108.

Lim, K., Wu, Y., & Jiang, S., 2016. Assessment of *Cryptosporidium* and norovirus risk associated with de facto wastewater reuse in Trinity River, Texas. Microbial Risk Analysis. In press. http://doi.org/10.1016/j.mran.2016.11.002.

Lim, K., Wu, Y., & Jiang, S. C., 2017. Assessment of cryptosporidium and norovirus risk associated with de facto wastewater reuse in trinity river, Texas. Microbial Risk Analysis, 5, 15-24.

Lodder, W. J., & de Roda Husman, A. M., 2005. Presence of noroviruses and other enteric viruses in sewage and surface waters in the Netherlands. Applied & Environmental Microbiology, 71(3), 1453-1461.

Mallory, Charles W., Waller, R., 1973. Application of selected industrial engineering techniques to wastewater treatment plants. United States Environmental Protection Agency, 107–110. EPA R2–73–176. Retrieved 2012-11-10.

Martorell, S., Soares, C. G., & Barnett, J., 2008. Safety, Reliability and Risk Analysis: Theory, Methods and Applications. CRC Press: Boca Raton, Florida.

Matsushita, T., Shirasaki, N., Tatsuki, Y., & Matsui, Y., 2013. Investigating norovirus removal by microfiltration, ultrafiltration, and precoagulation–microfiltration processes using

recombinant norovirus virus-like particles and real-time immuno-PCR. Water Research, 47(15), 5819-5827.

Messner, M. J., Chappell, C. L., & Okhuysen, P. C., 2001. Risk assessment for *Cryptosporidium*: a hierarchical Bayesian analysis of human dose response data. Water Research, 35(16), 3934-3940.

Messner, M. J., Berger, P., & Nappier, S. P., 2014. Fractional Poisson—a simple dose-response model for human norovirus. Risk Analysis, 34(10), 1820-1829.

Messner, M. J., & Berger, P., 2016. *Cryptosporidium* infection risk: Results of new dose-response modeling. Risk Analysis, 36(10), 1969-1982.

McBride, G. B., Stott, R., Miller, W., Bambic, D., & Wuertz, S., 2013. Discharge-based QMRA for estimation of public health risks from exposure to stormwater-borne pathogens in recreational waters in the united states. Water Research, 47(14), 5282-5297.

Milbrath, M., Spicknall, I., Zelner, J., Moe, C., & Eisenberg, J., 2013. Heterogeneity in norovirus shedding duration affects community risk. Epidemiology & Infection, 141(8), 1572-1584.

Mirchi, A., Madani, K., Watkins, Jr., D., & Ahmad, S., 2012. Synthesis of system dynamics tools for holistic conceptualization of water resources problems. Water Resources Management, 26, 2421-2442.

Moumouni, Y., 2014. A System Dynamics Model for Energy Planning in Niger." International Journal of Energy and Power Engineering, 3(6), 308.

National Center for Health Statistics. 2018. Final data for 2015. National vital statistics reports; Vol 66 no 1 (PDF). Retrieved 13 January 2018.

Nevecherya, I., Shestakov, V., Mazaev, V., & Shlepnina, T., 2005. Survival rate of pathogenic bacteria and viruses in groundwater. Water Resources, 32(2), 209-214.

Nordgren, J., Sharma, S., Kambhampati, A., Lopman, B., & Svensson, L., 2016. Innate resistance and susceptibility to norovirus infection. PLoS Pathogens, 12(4), e1005385.

NRC, 2012. Committee on the assessment of water reuse as an approach for meeting future water supply needs. Water reuse: Potential for expanding the nation's water supply through reuse of municipal wastewater. National Academies Press.

NRMMC-EPHC-NHMRC, 2008. Australian Guidelines for Water Recycling: Managing health and environmental risks (Phase 2): Augmentation of drinking-water supplies. National Resource Management Ministerial Council, Environment Protection and Heritage Council, National Health and Medical Research Council, Australian Government.

Nuanualsuwan, S., & Cliver, D. O., 2003. Capsid functions of inactivated human picornaviruses and feline calicivirus. Applied & Environmental Microbiology, 69(1), 350-357.

Nussbaum, E. M., Owens, M. C., Sinatra, G. M., Rehmat, A. P., Cordova, J. R., Ahmad, S., and Dascalu, S. M., 2015. Losing the Lake: Simulations to Promote Gains in Student Knowledge and Interest about Climate Change. International Journal of Environmental and Science Education, 10(6), 789-811.

NWRI, 2012. Ultraviolet Disinfection Guidelines for Drinking Water and Water Reuse. Third edition. Water Research Foundation: Denver, CO.

NWRI, 2013. Examining the Criteria for Direct Potable Reuse. National Water Research Institute: Fountain Valley, CA.

NWRI, 2016a. Potable Reuse Research Compilation: Synthesis of Findings. Final Report. WRRF-15-01. Water Environment & Reuse Foundation: Alexandria, VA.

NWRI, 2016b. Evaluation of the Feasibility of Developing Uniform Water Recycling Criteria for

Direct Potable Reuse. Expert Panel Final Report. National Water Research Institute:

Fountain Valley, CA.

NWRI, 2016c. Final report of an NWRI independent advisory panel: Recommended DPR

general guidelines and operational requirements for New Mexico. Fountain Valley (CA):

National Water Research Institute. http://www.nwri-usa.org/pdfs/New-Mexico-DPR-Panel-

General-Report(1).pdf (accessed 20 May 2017).

Ogorzaly, L., Bertrand, I., Paris, M., Maul, A., & Gantzer, C., 2010. Occurrence, survival, and

persistence of human adenoviruses and F-specific RNA phages in raw groundwater. Applied

& Environmental Microbiology, 76(24), 8019-8025.

Okhuysen PC, Jiang X, Ye L, Johnson PC, Estes MK., 1995. Viral shedding and faecal IgA

response after Norwalk virus infection. Journal of Infectious Diseases, 171:566–569.

Olivieri, A., Eisenberg, D., Soller, J., Eisenberg, J., Cooper, R., Tchobanoglous, G., Gagliardo,

P., 1999. Estimation of pathogen removal in an advanced water treatment facility using

monto carlo simulation. Water Science & Technology, 40(4-5), 223-233.

Olivieri, A. W., Seto, E., Cooper, R. C., Cahn, M. D., Colford, J., Crook, J., & Tchobanoglous,

G., 2014a. Risk-based review of California's water-recycling criteria for agricultural

irrigation. Journal of Environmental Engineering, 140(6), 04014015.

Olivieri, A. W., Seto, E., Danielson, R. E., Soller, J. A., & Cooper, R. C., 2014b. Applications of

quantitative microbial risk assessment (QMRA) to regulatory decision making. International

Environmental Modelling and Software Society.

Ottoson, J., Hansen, A., Björlenius, B., Norder, H., & Stenström, T., 2006. Removal of viruses, parasitic protozoa and microbial indicators in conventional and membrane processes in a wastewater pilot plant. Water Research, 40(7), 1449-1457.

Pachepsky, Y., Blaustein, R., Whelan, G., & Shelton, D., 2014. Comparing temperature effects on *escherichia coli*, *Salmonella*, and enterococcus survival in surface waters. Letters in Applied Microbiology, 59(3), 278-283.

Pang, L., Close, M., Goltz, M., Noonan, M., & Sinton, L., 2005. Filtration and transport of bacillus subtilis spores and the F-RNA phage MS2 in a coarse alluvial gravel aquifer: Implications in the estimation of setback distances. Journal of Contaminant Hydrology, 77(3), 165-194.

Park, S., Kim, B. J., & Jung, S. Y., 2014. Simulation methods of a system dynamics model for efficient operations and planning of capacity expansion of activated-sludge wastewater treatment plants. Procedia Engineering, 70, 1289-1295.

Parker, J., Fowler, N., Walmsley, M. L., Schmidt, T., Scharrer, J., Kowaleski, J., & Chen, J., 2015. Analytical sensitivity comparison between singleplex real-time PCR and a multiplex PCR platform for detecting respiratory viruses. PloS one, 10 (11), e0143164.

Parshionikar, S. U., Willian-True, S., Fout, G. S., Robbins, D. E., Seys, S. A., Cassady, J. D., & Harris, R., 2003. Waterborne outbreak of gastroenteritis associated with a norovirus. Applied & Environmental Microbiology, 69(9), 5263-5268.

Pecson, B. M., Ackermann, M., & Kohn, T., 2011. Framework for using quantitative PCR as a nonculture based method to estimate virus infectivity. Environmental Science & Technology, 45(6), 2257-2263.

204

Pecson, B. M., Trussell, R. S., Pisarenko, A. N., & Trussell, R. R., 2015. Achieving reliability in
potable reuse: The four Rs. Journal of American Water Works Association, 107(3), 48-58.

Pecson, B. M., Triolo, S. C., Olivieri, S., Chen, E. C., Pisarenko, A. N., Yang, C. C., & Trussell,
R. R., 2017. Reliability of pathogen control in direct potable reuse: Performance evaluation
and QMRA of a full-scale 1 MGD advanced treatment train. Water Research, 122, 258-268.

Pejic-Bach, M., & Ceric, V., 2007. Developing system dynamic model with step-by-step
approach. Journal of Information and Organizational Science, 31(1), 171-185.

Peng, X., Murphy, T., & Holden, N. M., 2008. Evaluation of the effect of temperature on the die-
off rate for *Cryptosporidium* parvum oocysts in water, soils, and feces. Applied &
Environmental Microbiology, 74(23), 7101-7107.

Percival, S. L., Yates, M. V., Williams, D., Chalmers, R., & Gray, N., 2013. Microbiology of
waterborne diseases: microbiological aspects and risks. Academic Press, 515-522.

Petterson, S., Ashbolt, N., 2016. QMRA and water safety management: Review of application in
drinking water systems. Journal of Water Health, 14(4), 571-589.

Phillips, G., Tam, C. C., Conti, S., Rodrigues, L. C., Brown, D., Iturriza-Gomara, M., &
Lopman, B., 2010. Community incidence of norovirus-associated infectious intestinal disease
in England: improved estimates using viral load for norovirus diagnosis. American Journal of
Epidemiology, 171(9), 1014-1022.

Qaiser, K., Ahmad, S., Johnson, W., & Batista, J., 2013. Evaluating water conservation and reuse
policies using a dynamic water balance model. Environmental Management, 51(2), 449-458.

Qaiser, K., Ahmad, S., Johnson, W., & Batista, J., 2011. Evaluating the impact of water
conservation on fate of outdoor water use: A study in an arid region. Journal of
Environmental Management, 92(8), 2061–2068

Qiu, Y., Lee, B. E., Neumann, N., Ashbolt, N., Craik, S., Maal-Bared, R., & Pang, X., 2015. Assessment of human virus removal during municipal wastewater treatment in Edmonton, Canada. Journal of Applied Microbiology, 119(6), 1729-1739.

Rao SSC., 2006. Oral rehydration for viral gastroenteritis in adults: a randomized, controlled trial of 3 solutions. JPEN Journal of Parenteral & Enteral Nutrition, 30, 433–9.

Reardon, R., DiGiano, F., Aitken, M., Paranjape, S., Kim, J. H., & Chang, S., 2005. Membrane treatment of secondary effluents for subsequent use. Water Environment Research Foundation/International Water Association.

Regli, S., Rose, J. B., Haas, C. N., & Gerba, C. P., 1991. Modeling the risk from *Giardia* and viruses in drinking water. Journal of American Water Works Association, 83(11), 76-84.

Rehan, R., Knight, M. A., Unger, A. J. A., Haas, C. T., 2013. Development of a system dynamics model for financially sustainable management of municipal watermain networks. Water Research, 47(20), 7184-7205.

Reungoat, J., Macova, M., Escher, B., Carswell, S., Mueller, J., & Keller, J., 2010. Removal of micropollutants and reduction of biological activity in a full scale reclamation plant using ozonation and activated carbon filtration. Water Research, 44(2), 625-637.

Rice, J., Wutich, A., & Westerhoff, P., 2013. Assessment of *de facto* wastewater reuse across the US: Trends between 1980 and 2008. Environmental Science & Technology, 47(19), 11099-11105.

Rice, J., Via, S. H., & Westerhoff, P., 2015. Extent and impacts of unplanned wastewater reuse in U.S. rivers. Journal of American Water Works Association, 107(11). E571-E581.

Rigotto, C., Hanley, K., Rochelle, P., De Leon, R., Barardi, C., & Yates, M., 2011. Survival of adenovirus types 2 and 41 in surface and ground waters measured by a plaque assay. Environmental Science & Technology, 45(9), 4145-4150.

Robertson, L.J., Hermansen, L., & Gjerde, B. K., 2006. Occurrence of *Cryptosporidium* oocysts and *Giardia* cysts in sewage of Norway. Applied & Environmental Microbiology, 72(8), 5297-5303.

Rose, J. B., Farrah, S. R., Harwood, V. J., Levine, A. D., Lukasik, J., Menendez, P., & Scott, T. M., 2005. Reduction of pathogens, indicator bacteria, and alternative indicators by wastewater treatment and reclamation processes. IWA Publishing: London, UK.

Rusuli, Y., Li, L., Ahmad, S., & Zhao, X., 2015. Dynamics model to simulate water and salt balance of Bosten Lake in Xinjiang, China. Environmental Earth Sciences, 74(3), 2499–2510.

Ryu, H., Alum, A., Mena, K., & Abbaszadegan, M., 2007. Assessment of the risk of infection by Cryptosporidium and Giardia in non-potable reclaimed water. Water Science & Technology, 55(1-2), 283-290.

Rzeżutka, A., & Cook, N., 2004. Survival of human enteric viruses in the environment and food. FEMS Microbiology Reviews, 28(4), 441-453.

Salvadori, M. I., Sontrop, J. M., Garg, A. X., Moist, L. M., Suri, R. S., & Clark, W. F., 2009. Factors that led to the Walkerton tragedy. Kidney International, 75, S33-S34.

Salveson, A., Snyder, S., & Macpherson, L., 2016. Guidelines for engineered storage for direct potable reuse. Water Environment & Reuse Foundation.

Scallan, E., Griffin, PM., Angulo, FJ., Tauxe, RV., & Hoekstra, RM., 2011. Foodborne illness acquired in the United States—unspecified agents. Emerging Infectious Diseases, 17, 16–22. http://dx.doi.org/10.3201/eid1701.P21101

Shrestha, E., Ahmad, S., Johnson, W., & Batista, J., 2012. The carbon footprint of water management policy options. Energy Policy, 42, 201-212.

Shrestha, E., Ahmad, S., Johnson, W., Shrestha, P., & Batista, J. R., 2011. Carbon footprint of water conveyance versus desalination as alternatives to expand water supply. Desalination, 280(1), 33-43.

Simmons, F. J., Kuo, D. H., & Xagoraraki, I., 2011. Removal of human enteric viruses by a full-scale membrane bioreactor during municipal wastewater processing. Water Research, 45(9), 2739-2750.

Simmons, K., Gambhir, M., Leon, J., & Lopman, B., 2013. Duration of immunity to norovirus gastroenteritis. Emerging Infectious Diseases, 19(8), 1260-1267.

Simonovic, S. P., & Rajasekaram, V., 2004. Integrated analyses of Canada's water resources: A system dynamics approach. Can. Water Resources, 29(4), 223-250.

Sjogren, R. E., 1994. Prolonged survival of an environmental *Escherchia coli* in laboratory soil microcosms. Water, Air, and Soil Pollution, 75(3-4), 389-403.

Sloss, E. M., 1996. Groundwater recharge with reclaimed water: An epidemiologic assessment in Los Angeles County, 1987-1991, P.41.Minnesota Historical Society.

Soller, J. A., Eftim, S. E., Warren, I., & Nappier, S. P., 2016. Evaluation of microbiological risks associated with direct potable reuse. Microbial Risk Analysis,

Snyder, S. A., von Gunten, U., Amy, G., Debroux, J., & Gerrity, D., 2014. Use of ozone in water reclamation for contaminant oxidation. WateReuse Research Foundation: Alexandria, VA.

Soller, J., Olivieri, A., Eisenberg, J., DeGeorge, J., Cooper, R., & Tchobanoglous, G., 2006. A public health evaluation of recreational water impairment. J. Water Health, 4, 1-19.

Soller, J. A., & Eisenberg, J. N., 2008. An evaluation of parsimony for microbial risk assessment models. Environmetrics, 19(1), 61-78.

Soller, J. A., Eftim, S. E., Warren, I., & Nappier, S. P., 2016. Evaluation of microbiological risks associated with direct potable reuse. Microbial Risk Anal, 5, 3-14.

Soller, J. A., Eftim, S. E., & Nappier, S. P. 2018. Direct potable reuse microbial risk assessment methodology: Sensitivity analysis and application to State log credit allocations. Water Research, 128, 286-292.

Stave, K., 2003. A system dynamics model to facilitate public understanding of water management options in Las Vegas, Nevada. Journal of Environmental Management, 67, 303-313.

Sterman, J. D., 2000. Business Dynamics: Systems Thinking and Modeling for a Complex World. McGraw-Hill: New York, NY.

Tamaddun, K., Kalra, A., & Ahmad, S., 2018. Potential of rooftop rainwater harvesting to meet outdoor water demand in arid regions. Journal of Arid Land, 10(1), 68-83.

Tchobanoglous, G., Leverenz, H., Nellor, M. H., & Crook, J., 2011. Direct potable reuse: A path forward. WateReuse Research Foundation: Alexandria, VA.

Tchobanoglous, G., Cotruvo, J., Crook, J., McDonald, E., Olivieri, A., Salveson, A., & Trussell, S. R., 2015. Framework for direct potable reuse. WateReuse Research Foundation: Alexandria, VA.

Teunis, P., Medema, G., Kruidenier, L., & Havelaar, A., 1997. Assessment of the risk of infection by Cryptosporidium or Giardia in drinking water from a surface water source. Water Research, 31(6), 1333-1346.

Teunis, P. F., Nagelkerke, N. J., & Haas, C. N., 1999. Dose response models for infectious gastroenteritis. Risk Analusis, 19(6), 1251-1260.

Teunis, P. F., Moe, C. L., Liu, P., E Miller, S., Lindesmith, L., Baric, R. S., Calderon, R. L., 2008. Norwalk virus: How infectious is it? Journal of Medical Virology, 80(8), 1468-1476.

Teunis, P., Sukhrie, F., Vennema, H., Bogerman, J., Beersma, M., & Koopmans, M., 2015. Shedding of norovirus in symptomatic and asymptomatic infections. Epidemiology & Infection, 143(8), 1710-1717.

Thurston-Enriquez, J. A., Haas, C. N., Jacangelo, J., & Gerba, C. P., 2005. Inactivation of enteric adenovirus and feline calicivirus by ozone. Water Research, 39(15), 3650-3656.

Teunis, P. F., Kasuga, F., Fazil, A., Ogden, I. D., Rotariu, O., & Strachan, N. J., 2010. Dose–response modeling of Salmonella using outbreak data. International Journal of Food Microbiology, 144(2), 243-249.

Trussell, R., Salveson, A., Snyder, S., Trussell, R., Gerrity, D., & Pecson, B., 2013. Potable reuse: State of the science report and equivalency criteria for treatment trains. WateReuse Research Foundation: Alexandria, VA.

Trussell, R., Salveson, A., Snyder, S., Trussell, R. S., & Gerrity, D., 2016. Equivalency of advanced treatment trains for potable reuse. Water Environment & Reuse Foundation: Alexandria, VA.

TWDB., 2015. Final Report: Direct Potable Reuse Resource Document. Report prepared for the Texas Water Development Board by Alan Plummer Associates, Inc.: Fort Worth, TX.

http://www.twdb.texas.gov/publications/reports/contracted_reports/doc/1248321508_Vol

1.pdf (accessed 9/3/2015)

USEPA, 1980. Wastewater in receiving water supply abstraction points. EPA/600/2-80/044. U.S.

Environmental Protection Agency, Washington, D.C.

USEPA, 1991. Guidance Manual for Compliance with the Filtration and Disinfection

Requirements for Public Water Systems Using Surface Water Sources. U.S.

Environmental Protection Agency, Washington, D.C

USEPA, 2002. USEPA Onsite Wastewater Treatment Systems Manual, Chapter 3, 2002.

USEPA, 2004. Estimated per capita water ingestion and body weight in the United States—An

update. EPA 822-R-00-001. U.S. Environmental Protection Agency, Washington, D.C.

USEPA, 2006a. National primary drinking water regulations: Ground Water Rule; Final Rule.

Federal Register. 40 CFR Parts 9, 141 and 142, Vol. 71, No. 216. U.S. Environmental

Protection Agency, Washington, D.C.

USEPA, 2006b. National primary drinking water regulations: Long term 2 enhanced surface

water treatment rule (LT2ESWTR); Final Rule. 40 CFR Parts 9, 141 and 142, 71 (654). U.S.

Environmental Protection Agency, Washington, D.C.

USEPA, 2006c. National primary drinking water regulations: Long Term 2 Enhanced Surface

Water Treatment Rule (LT2ESWTR); Final Rule. EPA 815-Z-06-001. U.S.

Environmental Protection Agency, Washington, D.C.

USEPA, 2010a. Long Term 2 Enhanced Surface Water Treatment Rule Toolbox Guidance

Manual. EPA 815-D-03-009. U.S. Environmental Protection Agency, Washington, D.C.

USEPA, 2010b. Quantitative Microbial Risk Assessment to Estimate Illness in Freshwater

Impacted by Agricultural Animal Sources of Fecal Contamination. Washington, D.C. EPA-

822-R-10-005.USEPA. 2014. Microbiological risk assessment tools, methods, and approaches for water media. Washington, D.C. EPA-820-R-14-009.

USEPA, 2012. Guidelines for Water Reuse. EPA/600/R-12/618. U.S. Environmental Protection Agency, Washington, D.C.

USEPA, 2015a. Human health ambient water quality criteria: 2015 update. EPA 820-F-15-001. U.S. Environmental Protection Agency, Washington, D.C.

USEPA, 2015b. Drinking Water Contaminant Candidate List 4; Notice. Federal Register. Vol. 80, No. 23. February 4, 2015.WHO, 2008. Guidelines for Drinking-water Quality. World Health Organization, Geneva, Switzerland.

USEPA, 2017. Potable Reuse Compendium. EPA/810/R-17/002. Environmental Protection Agency, Washington, D.C.

Venkatesan, A. K., Ahmad, S., Johnson, W., & Batista, J. R., 2011a. System dynamics model to forecast salinity load to the Colorado River due to urbanization within the Las Vegas Valley. Science of the Total Environment, 409(13), 2616-2625.

Venkatesan, A. K., Ahmad, S., Johnson, W., & Batista, J. R., 2011b. Salinity reduction and energy conservation in direct and indirect potable water reuse. Desalination, 272(1), 120-127.

WHO, 2008. Guidelines for drinking-water quality. World Health Organization: Geneva, Switzerland.

Winz, I., Brierley, G., & Trowsdale, S., 2009. The use of system dynamics simulation in water resources management. Water Resources Management, (23), 1301-1323.

Wu, G., Li, L., Ahmad, S., Chen, X., & Pan, X., 2013. A Dynamic Model for Vulnerability Assessment of Regional Water Resources in Arid Areas: A Case Study of Bayingolin, China. Water Resources Management, 27(8), 3085-3101.

Wu, Y., 2015. Quantitative microbial risk assessment of de facto water reuse practice: A case study of Trinity River, Texas. University of California, Irvine.

Wu, J., Dhingra, R., Gambhir, M., & Remais, J. V., 2013b. Sensitivity analysis of infectious disease models: Methods, advances and their application. Journal of the Royal Society, Interface, 10(86), 20121018.

Xiang, N., Sha, J., Yan, J., & Xu, F., 2013. Dynamic modeling and simulation of water environment management with a focus on water recycling. Water, 6(1), 17-31.

Yang, Y., & Griffiths, M. W. 2013. Comparative persistence of subgroups of F-specific RNA phages in river water. Applied & Environmental Microbiology, 79(15), 4564-4567.

Yates, M., & Gerba, C., 1983. Virus survival in groundwater. Paper presented at the Hydrology and Water Resources in Arizona and the Southwest,

Yates, M. V., Gerba, C. P., & Kelley, L. M., 1985. Virus persistence in groundwater. Applied & Environmental Microbiology, 49(4), 778-781.

Yi, J. Y., Lee, N., & Chung, M., 2016. Inactivation of bacteria and murine norovirus in untreated groundwater using a pilot-scale continuous-flow intense pulsed light (IPL) system. LWT-Food Science & Technology, 66, 108-113.

Zelner, J. L., King, A. A., Moe, C. L., & Eisenberg, J. N., 2010. How infections propagate after point-source outbreaks: an analysis of secondary norovirus transmission. Epidemiology, 21(5), 711-718.

Zhang, S., Chen, T., Wang, J., Dong, C., Pan, J., Moe, C., et al., 2011. Symptomatic and

asymptomatic infections of rotavirus, norovirus, and adenovirus among hospitalized children

in Xi'an, china. Journal of Medical Virology, 83(8), 1476-1484.

Zhang, K., Achari, G., Sadiq, R., Langford, C. H., & Dore, M. H., 2012. An integrated

performance assessment framework for water treatment plants. Water Research, 46(6), 1673-

1683.

Zhang, F., Ahmad, S., Zhang, H., Zhao, X., Feng, X., and Li, L., 2016. Simulating low and high

streamflow driven by snowmelt in an insufficiently gauged alpine basin. Stochastic

Environmental Research & Risk Assessment, 30, 59-75.

Zuma, F., Lin, J., & Jonnalagadda, S. B., 2009. Ozone-initiated disinfection kinetics of

Escherichia coli in water. Journal of Environmental Science & Health, Part A, 44(1), 48-56.

Zwietering, M. H., & Van Gerwen, S. J. C., 2000. Sensitivity analysis in quantitative microbial

risk assessment. International Journal of Food & Microbiology, 58(3), 213-221.

Erfaneh Amoueyan, Ph.D., EIT

Email: amoueyan@unlv.nevada.edu

EDUCATION

University of Nevada, Las Vegas	Spring 2018
Doctor of Philosophy in Environmental Engineering	
Babol Noshirvani University of Technology, Iran	Fall 2011
Master of Science in Environmental Engineering	
University of Mazandaran, Iran	Fall 2008
Bachelor of Science in Civil Engineering	

CERTIFICATION

Engineer in Training (EIT)· License 0T7776	June 2017

LANGUAGES

Fluent in Persian

RESEARCH EXPERIENCE

Research Assistant, University of Nevada, Las Vegas Aug 2014 –May 2018

Dissertation: Static and Dynamic Quantitative Microbial Risk Assessment of Potable Reuse Paradigms

- Developed and implemented static and dynamic quantitative microbial risk assessments to compare public health risk in various potable reuse scenarios
- Explored feasibility of ozone-biological filtration as an alternative for full advanced treatment trains consisting of reverse osmosis and advanced oxidation processes
- Identified critical parameters/operational conditions in implementation of potable reuse systems
- Provided recommendations for improvement of the decision-making processes in development, operational designs, and the overall reliability of potable reuse systems

RELEVANT EXPERIENCE

Engineering Intern May – Aug 2017
Carollo Engineers Inc, Sacramento, CA

- Conducted hydraulic analysis on water treatment projects
- Prepared Operations and Maintenance materials for water and wastewater projects
- Checked plans and specifications
- Worked on pipeline networks in water and wastewater projects
- Checked reports on potable reuse projects

Teaching Assistant, University of Nevada, Las Vegas 2014-2017

- Assisted the instructor with preparing course materials

215

- Taught concepts of microbial risk assessment in water reuse class
- Graded assignments, quizzes, and exams
- Held office hours to assist undergraduate students who needed additional guidance with assignments

COMPUTER SKILLS

- **Computer Programming languages:** Matlab, R
- **Engineering Applications:** Stella System Dynamics Software, Autocad, Qual2k
- **Other Applications:** MS Office, Photoshop, Minitab

CONFERENCES

- 11th IWA International Conference, Long Beach. (2017). "Quantitative Microbial Risk Assessment of Potable Reuse Treatment with Ozone and Biological Filtration." Oral presentation.
- 32nd Annual WateReuse Symposium, Phoenix. (2017). "Evaluating Human Health Risks Associated with Potable Reuse: Use of System Dynamics Models to Compare Reverse Osmosis and Ozone-Biofiltration." Oral presentation.
- 32nd Annual Tri-State Seminar, Las Vegas. (2016). "Quantitative Microbial Risk Assessment and Sustainability Framework for Potable Reuse." Oral presentation.
- UCOWR / NIWR / CUAHSI Conference, Henderson. (2015). "Evaluating the Possibility of Using Direct Potable Reuse Systems as Alternative Sources of Drinking Water in Las Vegas." Poster presentation.

PUBLICATIONS

Amoueyan, E., Ahmad, S., Eisenberg, J. N., Pecson, B., & Gerrity, D. (2017). Quantifying pathogen risks associated with potable reuse: A risk assessment case study for *Cryptosporidium*. Water Research, 119, 252-266.